



City Research Online

City, University of London Institutional Repository

Citation: Bufler, M. (2007). The ability of the corneal shape to adapt to acclimatisation with and without soft lenses during a change of altitude. (Unpublished Doctoral thesis, City, University of London)

This is the accepted version of the paper.

This version of the publication may differ from the final published version.

Permanent repository link: <https://openaccess.city.ac.uk/id/eprint/30332/>

Link to published version:

Copyright: City Research Online aims to make research outputs of City, University of London available to a wider audience. Copyright and Moral Rights remain with the author(s) and/or copyright holders. URLs from City Research Online may be freely distributed and linked to.

Reuse: Copies of full items can be used for personal research or study, educational, or not-for-profit purposes without prior permission or charge. Provided that the authors, title and full bibliographic details are credited, a hyperlink and/or URL is given for the original metadata page and the content is not changed in any way.

City Research Online:

<http://openaccess.city.ac.uk/>

publications@city.ac.uk

The ability of the corneal shape to adapt to acclimatisation with and without soft lenses during a change of altitude

Author: Manfred Bufler M.S. in Clinical Optometry (PCO)

The thesis is submitted in fulfilment of the requirements for the degree of
Doctor of Philosophy

City University London

Department of Optometry and Visual Science

Submission: February 2007

CHAPTER 1. ANATOMY AND PHYSIOLOGY OF THE CORNEA	20
1.1 Introduction	20
1.2 Corneal dimensions	20
1.3 Anatomy of the cornea	22
1.3.1 Embryology of the cornea	23
1.3.2 Epithelium	24
1.3.3 Bowman's layer.....	26
1.3.3.1 Cell adhesion of epithelium and stroma.....	26
1.3.4 Stroma	27
1.3.5 Descemet's membrane.....	29
1.3.6 Endothelium	30
1.4 Physiology of the cornea.....	31
1.4.1 Corneal metabolism.....	31
1.4.2 Epithelial metabolic pump functions.....	32
1.4.3 Endothelial metabolic pump functions.....	34
1.4.4 Stroma	34
1.4.5 Tear Film.....	35
1.5 Summary	37
CHAPTER 2. FACTORS AFFECTING CORNEAL PHYSIOLOGY	40
2.1 Introduction	40

2.2 Factors influencing corneal physiology caused by altitude	40
2.2.1 The determination of the influential factors	40
2.2.2 Effects of UV on corneal physiology	48
2.2.3 Cosmic radiation and corneal physiology	51
2.2.4 The influence of temperature on corneal metabolism.....	52
2.2.5 The influence of humidity on corneal physiology	53
2.2.6 Oxygen level and contact lens wearing effects on corneal physiology	58
2.2.6.1 Striae and folds	59
2.2.6.2 Hypoxia.....	61
2.2.6.3 Minimum partial oxygen pressure before swelling of the cornea ...	64
2.2.6.4 Signs and symptoms.....	66
2.2.7 The indirect influence of acclimatisation	67
2.2.7.1 Acclimatisation.....	71
2.2.7.2 Complications at high altitude	72
2.2.8 Hypothesis to be tested in this study.....	74
2.3 Summary	74
CHAPTER 3. METHODS	79
3.1 Introduction	79
3.2 Instruments	79
3.2.1 Protection against cosmic radiation	79

3.2.2 Protection against UV radiation	80
3.2.3 Instruments for the measurement of air pressure.....	82
3.2.4 Instruments for measuring altitude.....	83
3.2.5 Instruments used to measure temperature	84
3.2.6 Instruments for measuring humidity	85
3.2.7 Instruments for corneal inspection.....	87
3.2.8 Instruments for measuring intraocular pressure	87
3.2.9 Instruments for inspecting the central retina	90
3.2.10 Instruments for measuring corneal shape	91
3.2.10.1 The programme used to describe corneal shape	92
3.2.10.2 The quality of shape fitting statistical analysis	95
3.2.10.3 The role of a best fitted ellipsoid.....	96
3.2.10.4 Zernike polynomials	98
3.2.10.4.1 Spherical part of the Zernike polynomials.....	99
3.2.10.4.2 Angle-dependent part of the Zernike polynomials.....	99
3.2.10.4.3 The graphical demonstration of the Zernike polynomials.....	100
3.2.10.5 rms	101
3.2.10.6 Residual rms.....	102
3.3 Calibration of instruments used in this study.....	103
3.3.1 Altimeter and aneroid barometer.....	104

3.3.2 Thermometer	107
3.3.3 Hygrometer	110
3.3.4 Tonometry	112
3.3.5 Keratographer	117
3.4 Summary	125
CHAPTER 4. STANDARD MEASUREMENTS AT LOW ALTITUDE.	128
4.1 Introduction	128
4.2 Subjects and methods	128
4.2.1 Subjects.....	128
4.2.2 Anamnesis	129
4.2.3 Contact lenses used for subjects in the low altitude study	130
4.2.4 Methods	133
4.2.5 Results of the low altitude study	133
4.2.5.1 Distributions of residual rms values and significance testing for daily corneal shape change.....	135
4.2.5.2 Zernike coefficients for both subject groups	140
4.2.5.3 z-value.....	142
4.2.5.4 Association between residual rms and intra ocular pressure.....	144
4.2.6 Summary	146
CHAPTER 5. METHODS AND DESIGN OF THE STUDY AT HIGH ALTITUDE	147

5.1 Introduction	147
5.2 Electrical support	147
5.3 Preparation and test procedures	149
5.3.1 Preparation	149
5.3.2 Contact lenses used for subjects in the altitude study.....	149
5.3.3 The test procedure performed morning, noon, and evening	152
5.4 Description of the tour.....	155
5.4.1 The choice of the region for the tests.....	155
5.4.2 Equipment.....	157
5.4.3 The trekking tour.....	158
5.5 Summary	161
CHAPTER 6. HIGH ALTITUDE STUDY	163
6.1 Introduction	163
6.2 Data from the high altitude study.....	163
6.3 Descriptive statistics	164
6.4 Distributions of residual rms values and significance testing for the non contact lens wearers and contact lens wearers groups.....	168
6.5.1 Significance analysis and hypothesis testing.....	174
6.5.2 Hypothesis tests.....	176
6.5.2.1 Non-lens wearers' morning tests (MOR-NCL).....	176

6.5.2.2 Non-lens wearers' noon tests (NOON-NCL).....	178
6.5.2.3 Non-lens wearers' evening tests (EVEN-NCL).....	181
6.5.2.4 Contact lens wearers morning tests (MORN-CL).....	183
6.5.2.5 Contact lens wearers' noon tests (NOON-CL)	185
6.5.2.6 Contact lens wearers evening tests (EVEN-CL).....	187
6.5.2.7 A short summary of the tests:	189
6.5.3 Maximum and minimum residual rms values described graphically	190
6.6 Corneal shape change during the test period compared to corneal shape change during normal conditions	191
6.7 Associations between the various meteorological parameters.....	194
6.8 z-values	198
6.9 Altitude and z-value.....	200
6.10 Results of eye examinations during the test period	202
6.11 Association between residual RMS values and other parameters.....	205
6.11.1 Association between residual rms and humidity	205
6.11.2 Association between residual rms and air pressure	207
6.11.3 Association between residual rms and temperature	208
6.11.4 Associations between residual rms and altitude	210
6.12 Summary and discussion.....	212
CHAPTER 7. DISCUSSION AND SUMMARY	218

7.1 Introduction	218
7.2 Corneal shape change at low altitude.....	219
7.2.1 Keratographer accuracy considered in detail.....	219
7.2.2 Measurement of IOP	221
7.2.3 Low altitude study	222
7.2.3.1 Tests of significant daily corneal shape change	222
7.2.3.2 Change in z-value (the distance between the highest and deepest points of a cornea).....	224
7.3 Corneal shape change at high altitude	225
7.3.1 Hypothesis test	225
7.3.2 Meteorological data and its influence on the test subjects.....	226
7.3.3 The range of the maximum and minimum z-values.....	227
7.3.4 Eye inspection	229
7.4 Addressing the three questions posed in Chapter 7 section 1.....	230
7.5 Suggestions for further research	231
7.6 Main conclusions.....	232
REFERENCES.....	233
APPENDIX.....	248
Assumptions and definition of terms.....	249

Figures and tables:

Figures

Chapter 1

Figure 1.2-1	21
Mexican hat	
Figure 1.2-2	22
Refract. index and corn. hydration	
Figure 1.3-1	23
Corneal layers	
Figure 1.3.1-1	24
Optic vesicle	
Figure 1.3.2-1	25
Cut through corn. epith.	
Figure 1.3.3-1	26
Bowman's layer	
Figure 1.3.4-1	27
Structure of stroma	
Figure 1.3.4-2	28
Stromal fibrils	
Figure 1.3.5-1	29
Posterior stroma	
Figure 1.3.6-1	30
Endothelium	
Figure 1.3.6-2	31
Endothelium cell density	

Figure 1.4.1-1	32
----------------	----

Corneal metabolism

Figure 1.4.2-1	33
----------------	----

Cl⁻ transport in epithelium

Figure 1.4.5-1	35
----------------	----

Tear film

Chapter 2

Figure 2.2.1-1	42
----------------	----

Effects of temperature on air pressure

Figure 2.2.1-2	47
----------------	----

Solar wind

Figure 2.2.2-1	50
----------------	----

Corneal transmission of UV-radiation

Figure 2.2.5-1	54
----------------	----

Evaporation of tears

Figure 2.2.5-2	57
----------------	----

Mires projected on corneas

Figure 2.2.6.1-1-3	60
--------------------	----

Striae

Figures

Figure 2.2.6.3-1	64	Figure 3.2.10.4-1	98
Corneal swelling		Zernike polynomials	
Figure 2.2.6.3-2	65	Figure 3.2.10.4.3-1-6	100
Average corn. swelling		Aberrations	
Figure 2.2.7-1	72	Figure 3.2.10.4.3-7-11	101
Pulse during		Aberrations	
Acclimatisation		Figure 3.3.1-1	104
		Scatterplot altimeter	
		test 1	
		Figure 3.3.1-2-3	105
		Scatterplot altimeter	
		test 1, Altman Bland	
		plot altimeter test 1	
		Figure 3.3.1-4	106
		Altman Bland plot	
		altimeter test 2	
		Figure 3.3.2-1	107
		Scatterplot therm.	
		Figure 3.3.2-2	108
		Scatterplot therm.	
		Figure 3.3.2-3	109
		Altman-Bland plot	
		thermometers	
		Figure 3.3.3-1	111
		Scatterplot hygrometer	

Chapter 3

Figure 3.2.2-1	81
Transmission of UV	
radiation	
Figure 3.2.6-1	86
Assmann-Aspirations	
psychrometer	
Figure 3.2.7-1	87
Slit lamp	
Figure 3.2.9-1	91
Retinal haemorrhages	
Figure 3.2.10-1-1	94
Fluorescein pictures	
Figure 3.2.10.3-1	97
Wave fronts	
Figure 3.2.10.3-2	97
Ideal ellipsoid	

Figures

Figure 3.3.3-2	112	Figure 4.2.5-1	135
Altman-Bland plot hygrometers		Box and Whisker plot resrms values	
Figure 3.3.4-1-2	115	Figure 4.2.5.1-1	136
Altman-Bland plot tonometers		Distribution of n.- cl wearer samples	
Figure 3.3.4-3	116	Figure 4.2.5.1-2	139
Altman-Bland plot tonometers		Distribution of cl wearer samples	
Figure 3.3.5-1	119	Figure 4.2.5.4-1	144
Zernike coefficients		Scatterplot of mean IOP values	
Figure 3.3.5-2	120	Figure 4.2.5.4-2-3	145
Zernike coefficients		Scatterplot of mean IOP values	
Figure 3.3.5-3-4	123		
Altman-Bland plot keratographer			
Figure 3.3.5-5	124		
Altman-Bland plot keratographer			
Chapter 4		Chapter 5	
Figure 4.2.3-1	132	Figure 5.2-1	147
Contact lens data		Electrical support	
		Figure 5.3.2-1	151
		Contact lens data	
		Figure 5.3.2-2	152
		Contact lens data	
		Figure 5.3.3-1	153
		Soft lens fitting test	

Figures

Figure 5.4.1-1	155	Figure 6.4-19-24	173
Kyangjin Kar		Distribution of cl	
Figure 5.4.1-2	156	wearer samples	
Nepal map		Figure 6.5.2.1-1	178
Figure 5.4.2-1	157	Box and whisker	
Equipment		plot n-cl morning	
Figure 5.4.2-2	157	Figure 6.5.2.2-1	181
Measuring		Box and whisker	
corneal shape		plot n-cl noon	
Figure 5.4.3-1	161	Figure 6.5.2.3-1	183
Altitudes in Nepal		Box and whisker	
		plot n-cl evening	
Chapter 6		Figure 6.5.2.4-1	185
		Box and whisker	
Figure 6.3-1	166	plot cl morning	
Box and Whisker		Figure 6.5.2.5-1	187
plot resrms values		Box and whisker	
Figure 6.4-1-4	169	plot cl noon	
Probability plot		Figure 6.5.2.6-1	189
Figure 6.4-5-10	170	Box and whisker	
Probability plot		plot cl evening	
Figure 6.4-11-12	171	Figure 6.5.3-1	190
Probability plot		3D graphics of	
Figure 6.4-13-18	172	Zernike functions	
Distribution of n.-		Figure 6.6-1-3	192
cl wearer samples		Probability plot	

Figures

Figure 6.6-4-5	193
Gamma frequency	
Figure 6.6-6	194
Gamma frequency	
Figure 6.7-1-3	197
Scatterplots of surrounding cond.	
Figure 6.9-1	202
Z-value and altitude	
Figure 6.11.1-1	206
Association betw. Residual rms and humidity	
Figure 6.11.2-1	208
Association betw. Residual rms and air pressure	
Figure 6.11.3-1	209
Association betw. Residual rms and temperature	
Figure 6.11.4-1	211
Association betw. Residual rms and altitude	

Tables

Chapter 2		Table 3.3.1-1	104
		Altimeter test	
Table 2.2.1-1	43	Table 3.3.3-1	111
Air pressure at altitude		Hygrometer test	
Table 2.2.1-2	46	Table 3.3.4-1	114
Water vapour		Tonometer test	
Table 2.2.5-1	56	Table 3.3.5-1	122
Air conditions during flights		Zernike coefficients	
Table 2.2.6.1-1	59	Chapter 4	
Striae		Table 4.2.5-1	134
Table 2.2.7-1	68	Residual rms values at low altitude	
Erythrocytes at high altitude		Table 4.2.5.1-1	138
Table 2.2.7-2	69	F-test of non-cl wearer samples	
CO ₂ , O ₂ in blood		Table 4.2.5.1-2	139
Table 2.2.7-3	70	F-test of cl wearer samples	
Heamoglobin saturation		Table 4.2.5.1-3-4	141
Chapter 3		Zernike coefficients	
Table 3.2.2-1	80		
Transmission of UV radiation			
Table 3.2.8-1	89		
Tono-Pen factor			

Tables

Table 4.2.5.1-5-6	141	Table 6.5.2.1-1-2	177
Ellipsoid data		Hypthesis test n.-	
Table 4.2.5.3-1	144	cl morning	
Z-values at low		Table 6.5.2.2-1-2	179
altitude		Hypthesis test n.-	
		cl noon	
Chapter 5		Table 6.5.2.3-1 &	181
		Table 6.5.2.3-2	182
Table 5.3.2-1	150	Hypthesis test n.-	
Residual rms		cl. evening	
reference data		Table 6.5.2.3-3	183
		Duncan's MRT	
Chapter 6		test	
		Table 6.5.2.4-1-2	184
Table 6.3-1	165	Hypthesis test cl	
Residual rms		morning	
values at high		Table 6.5.2.5-1	185
altitude		Hypthesis test cl	
Table 6.3-2	166	noon	
Zernike		Table 6.5.2.5-2	186
coefficients		Mean values of	
Table 6.3-3-4	167	altitude samples	
Zernike		Table 6.5.2.6-1	187
coefficients		Hypthesis test n.-	
Ellipsoid data		cl evening	

Tables

Table 6.5.2.6-2-3	188
Mean values of altitude samples, Duncan's MRT test	
Table 6.7-1	196
Surrounding conditions	
Table 6.8-1	198
Z-values at high altitude	
Table 6.8-2	199
Z-values at high altitude	
Table 6.9-1	201
Z-value and altitude	
Table 6.10-1	204
Eye signs	
Table 6.10-2	204
Cl movement	
Table 6.11.4-1	212
Mean r-values	

Word Of thanks

Some assistance was required to complete this work.

I would like to express my thanks to the following persons for their help:

Professor David Edgar

Dr. Luis Diaz-Santana

Professor Dr. Bernd Lingelbach

Professor Dr. Roger Buckley

I would also like to express my appreciation for the support provided by those persons involved in the study (the tested subjects) and my family.

I grant powers of discretion to the University Librarian to allow this thesis to be copied in part without further reference to me. This permission covers only single copies made for study purposes.

Abstract

Changes in corneal shape at altitude have not been the subject of research, but are relevant to mountaineers. Chapters 1 and 2 of this thesis review the literature of the anatomy and physiology of the cornea, and factors affecting corneal physiology. Among these factors, and of particular relevance to mountaineers, is that the oxygen concentration in the atmosphere is reduced at high altitude and could contribute to corneal oedema and corneal shape change. When the cornea is subjected to reduced oxygen levels at low altitude there is no consensus as to the level of oxygen which leads to corneal oedema, but some researchers have found the critical oxygen level to be sufficiently high to lend support to the anecdotal reports from high altitude mountaineers that reduced visual acuity does occur at high altitudes (e.g. the summit of Mt. Everest), presumably as a result of corneal oedema. However, there are no reports in the literature that ascending to an altitude of 15 000 ft has any influence on visual acuity. It appears that light scatter induced by a possible oedematous reaction of the cornea to hypoxia at altitudes of up to 15 000 ft is not sufficient to have any influence on visual acuity. Other influential factors apart from low oxygen levels, such as low humidity, low temperature, and interactions between the meteorological factors described as weather, could also have an influence on corneal shape change. A low pressure chamber is an ideal instrument to test each influential factor while other factors are kept constant, however the weather can not be simulated unless experiments are carried out under the natural conditions experienced in the real world. The hypothesis to be tested in the experimental work described in this thesis is that "the cornea is able to adapt to changing conditions and exhibits no significant change in the corneal shape up to 16,400 ft." Measurements were taken during a high-altitude trek in Nepal and the equipment used and its validation is described in Chapter 3 for measurements of air pressure, altitude, temperature, and humidity. Calibrations against a suitable gold standard and/or manufacturers' tolerances were undertaken and found to be satisfactory for all instruments to be taken on the trek. A lack of repeatability and validity for the Tono-Pen® XL tonometer had to be accepted because, for safety reasons, IOP had to be measured from the sclera on the trek. There is evidence to suggest that the Tono-Pen manufacturer's conversion table to convert from measurements taken from the sclera at the limbus rather than from the cornea may be inaccurate. Details are given of the method for measuring corneal shape using an Oculus keratographer, whose output was converted into combined variables consisting of Zernike polynomials and an ellipsoid. A residual rms value was generated from the Zernike polynomials and was used to describe corneal shape change. Repeatability of the residual rms measurements was not as good as anticipated. However, it was comparable between the two keratographers tested and the variability was regarded as acceptable.

The research detailed in this thesis investigates corneal shape change in 11 normal subjects, aged 35 to 54 years, over a period of four days at low altitude (Chapter 4) and in 9 normal subjects, aged 45 to 60 years, on a three week high-altitude trekking tour of Nepal, which reached an altitude of 16,400 feet (Chapter 6). In both studies, measurements were taken three times each day (morning, noon, and evening). Both samples included three subjects who wore soft contact lenses, to investigate if any aspect of corneal shape change was different among contact lens wearers. For all contact lens wearers, the fit and comfort of the lenses were checked during an examination of both the anterior and posterior eye. For the low altitude study (Chapter 4) descriptive statistics reveal a slight tendency for residual rms values to be higher in the small sample of contact lens wearers.

No significant corneal shape change with time of day was detected for either the non contact lens wearer category ($p = 0.808$) or for the contact lens wearer category ($p = 0.210$). No significant change in corneal shape was found over four days for either the non contact lens wearer category ($p = 0.62$, $p = 0.32$, $p = 0.11$) or for the contact lens wearer category ($p = 0.11$, $p = 0.09$, $p = 0.35$) for morning, noon or evening tests respectively. Chapter 5 describes the complex logistics of the trek, which was organised by the author to allow the battery of tests to be completed at high altitude.

In the high altitude study (Chapter 6), residual rms values were analysed with the data categorised according to 5 altitude levels (altitude samples). Descriptive statistics generally show higher sample mean residual rms values at high altitude, greater maximum residual rms values at high altitude, and greater residual rms values in the contact lens wearers. There are statistically significant increases in residual rms values with altitude, identified by ANOVA testing, for both non contact lens wearers ($p = 0.0061$) and contact lens wearers ($p = 0.0002$) for their evening tests.

The low altitude reference sample 1 (up to 3,280ft) had a statistically significantly lower mean residual rms value than samples 2 (3,280 to 6,560ft) and 5 (above 13,120 ft) for both contact lens wearers and non wearers, and sample 1 mean was also statistically significantly lower than sample 4 (9,840ft to 13,120ft) for the non wearers. The meteorological data revealed a very stable weather situation throughout the entire testing phase of the trek. For each eye tested there was very little or no evidence for any linear association between residual rms and humidity ($r_{\text{mean}} = 0.24$), air pressure ($r_{\text{mean}} = 0.18$), temperature ($r_{\text{mean}} = 0.20$), or altitude ($r_{\text{mean}} = 0.19$). Transient retinal vasculature changes occurred in two subjects. The degree of contact lens movement increased for all three subjects during the trek.

The z-value, the distance between the highest and deepest point of the corneal shape described by the Zernike coefficients, was analysed at both low and high altitude for each subject. There is a tendency for the mean z-values for contact lens wearers to be higher than those of the non contact lens wearers at both low and high altitude. The findings from this study suggest that contact lens wear causes an increase in z-values irrespective of altitude. There is also a tendency for a greater range of z-values to be found in contact lens wearers. The risk of contact lens wear inducing irritations rises dramatically when movement of the contact lens is influenced by a very variable z-value. This elevated range of z-values at high altitude should undoubtedly be taken into consideration during lens fitting for mountaineers who wish to ascend to high altitudes.

The conclusions of this thesis should be interpreted with caution, due to the small samples; however the hypothesis is rejected for the evening measurements. The corneal shape changes detailed in this thesis are likely to be the result of a combination of a reduced oxygen partial pressure at high altitudes, possibly exacerbated by fatigue, and, for contact lens wearers, the effects of the contact lens on the cornea. Unfortunately, there was limited time available to complete the battery of tests at altitude and limited electrical power on the trek. These factors limited the number and range of tests that could be carried out, and as a result no measurements of visual function with altitude were included in the study.

The main aim of this hypothesis is to investigate how the corneal shape changes with and without contact lenses at low altitude and during an ascent up to an altitude of 16 400 ft. Changing surrounding conditions and a steady decrease in oxygen levels during ascent are the main factors that determine how the human body acclimatizes. For contact lens fitting in trekkers and mountaineers, it is essential to know how the corneal shape is influenced by altitude. The z-value, which is the distance between the highest and lowest point of the corneal contour, has been introduced to investigate possible associations between contact lens movement and corneal shape change. Further associations between a range of possible influencing factors (i.e. humidity, air pressure, temperature, and altitude) and residual rms values are explored.

Chapter 1. Anatomy and Physiology of the cornea

1.1 Introduction

This chapter is a literature review of relevant aspects of the human cornea. The main focus of this thesis is on changes to the cornea with altitude, hence the importance of the anatomy and physiology of this structure.

The dimensions and the corneal shape are divided into different zones and presented as a basis for further shape considerations. Additionally, the layers of the cornea are described and some factors regarding the corneal metabolism are shown to be the main factors responsible for the tissues' transparency.

1.2 Corneal dimensions

The geometrical shape which best describes the rim around the cornea is an ellipsoid.

It covers a horizontal length which ranges from 11.0 – 12.5 mm (mean 11.6 mm) and a vertical height ranging from 10.0 – 11.5 mm (mean 10.7 mm) (Baron, 1981). The description of the corneal profile has been steadily improving in its accuracy for about two hundred years.

In the 1820s, the French ophthalmologist Ferdinand Cuignet provided the first description of a method for studying images reflected off the anterior corneal surface. A light was projected onto a target that was held in front of the patient's eye. The light, target, patient, and observer were positioned so that the observer could visualize the image of the target on the patient's cornea. Distortion of the reflected image could then be qualitatively interpreted by the observer.

In 1880, A. Placido devised a keratometry target that is still in use today. The target was a disk with alternating black and white circles. The disk had a hole in its centre through which the observer could visualize the patient's cornea (Schanzlin, and Robin, 1992).

Watkins (1966) described the corneal profile as being like a Mexican hat, and he subdivided the corneal shape into three zones (Fig. 1.2-1).

- The central zone measured 5 mm in diameter and is known as the spherical optical zone.
- This area is followed by the elliptical zone of 1.75 mm width around the central zone.
- Finally, the third zone has a parabolic shape which extends for 1.25 mm at the periphery of the cornea.

The central radius of a normal human cornea is between 7.0 mm and 8.5 mm (Baron, 1981).

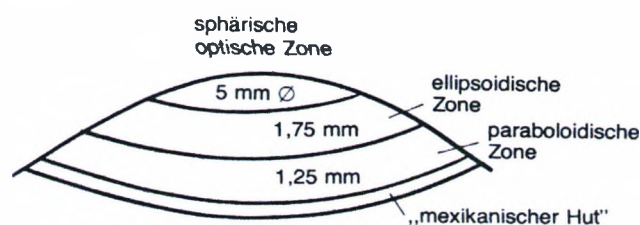


Figure 1.2-1 The corneal profile is described as a three zone shape resembling a “Mexican hat”. Each zone is defined by a geometrical shape. (Watkins, 1966)

Nowadays, mathematical algorithms are used to describe the images on the corneal surface, which are projected by a target- like grid or “Placido disc” (Schanzlin, and Robin, 1992).

The thickness of the cornea is not constant. It increases from the centre towards the limbus. The normal central corneal thickness is between 0.49 mm and 0.56 mm. At the limbus the thickness ranges from 0.7 mm to 0.9 mm (Kanski, 1995).

Meek, et al (2003) demonstrated that the corneal refractive index $n_e \approx 1.362$ depends on the hydration of the tissue.

They used Gladstone and Dale's law and measured the changing refractive index of a dissected corneal stroma during hydration, which allowed them to derive the following formula:

$$n'_s = 1.335 + 0.04/(0.22 + 0.24H)$$

$$\text{Tissue hydration (H)} = (\text{Average Wet Weight} - \text{Dry Weight})/(\text{Dry Weight})$$

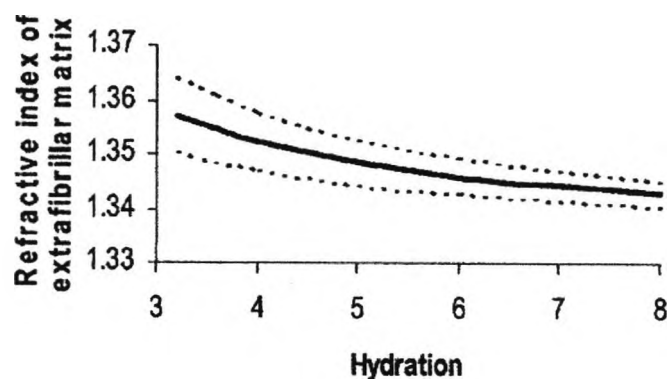


Figure 1.2-2 As the hydration of the stroma increases from $H = 3.2$ to $H = 8$, the “refractive index” of the stroma decreases. (Meek et al, 2003)

These changes in the “refractive index of the stromal extrafibrillar matrix” are based on the fact that the fibril distance gets bigger when the stroma swells (Figure 1.2-2). Hence, it follows that the gaps between the fibrils are filled with fluid which has a lower refractive index than the fibrils.

1.3 Anatomy of the cornea

Anatomically, the cornea consists of the following five layers:

Epithelium, Bowman's layer, stroma, Descemet's membrane, and endothelium (Fig. 1.3-1). Only the epithelium is derived from the ectoderm cells at 4 to 5 weeks of gestation. The other four layers are derived from the mesenchymal cells (Naumann, 1997).

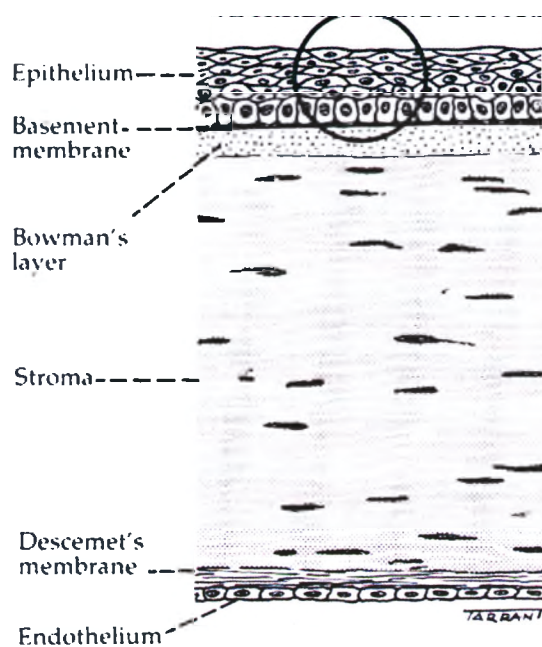


Figure 1.3-1 The five human corneal layers. (Kanski, 1995)

1.3.1 Embryology of the cornea

The following embryological stages lead to the creation of the five corneal layers:

- At 5 to 6 weeks of gestation the lens vesicle detaches and the adjacent surface ectoderm from which it has budded gives rise to the corneal epithelium, which is 1 to 2 cells thick with a gossamer underlying basement membrane (Figure 1.3.1-1).
- Between 8 weeks and 5 months, the corneal epithelium goes through many changes. The number of epithelial cell layers increases from 1 to 2 at 8 weeks to 3 to 4 at 19 weeks, and to 4 to 5 at 27 weeks, increasing to the adult level of 6 to 7 layers by 36 weeks of gestation.

- After 5 weeks of gestation a loose acellular layer, destined to become corneal stroma, has formed and comprises collagen fibrils.
- Perilimbal mesenchymal cells that migrate between the lens and the acellular stroma at 6 weeks of gestation form the corneal endothelium.
- At 13 weeks a palisade of fine filaments is observed extending perpendicular to the basal lamina into the anterior stroma. This may be a precursor to Bowman's layer. Descemet's membrane has been detected from 8 weeks of gestation (Kaufman, and Alm 2003).
- At the beginning of the 5th month all five corneal layers are existent (Naumann, 1997).

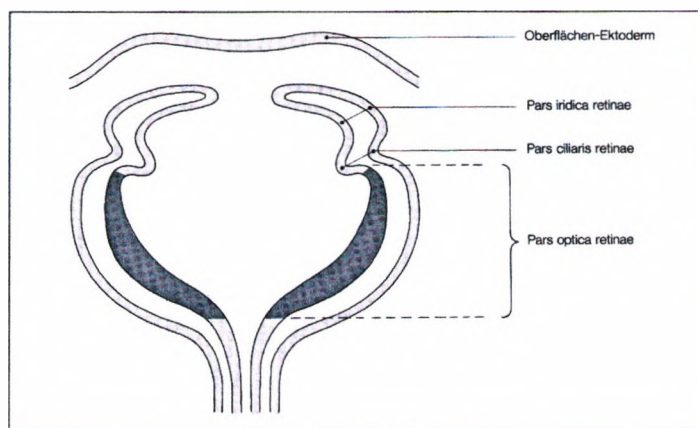


Figure 1.3.1-1 The optic vesicle at the second month of pregnancy.
(Naumann, 1997)

1.3.2 Epithelium

The human epithelium consists of three types of cells; a single layer of basal columnar cells, two to three rows of wing cells, and two layers of long and thin surface cells joined by bridges (Kanski 1995). These three types of cells build five to seven cell layers and the epithelium is 50 µm thick (Freyler, 1985). The basal cells, in which mitosis occurs, adhere to a basement membrane. The daughter cells, as a result of cell division, move towards the surface of the cornea and begin to differentiate, forming one to three layers of wing cells (Figure 1.3.2-1). The superficial cells finally degenerate and are sloughed from the corneal surface.

Basal cells have a higher level of metabolic and synthetic activity than the more superficial cells and therefore have more prominent mitochondria, endoplasmic reticulum, and Golgi apparatus (Kaufman, and Alm, 2003).

The cell division process results in turnover of the entire epithelium every 7 to 10 days. Thus the cells are able to regenerate in an excellent manner, and therefore the epithelium does not scar. This is one of the reasons why cellular epithelium serves as the major protective barrier against penetration of pathogens into the deeper stroma. (Catania, 1995).

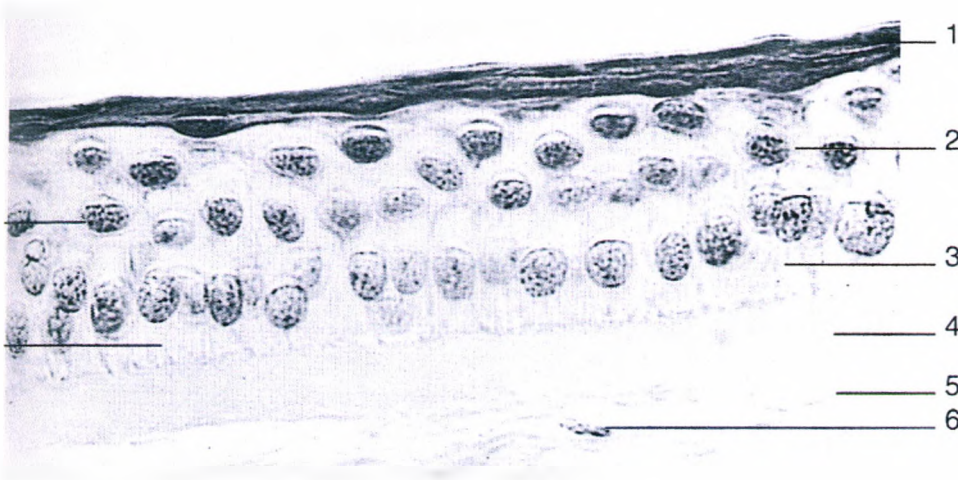


Figure 1.3.2-1 Human epithelium stained with Haematoxylin – Eosin. The magnification is 500 times. 1. Superficial cells 2. Wing cells 3. Basal cells 4. Bowman's membrane 5. Stroma 6. Keratocyte. (KÜHNEL, 1999)

The basal cells of the epithelium rest on a basement membrane, or basal lamina, that is approximately 40 to 60 nm thick. This membrane is similar in structure and composition to the basal laminas of other squamous epithelia.

It contains type 4 collagen, laminin, the proteoglycan perlecan, fibronectin, and fibrin (Kaufman, and Alm, 2003).

1.3.3 Bowman's layer

Bowman's layer lies beneath the basement membrane and is approximately 8 - 14 μm thick (Freylar, 1985). The structure is revealed to be made of randomly arranged collagen fibrils. These are probably, at least in part, type 1 collagen (Figure 1.3.3-1). Bowman's layer is acellular and may be considered a modified superficial layer of the stroma. It could be said that the anterior-most stromal layer is Bowman's layer (Kaufman, and Alm, 2003).

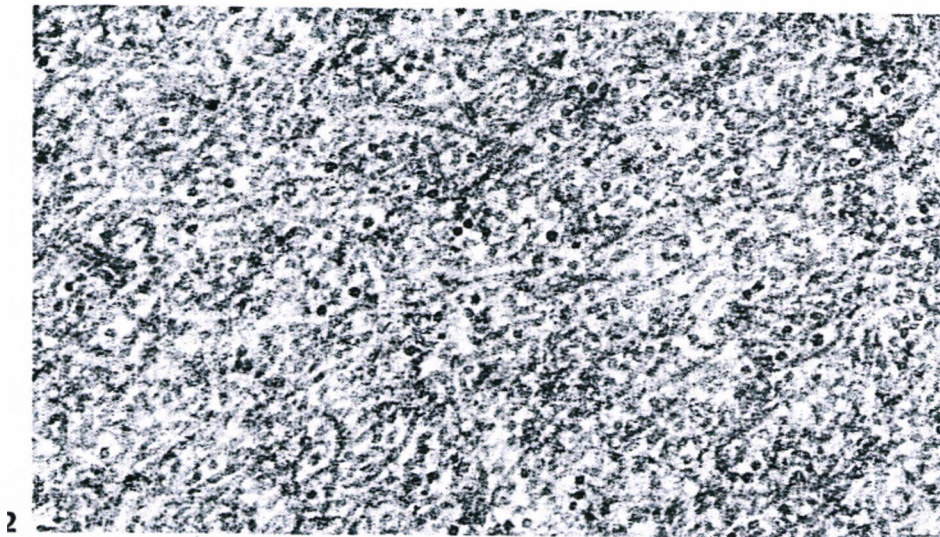


Figure 1.3.3-1 Bowman's layer consists of 14 – 27 nm thick collagen fibrils. Magnification of 42,500 times. (KÜHNEL, 1999)

1.3.3.1 Cell adhesion of epithelium and stroma.

The basal cells of the epithelium adhere to their basement membrane and underlying connective tissue stroma via a series of linked structures collectively termed the adhesion complex (Smolin, and Thoft, 1994). These linked structures contain a high quantity of type 1 and type 5 collagen (Kampik, and Grehn, 1996).

Additionally, these structures and the basement membrane are products of the basal cells of the epithelium. On the outside of the basal cell membrane a thin electron- dense line runs parallel to the cell membrane, and from it fine anchoring filaments extend through towards the electron dense zone of the basement membrane. On the opposite side of the basement membrane, anchoring fibrils insert. These anchoring fibrils consist of type 7 collagen and pierce 1 – 2 μm into the anterior Bowman´s layer. In small patches of the basement membrane, there appears material termed anchoring plaques and the cross-banded anchoring fibrils forming a complex network that is interwoven with the conventionally cross banded type 1 collagen fibrils (Smolin, and Thoft, 1994).

These data indicate the importance of the anchoring fibril network penetration into the anterior stroma in adhesion of the basement membrane and its epithelium.

1.3.4 Stroma

The stroma makes up 90% of the corneal thickness (Figure 1.3.4-1). The middle connective tissue layer is approximately 500 μm thick (Smolin, and Thoft, 1994).

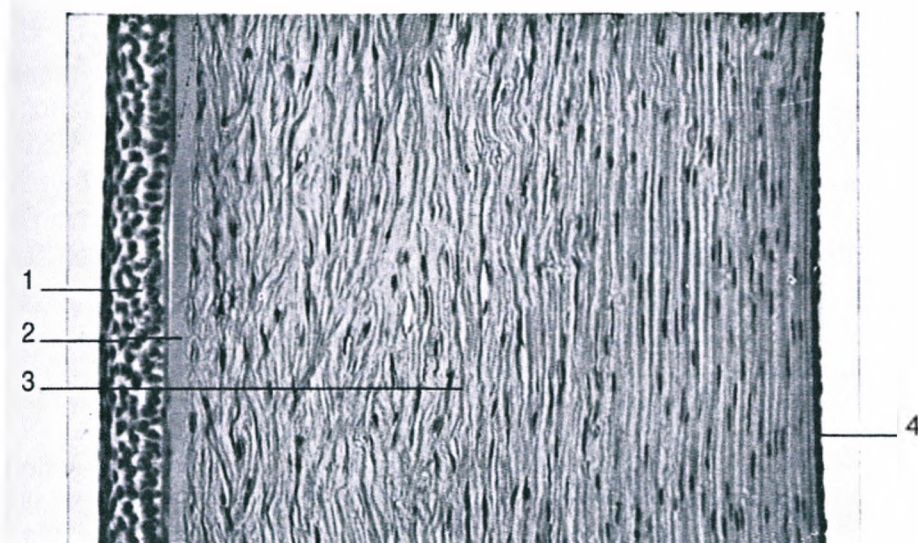


Figure 1.3.4-1 The structure of four human corneal layers. 1. Epithelium 2. Bowman´s layer 3. Stroma 4. Endothelium. Magnification of 50x, (KÜHNEL, 1999)

The corneal stroma is an extracellular matrix consisting of collagen and amorphous ground substance (proteoglycans, glycoproteins, and proteins). Collagen is the major structural component of the stroma, accounting for 12-15% of its wet weight or approximately 70% of its dry weight. The collagen fibrils measure 23 – 35 nm in diameter and they lie parallel to the corneal surface (Berman, 1991). The extraordinary parallel structure of the corneal fibrils is mainly responsible for the stromal transparency (Figure 1.3.4-2). This parallel structure is based on proteoglycans which keep the distance constant between fibrils (Hockwin, 1985).

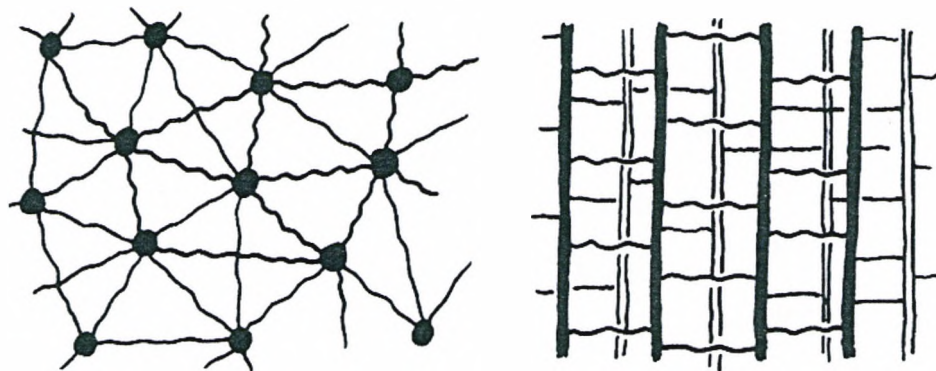


Figure 1.3.4-2 Schematic representation of the structure of the corneal stroma. Here the long lines describe the fibrils and the wavy lines demonstrate proteoglycans between the fibrils. (Hockwin, 1985)

The fibrils themselves are primarily made of type 1 collagen, with lesser amounts of type 3, type 5 and type 6 collagen. The collagen fibrils are surrounded by a polyanionic extracellular matrix, which may be important in maintaining the fairly constant separation distance of 60 nm between the centres of the fibrils. They are packed in parallel arrays, which make up the 300 to 500 lamellae of the stroma. The lamellae extend from limbus to limbus and are oriented at various angles to one another (Kaufman et al, 1998).

The cornea is richly supplied by sensory nerve axons, and their associated Schwann cells are found in the anterior and middle third of the stroma from the first division of the trigeminal nerve, named the ophthalmic division.

As with other sensory nerves, the pattern of distribution is divided along the vertical midline of the head (Blaustein, 1996).

1.3.5 Descemet's membrane

Descemet's membrane is the basement membrane of the corneal endothelium. It is synthesized by the endothelium and assembled at the basal surface of the cell layer (Figure 1.3.5-1). It increases in thickness during life.

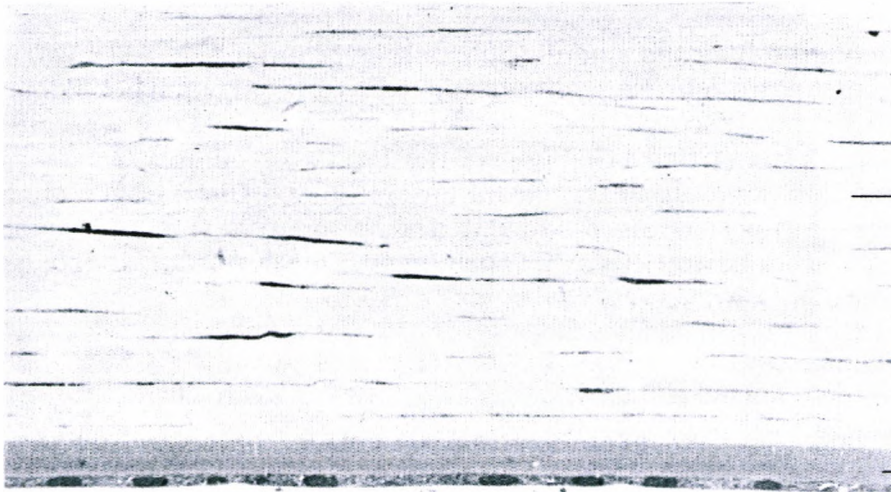


Figure 1.3.5-1 Light micrograph of the posterior central cornea illustrating posterior stroma, and Descemet's membrane. Magnification of 800 times. (KÜHNEL, 1999)

At birth, the human Descemet's membrane is approximately 3 μm thick, but by late adulthood the width can measure up to 12 μm . The anterior one half to one third is the fetal or oldest layer which displays a 100 - 110 nm long banded type 8 collagen pattern. The posterior layer is not banded and appears as amorphous matrix in the same manner as all other basement membranes. The regional thickness and structure varies (Smolin, and Thoft, 1994). Berman (1991) describes how both type 4 and type 8 collagen can be selectively extracted.

1.3.6 Endothelium

The single layer of approximately 400 000 cells, 4 to 6 μm thick, on the posterior corneal surface is named the endothelium. These cells are predominantly hexagonal in shape and approximately 20 μm wide. The outline at the level of Descemet's membrane is irregular because of the marked infolding and interdigitation between adjacent cells. However the posterior cell membrane is coated by a viscous substance, which is possibly of endothelial origin.

The cytoplasm of the cells have many mitochondria and elaborate smooth and rough endoplasmic reticulum, as well as a Golgi complex, all of which are characteristic of cells actively involved in metabolic energy production and molecular synthetic processes (Kaufman et al, 1998). The endothelium cells are not able to undergo mitosis in adult human beings. However, the endothelium cells are able to enlarge (Hockwin, 1985).

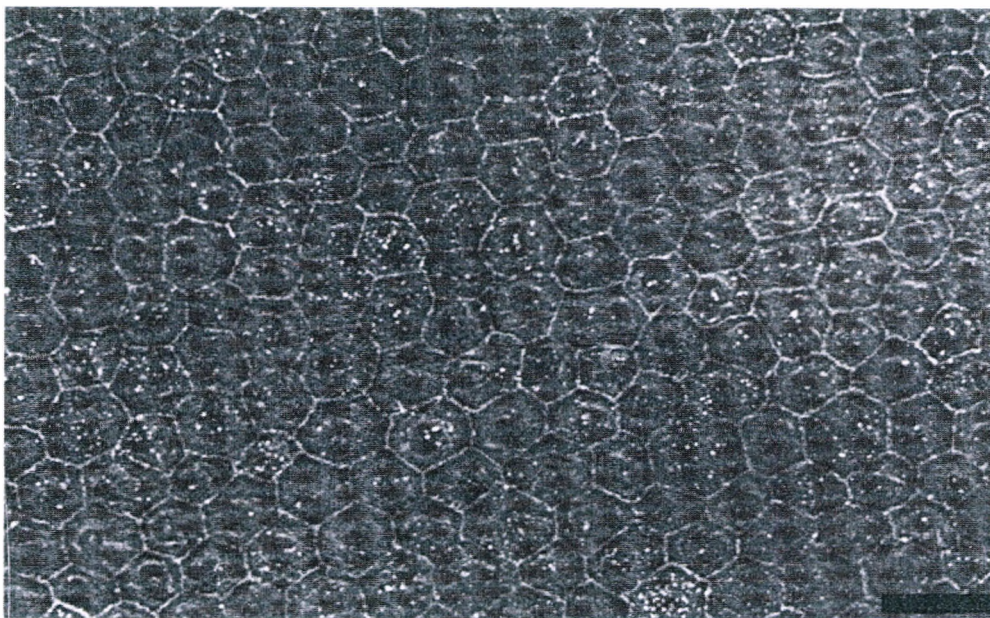


Figure 1.3.6-1 Scanning electron micrograph of the central endothelium showing a regular cellular mosaic. (Bar 30 μm). (Kaufman et al, 1998)

To determine the variation of cell size the coefficient of variation (CV) has been introduced. The normal endothelium has a CV of approximately 0.25. An increase in this value means that the cell size is variable, known as polymegathism. This may indicate a stressed or unstable endothelium in which cell volume is not adequately regulated or in which the cytoskeleton is abnormal (Kaufman, and Alm, 2003).

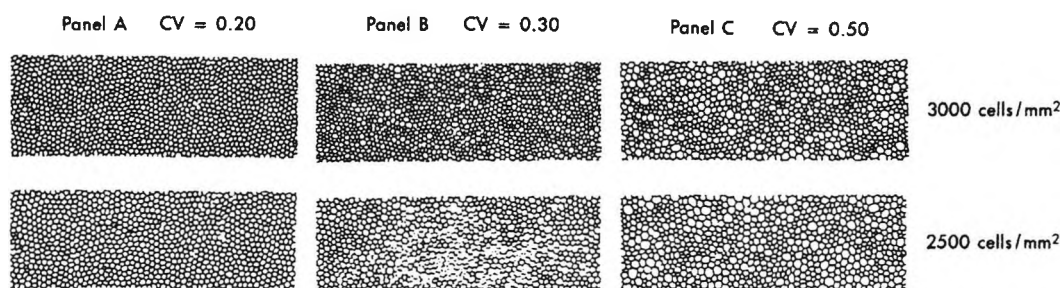


Figure 1.3.6-2 Variability in cell density and coefficient of variation (CV) of cell size. (Kaufman, and Alm, 2003)

1.4 Physiology of the cornea

The cornea is an avascular transparent tissue which is supplied with nourishment by aqueous humour, tear film, and blood vessels at the limbus. The basis of corneal physiology is mainly related to the corneal epithelial and endothelial barrier and metabolic pump functions. If there is any disturbance the cornea increases in thickness, becomes oedematous and shows a decrease in corneal transparency (Sachsenwenger, 1994).

1.4.1 Corneal metabolism

The corneal cells are actively involved in maintaining the function of molecular synthesis and volume regulation. Much of the energy for these processes is derived from metabolites of glucose by both aerobic and anaerobic pathways.

The bulk of the glucose used ($105 \mu\text{g}/\text{cm}^2/\text{hr}$) is derived from the aqueous humour. However, negligible amounts enter the cornea from the tears and the limbus.

The CO_2 which is a metabolic by-product of aerobic/anaerobic pathways is eliminated easily by the cornea. The reason for this is based on the high permeability to CO_2 of the corneal membranes and an active carbonic anhydrase system of the endothelium. By contrast, the elimination of lactate is not as easily accomplished. The barrier properties of the superficial corneal epithelial cells preclude the transfer of significant amounts of corneal lactate to the tears (Figure 1.4.1-1). Instead, lactate must be removed by diffusion across the stroma and endothelium into the aqueous humour (Kaufman et al, 1998).

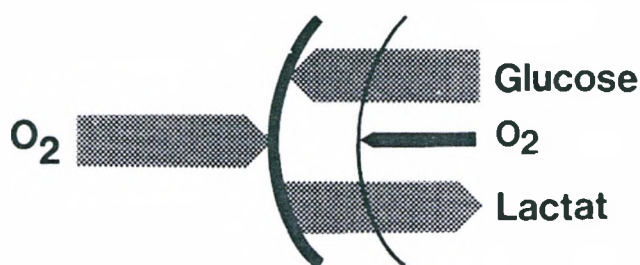


Figure 1.4.1-1 Metabolism of the cornea. (Hockwin, 1985)

Hockwin (1985) explains that 85% of glucose, delivered to the cornea, is transformed to lactate by the cells of the cornea and only 15% is metabolised to CO_2 . Less oxygen supply leads to a reduced ATP/ADP quotient immediately (ATP = Adenosine 5' triphosphate, ADP = Adenosine 5' diphosphate).

1.4.2 Epithelial metabolic pump functions

The epithelium has been described as a “tight” ion-transporting cell layer that functions both as a protective barrier and as an accessory fluid secreting layer that augments the endothelial regulation of stromal hydration. 15% of water that leaves the stroma may be transported by the Cl^- dependent pump. The movement of Cl^- from the stroma to the tear film appears to be modulated by several types of receptors.

First are the β -adrenergic and serotonergic receptors, which are coupled to the activation of adenyate cyclase and the stimulation of cAMP synthesis, and second are the phorbol ester receptors, which activate protein kinase C. Dopamine and possibly muscarinic cholinergic agents may also play a role in Cl^- transport (Berman, 1991).

Na^+ ions are transported from the tears to the stroma. They might neutralize the anionic groups of the glycosaminoglycans and reduce or prevent their ability to swell. However, other ion transport systems show net flow of Na^+ across the epithelium from stroma to tears. Nevertheless, the epithelium contains an active Na^+ transport system from tears to stroma. This transport system is inhibited by Ouabain, specific inhibitor of Na^+ / K^+ ATPase (Figure 1.4.2-1). Amiloride-sensitive channels do elevate the inflow of Na^+ .

Net Na^+ absorptive transport and net Cl^- secretory transport can occur simultaneously only under special experimental conditions. In the living eye, the epithelium generates an electrical potential of about - 30 mV on the tear film side (Kaufman et al, 1998).

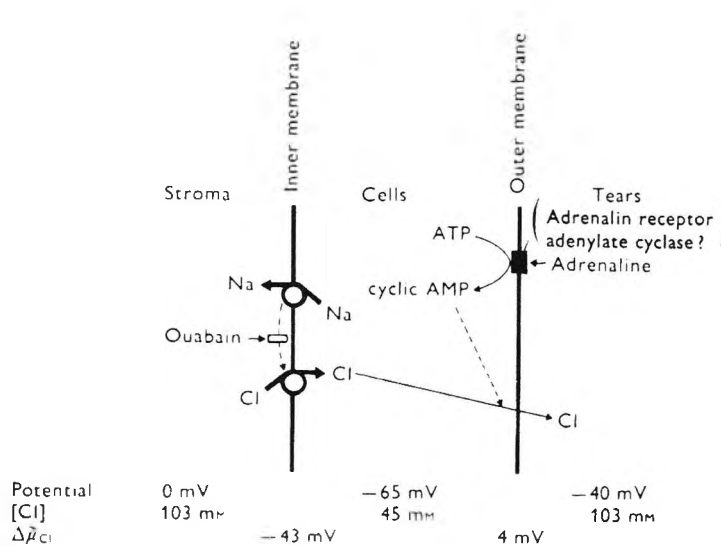


Figure 1.4.2-1 Model for the action of adrenaline in the stimulation of epithelial Cl^- transport. $\Delta\mu_{\text{Cl}^-}$ is called the electrochemical potential gradient and electrical concentration (Cl) is listed across the outer and inner membranes. (Kaufman et al, 1998)

1.4.3 Endothelial metabolic pump functions

The stroma tends to imbibe water as a result of the charge characteristics of the proteoglycans of the stromal ground substance. Two factors prevent stromal swelling and maintain 78% of normal water content. These are the barrier and pump function of the endothelium. The barrier is incomplete compared with the epithelial barrier.

When the endothelium is disrupted, an in-vitro cornea swells at 127 $\mu\text{m/hr}$.

When the metabolic pump is inhibited, the cornea swells at approximately 33 $\mu\text{m/hr}$. The normal leakage of the intact cell layer as a result of an incomplete barrier leads to inflow of fluid which is the source of nutrients including glucose and amino acids for the cornea. 6 to 8 ml/hr of water is moved by the endothelium from the stroma to aqueous humour (Kaufman, and Alm, 2003).

The energy-requiring pumps in the endothelium remove the fluid that enters the stroma. There is a transport of both Na^+ and HCO_3^- across the endothelium from the stroma to the aqueous humour.

The energy- dependent transport of Na^+ and HCO_3^- is mediated by Na^+ / K^+ ATPase and HCO_3^- dependent ATPase respectively. Carbonic anhydrase may also be involved indirectly in the transport of HCO_3^- . Ouabain plays an important role as a specific inhibitor of Na^+ / K^+ ATPase (Berman, 1991).

1.4.4 Stroma

The activities of the major diffusible ions (Na^+ , K^+ , and Cl^-) are similar in the stroma and the aqueous humour. However, the concentrations are higher in the stroma. The negative charge of glycosaminoglycans is primarily responsible for the abundance of Na^+ and K^+ in the stroma. If the stroma swells, the diameter of the collagen fibrils remains constant, and if the stroma dehydrates the driving force for fluid inflow (swelling pressure gradient) increases exponentially.

At normal hydration, the stromal swelling pressure is approximately 80 g/cm^2 or 55 mm Hg. The relationship between IP (stromal inhibition pressure), IOP (intra ocular pressure) and SP (stromal swelling pressure) is shown by the following formula: $IP = IOP - SP$ (Kaufman et al, 1998).

1.4.5 Tear Film

The tear film maintains a moist environment for the epithelial cells of the cornea. It forms a smooth refractive surface over the cornea, transports metabolic products to and from the epithelial cells and cornea, and protects the cornea and conjunctiva against noxa. This $7 \mu\text{m}$ thick film is composed of three layers; lipid layer, aqueous layer (thickest layer), and mucous layer (Figure 1.4.5-1). Every layer is produced by a different type of gland.

The lipid layer is built by meibomian glands and glands of Zeis, the aqueous layer is produced by the main lacrimal gland and accessory glands of Krause and Wolfring, and the mucous layer is a product of goblet cells and glands of Henle and Manz (Burk, and Burk, 1996).

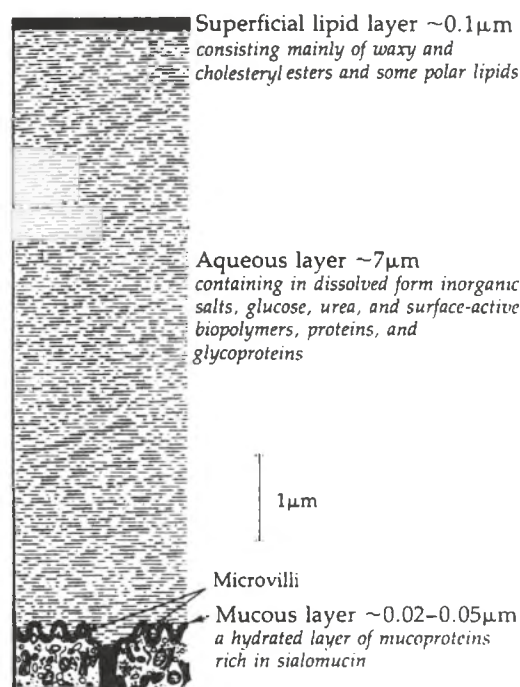


Figure 1.4.5-1 The three layers of the corneal tear film. (Smolin, and Thoft, 1994)

Cholesteryl esters and some polar lipids give the lipid layer an oily character. When the lid opens the lipid layer begins to spread and inhibit the evaporation of the tears. The aqueous layer mainly consists of HO_2 , inorganic salts, glucose, urea, surface-active biopolymers, proteins, and glycoproteins. All known immunoglobulins and the entire complement pathway are found in normal human tears.

Protecting the cornea as well as possible, the tear film should cover the complete cornea. However, the epithelium surface is hydrophobic. Here, the mucous layer, which contains mucus (an extremely hydrophilic substance), helps to solve that problem and maintains the stability of the tears on the surface of the cornea. Enough mucus has to be present so that lipid coming into contact with mucus has no influence on the stability of the tear film.

Evaporation of aqueous fluid leads to an elevated contamination of mucus with lipid. Hence, it follows that the mucus becomes hydrophobic and a dry spot forms. Blink rate and the consistency of tears interact to avoid dry spots (Smolin, and Thoft, 1994).

Mieyal, Dunn, and Schwartzman (2001) tested the quantity of HETE and HETrE (HETE = hydroxyeicosatetraenoic acid, HETrE = hydroxyeicosatrienoic acid) in the tear film in cases of corneal inflammations such as herpes simplex keratitis, superficial punctate keratitis, iridocyclitis, corneal foreign body and corneal hypoxia. The presence of 12-HETrE in the tear film is consistent with its hypothesized role as a paracrine mediator of inflammation. In addition, the ocular surface inflammation stemming from diverse causes was associated with an increased 12-HETrE level. Concentrations were especially high in contact lens-related inflammations in which seven patients had to sleep with their lenses. They had acute red eyes as in the case of hypoxia. This is believed to be a major factor in contact lens-induced inflammation and has been shown to promote an elevated synthesis of 12-HETE and 12-HETrE.

1.5 Summary

The cornea is an avascular transparent tissue. The horizontal length ranges from 11.0 – 12.5 mm and the vertical height ranges from 10.0 – 11.5 mm.

The corneal profile could be described by a summary of three geometrically shaped zones. The centre is described as a spherical zone, the second one as an ellipsoid, and the third zone is comparable with a parabolic shape. Nowadays, complex mathematical algorithms are used to describe the corneal surface as exactly as possible.

Anatomically, the cornea consists of five layers; epithelium, Bowman's layer, stroma, Descemet's membrane, and endothelium. The epithelium is derived from ectoderm cells and the others are derived from mesenchymal cells. All five layers are detectable by the beginning of the 5th month of gestation.

However, the epithelium increases to adult levels by 36 weeks of gestation.

The adult level shows three different types of cell; basal columnar cells, wing cells and surface cells. These cells form a 50 µm thick tissue which consists of five to seven layers. The basal cells have a higher level of metabolic and synthetic activity than the more superficial cells. Generally speaking, the whole epithelium regenerates in an excellent fashion, and it serves as a protective barrier against penetration. Additionally, only epithelium and endothelium consist of a cell agglomeration. The other three layers' structure is mainly composed of collagen fibrils among other components. Every structure of the following three layers consists of different types of collagen fibrils.

<u>Layer</u>	<u>Fibril collagen type</u>
Bowman's layer	1, 5 anchoring Fib. 7
Stroma	1, 3, 5, 6
Descemet's membrane	4, 8

Bowman's layer may be considered as a modified superficial layer of the stroma. It is approximately 8 - 14 µm thick. Anchoring collagen fibrils type 7 pierce 1 – 2 µm into Bowman's layer and form fine anchoring filaments.

These anchoring filaments adhere to the epithelium at the stroma. The stroma makes up 90% of the cornea. Centrally it is approximately 500 μm thick and it is transparent. This is the result of the very parallel structure of the collagen fibrils. Here, Proteoglycans are responsible for the parallel structure.

Descemet's membrane is the basement membrane of the corneal endothelium. It is synthesized by the endothelium and its thickness depends on the age of the cornea (approximately from 3 to 12 μm thickness).

The endothelium is a single cell layer which contains approximately 400 000 cells and is 4 – 6 μm thick.

These cells are predominantly hexagonal in shape, they contain characteristic metabolic utilities for energy production and synthetic processes, and they are able to enlarge. A variable cell size is described by the coefficient of variation (CV).

If the value of CV is greater than 0.25, then the cell size is variable which is known as polymegathism.

The nourishment of the cornea is mainly supplied by the aqueous humour and tear film. Limbal blood vessels do not play an important role in delivering nourishment to the cornea. Different pumps in the epithelium and endothelium keep the osmotic pressure in balance and supply the metabolic process with essential products. These pump systems transport ions into and out of the corneal tissue.

In the epithelium two important transport systems are the net Na^+ absorptive transport system and the net Cl^- secretory transport system.

Two factors of the endothelium prevent corneal swelling, first the leakage barrier and second the pump function. A disruption of the endothelium leads to corneal swelling at a rate of 127 $\mu\text{m/hr}$. The power supply of the pump function is guaranteed by mitochondria positioned in the endothelium cells. There is transport of both Na^+ and HCO_3^- across the endothelium from the stroma to the aqueous humour.

The reason for the high energy consumption to pump fluid out of the stroma is that glycosaminoglycans have a negative charge. The following formula demonstrates the relationship between intra ocular pressure (IOP) and stromal swelling pressure (SP):

$$\text{Stromal inhibition pressure (IP)} = \text{IOP} - \text{SP}.$$

The tear film is a 7 μm thick fluid film on the surface of the corneal epithelium. It consists of three layers; lipid layer, aqueous layer, and mucous layer. The oily lipid layer inhibits evaporation of tears. The thickest layer, the aqueous layer, mainly consists of water. However, the surface of the corneal epithelium is hydrophobic.

Mucus, a very hydrophilic substance of the mucous layer, is the solution used to stabilize the hydrophilic film on the surface of the cornea. When tears evaporate lipid contacts mucus and then the mucus becomes hydrophobic. The consistency of tears and the blink rate play an important role in avoiding dry spots on the corneal surface.

Chapter 2. Factors affecting corneal physiology

2.1 Introduction

During an ascent to high altitudes, changing surrounding conditions such as humidity, temperature, oxygen levels in the air, UV radiation, and cosmic radiation have a direct, and an indirect, influence on corneal physiology.

The indirect influence is derived from the way in which the human body adapts to the changing conditions, described above, during acclimatisation. The physical effort exerted by the human gaining altitude also affects the cornea.

In this chapter the factors which have an influence on changes in corneal shape will be described. Also, contact lens wear is discussed in the context of its effect on corneal physiology. This is particularly relevant to this thesis because three of the subjects who ascended to high altitude were contact lens wearers. Finally, the hypothesis to be addressed in this study is stated.

2.2 Factors influencing corneal physiology caused by altitude

2.2.1 The determination of the influential factors

Karaküçük and Ertuğrul Mirza (2000) noted that altitude has potential undesirable effects on the human body and eye. Butler (1999) explained that, before the effects of altitude on the eye are examined, it is useful first to review the changes in the physical environment during such an exposure. He described that a mountaineer who ascends up to high regions is confronted with less oxygen in the air, drier air, a higher amount of both UV and cosmic radiation, and a lower temperature compared with sea level. Interestingly, these factors are often described in contact lens related studies as being reasons for contact lens wear becoming uncomfortable.

For example, Andresko, and Schoessler (1980) tested the dehydration of soft contact lenses in their study. Before discussing their results, they noted that many patient-related factors probably control the amount and speed of evaporation, including the rate and completeness of blink, tear volume and osmolarity, and palpebral aperture size. Environmental factors such as air temperature, relative humidity and wind velocity have an influence on lens dehydration. Outdoors, under natural conditions, these factors interact in a very complex manner to form the system which we know as weather.

Before the different factors which affect corneal physiology are discussed, some important observations are warranted from a physics perspective. Our atmosphere consists of molecules which press on the surface of the earth. This pressure is named atmospheric pressure and is the sum of the pressure of all the gases that make up the air. The pressure of one gas is referred to as partial pressure. Oxygen accounts for about 21% of air (Butler, 1999). With air density as a measure of the quantity of gas molecules in the air, one can say that when the air pressure is lower than normal, there are fewer gas molecules such as oxygen molecules in the air (Bohl, and Elmendorf, 2005).

The higher the altitude, the lower the weight of the air mass that presses on the deeper-lying air masses. Generally, this is the reason for a lower density level of air molecules in high regions compared to deeper lying areas. Further, more pressed air in deeper regions leads to a faster change of air pressure during a change of altitude. In addition, the air pressure depends on the ambient temperature and hence on the weather. When a surface is warmed up by the energy of the sun, the air around the surface also warms up until its temperature is high enough to form an air bubble which rises up to a higher area. During the ascent, the temperature in the air bubble decreases as a result of an expansion of its volume.

If an air bubble is colder than its surroundings, it descends, its volume diminishes as a result of elevating pressure, and therefore the temperature increases in the bubble until it reaches a point when the surrounding air has the same temperature.

The following can be derived: the air pressure of cold air is greater than that of warm air. However, during an ascent up to higher altitudes the atmospheric pressure of cold air decreases faster than that of warm air.

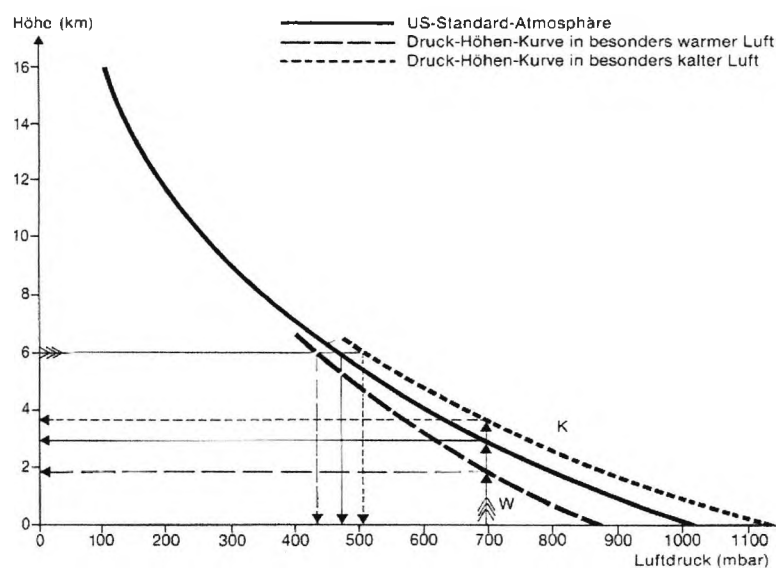


Figure 2.2.1-1 The effects of air temperature on atmospheric pressure at varying altitudes. The three curves are from left to the right; W = the air is very warm, US standard atmosphere, and K = the air is very cold. (Häckel, 1999)

Figure 2.2.1-1 shows the interaction of temperature and atmospheric pressure with the help of three curves. One curve shows air pressure changes measured on a cold day, the second describes the atmospheric pressure on a very warm day, and the third curve represents the US standard atmosphere.

For example, an air pressure of 700mbar measured at an altitude of about 1900m on a very warm summer's day could be measured at an altitude of 3800m on a very cold day. Similarly, if we consider an air pressure measured at 500mbar, this would be recorded at an altitude of approximately 5000m on a warm day and approximately 6200m on a cold day.

This example shows that an identical air pressure can be measured at higher lying regions on a very cold day compared with a warm day. If we look at the altitude differences of cold or warm days respectively, the air pressure changes more rapidly on a cold day (Häckel, 1999).

The low density of the atmosphere at high altitudes corresponds to the low oxygen level there (Table 2.2.1-1). This hypoxic effect is the reason why the respiration rate of mountaineers becomes shorter at high altitudes (Madigan, and Martinko, and Parker, 2000).

h/m//ft	p/kPa	p/Torr
0	101.30	760
500//1640	95.50	716
1000//3280	89.90	674
1600//5250	83.50	627
2000//6560	79.50	596
2600//8530	73.80	553
3000//9840	70.10	526
3600//11,810	64.90	487
4000//13,120	61.60	462
4600//15,090	57.00	427
5000//16,400	54.00	405
5600//18,370	49.80	374

Table 2.2.1-1 The effects of altitude on air pressure. Air pressure in mbar = kPa x 10, where kPa = kilogram Pascal unit of air pressure. Torr = 133.3224 Pa. (Kuchling, 1986)

With the following formula we are able to calculate the air pressure at every altitude.

This formula applies up to 36,090 ft of altitude and 15° C at sea level. A change in air pressure takes place in relation to temperature at every altitude up to 36,090 ft:

$$p_h = 101.3 \text{ kPa} (1 - 6.5h/288 \text{ km})^{5.255}$$

p_h = air pressure (altitude dependent), h = height in km. (1 km = 3280.84 ft)

kPa = kilogram Pascal unit of p_h (10kPa = 1hPa = 1mbar) (Kuchling, 1986).

The temperature and the air pressure are tightly related to humidity. In winter, dry air causes frequent complaints from patients about discomfort with their contact lenses. The quantity of water vapour in the air can vary considerably, and depends on the temperature, the time of day, and the terrain, including features such as vegetation, lakes, rivers, glaciers etc. Water vapour does not have the same characteristics of gas, in the sense that when the volume of water vapour is reduced, the water vapour pressure increases until the maximum water vapour pressure is achieved.

A further reduction in the volume has no further influence on the pressure. This is only possible because part of the water vapour condenses into water. However, when the volume of the water vapour expands, the water vapour pressure reduces and the air is unsaturated with water.

Other gases in the air surrounding water which evaporates have no influence on the development of water vapour (Hupfer, and Kuttler, 2005).

The maximum water vapour pressure in the air is referred to as water vapour pressure of saturation. The water vapour pressure of saturation is dependent on the temperature and is reached when the condensation and water vapour are in balance. No more fluid evaporates. The lower the temperature, the lower the water vapour pressure of saturation (Etling, 1996).

The following example demonstrates the interaction of water vapour condensation, temperature, and wind:

If the air is saturated with water vapour, for example near a lake, then the wind carries some water vapour away. As a result the air around the lake becomes unsaturated. Hence it follows that the water and the water vapour are no longer in balance, which means that the water begins to evaporate once again.

When the temperature goes down, the water vapour pressure of saturation declines as well.

When the water vapour pressure of saturation falls under the momentary water vapour pressure, the water vapour condenses into water, the water vapour pressure falls and the ground becomes wet. The quantity of condensation into water depends on the difference between the water vapour pressure and the water vapour pressure of saturation.

In high regions compared to low regions, for example, dry air is the result of more wind, less vegetation, low temperature and glaciers. Because of all this there is less water to evaporate at altitude.

The humidity of the air (in %) is defined as follows:

The water vapour pressure of saturation is the basis for f_{\max} (Table 2.2-1).

f_{\max} = the possible maximum water vapour mass in the air / the volume of the humid air (kg/m^3)

The maximum humidity of the air (f_{\max} (kg/m^3)) is measured when the air is saturated.

f_{absolute} = the water vapour mass in the air / the volume of the humid air (kg/m^3)

The absolute humidity of the air (f_{absolute} (kg/m^3)) is measured in given conditions at the moment when the air is saturated or unsaturated.

The water vapour pressure is lower than or equal to the water vapour pressure of saturation.

$$f_{\text{relative}} = f_{\text{absolute}} / f_{\max} \times 100 (\%)$$

The relative humidity of the air (f_{relative} (%)) is the proportion of the real water vapour mass in the air to the possible maximum water vapour mass multiplied by 100.

The maximum humidity, the absolute humidity and the relative humidity all depend on the temperature.

The relative humidity is measured in percentage terms with a hygrometer. 100% humidity means that the air is saturated but it does not mean the quantity of water vapour (kg/m^3) in the air is the same as the quantity of gas (kg/m^3) in the air. The maximum water vapour mass is less than the quantity of the air mass (Kuchling, 1986).

$t/^{\circ}\text{C}$	p/kPa	p/Torr	$f_{\text{max}}/\text{g/m}^3$	$t/^{\circ}\text{C}$	p/kPa	p/Torr	$f_{\text{max}}/\text{g/m}^3$
-5	0.401	3.01	3.25	12	1.401	10.51	10.67
-4	0.437	3.28	3.53	13	1.497	11.23	11.36
-3	0.463	3.47	3.83	14	1.597	11.98	12.08
-2	0.517	3.88	4.14	15	1.704	12.78	12.84
-1	0.563	4.22	4.49	16	1.817	13.63	13.65
0	0.611	4.58	4.85	17	1.937	14.53	14.50
1	0.656	4.92	5.20	18	2.062	15.47	15.39
2	0.705	5.59	5.57	19	2.196	16.47	16.32
3	0.757	5.68	5.95	20	2.337	17.53	17.32
4	0.813	6.10	6.37	21	2.486	18.65	18.35
5	0.872	6.54	6.80	22	2.642	19.82	19.44
6	0.935	7.01	7.27	23	2.809	21.07	20.60
7	1.005	7.54	7.79	24	2.984	22.38	21.81
8	1.072	8.04	8.28	25	3.168	23.76	23.07
9	1.148	8.61	8.83	26	3.361	25.21	24.40
10	1.227	9.20	9.41	27	3.565	26.74	25.79
11	1.312	9.84	10.02	28	3.780	28.35	27.26

Table 2.2.1-2 Data illustrating that the water vapour pressure of saturation (p/kPa and P/Torr) and the maximum water vapour mass ($f_{\text{max}}/\text{g/m}^3$) are temperature dependent. (Kuchling, 1986)

A low density of air molecules at high altitude absorbs and reflects a small amount of cosmic and UV radiation. Thus the intensity of cosmic and UV radiation rises the higher the mountaineers ascend.

Cosmic radiation consists of 98% nuclei; with only 2% made up of electrons or positrons. The nuclear component consists of about 87% hydrogen, about 12% helium and about 1% heavier nuclei.

At certain locations on the earth the magnetic field provides an effective shield against cosmic ray particles of lower energy. Charged particles moving through the field maintain their energy but are deflected by the Lorentz force (Heinrich, Roesler, and Schraube, 1999). But there are considerable differences in the amount of cosmic radiation between polar regions and equatorial regions. This stems from geomagnetic shielding. The maximum radiation is at the magnetic equator, where particles move perpendicular to the field (Tommasino, 1999).

The surface of the sun occasionally releases large amounts of energy in local outbursts of γ -rays, hard and soft x-rays and radio waves. These large bursts of energy are referred to as solar flares and the energy released can increase by a

factor of more than 100 times in a brief amount of time.

Solar flares are very rare events and are unpredictable in terms of their energy spectrum. The particle flux of cosmic radiation, however, is very calculable. It fluctuates over an eleven-year cycle.

There are different models for describing the quantity of energy emitted in the form of cosmic radiation, which is referred to as particle flux. One of the best models is the Badhwar model (Figure 2.2.1-1).

This model describes the eleven year sun particle flux by a sine function. It is based on the different intensity of solar wind.

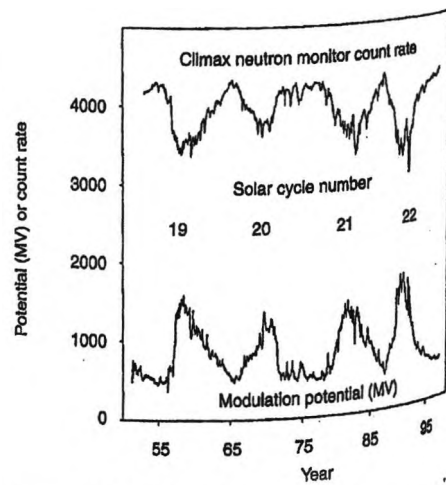


Figure 2.2.1-2 The particle flux of the sun can be described by a sine function, with an 11 year cycle. The variations in intensity of the solar wind over time can be measured by the modulation potential (U) and the neutron monitor. (Heinrich, Roesler, and Schraube, 1999)

This different intensity is described by a negative electrical modulation potential U . Figure 2.2.1-1 shows that the minimum modulation potential is about 200 mV and the highest point about 1800 mV.

In other words, the chance that nuclei will hit human cells during the maximum period is nine times higher than during the minimum period. This difference can be compared to the difference in the amount of cosmic radiation at high regions and sea level. (Heinrich, Roesler, and Schraube, 1999).

Butler (1999) states that there are three types of UV radiation; UV A - (320 - 400 nm), UV B - (290 - 320 nm) and UV C (100 – 290 nm). Almost all UV C radiation is absorbed by the earth's ozone layer.

The most important cell constituent that radiation affects is DNA, which carries about 100,000 genes, each of which controls a discrete hereditary characteristic. These genes provide instructions for cell division and for the synthesis of proteins that provide many of the structural components of the cell, in addition to the numerous enzymes promoting and controlling cellular activity.

Damage to genes may cause cell death or inhibit cell division; more insidiously, it may modify a genetic sequence in viable cells (Smith, 1999).

2.2.2 Effects of UV on corneal physiology

UV radiation does not ionize but the energy in UV radiation does change the structure of proteins and the DNA, leading to cell damage, depending on the dose and the duration of radiation. UV radiation with a wavelength of 260 nm is most responsible for cell death because of the effect on DNA. The Purine base and the Pyrimidine base absorb maximally at 260nm.

Aromatic amino acids like tryptophan, phenylalanine and tyrosine also absorb UV radiation having a maximum wavelength of absorption of 280 nm in proteins (Madigan, Martinko, and Parker, 2000).

When considered in more detail, there are two types of series of cellular events which, when triggered, can change the phosphorylation levels of p53 protein resulting in cell cycle arrest and apoptosis. These two cellular events are eliciting stress-induced signalling pathways and DNA damage.

A significant phosphorylation of p53ser15 serum was found in rabbit epithelium cells as a result of UV radiation exposure. This plays an important role regarding signalling events leading to apoptosis. UV radiation induced corneal epithelial injury can affect corneal barrier function and in turn increase susceptibility to infection, and the development of corneal opacity (Wang, Dai, and Lu, 2005). For example, subjects with cortical cataracts have on average a 21% higher exposure to ultraviolet B radiation than subjects with no cataract (Taylor et al, 1988).

Acute exposure to high levels of UV radiation may result in UV photokeratitis, whereas chronic exposures may be associated with cortical lens opacities, posterior subcapsular lens opacities, pterygia, and squamous cell carcinoma of the conjunctiva (Butler, 1999).

Kolozvári et al (2002) tested the UV absorbance of the corneal layers from 240 nm to 400 nm. The measurements were carried out on twenty dissected human corneas within six hours after death.

The cornea absorbed the tested range of UV radiation effectively. In particular, the epithelium and Bowman's layer are especially important in preventing damage from UV-B radiation. These layers have significantly higher absorption coefficients than that of the stroma for UV spectra shorter than 310 nm. However, the stroma has the most significant absorbance because of its thickness (Figure 2.2.2-1).

The significant absorbance of the cornea in the UV-B and -C spectra appears to be due to high amounts of tryptophan residues in the proteins of the stroma and the high ascorbic acid content of the epithelium.

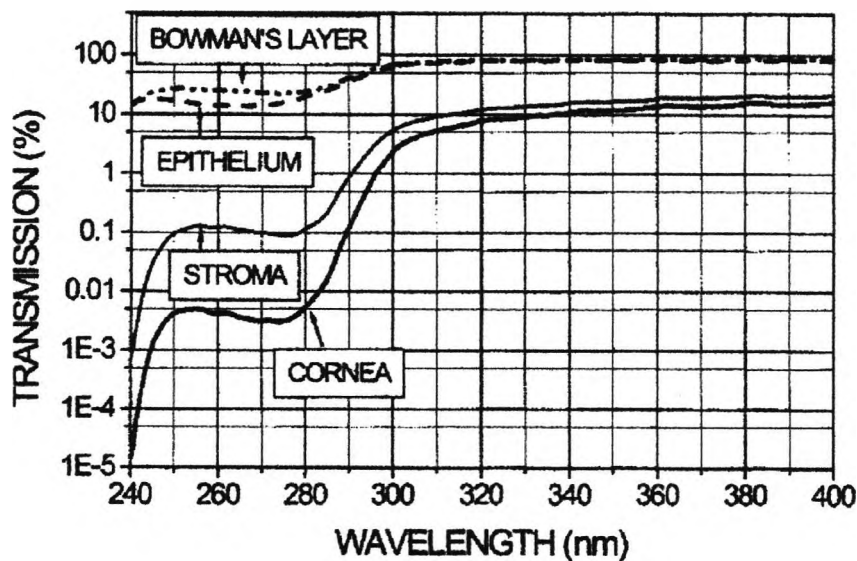


Figure 2.2.2-1 Transmission curves illustrating the important role of the cornea in absorbing UV radiation. (Koložvári, Nógrádi, Hopp, and Bor, 2002)

Changes in corneal structure which is exposed to UV radiation are described by Pitts, Bergmanson, and Chu (1987). They anaesthetised the eyes of eight Macaques *mulatta*. A 5000 W, high pressure Xe-Hg lamp provided a continuous spectrum from 200 to 5000 nm. The primate cornea was exposed to 300 nm UV radiation with five levels of radiant exposure (0.08, 0.15, 0.23, 0.45, and 0.60 Jcm⁻²). Some epithelial cells are more resistant to UV radiation damage than others, but there was no injury recorded in any of the corneal basement membranes regardless of the radiation exposure level.

Increased levels of exposure caused an increasing number of keratocytes to react, first with intracellular vacuoles and, later, with fragmentation of processes and nuclear disintegration. Stromal oedema was present at 0.08 Jcm⁻² and there was severe stromal and endothelial damage in the form of oedema and cytolysis at a 0.6 Jcm⁻² UV radiation level. At eight days post-exposure, the corneal epithelium had returned to a normal 5 to 6 cell thick layer.

Damaged endothelial cells showed a reduced number of mitochondria, endoplasmic reticulum, vacuoles and abnormal lateral sides, of which the latter may indicate polymegathism. In spite of this, stromal oedema vanished.

After testing the eyes of nine rabbits, Podskochy (2004) noted that the epithelium strongly absorbs UV radiation with a wavelength of 280 nm at a dose producing biomicroscopically significant keratitis (0.12 Jcm^{-2}).

Some eyes were scraped manually with a corneal knife (first group), some eyes were de-epithelialized by scraping (second group), and some were only treated by UVR (third group).

The third group showed a loss of epithelial cells, the first group showed a loss of epithelial cells and keratocytes in the anterior quarter to half of the corneal stroma, and the de-epithelialization group developed very deep stromal damage with complete loss of keratocytes throughout the entire thickness of the stroma in the UV radiation exposed area.

2.2.3 Cosmic radiation and corneal physiology

The main difference between cosmic radiation and UV radiation is that UV radiation does not ionise but cosmic radiation has more energy than UV radiation and as a result it ionizes. The ionization has an indirect influence on cell mutation. Free radicals are the most effective agents created by ionization. The most important free radicals are hydroxyl radicals OH. Free radicals react with macromolecules, thus rendering the macromolecules inactive. This effect also leads to cell damage. Depending on the dose of cosmic radiation, the cell damage can become pathological (Madigan, Martinko, and Parker, 2000).

The human body has lived with cosmic radiation for thousands of years and, in addition, is able to repair cell damage to a limited extent.

Nelson and Tobias (1983) tested the influence of heavy ions on corneal tissue. The measurements were taken on 52 eyes which were removed from albino rats. The heavy ion beams utilized to irradiate the corneas were carbon at 474 MeV/amu, neon at 6 MeV/amu, argon at 3 MeV/amu, and iron at 600 MeV/amu. Exposure time generally ranged from 1 minute to 2 minutes. This work demonstrates that heavy ion beam irradiation of biological tissue causes microstructural damage to plasma membranes.

2.2.4 The influence of temperature on corneal metabolism

Temperature plays a central role in all meteorological phenomena.

The influence of temperature on the quantity of water vapour and oxygen in the air makes it necessary to discuss how temperature affects the eye, especially the cornea. Generally, the higher one ascends, the lower the temperature.

Karaküçük, and Ertuğrul Mirza (2000) noted that there is no uniform conclusion in the literature as to the changes in intraocular pressure at high altitudes. But intraocular pressure changes may partly be affected by cold air at high altitude. Cold air causes a decrease in intraocular pressure by causing a decrease in episcleral venous pressure.

Stapleton et al, (2004) demonstrated significant differences in corneal sensitivity between 20 °C and 34 °C stimulus temperature. Sensitivity for low temperature stimuli is higher than for high temperature stimuli.

Acosta, Belmonte, and Gallar (2001) asked sixteen human subjects (8 male and 8 female, aged 19-27 years) to describe the sensation when their eyes were exposed to different surrounding conditions simulated by a gas aesthesiometer. Corneal stimulation with cold air was described as cooling and in some cases as slightly unpleasant. On the other hand, hot air stimulation was described as irritating, like a combination of burning and stinging. They described these responses as “sensation combinations”. The cornea is an avascular tissue which is innervated almost exclusively by thin myelinated and unmyelinated trigeminal ganglion neurones that belong to the classes of high-threshold mechanosensory, polymodal and cold primary sensory neurones.

Cold air stimulated feeling is derived by innervation of the cold-sensitive and polymodal sensory neurons, and warm air stimulated feeling becomes painful when the population of polymodal nociceptive neurones is recruited.

Temperature is one of the fundamental parameters of tissue metabolism. For a thermal increment or decrement of 10 °C, metabolic rate changes by a factor of two to three.

To establish the environmental influences on ocular temperature, Freeman and Fatt (1973) placed a rabbit in a restraining box which permitted immobilization of the animal. An air blower was positioned at different distances in front of rabbits' eyes during which the temperature of the corneal surface was measured. For warm air at 23 °C, the corneal surface temperature is 34.0 ± 0.3 °C. When the ambient temperature drops, the cornea becomes colder in a linear fashion. The effect of air velocity on the transport of water away from the tear film is small because of the resistance to water transport imposed by the oily layer on the tears.

The rate of water loss to the air from the tear layer is linearly dependent upon the relative humidity. Finally, the cornea has a highly reduced relative metabolic activity when the ambient temperature is low.

Singh and Bhinder (2003) measured humidity and temperature in a closed chamber which was positioned in front of the eye. The study was conducted in 40 dry eyes and 20 normal eyes ranging in age from 11 to 61 years. Dry-eye patients had an average temperature of 26.18 ± 1.04 °C and normal eyes had an average temperature of 27.20 ± 1.36 °C. In normal eyes a temperature difference of 0.1 °C (dry eyes 0.0 °C) and humidity difference of < 1% (dry eyes > 1%) were measured between closed and open eye positions.

Dixon and Blackwood (1991) noted a corneal temperature of 33.7 °C in their study.

2.2.5 The influence of humidity on corneal physiology

Evaporation of water molecules from the intact precorneal tear film occurs by internal diffusion into the ambient air when relative humidity is lower than 100%.

External diffusion will dominate the water evaporation from the precorneal tear film. Here, high air velocity enhances the evaporation of water, resulting in a faster corneal temperature decrease.

A lower corneal temperature than usual leads to an increase in blinking frequency. Figure 2.2.5-1 demonstrates the interactions between temperature, relative humidity, air velocity, and contact lens wearing and the evaporation of the tear film (Wolkoff et al, 2005).

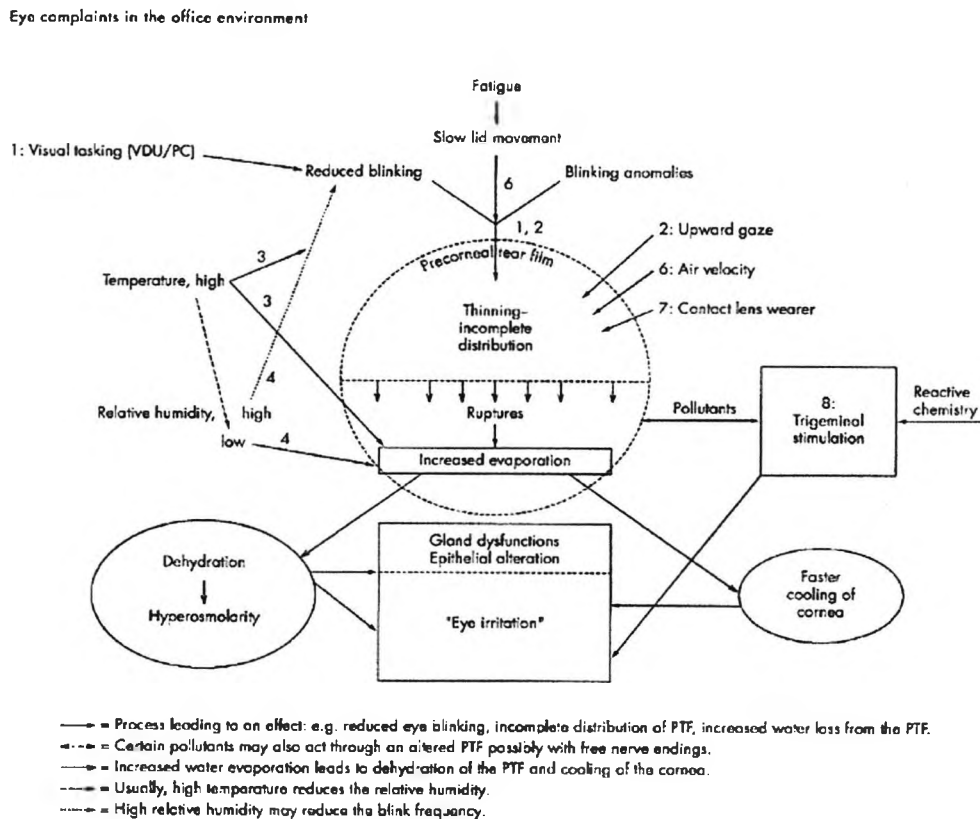


Figure 2.2.5-1 Diagram of processes resulting in alterations to the precorneal tear film. (Wolkoff, Nojgaard, Troiano, and Piccoli, 2005)

Mathers, Binarao, and Petroll (1993) developed an instrument to measure the water evaporation from the ocular surface. They fitted a pair of goggles tightly over the skin around the eyes of 18 normal eye- and 15 dry eye patients. Dry air was pumped into the evaporation chamber in front of the eye containing a humidity sensor that was then sealed. The temperature and relative humidity were recorded on the paper strip chart for a 2 min period with the eye closed. Dry air was pumped into the chamber again, and this procedure was repeated with the eye open for another 2 min.

Then the water evaporation of the skin surface was subtracted from the difference of open eye- and closed eye humidity.

The following values were calculated as a normal rate of evaporation at 30 % relative humidity; for normal eyes 0.14 ± 0.6 micro litre/min and for dry eyes 0.43 ± 0.19 micro litre/min.

The epithelial pump- and endothelial leakage-pump mechanism are responsible for maintaining a consistent corneal water hydration of 78%. The relative humidity of the air does have an influence on the evaporation of tears.

Therefore, it may have an influence on the epithelial pump mechanism.

In this way, humidity could affect the de-swelling function of the human cornea. This is the background to the study by Bourassa, Benjamin, and Boltz (1991). They tested de-swelling of sixteen corneas in a humidity chamber after corneal swelling was induced by a thick hydrogel contact lens. Three different sessions on three separate days were conducted under three different levels of humidity (25%, 60%, and 85% relative humidity), for every subject. Two sessions were completed with the help of goggles (0%, and 100% relative humidity). The time span from shortly after the thick hydrogel contact lens was removed until the point at which the cornea achieved normal thickness was a measure for the influence of humidity on corneal metabolism.

Interestingly, no humidity level exerts an over-riding influence on corneal recovery time from oedema.

This finding agrees with the conclusion of the following study.

Assessment of corneal hydration control is based on two different data sets.

First, the Open-eye steady-state (OEES), in which the corneal thickness is often measured over a period of time.

Second, the percentage corneal thickness recovery per hour (PRPH), in which a thick contact lens is put in front of the cornea for 2 hrs. After the lens is removed, the corneal thickness is measured until the cornea has recovered from the contact lens induced hypoxia.

Cohen, Polse, Brand, and Mandell (1990) described the influence of humidity on these two tests. This study showed that OESS corneal thickness is relatively stable when the cornea is exposed to large changes in humidity.

In conclusion, it seems unlikely that normal humidity changes in the clinical laboratory environment would have any substantial effect on the corneal de-swelling response.

A questionnaire on eye comfort has been developed by collaboration between the Air Safety Department and the Association of Flight Attendants USA. Of the 774 volunteers, 95% reported some eye discomfort in an aircraft.

85% of all contact lens wearers had dry eye symptoms after a 5 hour flight (Eng, 1979).

Eng, Harada, and Jagermann (1982) demonstrated the influence that climate in an aeroplane has on the contact lens surface during two plane flights. They projected mires on to the surface of the lenses.

Figure 2.2.5-1 shows the respective change in humidity, atmospheric pressure, and lens surface pattern during the first 35 min. of a flight.

Seven subjects, five women and two men, were provided with Bausch & Lomb Softlenses®.

The average age of the subjects was 33.4 years, with a range from 14 to 50 years.

Environmental Conditions					
		Preflight	Takeoff + 2hrs	Takeoff + 4 hrs	Postflight
Humidity	I	47%	11%	11%	50%
	R	65%	11%	11%	50%
Atmospheric Pressure	I	1015 mb	875 mb	875 mb	1015 mb
	R	1015 mb	875 mb	875 mb	1015 mb
Temperature	I	24°C	24°C	24°C	24°C
	R	24°C	24°C	24°C	24°C

I = Initial Flight

R = Return Flight

Table 2.2.5-1 The change in humidity, atmospheric pressure and temperature during two flights are shown here. Flight 1 = I, Flight 2 = R. (Eng, Harada, and Jagermann, 1982)

During both flights the cabin humidity declined from 47% (flight I) and 65% (flight R) to 11% while the atmospheric pressure was held constant during flight at 875 mbar.

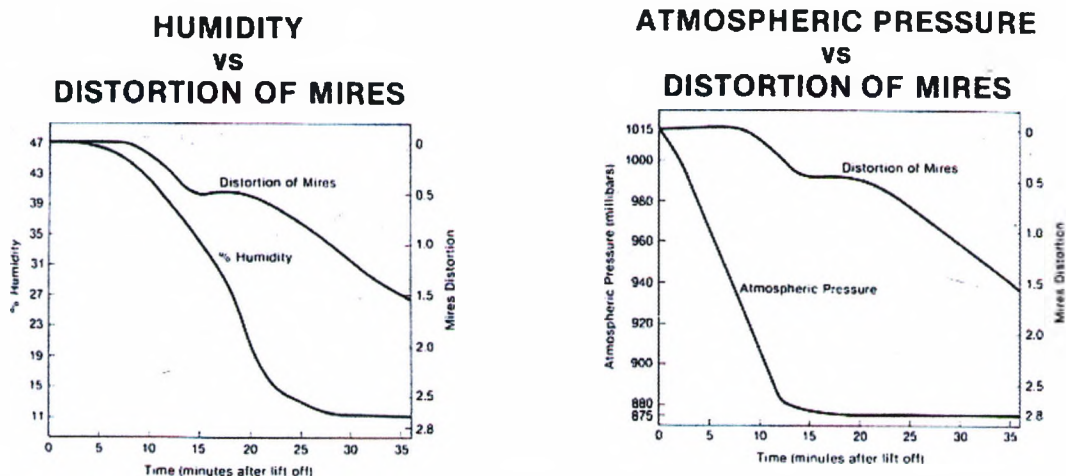


Figure 2.2.5-2 Rate of change in humidity and distortion of mires (projected patterns on lens surface) during the first 35 minutes of a flight, for 7 subjects wearing soft contact lenses. The keratometric patterns were graded on a scale from 0 to 3. No observable change was indicated by 0, and 3 indicated a severe change. Note that the distortion roughly follows the decline in per cent humidity, especially in the first 15 minutes. Atmospheric pressure was also measured. Note also that the distortion does not follow the decline in pressure as well as it followed the decline in per cent humidity (Abscissa, time (minutes after lift off) ordinate, humidity and in the second graphic atmospheric pressure (millibars)). (Eng, Harada, and Jagermann, 1982)

The most noticeable change in lens fitting occurred when the humidity was sharply reduced. After this, the amount of pattern distortion was variable with occasional improvements. Perhaps there was some compensation by the tear glands and/or some adjustment in the blink rate to counter the effects of the low humidity.

Mires were projected onto the surface of the soft lenses when the atmosphere was very dry, with a minimum humidity of about 11%. With a soft lens in front of the cornea, more tears evaporate in dry air conditions compared to when not wearing a soft lens.

As a result, the surface of the soft lens becomes dry in a very short time. The lens surface is then no longer smooth and the quality of the projected mires is reduced.

It is not possible to say whether the mire deformation comes from the dry contact lens surface or from contact lens shape change, or from changes in the corneal shape or all of the above.

Further possible evidence that low humidity could have an influence on the corneal shape comes from the “Jet Set Syndrome”. It can occur during a long flight. This is corneal oedema resulting from prolonged air travel. The main factor is low humidity (Casebeer, 1973).

2.2.6 Oxygen level and contact lens wearing effects on corneal physiology

Normal corneal metabolism depends on a critical level of oxygen. Below this level a series of acute corneal responses occur, including an increase in stromal lactate, a reduction in intercellular pH and an increase in corneal hydration (Polse et al, 1990).

Klyce (1981) attempted to resolve some of the speculation concerning corneal oedema associated with the tear film and hypoxia. Tests were performed with enucleated rabbit eyes. The results provide firm support for the hypothesis that stromal lactate accumulation and subsequent osmotic imbalance are the major short-term factors involved.

In his article Berke (2002) described that hypoxia induces corneal oedema, promotes the risk of infection and reduces sensitivity to pain.

85% of the epithelial energy is produced by anaerobe glycolysis, while in the corneal endothelium the proportions are 70 % anaerobic and 30 % aerobic. The endothelium has the most mitochondria of all the corneal layers. The stroma has hardly any cells so it needs less energy than the aforementioned layers. A high anaerobe energy production results in a high lactate concentration. Additionally, the risk of a cell membrane injury rises too.

The quantity of lactate in the cornea is 12.4 $\mu\text{mol/g H}_2\text{O}$, which contrasts with the quantity of lactate in the blood which is 2.1 $\mu\text{mol/g H}_2\text{O}$. Only after a long period of physical effort does the blood lactate concentration rise up to the corneal level. The epithelium and the upper part of the stroma get oxygen from the air and the conjunctival blood vessels.

However, the endothelium and the deeper part of the stroma are supplied with oxygen by the aqueous humour. Hence it follows that a slight disturbance of the oxygen supply may induce oedema.

When the stroma swells more than 4%, vertical striae can be seen. After swelling more than 8%, Descemet folds appear.

2.2.6.1 Striae and folds

Polse, Sarver, and Harris (1975) compared the amount of corneal swelling during lens wearing with two different types of contact lenses.

Twenty-seven patients were tested wearing both the “F” and “N” series Bausch and Lomb Soflens™ (polymacon) contact lenses. They described corneal swelling and when striae were observed.

The following table shows the results:

“F” Series Lenses - Increase in Corneal Thickness				“N” Series Lenses - Increase in Corneal Thickness			
Observation		0 - 4%	> 4%	Observation		0 - 4%	> 4%
of Striae	No	21	11	of Striae	No	18	10
	Yes	1	21		Yes	7	10
	Sum	22	32		Sum	25	20

Table 2.2.6.1-1 Increase in corneal thickness and presence of striae with both F and N series Bausch & Lomb Soflens contact lenses. (Polse, Sarver, and Harris, 1975)

Striae occurred when the corneal thickness increased by about or greater than 4%, so it appears that the type of the contact lenses has an influence on the presence of striae. The “F” series contact lenses have flatter posterior apical radii than the “N” series, therefore producing less oedema. In 65.6% of “F” series and 50% of “N” series lens measurements, striae were observed when the corneal thickness increased more than 4%. However in 4.5% of “F” series and 28% of “N” series lens measurements, striae were observed when the corneal thickness was less than 4%.

The corneal thickness also changed on three subjects wearing “F” series Soflens™ lenses, who were monitored over a 48h period including during 12 hours of wearing followed by a 36 h period after lens removal.

All the subjects had been wearing hydrogel lenses for at least two months prior to the measurements.

The subjects showed different thickness response profiles during the test period (Figures 2.2.6.1-1 to -3).

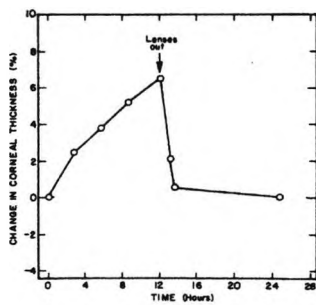


Figure 2.2.6.1-1 Corneal swelling profile type 1 “F” series lenses. (Polse, Sarver, and Harris, 1975)

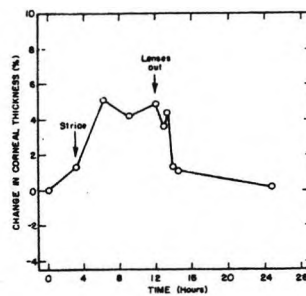


Figure 2.2.6.1-2 Corneal swelling profile type 2 “F” series lenses. (Polse, Sarver, and Harris, 1975)

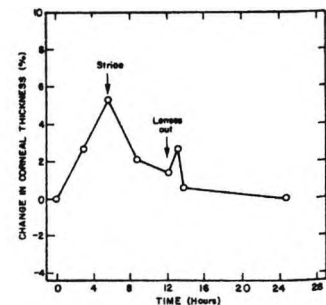


Figure 2.2.6.1-3 Corneal swelling profile type 3 “F” series lenses. (Polse, Sarver, and Harris, 1975)

In spite of three subjects wearing the same kind of contact lenses, three different corneal swelling profiles were found (Fig. 2.2.6.1-1-3).

The study shows the following results with respect to striae:

Almost 50% of the subjects demonstrated vertical striae during and after adaptation. The appearance of striae correlates with the development of corneal oedema. Whether or not corneal oedema causes vertical striae is not known.

However, striae have been observed in some patients with oedematous corneas following cataract extractions. In these eyes, the striae occur in the oedematous areas of the cornea and disappear when the oedema subsides. In any case, it is of clinical interest that significant amounts of oedema usually accompany the appearance of striae, and this suggests that when striae are observed, there is a high probability of oedema being present.

Additionally, folds and haze were determined as important signs to form the basis for clinical decisions (Efron et al, 2002)).

They stated that the human cornea swells by about four per cent in thickness during eye-closure overnight. This swelling and de-swelling is known to directly reflect changes in corneal hydration because the cornea can change thickness only in the anterior-posterior axis.

Thus, a 4% increase in corneal thickness represents a 4% increase in stromal water content or 4% oedema. Shortly before and after thirteen subjects wore Bausch & Lomb one day soft lenses on one eye over-night confocal microscopy, ultrasonic pachometry and slit lamp biomicroscopy were performed. Pachometry confirmed that the cornea had swollen by $11.8 \pm 3.8\%$ in the lens wearing eye and $2.1 \pm 1.9\%$ in the non-lens wearing control eye.

With the confocal microscope long dark lines could be observed in the posterior stroma of the lens wearing eye. The thickness of the lines and the total number of lines were greater at higher levels of oedema. Striae, as distinct from folds, were not seen with the confocal microscope.

2.2.6.2 Hypoxia

The clinical response to contact lens wear and laboratory hypoxia-induced corneal swelling studies have hinted that there is a wide variability in corneal oxygen demand in the normal population. Quick measurement of corneal oxygen consumption (Q_c) could be useful in studying the effects of contact lens wear on the metabolic status of the cornea.

The measurements could be carried out with a soft contact lens which was soaked over-night in a solution consisting of 1:9 part mixture of the oxygen-sensitive phosphorescent dye Pd meso-tetra porphine and bovine serum albumin. This stained lens should be rinsed before insertion. The phosphorescence is determined by flash illumination. After testing four subjects, an oxygen consumption of $2.2 * 10^{-4}$ mL O₂/cm³ *sec was stated (Bonanno et al, 2002).

Nguyen et al (2003) selected 30 non contact lens wearers to find out how the variability in hypoxia-induced corneal swelling is associated with a variable corneal metabolism and endothelial function.

Percent corneal thickness recovery per hour (PRPH), open-eye-steady-state (OESS), endothelial cell density, and tear oxygen tension beneath thick and thin hydrogel lenses were considered. Tear oxygen tension was measured in open eyes and shortly after the eyes were closed for five minutes. The difference between both kinds of tension values gives information about corneal oxygen consumption. PRPH and OESS values were significantly influenced by lens thickness. There were no associations between corneal swelling and endothelial cell density. In consideration of corneal oxygen consumption they come to the conclusion that contact lens-induced corneal swelling is associated with corneal metabolic and endothelial activities.

In 1973 Bailey and Carney had already determined that, at least in the short term, hydrophilic contact lens wearing does cause a significant increase in the corneal thickness. The eye had been measured with a Haag Streit Pachometer and a Bausch & Lomb Keratometer after the subjects removed a soft lens from one eye. No contact lens was fitted on the other eye.

The experiment was performed with Bionite lenses and Hydron lenses. The range of changes in the corneal thickness was 3.1% - 8.3% and the range of changes in the radius of curvature was 0.01 – 0.08 mm after a wearing time of 4 ³/₄ h - 7 ¹/₂ h.

Despite normal conditions, a change occurred in the thickness of the cornea which was induced by a contact lens. The cornea with the contact lens becomes thicker but the cornea without the lens also increases its thickness slightly.

This phenomenon was not taken into consideration in the analysis of the results. When the thickness of both corneas is compared after removing the lenses, the measured change in the corneal thickness would be less than the real change.

Uniacke, Augsburger, and Hill (1971) described the swelling which occurs in the corneal epithelium in response to an oxygen-free atmosphere. The epithelia showed the most pronounced thickness increase during the first hour. The cells in these outermost three to four layers of the epithelium increased to two to three times their normal sagittal thickness.

Corneal sensitivity declined at low oxygen levels. These measurements were performed using corneas from forty-two rabbits, which were dissected from their eyes. Measurements performed directly on living tissue do not suffer from the same uncertainties as morphometry derived from preserved tissues.

Clinical epithelial oedema is, however, a common sign related to the hypoxic effect of contact lens overwear. Hapnes, in 1980, performed a test in a low-pressure chamber. Five subjects were placed in the chamber wearing HEMA lenses. The temperature was 21 degrees Celsius, the humidity was 41 - 43% and the air pressure was a simulated 18,000 ft. Three subjects developed deposits on the tear film of both eyes after two hours. All subjects exhibited irritation after four hours. The experiment was terminated before stromal oedema developed. Each test subject was provided with an oxygen mask, providing an oxygen supply equal to 155 mm Hg. Partial pressure is 159 mm Hg at sea level (Butler, 1999).

However, Eng, Rasco, and Manrano (1978) described the effects of low atmospheric pressure on soft contact lenses when subjects breathe pure oxygen in a low-pressure chamber. The tests were taken at altitudes of up to 30,000 ft. There were no significant changes in visual acuities, refraction, wearability or bio microscopy after three hours.

The Hapnes and the Eng, Rasco, and Manrano studies were performed on subjects wearing oxygen masks while staying in a low-pressure chamber. The subjects breathed pure oxygen.

In comparison to the Hapnes study, the Eng, Rasco, and Manrano study was carried out at lower humidity levels and less partial pressure of oxygen around the tested eyes, but there were no corneal changes. These two studies merely indicate the influence of conditions on contact lens-wearing. The body of each test subject did not have to adapt to the changing conditions. No acclimatisation of the intrinsic system was necessary.

2.2.6.3 Minimum partial oxygen pressure before swelling of the cornea

The following studies were performed to find out the minimum dose of air pressure associated with corneal swelling. In 1970 Polse and Mandell showed that we need a minimum of 11 to 19 mm Hg air pressure to prevent corneal swelling.

Mandell and Farrell (1980) exposed 28 human corneas to partial oxygen pressures of 6.9, 17.1 and 22.2 mmHg in a gas goggle.

Corneal swelling was measured by pachometry for a period of 4 hours.

The average corneal swelling after 4 hours was 5.07%, 2.13%, and 1.66% at 0.95%, 2.34%, and 2.77% oxygen levels respectively (Fig. 2.2.6.3-1). The “corneal swelling air pressure threshold“ was 23 to 37 mm Hg \pm 8.7 mm Hg.

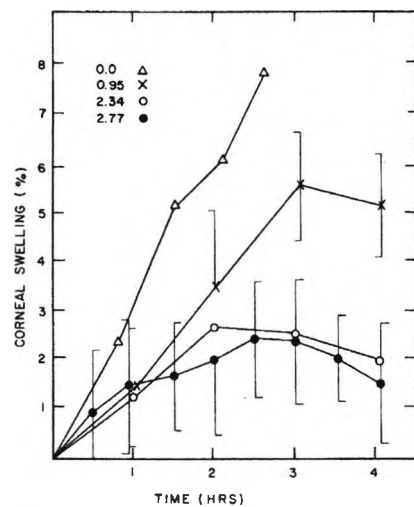


Figure 2.2.6.3-1 Average corneal swelling response at three oxygen concentrations (0.95%, 2.34%, and 2.77% oxygen). Also shown (Δ) are data from a previous study at zero oxygen level (100% nitrogen). (Mandell and Farrell)

These two studies suggest that an air pressure sufficient to cause corneal swelling is unlikely to be reached at high altitude, for the oxygen pressure at 8850 m (equivalent to the peak of Everest) is calculated to be 45mmHg. But these findings are not consistent with the frequently observed anecdotal reports from high altitude mountaineers of reduced visual acuity that occurs at high altitudes, presumably as a result of corneal oedema. However, both these studies were beset by two problems: the short exposure periods and the limited range of oxygen concentrations used.

To deal with these problems, Holden, Sweeney, and Sanderson (1984) conducted a test over an 8-hour period with an oxygen level ranging from 1% to 21 % (Fig. 2.2.6.3-2). This resulted in a minimum oxygen tension to prevent corneal swelling being measured at 74 mmHg (10.1%). This level induced an increase in corneal thickness of 0.3%, which was considered an acceptable level by Holden and Sweeney. This critical oxygen tension is considerably higher than that estimated by Mandell and Farrell, and would theoretically be reached at an altitude of approximately 18,000ft.

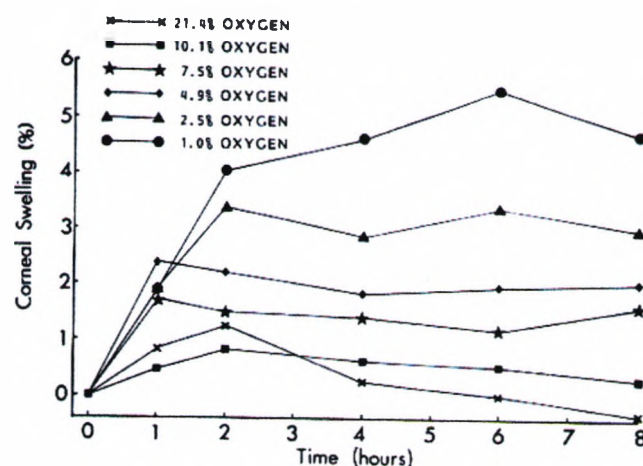


Figure 2.2.6.3-2 Average corneal swelling (n = 8) over time for a range of oxygen concentrations. (Oxygen concentration 1.0%, 2.5%, 4.9%, 7.5%, 10.1% and 21.4%). (Holden, Sweeney, and Sanderson, 1984)

In a study conducted in 1984, Holden and Mertz explained that the critical lens oxygen transmissibility for open eye wear is based on an estimated oxygen level of 5×10^{-9} (cm x ml o₂) (sec x ml x mmHg) (DK/L), as has been suggested elsewhere.

They performed tests on ten different kinds of soft contact lenses on seven men and three women.

When a hydrogel contact lens is worn, the maintenance of normal corneal function depends primarily on sufficient oxygen diffusion through the lens material. The oxygen transmissibility of such a lens (DK/L) is directly proportional to the oxygen permeability (DK) of the material polymer and inversely proportional to the thickness of the lens (L). This is a function which describes the water content in hydrogel materials. The extended wearing time of contact lenses has been tested on five subjects over a period of 35 hours. The daily wearing of contact lenses has also been tested on five subjects over a period of 12 hours.

For daily wear, a standard low water content lens (HEMA) with a maximum thickness of 33 μm and higher water content material such as Duragel 75 with a maximum thickness of 166 μm have been suggested.

2.2.6.4 Signs and symptoms

A retrospective study was performed to review the clinical characteristics of peripheral corneal infiltrates in contact lens wearers. Infiltrates associated with contact lens wear were reviewed in 52 patients. Six per cent of the subjects were wearing rigid gas permeable contact lenses. Forty-four patients presented with a single infiltrate, while eight patients had multiple infiltrates. The majority had minimal conjunctival inflammation, an anterior stromal cellular reaction and minimal anterior chamber activity (Donshik, Suchecki, and Ehlers, 1995).

Lemp, Mathers, and Sachdev (1990) showed a statistically significant enlargement of central epithelium cells as a result of extended lens wearing. The corneas of 48 subjects were photographically documented for evaluation. Flynn, et al (1987) found that bubble formation begins when soft contact lenses are worn at an altitude of 6,000 ft. The position of the bubbles was peripheral.

The quantity and the size of the bubbles depended on the altitude. They did not disappear when the subject blinked, but had no effect on vision or corneal epithelial integrity.

The study was performed under artificial conditions in a low-pressure chamber and in an aeroplane.

2.2.7 The indirect influence of acclimatisation

Generally speaking, the higher mountaineers ascend, the lower the oxygen partial pressure, the lower the temperature, and the lower the humidity. The human body has to adapt to these changing surrounding conditions. A healthy mountaineer ascends to an altitude of about 8500 ft without any adaptation problems. Ascending higher, hypoxic signs are established.

For example, hyper ventilation and an elevated pulmonary arterial pressure are typical reactions of the body to compensate for the low oxygen levels at greater altitude. A high dose of UV radiation at high altitude could be seen as an additional stress factor on organ adaptation (Fischer, 2005).

The cornea is an avascular tissue but parts of the cornea are supplied with oxygen by limbal and conjunctival blood vessels.

A change in blood parameters such as a higher pH value and a lower 2,3 Bisphosphoglycerate concentration reduce the splitting off of oxygen from haemoglobin. This has an influence on the metabolic activity of every tissue in the body, including the cornea. The kidney reacts by releasing a higher level of erythropoietin which enhances the production of erythrocytes in the red bone marrow because of the effect of a lower oxygen supply. A higher "red blood cell count rate" than normal is named Hyperaemia or Polycythaemia.

Hyper ventilation leads to a reduced CO₂ level in blood. The lower CO₂ level is compensated by cleaving Bicarbonate molecules in the liver. Hence, it follows that the blood pH value alters in an alkaline direction called respiratoric alkalosis (Kreutzig, 1997; Forth et al, 2001; Jefferson et al, 2002).

The effect of altitude on several metabolic processes had been studied on 30 human volunteers ascending Mount Aconcagua in Argentina, which has a 23,000 ft summit.

The changes observed in the acid-base balance, in liver functions and in some other standard examinations were discussed with regards to acclimatisation. It was demonstrated that the compensational capacity of the organism is limited at altitudes above 18,000 ft. At 20,400 ft the blood pH tends to be less alkaline than expected (8800ft pH 7.370 ± 0.023 , 20,400ft pH 7.469 ± 0.025). The quantity of erythrocytes in blood increased only slightly from the starting level of 5.48 ± 0.27 (mill./mm³) during the ascent and descent, which began at an altitude of 8,800 feet and featured an ascent to an altitude of 20,400 feet. When the subjects returned to 8,800 feet a value of 5.51 ± 1.50 (mill./mm³) was measured (Tab. 2.2.7-1). In spite of a respiratory alkalosis the total acid-excretion in urine increases at 20,400 ft. The capacity of the liver for the acetylation of orally administered sulphonamides decreases with increasing altitude. At 20,400 ft only half of the test sulphonamide is excreted as an N₄-acetylated compound.

Erythrocyte (mill./mm ³)		
Altitude	n	Control group
8800ft tour beginning	15	5.48 ± 0.27
8800 ft tour end	15	5.51 ± 1.50
Haemoglobin (g/100ml)		
Altitude	n	Control group
8800ft tour beginning	15	15.90 ± 0.95
8800ft tour end	15	15.90 ± 1.31

Table 2.2.7-1 Erythrocyte concentration (mill./mm³) and haemoglobin were measured at an altitude of 8,800 ft at the beginning and at the end of a stay at higher altitude. (Albrecht and Albrecht, 1967)

SGPT-activity shows a slight increase. An intensified hemopoiesis with a consecutive increase in the erythrocytes, a much lower increase in blood pH, better liver acetylation capacity and a significant anticatabolic effect has been observed in a treated group (Albrecht, and Albrecht, 1967).

Malconian, et al (1993) measured the alveolar gas O₂ (P_{AO₂}) and CO₂ (P_{ACO₂}). The test subjects were eight men between the ages of 21 and 31 years. The subjects were tested in a low pressure chamber. Six subjects were tested across the entire period of about 34 days. The barometric pressure (PB) was reduced step by step and the oxygen pressure (P_{iO₂}) commensurately. Table 2.2.7-2 shows the differences between the oxygen pressure, the alveolar oxygen gas tension and the alveolar carbon dioxide gas tension.

The higher the simulated altitude the lower the oxygen pressure, the alveolar oxygen gas tension and the alveolar carbon dioxide gas tension.

When the alveolar oxygen gas tension (PAO₂) and the alveolar carbon dioxide gas tension (PACO₂) were considered from sea level to 19000 ft it emerged that the values of PAO₂ decreased faster than the PACO₂ values.

Day	n	PB (mm Hg)	P _{iO₂} (mm Hg)	Elev* (m)	PAO ₂ (mm Hg)	S.D.†	PACO ₂ (mm Hg)	S.D.†	R‡
1	8	760	149	0	104.3	10.0	38.2	4.3	0.82
3	8	575	111	2360	63.2	9.0	38.2	3.5	0.77
4	8	501	95	3500	53.8	3.8	37.6	4.0	0.89
5	8	482	91	4100	53.8	5.3	31.6	2.9	0.82
6	8	463	87	4300	50.0	7.2	29.5	3.7	0.76
7	8	447	84	4600	46.9	5.0	28.5	2.8	0.73
9	8	428	80	4900	47.5	5.4	26.4	3.8	0.78
12	8	412	76	5200	48.7	7.8	25.0	4.8	0.88
13	8	397	73	5500	41.0	6.7	25.8	4.2	0.76
14	8	380	70	5800	40.6	6.1	25.6	3.5	0.85
15	8	380	70	5800	43.4	6.2	23.4	3.9	0.86
16	8	380	70	5800	43.4	5.2	22.6	3.0	0.83
17	7	364	66	6100	40.3	3.7	23.7	2.5	0.89
18	7	349	63	6460	36.7	3.8	23.1	3.0	0.84
19	7	349	63	6460	39.5	2.2	18.5	1.8	0.74
20	7	349	63	6460	35.7	5.4	21.3	4.0	0.73
21	7	380	70	5800	45.0	4.6	22.0	3.4	0.87
22	7	349	63	6460	36.9	4.0	21.2	3.2	0.77
23	7	349	63	6460	35.2	3.0	22.0	3.0	0.74
24	7	347	63	6480	38.0	3.6	19.9	2.4	0.76
25	7	335	60	6750	35.7	3.2	20.5	2.9	0.80
26	7	314	56	7200	31.2	3.0	18.6	2.0	0.71
27	7	307	54	7400	30.6	3.0	17.5	2.1	0.69
30	7	295	52	7700	32.4	4.4	14.9	3.4	0.72
31	7	289	51	7850	31.9	2.0	17.0	1.8	0.88
34	6	273	47	8300	30.2	2.7	14.7	2.2	0.83
34	6	263	45	8550	31.0	3.1	13.9	2.3	0.97

Table 2.2.7-2 Elev = the terrestrial elevation, and is greater than altitude estimated from the ICAO Standard Atmosphere.

PD = barometric pressure

PiO₂ = oxygen pressure, PAO₂ = alveolar oxygen gas tension

† S.D. indicates one standard deviation from the mean.

‡ R is the expiratory exchange ratio from the alveolar air equation.

(Malconian et al, 1993)

Maurice, et al (1995) tested hemoglobin oxygen saturation along with other parameters such as, for example, visual fields, and contrast sensitivity. The tests were performed on twelve subjects aged 19 to 30 years at simulated altitudes of 7,000 ft and 12,000 ft. The saturation of hemoglobin with oxygen in percentage terms was measured using a colorimetric transdermal pulse oximeter (Nellcor Inc., Hayward, CA). Although the subjects were exposed to each at simulated altitude for a very short time of about 80 min. hemoglobin saturation levels were significantly different at different altitudes (Tab. 2.2.7-3). (ANOVA, $F = 17,934$, $df = 2,22$, $p = 0.0001$)

Subject	Hemoglobin saturation		
	Sea Level	7,000 ft	12,000 ft
1	99.5	95.25	89.00
2	100	95.25	82.00
3	98.25	97.25	94.75
4	99.75	97.25	82.30
5	100	97.50	88.75
6	99.50	95.25	88.00
7	100	96.25	96.25
8	99.00	96.50	96.50
9	98.50	96.75	95.50
10	100	98.75	89.00
11	100	96.75	97.25
12	100	95.50	97.25

Table 2.2.7-3 Percentage Hemoglobin Saturation for subjects at three stations of altitude. (Maurice, Garner, Legg, and Faris, 1995)

2.2.7.1 Acclimatisation

The ability of the body to adapt to changing surrounding conditions is referred to as acclimatisation. The human body is able to acclimatize up to 17,000 ft. The reason for almost all deaths at high altitudes is hypoxia. Being well acclimatized is more important than being in good condition.

Acclimatisation takes place in several steps:

The first step begins at 9,000 ft, while the following steps are every 1,500 ft. The acclimatisation time varies. No further acclimatisation is possible above about 17,000 ft (Albrecht, and Albrecht, 1967).

People who have been acclimatized to high altitudes have a higher concentration of haemoglobin that helps them maintain oxygen delivery to tissues.

One measurement of a body's level of acclimatisation is the pulse when the person is calm and relaxed. It is taken directly after the subject wakes up. After reaching an unusual altitude, this pulse increases over the first two days to up to 60% above the level measured in a familiar environment. Beginning on the second day, it declines in an almost linear fashion until the normal pulse rate is reached again about 5 ½ days later.

Acclimatisation has then been reached to its fullest extent.

This linear curve for the pulse recovery only occurs when the body acclimatizes properly. For this reason the first 5 ½ days of the acclimatisation are also referred to as the critical phase (Figure 2.2.7.1-1). Other problems related to altitude include thrombosis, frostbite, thromboembolism, exhaustion and inappropriate reaction by the central nervous system as a result of hypoxia (Berghold, Schaffert, and Pallasman, 1991).

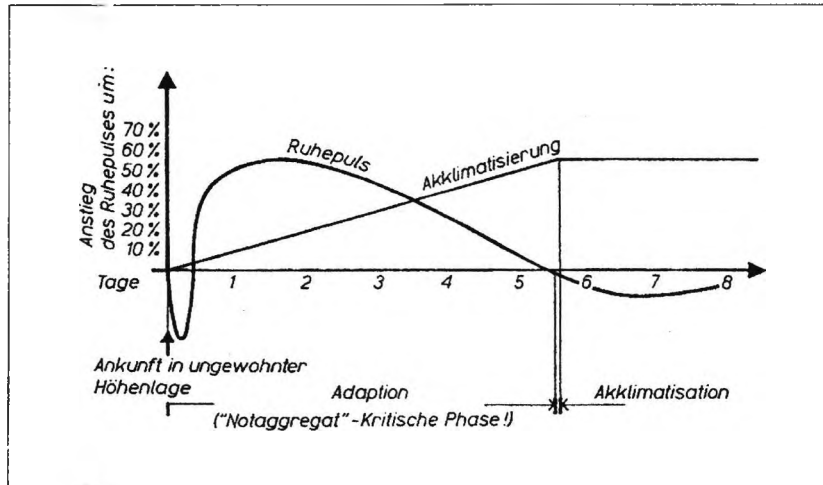


Figure 2.2.7-1 The Ruhepuls is the pulse, which is measured immediately after awakening. The graphic shows the change of the Ruhepuls with the acclimatisation measured in days. (Abscissa days of acclimatisation, ordinate the change of the Ruhepuls %). (Berghold, Schaffert, and Pallasman, 1991)

2.2.7.2 Complications at high altitude

Low oxygen level is the main reason for the high risk of sickness at high altitude. Acute mountain sickness (AMS) is the most common manifestation of altitude sickness and involves headache, loss of appetite, light-headedness, breathlessness, nausea, fatigue, and insomnia. Typically, symptoms begin 2 or 3 hours after ascent, but the condition is generally self-limiting and most of the symptoms disappear after 2 or 3 days. However, insomnia may persist. Descent to low altitude rapidly reverses acute mountain sickness. The precise pathogenesis of acute mountain sickness is not understood. Mild cerebral oedema may occur secondary to increased cerebral blood flow and perhaps altered permeability of the blood-brain barrier. Additionally, hyperaemia induced by hypoxia elevates the thrombosis risk (West, 2004).

AMS is potentially life-threatening. But it is avoidable because it occurs as a consequence of insufficient attention being paid to the specific conditions, as well as incorrect behaviour by individuals with respect to altitude (Berghold, Schaffert, and Pallasman, 1991).

In addition to AMS, chronic mountain sickness is diagnosed sometimes in patients who stay for a longer time at high altitude.

Polycythaemia usually develops at high altitudes in response to systemic hypoxia. In some cases, erythrocytosis is severe, leading to chronic mountain sickness. The crucial factor is how long the mountaineer stays at a high altitude (Jefferson et al, 2002).

Twenty-six selected subjects were tested to see whether the angiotensin-converting enzyme-inhibitor enalapril helps to reduce the erythrocyte mass, promoting a better blood flow and reducing blood pressure.

The results show that in patients with altitude polycythaemia, long-term treatment with low doses of enalapril have safely prevented an increase in arterial blood pressure and progressively reduced packed cell volume, haemoglobin concentration and proteinuria (Plata et al, 2002).

Other possible diseases are high altitude pulmonary oedema and high altitude cerebral oedema. High altitude pulmonary oedema is a potentially fatal condition that typically occurs 2 to 4 days after ascent to altitudes above 10,000 ft. The pathogenesis is still a subject of study, but strong evidence indicates that it is triggered by pulmonary hypertension as a result of hypoxic pulmonary vasoconstriction. High altitude pulmonary oedema may be preceded by acute mountain sickness, but this is not always the case.

High altitude cerebral oedema is rare but potentially very serious. The condition often follows acute mountain sickness, and many people think that the two are closely related and that high altitude cerebral oedema is the extreme end of the spectrum. Hallucination has been described, and serious cases involve coma followed by death. The pathogenesis is almost certainly cerebral oedema, possibly related to an increased oedema with swollen flattened gyri. The cardinal rule in treatment is descent to a lower altitude as quickly as possible. Oxygen should be administered if possible (West, 2004).

2.2.8 Hypothesis to be tested in this study

One should expect the following conditions at high altitudes: a low oxygen level, low partial oxygen pressure, dry air, elevated dose of cosmic radiation and UV radiation, and low temperature. The literature indicates that these conditions have an influence on corneal metabolism.

Given the corneal changes described in the literature and the facts discussed in this chapter, this study was designed to investigate the following hypothesis:

“The cornea is able to adapt to changing conditions and does not exhibit a significant change in corneal shape up to 16,400 ft.”

If the cornea is unable to adapt to marked changes in altitude this raises several further questions which will be addressed in this study:

- How does the corneal shape change, at low and high altitudes, both with and without contact lenses being worn?
- Is the extent of the corneal shape change relevant to comfortable contact lens wear?
- What are the main influencing factors at work in corneal shape change?

2.3 Summary

Every environment, for example a forest, park, or inside a house has its own micro climatic conditions which can change continuously. A major change of climatic conditions occurs between sea level and ascent to high altitude. In order to establish the effect of this change we should investigate the influence of relevant meteorological factors and their interactions. Standard meteorological factors are air pressure, humidity, temperature, wind velocity, and the daily sunshine period which gives a measure of the energy of the Sun which reaches the Earths' surface. The air pressure depends on the thickness of the air layer which presses on the surface.

The higher the altitude of the air considered, the thinner the air layer above and therefore the lower the air pressure. A further important role is played by the air density. A cold temperature induces a high density of air molecules so the air pressure increases. However, a warm temperature has the opposite effect. Water molecules do have a special property in the air. Water is found in three states, vapour, liquid, and ice. Variable air pressure and air temperature transform water from one state into another, continuously. If a defined volume of water vapour is pressed, its pressure rises until the maximum pressure of water vapour is achieved then the water vapour condenses. Here, a hygrometer would show 100% humidity.

This is based on the fact that a hygrometer measures the proportion of real water mass and maximum water mass in the air as a percentage. Dry air, low air density, and a thin air layer are mainly responsible for the high doses of UV radiation and cosmic radiation at high altitude. Both types of radiation affect the cornea in different ways. Cosmic radiation does ionize and has more energy than UV radiation. Both damage corneal cells depending on the dose of radiation.

The corneal epithelium and Bowman's layer absorb UV B radiation effectively. The stroma absorbs a higher quantity of UV B radiation because of its thickness. However, intensive corneal exposure disturbs cell metabolic activities which lead to apoptosis. Photokeratitis is one disease that can result after a high dose of radiation exposure.

Temperature is one of the fundamental parameters of tissue metabolism. When the ambient temperature drops, the corneal temperature falls linearly. Sensory nerves in the cornea distinguish the feeling of warm and cold temperature. The normal corneal temperature is described as 33.7 degrees Celsius. Additionally, temperature is a main indicator for the maximum water mass which could be in the air. Thus temperature is a major influential factor for evaporation and condensation.

An enhanced tear film evaporation results in an increase in blinking frequency.

A normal rate of evaporation is calculated at 30 % relative humidity for normal eyes to be 0.14 ± 0.6 micro litre/min and for dry eyes to be 0.43 ± 0.19 micro litre/min. The epithelial pump and endothelial leakage-pump mechanisms are responsible for maintaining a consistent corneal water hydration of 78%. Higher tear film evaporation does not have any influence on corneal swelling and de-swelling functions. Studies on long-term and short-term flights show irritation of the corneas with and without contact lenses, which are mainly induced by the low humidity under these conditions.

Low oxygen level is another problem which induces disturbances in corneal metabolism. Less energy would be produced by the corneal cells and the effect of this is seen in an elevated lactate level in the corneal tissue. The cornea swells as a result of an osmotic imbalance. At levels of swelling of 4% and higher, striae are seen and at higher than 8% folds are produced. A slit lamp is a better instrument of choice than a confocal microscope to differentiate striae and folds because it is not possible to see any differences between striae and folds with confocal microscopy.

Contact lens induced increases in corneal thickness have been the subject of many studies. Three main values are used to describe the corneal metabolic status. The first is the Open-eye steady-state (OESS), where the corneal thickness is often measured over a period of time. The second is the percentage corneal thickness recovery per hour (PRPH). Here a thick contact lens is put in front of the cornea for 2 hrs and after the lens is removed the corneal thickness is measured until the cornea has recovered from the contact lens induced hypoxia. The third is the corneal oxygen consumption (Q_c), a measure of the quantity of oxygen which passes the corneal surface with the help of an oxygen sensitive indicator "Pd meso-tetra porphine".

When PRPH, OESS, and corneal oxygen consumption measurements are considered, one comes to the conclusion that contact lens-induced corneal swelling is associated with corneal metabolic and endothelial activities.

Following testing to identify the minimum oxygen level (artificially induced at low altitude) before the cornea swells, the results range from 11 mmHg to 74 mmHg, with little consensus in the literature. However, there are frequently observed anecdotal reports from high altitude mountaineers of reduced visual acuity occurring at high altitudes, presumably as a result of corneal oedema. The human body is generally regarded as being able to acclimatize up to about 18,000 ft of altitude and the the oxygen level is about 70 mmHg there. It is possible that the cornea may swell when the oxygen level is below 74 mmHg. Acclimatisation is defined as the ability of the body to adapt to changing surrounding conditions. It takes place in several stages. Slight differences may be found in published studies regarding the stages in the acclimatisation process. The first stage begins at 9,000 ft, while the following stages are every 1,500 ft. The acclimatisation time varies but no further acclimatisation is possible above about 17,000 ft. People who have been acclimatized at high altitude have a higher concentration of haemoglobin that helps them maintain oxygen delivery to tissues. But a negative aspect of hyperaemia is the elevated thrombosis risk.

The blood pressure measured shortly after awakening describes the status of acclimatisation. The failure to acclimatize is comparable to crossing a motorway with closed eyes. The following symptoms can be detected; headache, loss of appetite, light-headedness, breathlessness, nausea, fatigue, and insomnia. The appearance of these signs and symptoms characterises acute mountain sickness (AMS). It is the most common manifestation of altitude sickness and must be watched very carefully because it is potentially life-threatening. People who stay at high altitude for a long period of time can also fall ill (chronic mountain sickness). Other possible diseases are high altitude pulmonary oedema and high altitude cerebral oedema.

Given the many corneal changes associated with altitude, especially corneal oedema, and the other effects of altitude described in this chapter one can put forward the following hypothesis:

“The cornea is able to adapt to changing conditions and does not exhibit a noticeable change in the corneal shape up to 16,400 ft.”

If the cornea is unable to adapt to marked changes in altitude this raises further questions:

- How does the corneal shape change with and without contact lenses being worn?
- Is the amount of the corneal shape change relevant to contact lens wearing?
- What are the main influencing factors at work here?

This hypothesis and the supporting questions are addressed in the remainder of this thesis.

Chapter 3. Methods

3.1 Introduction

This chapter describes the equipment used in the study and methods employed to test the hypothesis and to answer the questions raised at the end of chapter 2. In addition, the mathematical equations involved are explained, especially as regards the corneal shape. Finally, calibration of the instruments used in this study is described in detail.

3.2 Instruments

The literature indicates that low humidity, low oxygen rate, low air pressure and low temperature all have an influence on corneal metabolism. In particular, an elevated lactate level produces, among other corneal changes, corneal oedema and lower tear formation. Furthermore, corneal swelling could eventually cause corneal shape to change. It is important to know how these factors influence corneal shape during ascent to high altitudes.

3.2.1 Protection against cosmic radiation

Chapter 2 noted that high doses of cosmic radiation and UV radiation could be expected at high altitude. Both types of radiation lead to cell damage, the extent of which depends on the amount of radiation. The question of how to protect against a high dose of both radiations will now be addressed.

As noted in the previous chapter, if measurements are performed during the minimum phase of cosmic radiation at high altitudes, the amount is the same as when measurements are performed during the maximum phase of cosmic radiation at sea level.

Furthermore, Solar flares are unpredictable, and these are a risk factor, but it is not possible to prepare for them. There is only one counter-measure that can be taken. After the measurements have been recorded at high altitude, one needs to establish whether solar flares have been detected during the test phase. During this study, information on Solar Flares was obtained from the Meteorological Institute in Munich.

3.2.2 Protection against UV radiation

The best protection against UV radiation is wearing sunglasses with high rates of UV absorption. All subjects were instructed to wear sunglasses during the test phases with lenses offering a very high percentage of UV absorption; this ensures that UV radiation has no significant influence on the results. The Essilor Orma extreme 2 lens absorbs sufficient UV radiation to protect the eyes during the stay in Nepal. The following graph and table show the percentage transmission of wavelengths through the Essilor lens for wavelengths from 280 nm to 780 nm. The measurements were carried out using a Beckman spectral photometer, model DU 70:

Transmission in % of wave lengths in steps of 2 nm						
Wave l.	280-314	316	318	320	322	324, 326
Transm.	0.07	0.08	0.07	0.08	0.07	0.08
Wave l.	328-336	338, 340	342, 344	346, 348	350, 352	354
Transm	0.07	0.08	0.07	0.08	0.07	0.08
Wave l.	356-372	374	376	378-396	398, 400	402
Transm	0.07	0.08	0.07	0.08	0.01	0.00

Table 3.2.2-1 Transmission (%) of every wavelength from 280 nm to 402 nm in steps of 2nm for the Essilor Orma extreme 2 lens (Essilor).

Extreme 2

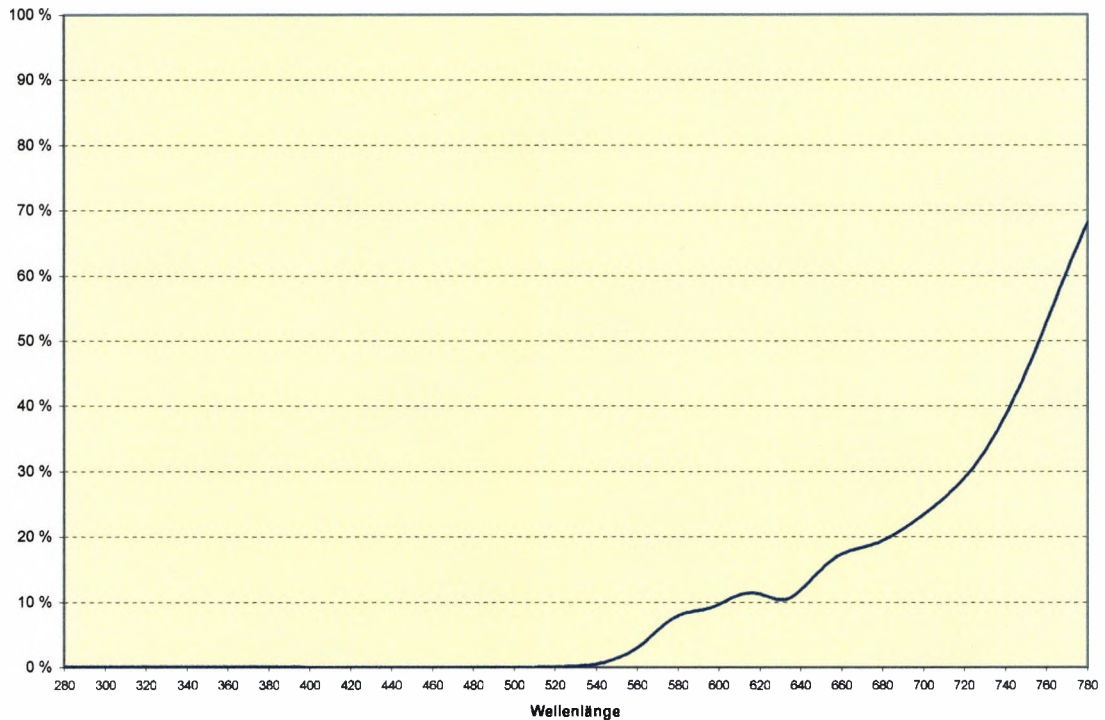


Figure 3.2.2-1 Transmission (%) of wavelengths (wellenlänge) from 280 nm to 780 nm for the Essilor Orma extreme 2 lens (Essilor).

In table 3.2.2-1 the transmission quoted is for the complete range of radiation at every wavelength, and not the summary of all wavelengths the glass is exposed to during the measurement period. It should be noted that every wavelength between 402 nm and 520 nm transmitted less than 0.09 %.

Before the test instruments are discussed, there is a very important consideration to address. Carrying out some types of measurements could have an influence on the results of measurements which follow. Therefore the tests were divided into two groups, the primary group and the secondary group. The primary group comprises the instruments used to test the hypothesis. Here the primary tests are the altitude measurements and the corneal shape measurements.

The altitude recorded reveals the information needed to indicate the acclimatisation stage reached during the trek and the corneal shape measurement allows identification of the corneal shape changes that have occurred during acclimatisation. Tests belonging to the secondary group are taken to document meteorological conditions and to examine the health status of every tested eye. Under no circumstances must a test belonging to the second group be allowed to have an influence on tests from the first group. This must be considered when choosing suitable instruments.

3.2.3 Instruments for the measurement of air pressure

Air pressure can be measured in different units. The pressure units are millibar (mbar), inches of mercury (in Hg), and pound-force/square inch (lbf/in²).

1 in Hg = 33.864 mbar = 33.864 hecto Pa

1 pound force/square inch = 68.95 mbar (Kuchling, 1986)

The scale of the barometer used in this study is standardized in unit mbar/hPa. Normally, the barometer system consists of a box, a transfer chain, a needle, and a scale.

The box is a small, round airtight metal cover with a vacuum inside. The best instruments have older boxes inside, because they are more reliable than newer ones. They are usually about two years old. The air pressure presses against the box, and when the air pressure changes, the thickness of the box also changes accordingly. The greater the surface area, the more the thickness changes.

Therefore, the greater the surface area of the box, the better the quality of the barometer.

However, a big box is more difficult to manufacture than a small one. Thus, a high-quality barometer contains more than one box, a very thin transfer chain, a long, fine needle and a standardized scale (Schirmer et al, 1989).

More exact measurements can be taken with a mercury barometer. It consists of a glass capillary tube, about one meter long, which is filled with mercury and placed in a perpendicular position with the open end in a mercury-filled bowl. The upper end of the capillary tube is closed, thus the weight of mercury pulls down until the force of a developed vacuum (Torricelli-Vacuum) in the upper part of the capillary is strong enough to hold the mercury in balance. Now the height of mercury in the capillary tube depends on the momentary air pressure which presses on the surface of mercury in the bowl. The use of Mercury makes this instrument potentially injurious to health and it is not easy transportable (Häckel, 1999).

A Fischer precision-aneroid barometer was the instrument selected for this study. This barometer is comparable with the Fischer model nr 104-002, however it has been modified for high altitudes. The accuracy of the measurements from 400 hPa to 900 hPa is ± 1 hPa. It is sturdy enough to be carried, together with other instruments, in a small container with limited space. The use of an electrical barometer was discounted for fear that the instrument would not function when the temperature drops.

3.2.4 Instruments for measuring altitude

Altimeters and barometers function in a similar way. Altimeters measure in units of meters (m) or feet (ft). $1 \text{ ft} = 0.3048 \text{ m}$ (Kuchling, 1986). There are many different types of altimeter. Altimeters can be divided into two groups. The first group consists of mechanical instruments (with one box, or two boxes inside) and the second group comprises electronic instruments with a pressure-sensitive electronic system inside. Most electronic altimeters look like watches. Some of these altimeters are multifunctional.

With these multifunctional instruments it is possible to retrieve data such as time, altitude, a summary of altitude differences as the mountaineer ascends over a defined period of time, and how fast a mountaineer ascends during a defined period of time.

But no altimeter is able to distinguish whether air pressure differences come from weather changes or from ascending.

It is therefore important to use a barometer to test whether the weather has had an influence on the altimeter measurements. All the other functions except for time and altitude are not precise enough for statistical consideration in this study. One additional risk factor is that all electronic altimeters need a battery.

A Thommen altimeter 7000 was used for this study (the name of manufacturer is Thommen). This precision system, made in Switzerland, was perfected several years ago. It is a mechanical altimeter with two boxes inside. Any changes in thickness of the two boxes are transformed by gearwheels, which are embedded with 19 jewels to minimize friction.

The precision of the measurements is ± 8 m. During the instrument calibration and testing procedure, two maps from the German Alpine Club were used. The altitudes at some map locations were stated, so it was possible to compare the measurements on the altimeter with the data stated on the two maps Nr. 0/10 and Nr. 0/11 (Aufschnaiter, Miehe, and Schneider, 1990).

3.2.5 Instruments used to measure temperature

Temperature is measured in the following units: degrees Celsius ($^{\circ}$ C), degrees Fahrenheit ($^{\circ}$ F), and Kelvin (K).

Degrees Celsius = (degrees Fahrenheit – 32) * 5/9

Degrees Fahrenheit = (9/5 * degrees Celsius) + 32

Kelvin = 273.15 + degrees Celsius (Kuchling, 1986)

There are three main types of thermometer: bimetal thermometers, fluid thermometers and electronic thermometers.

Bimetal thermometers are based on the principle of using two connected metals with different temperature extension coefficients.

The warmer the bimetal, the more the bimetal bends in the direction of the metal with the lower temperature extension coefficient. This type of thermometer is very sturdy but not as precise as fluid thermometers. Fluid thermometers are produced with different fluids inside.

Fluids frequently used include mercury, toluene, and pentane. Every fluid has different characteristics with respect to factors such as, for example boiling point or melting point. These characteristics are very important in defining the range of temperatures in which the fluid is used. Mercury thermometers have a wide range and mercury reacts very quickly and precisely to temperature changes.

Portable electronic thermometers need a battery because the electronic resistance of a metal is measured. The temperature influences the power of a metal to resist an electric current passing through it (Schirmer et al, 1989).

A Mercury thermometer with a standardized scale and a tolerance of plus/minus 0.5 degrees Celsius was chosen for the study. The unit of the scale is degrees Celsius and the range of the scale is +50 degrees to -30 degrees. The thermometer (Möller Therm, model number 106705) was delivered in a metal cover, ideal for transport in Nepal.

3.2.6 Instruments for measuring humidity

The absolute humidity indicates the quantity of water (kg) in a defined volume (m^3) of air. The relationship between the real water mass in the air and the maximum water mass in the air is expressed with the help of a hygrometer.

Normally air humidity is measured as a percentage (%) and referred to as relative humidity (f_{relative}) of the air. The value demonstrates how much water has to evaporate until a maximum of water vapour is reached. In other words 100 % relative humidity means water evaporation and water condensation are in balance (see chapter 2.2.1).

In this study, humidity is used as an indicator of tear film evaporation and loss of water through breathing and sweating.

There are several kinds of hygrometers. Two systems are worth consideration here. The first functions with a hair. The length of the hair is measured, as it is a function of humidity. Old hygrometers used to contain human hair. Lipids were removed from the human hair before it was placed in the hygrometer. Later horsehair was used and now Durotherm strings are installed in high-quality instruments.

The second type consists of two thermometers and is named a psychrometer.

Here the air temperature is measured with one thermometer and the evaporation temperature is measured with the other, which is partly wrapped into a wet fabric.

The difference between the two measurements is a measure of the humidity. The principle behind this is based on the fact that water cools when it evaporates.

When the water mass in the air reaches maximum levels, no more water evaporates and both thermometers show the same temperature. The more water evaporates into the air, the bigger the difference in the two temperatures measured.

An Assmann-Aspirations psychrometer includes additional radiation protection and a pump which pumps air along both thermometers (Schirmer et al, 1989).

This measurement is complicated in a natural setting, such as during a trekking tour. The water for evaporation has to be distilled and it should always have the same temperature as the air around the thermometers. The whole instrument has to be kept clean during the measurement. For this reason the precision hair hygrometer Fischer model nr 122.01 was used on the trek. It has a standardized scale and a scale tolerance of plus/minus 1.0% and measurement tolerance of $\pm 3\%$.

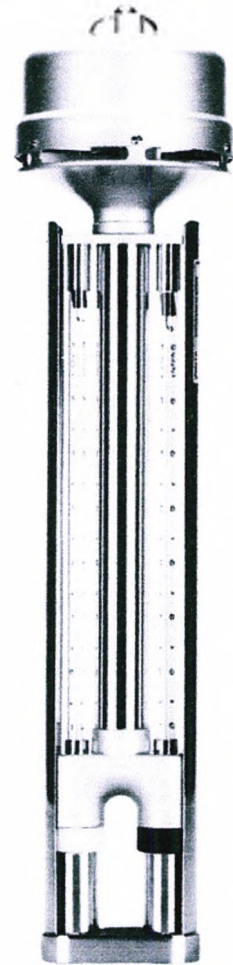


Fig. 3.2.6-1 (Appendix)
Assmann Aspirations-
psychrometer.

3.2.7 Instruments for corneal inspection

A slit lamp is needed to determine corneal oedema, other corneal changes, blood vessel changes and other data relating to the anterior segment of the eye. A conventional slit lamp is quite large and difficult to transport, however, plus it also requires a lot of electrical power. This made it difficult to take such a slit lamp on the study trek.

After a search of several months to find a suitable slit lamp, some brief information was discovered on the smallest slit lamp in the world. It is a hand-held slit lamp type 510L (distributor: Mediconsult Intraocular GmbH) with a magnification of x5 and a variable slit width.

This hand-held slit lamp consists of a magnifying glass with a power of 20D, giving a possible magnification of about x5, plus a pocket light with a variable slit (Figure 3.2.7-1). The hand-held slit lamp was delivered in a hard plastic case. The slit lamp is protected against damage in the hard case so it could be transported safely to and in Nepal.

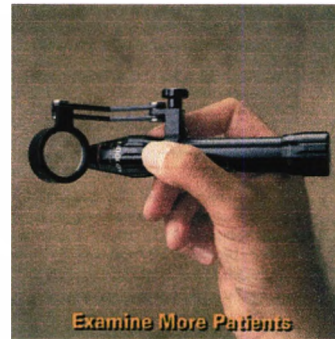


Figure 3.2.7-1 The smallest slit lamp in the world. The angle is variable between the pocket light and magnifying glass. The slit width can also be varied.

3.2.8 Instruments for measuring intraocular pressure

The unit used to indicate intraocular pressure is millimetres of mercury (mmHg)
 $1 \text{ mmHg} = 1,333 \text{ mbar}$ (Kuchling, 1986)

There are two main types of tonometer: contact and non-contact. Topical anaesthetics and fluorescein are needed for contact tonometry. The tonometer used in this study should be lightweight, small, easy to handle, and the measurements should not have an influence on the tears and the corneal surface. Useful contact tonometers are, for example, the Perkins hand-held Goldmann tonometer, the Ocuton A, an automatic hand-held Goldmann tonometer, and the Tono-Pen.

Another interesting contact tonometer is the phosphene tonometer.

The advantages of contact tonometry are:

- Its reference standard for accuracy
- It is easy to check the calibration
- It seldom goes out of calibration
- It displaces little aqueous
- Repeatability of readings
- It is extremely quick to perform with a cooperative patient
- Minimum disruption of corneal epithelium
- It is relatively inexpensive to buy and operate
- It is compact

The disadvantages of contact tonometry are:

- The need for topical anaesthesia and fluorescein,
- Poor or invalid results with an oedematous cornea,
- It is easily influenced by external pressure (Lewis, and Fingeret, 1993)

During the trek, the test subjects IOP was to be measured three times a day. If topical anaesthesia was used, the corneal sensitivity and the quantity of tears would be reduced. Lamberts, Forster, and Perry (1979) showed that topical anaesthetics reduce the volume of tears on the cornea and conjunctiva. This has an effect on the corneal shape and the risk of corneal infections rises.

Fluorescein in solution is a high-risk factor with respect to bacterial contamination. Fluorescein strips are much less risky in a clinical situation, but the water is not always clean in Nepal. The risk of an eye infection is hence too great when topical anaesthetics and fluorescein are given three times a day.

The phosphene tonometer is a very interesting tonometer for use at altitude, but it was not available before we started the Nepal tests. This left only one realistic choice, the Tono-Pen, a contact hand-held tonometer.

After telephone discussions with the distributor, Mentor, a specialist gave assurances that it would be possible to measure IOP on the sclera with the Tono-Pen XL. A paper from Khen, et al (1991) supported this view. They tested the accuracy of Tono-Pen XL measurements from the sclera at the limbus and from the cornea. Table 3.2.8-1 shows the correction factors used when measurements were performed on the sclera (Table 3.2.8-1).

Instrument reading (mm Hg) (Tono-Pen XL used on sclera)	Correction Factor (mmHg)
10	-6.0
15	-5.0
20	-3.0
25	-2.0
30	-1.0

Table 3.2.8-1 On average the Tono-Pen XL will read 4mm high when used on the sclera. This is an average figure, however, and the difference is greater in soft eyes and less in hard eyes.

Unfortunately, this difference does not change in a linear fashion. The correction factors given in this table were used in this study. (Khen et al, 1991)

For example, if a patient, measured at the limbus, has a pressure reading of 20mmHg on the instrument, his true pressure would be 17 mmHg. In the current study, all measurements were taken at the limbus on the scleral side and the same point on every eye was always used when performing the measurements. The IOP was then calculated using the correction factor. The great advantage of this method was that no drugs had to be used. The disadvantage was that the measurements which were performed with the Tono-Pen XL are not as precise as the measurements carried out with the Perkins hand- held Goldmann tonometer but, as explained before, the risks associated with topical anaesthetics and fluorescein at high altitude were too great.

3.2.9 Instruments for inspecting the central retina

A Welch Allyn ophthalmoscope number 11730 was used for central retinal inspection. The author has used the Welch Allyn ophthalmoscope for some years now and is, therefore, very familiar with this instrument. For peripheral retinal inspection, two medications can be used to produce the necessary dilation of the pupils: A muscarine antagonist and an alpha agonist. When the eye inspection is performed twice a day – in the morning and in the evening – these drugs may produce side effects, especially in higher doses.

Due to the reduced cell metabolism as a result of the lower amount of oxygen at high altitudes, a higher dosage of these drugs is necessary and the drugs have a longer effect. Hence, the risk of side effects is not insignificant. With regard to the eyes, the muscarinic antagonist also reduces the accommodation of the eye (Lüllmann, Mohr, and Ziegler, 1996), and any inability to focus clearly at altitude could be fatal if it results in a fall.

With alpha agonists, side effects include constriction of the diameter of blood vessels, causing the heart rate to be elevated and the blood pressure to rise (Lüllmann, Mohr, and Ziegler, 1996). At high altitudes there is less oxygen, and cells produce less energy because of the reduced aerobic citrate cycle the cells need for normal cell function. More erythrocytes are produced to transport more oxygen to the cells. The blood becomes thicker. Therefore, the risk of thrombosis rises when the blood vessel diameter also becomes smaller. Physical effort at high altitude already induces a high heartbeat rate and higher blood pressure. The use of drugs which also induce the same effect is potentially dangerous.

A further disadvantage of using mydriatics to dilate the pupil is that when the pupil is widened a higher dose of UV radiation reaches the retina.

A study performed by Schumacher and Petajan (1975) revealed the typical retinal change that occurs at high altitude. The eyes of 47 subjects were inspected on Mt. McKinley (summit 20,300 ft). At below 14,200 ft there were no significant retinal changes, while at 14,200 ft and higher the retinal changes were described as significant. There is no information as to how this significance was calculated. The typical retinal change (haemorrhage) is positioned in the central area of the retina (Figure 3.2.9-1). This change can also be seen with an ophthalmoscope without the aid of diagnostic drugs.

Due to the risk factors described above, diagnostic drugs for widening the pupils were not used. The eye inspections were instead performed in a tent to reduce the light intensity around the eye.

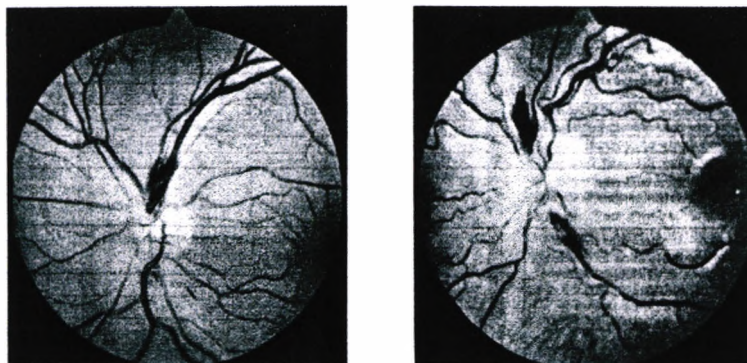


Figure 3.2.9-1 Typical examples of retinal haemorrhages observed at high altitude.
(Schumacher and Petajan, 1975)

3.2.10 Instruments for measuring corneal shape

At present the best instrument for inspecting corneal shape is a keratographer. There are many systems on the market.

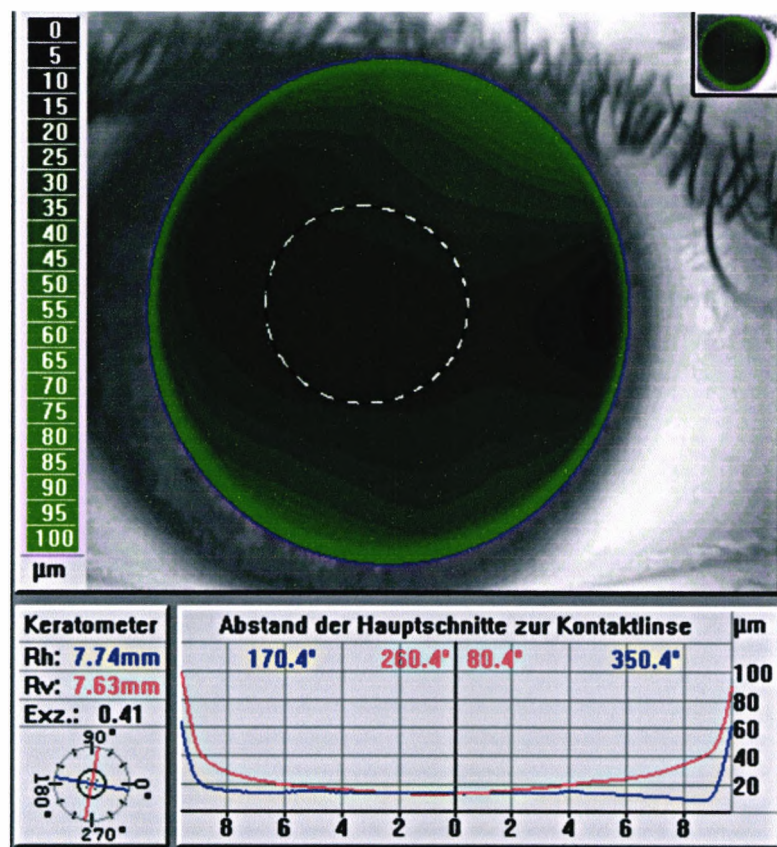
The Oculus keratographer in combination with a laptop (Model Artist with 366 MHz Pentium 2, 62 MB RAM and 4634 MB hard disk) was taken on the trek to measure the corneal shape in Nepal. It is possible to operate the system with a laptop, but the measuring instrument requires the correct electrical power. The Oculus system uses 22000 measurement points on the corneal surface, calculated with the aid of twenty-two Placido circles projected onto the surface of the cornea. However, the main reason for choosing this system was that the company made it possible to use its database. The normal keratographer programme is not very useful for statistics because picture differences can only be evaluated subjectively.

3.2.10.1 The programme used to describe corneal shape

Lingelbach (1999) described the optical quality of the cornea with the aid of an ellipsoid and Zernike coefficients. After they had published their article, Mrs. Lingelbach dipl. Ing. (FH) and Professor Bernd Lingelbach wrote a special programme which is designed to transform all of the keratographer programme base data from a cornea into a mathematical description of corneal shape. This description consists of two parts. The first part is an ellipsoid and the second part is calculated with Zernike polynomials. Every measurement is thus based on 20 values, two values for an ellipsoid, eleven Zernike coefficients and seven angles. The Zernike data shows the different kinds of lens errors for the cornea. Measurements which are calculated with more than eighteen Zernike values are problematic because either the tear film thickness varies across the cornea or denatured proteins on the cornea have an influence on the results.

The manufacturer installed a special button named "Zernike" on the contact lens-fitting side of the keratographer programme. The Zernike button makes it possible to get the base data from every observed measurement with the keratographer programme.

When the Zernike button is pressed the keratographer base data are taken by the Lingelbach programme which transforms the keratographer data into a combination of an ellipsoid and Zernike polynomials as described above. The quality of the Lingelbach programme corneal shape fitting can be tested on the contact lens page of the Oculus programme, because the Oculus contact lens programme is able to use the Lingelbach programme file format for describing the ellipsoid-Zernike shape as a contact lens fluorescein picture on the surface of the subject's eye. Every fitting of a considered corneal shape can be visually checked at this stage before it is taken for further mathematical and statistical consideration (Figure 3.2.10.1-1).



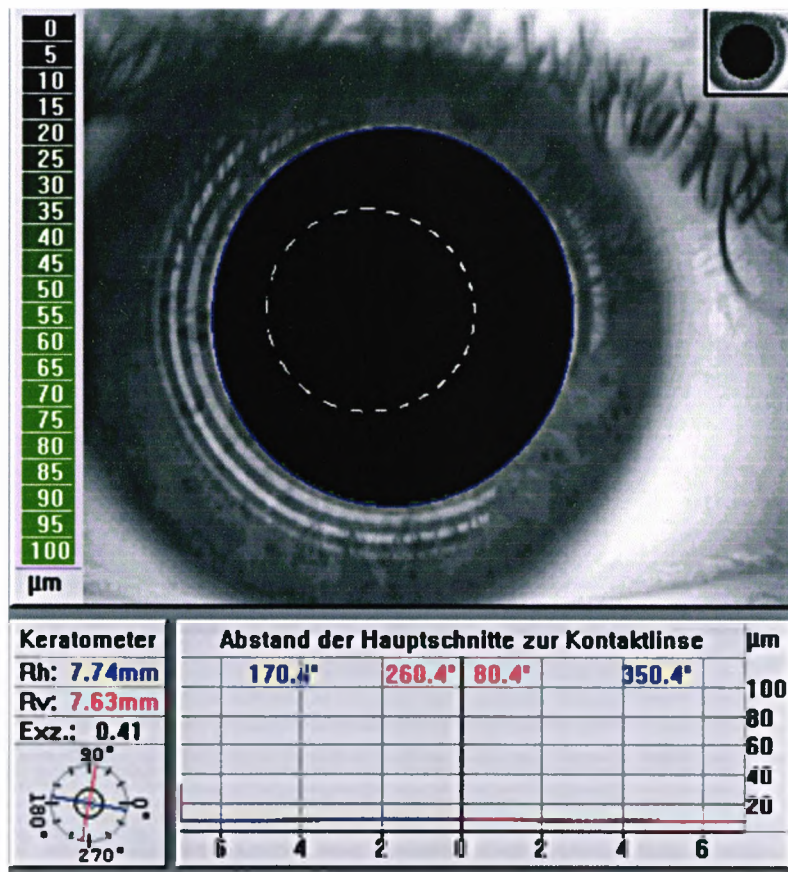


Figure 3.2.10.1-1 Output from the Oculus Keratographer. The upper picture shows a contact lens fluorescein simulation and the lower is taken as a visual measure for the quality of the ellipsoid-Zernike shape description.

Shortly before the tour to Nepal began, Professor Bernd Lingelbach sent the special Zernike programme to the author. The programme was the first version called Zernik1. After returning from Nepal, the database was transformed into the Zernike data for statistical analysis purposes.

After performing some basic statistical calculations (median, minimum, maximum, range, standard deviation, and variance), it was discovered that the variation of the corneal shape was very large. To investigate this surprising result a programme was written to test whether all the computed corneal shapes from one eye conformed with each other as they should. The programme was used to make a cut through the three-dimensional corneal shape calculated with the Zernike coefficients plus ellipsoid values from Professor Bernd Lingelbach's programme.

The front of the cut is two-dimensional, it is perpendicular to the base of the three-dimensional graphic, and it is possible to cut in all directions. All the two-dimensional cuts on one eye were traced onto one graph. Three graphs were drawn for each eye.

The first graph contained cuts with an angle of 0° , the second contained cuts with an angle of 45° , and the third contained cuts with an angle of 90° . After performing this test, it was clear that the three-dimensional ellipsoids - Zernike graphs did not exactly conform to one another. As a result, a new version of the programme, called Zerniklneu, was written by Mrs. Lingelbach dpl. Ing. (FH), taking into account the changes we had discussed. Using the new version of the programme, the keratographer database was converted to the ellipsoid-Zernike form, and then transformed into a format for statistical evaluation. These Zernike data were tested with perpendicular cuts as explained above. Spot checks were carried out to test the ellipsoid-Zernike data with three-dimensional graphs. In this manner, seven versions of the programme were written and tested until all the three-dimensional graphs conformed to each other.

The main difference between the first and the latest version is that the first version calculates every measurement separately. The latest version calculates one measurement and defines this measurement as the main one (which is referred to as the master). The corneal shapes which were calculated from all the remaining measurements of the eye examined were centred on the master three-dimensionally during the calculation. Thus the Zernike coefficient differences describe the real corneal shape differences for the eyes under consideration.

3.2.10.2 The quality of shape fitting statistical analysis

In terms of statistics there are some important considerations to be considered with respect to the Zerniklneu program.

In chapter 3.2.10.1 it was noted that the Zernikneu programme consists of two parts. Both parts of the programme - the master fitting and the other measurement fittings are calculated with the aid of iteration.

Two conditions have to be fulfilled. First of all, the z-scores of the database and the curve fitting have to be at a minimum and, secondly, the standard deviation has to be less than 0.0001. It is not useful to use a value smaller than 0.0001 for the standard deviation as a measurement of the quality of the shape fitting, the reason being that proteins in the tear film would have an influence on the results of the hypothesis test. The tear film is only 0.007 mm thick (Chapter 1.4.5) and is therefore too small to have an influence on the results of corneal shape change. However, no circles can be reflected from the cornea without a tear film in front of its surface, therefore subjects were instructed not to interrupt eye blinking during the measurement process.

3.2.10.3 The role of a best fitted ellipsoid

The best symmetrical form to describe the corneal shape is an ellipsoid. The data for an almost ideal ellipsoid would be the best in describing a typical corneal shape.

A combination of a geometrical form and Zernike polynomials makes it easier to turn and to transform graphs than is possible using only Zernike polynomials. Two values, first the central radius, and second g , where ($g = 1 - \epsilon^2$) define an ellipsoid.

Both values are calculated in the period during which the master is fitted.

This ellipsoid is taken for every other corneal shape description of the same eye. In other words, one ellipsoid is used for all measurements of one eye.

That ensures that any changes in the corneal shape are expressed only by the Zernike polynomials.

Figure 3.2.10.3-1 shows the appearance the wave fronts take on an ideal optical surface:

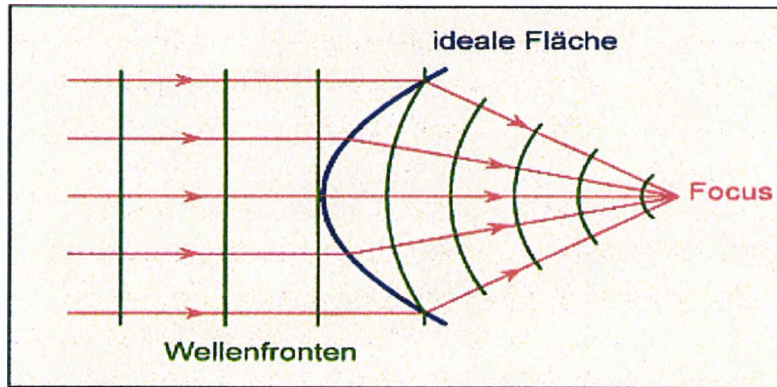


Figure 3.2.10.3-1 An ideal optical surface demonstrated using wave fronts.

The following mathematical condition has to be met for an ideal optical surface:

For a material of refractive index (n), and length (l): $n \cdot l = l_1 + n \cdot l_2$ (Figure 3.2.10.3-2)

The optical length has to be the same at every point of an ellipsoid so that the ellipsoid has no lens aberrations.

The formula used to calculate an ellipsoid is:

$y^2 = 2r_0x - gx^2$, where $g = 1 - \epsilon^2$, $r_0 =$ central radius, and $\epsilon =$ eccentricity.

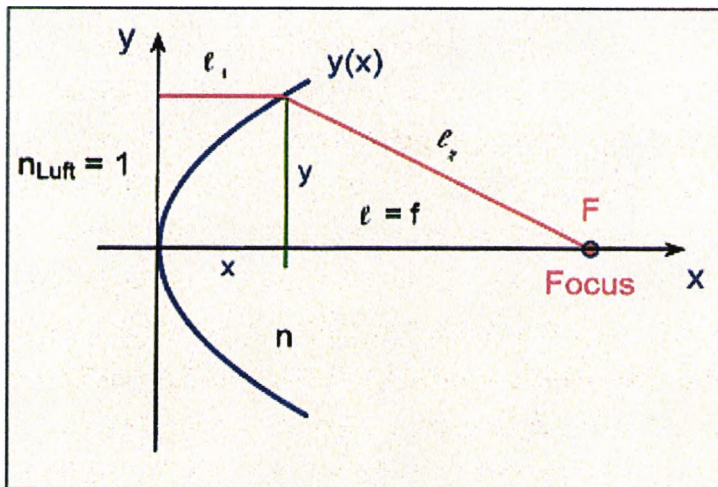


Figure 3.2.10.3-2 The condition for an ideal ellipsoid is $n \cdot l = l_1 + n \cdot l_2$.

When l_1 and l_2 are described so that they depend on y (Figure 3.2.10.3-2) and both lengths are entered in the formula $n \cdot l = l_1 + n \cdot l_2$ the formulae then have to be manipulated so that y^2 is positioned alone on one side of the equation.

After this it is possible to eliminate y^2 , replacing it with the help of the ellipsoid formula. The result of the calculation is that an ideal ellipsoid has an eccentricity ϵ , where $\epsilon = 1/n$. In this study, n is the corneal refractive index of 1.332. The cornea should have an eccentricity of $\epsilon = 0.751$ (Lingelbach, 1999).

3.2.10.4 Zernike polynomials

Zernike polynomials are circle polynomials, i.e. the basis for Zernike polynomials is a circle. The rims of contact lenses are circular and the projected Placido circles represent the basis for Zernike polynomials. All the measurement points lie on Placido circles. Therefore the Zernike polynomials are ideal for describing the corneal shape resulting from the measurement points. Furthermore, every coefficient corresponds to a lens error defined with the help of wave fronts.

The Zernike coefficient functions are calculated using the following formulae:

$$\rho(\rho, \vartheta) = \sum a_{n,m} \cdot Z_{n,m}(\rho, \vartheta), \quad \rho = \frac{h}{h_{\max}}$$

$$Z_{n,m}(\rho, \alpha) = \sum_{k=0}^{\frac{n-m}{2}} \frac{(-1)^k (n-k)!}{k! \left(\frac{n+m}{2} - k\right)! \left(\frac{n-m}{2} - k\right)!} \rho^{n-2k} \cos(m(\alpha - \alpha_{n,m}))$$

Figure 3.2.10.4-1 The formulae for the Zernike polynomial functions. $m \leq n$, $n-m = 2, 4, 6 \dots$ (Lingelbach, 1999)

For our purposes, the basis of the Zernike polynomials is a circle with the radius being one, and thus the convergence criteria of Zernike polynomials are fulfilled. The radius is standardized using the following formula:

$$\rho = h/h_{\max} \text{ (Figure 3.2.10.4-1).}$$

h is the distance of a point on the corneal shape which is considered measured from the centre of the shape.

h_{\max} is the radius of the corneal surface that is calculated. The area of every calculated corneal shape has a basic radius of 3.5 mm.

Only subjects with regular corneas were chosen (with the maximum corneal astigmatism of 4.5 diopters in subject 1.22). In such subjects, Zernike polynomials to the order of six in combination with an ellipsoid were sufficient to represent well the possible corneal shape changes.

Zernike coefficients are used to describe corneal shape as follows:

$$a_{0,0}, a_{2,0}, a_{4,0}, a_{6,0}, a_{1,1}, a_{3,1}, a_{5,1}, a_{2,2}, a_{4,2}, a_{3,3}, a_{4,4}$$

The following lens errors are described by the Zernike coefficients.

The functions result from using the formulae, as shown in Fig.3.2.10.4-1:

3.2.10.4.1 Spherical part of the Zernike polynomials

Piston	$Z_{0,0}(p) = a_{0,0} * 1$
Defocus	$Z_{2,0}(p) = a_{2,0} * (2p^2 - 1)$
Sph. Aberration1	$Z_{4,0}(p) = a_{4,0} * (6p^4 - 6p^2 + 1)$
Sph. Aberration2	$Z_{6,0}(p) = a_{6,0} * (20p^6 - 30p^4 + 12p^2 - 1)$

3.2.10.4.2 Angle-dependent part of the Zernike polynomials

Tilt	$Z_{1,1}(p, \alpha) = a_{1,1} * p \cos(\alpha - \alpha_{1,1})$
Coma1	$Z_{3,1}(p, \alpha) = a_{3,1} * (3p^3 - 2p) \cos(\alpha - \alpha_{3,1})$
Coma2	$Z_{5,1}(p, \alpha) = a_{5,1} * (10p^5 - 12p^3 + 3p) \cos(\alpha - \alpha_{5,1})$
Astigmatism1	$Z_{2,2}(p, \alpha) = a_{2,2} * p^2 \cos 2(\alpha - \alpha_{2,2})$
Astigmatism2	$Z_{4,2}(p, \alpha) = a_{4,2} * (4p^4 - 3p^2) \cos 2(\alpha - \alpha_{4,2})$
Triangular	$Z_{3,3}(p, \alpha) = a_{3,3} * p^3 \cos 3(\alpha - \alpha_{3,3})$
Ashtray astig.	$Z_{4,4}(p, \alpha) = a_{4,4} * p^4 \cos 4(\alpha - \alpha_{4,4})$

3.2.10.4.3 The graphical demonstration of the Zernike polynomials

The extension of a corneal shape which is described with the help of Zernike polynomials here is standardized with radius one (distance of a considered point to the centre of the corneal shape /3.5 mm) therefore the abscissa has no unit. The ordinate is not standardized.

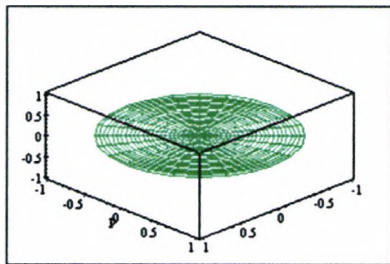


Figure 3.2.10.4.3-1 Piston

$$Z_{0,0}(p) = a_{0,0} * 1$$

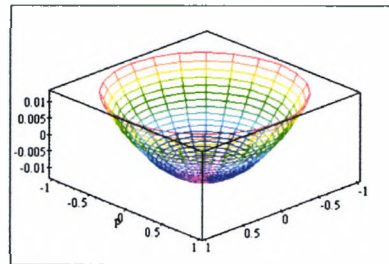


Figure 3.2.10.4.3-2 Defocus

$$Z_{2,0}(p) = a_{2,0} * (2p^2 - 1)$$

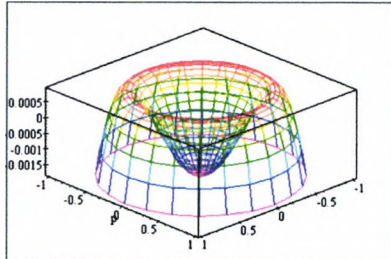


Figure 3.2.10.4.3-3 Sph. Aberration 1

$$Z_{4,0}(p) = a_{4,0} * (6p^4 - 6p^2 + 1)$$

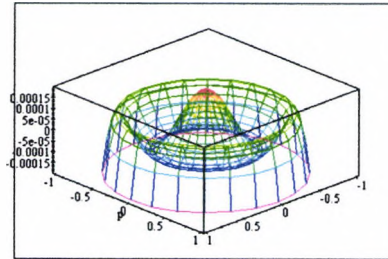


Figure 3.2.10.4.3-4 Sph. Aberration 2

$$Z_{6,0}(p) = a_{6,0} * (20p^6 - 30p^4 + 12p^2 - 1)$$

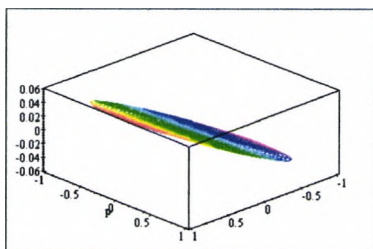


Figure 3.2.10.4.3-5 Tilt

$$Z_{1,1}(p,v) = a_{1,1} * p \cos(\alpha - \alpha_{1,1})$$

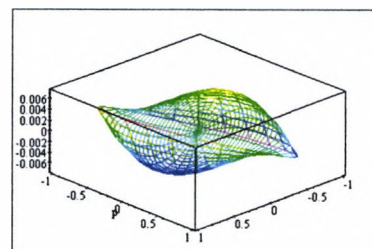


Figure 3.2.10.4.3-6 Coma 1

$$Z_{3,1}(p,v) = a_{3,1} * (3p^3 - 2p) \cos(\alpha - \alpha_{3,1})$$

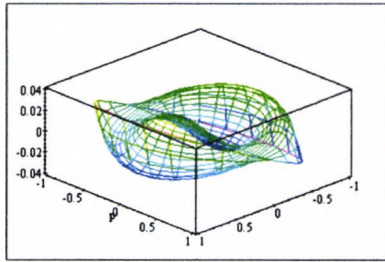


Figure 3.2.10.4.3-7 Coma 2

$$Z_{5,1}(p,v) = a_{5,1} * (10p^5 - 12p^3 + 3p) \cos(\alpha - \alpha_{5,1})$$

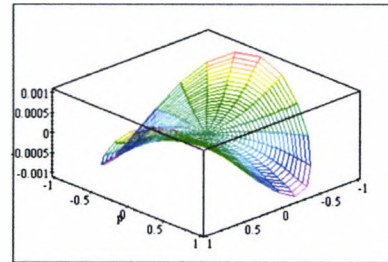


Figure 3.2.10.4.3-8 Astigmatism 1

$$Z_{2,2}(p,v) = a_{2,2} * p^2 \cos 2(\alpha - \alpha_{2,2})$$

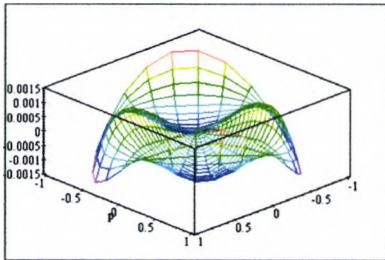


Figure 3.2.10.4.3-9 Astigmatism 2

$$Z_{4,2}(p,v) = a_{4,2} * (4p^4 - 3p^2) \cos 2(\alpha - \alpha_{4,2})$$

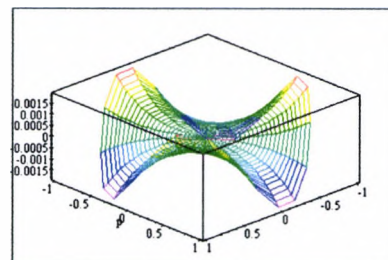


Figure 3.2.10.4.3-10 Triangular

$$Z_{3,3}(p,v) = a_{3,3} * p^3 \cos 3(\alpha - \alpha_{3,3})$$

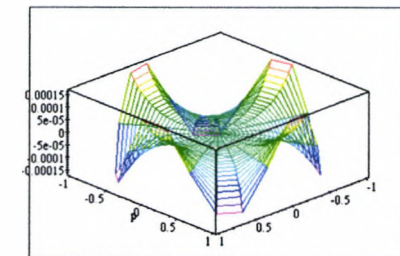


Figure 3.2.10.4.3-11 Ashtray astig.

$$Z_{4,4}(p,v) = a_{4,4} * p^4 \cos 4(\alpha - \alpha_{4,4})$$

3.2.10.5 rms

The variable rms represents a corneal shape which is expressed by Zernike polynomials. It gives information about how flat or steep wave fronts are. The variable rms is calculated in three steps.

The following mathematical steps are required:

$$\begin{array}{ll}
\text{for } n, m \in N_0 & \text{for } n, m \in N \\
m = 0 & \text{when } m = 1 \text{ then } n = 1, 3, 5 \\
n = 2, 4, 6 & \text{when } m = 2 \text{ then } n = 2, 4 \\
& \text{when } m = 3 \text{ then } n = 3 \\
& \text{when } m = 4 \text{ then } n = 4
\end{array}$$

$$a = \sum_{n=2}^6 \left(\frac{a_{n,m}}{\sqrt[3]{(n+1)}} \right)^2 \quad b = \sum_{m=1}^4 \sum_{n=1}^5 \left(\frac{a_{n,m}}{\sqrt[3]{2*(n+1)}} \right)^2$$

$$rms = \sqrt[3]{a + b}$$

3.2.10.6 Residual rms

Residual rms values, which represent the change in the corneal shape, are taken for testing the corneal shape change during the mountaineers' trek in Nepal.

This variable is called the residual root mean square value.

It is calculated as follows:

The mean is calculated for each of the Zernike coefficients

($a_{2,0}$, $a_{4,0}$, $a_{6,0}$, $a_{1,1}$, $a_{3,1}$, $a_{5,1}$, $a_{2,2}$, $a_{4,2}$, $a_{3,3}$, $a_{4,4}$) recorded throughout the trek for each eye. Then the differences are computed between the Zernike coefficients for a keratographer measurement and the calculated mean coefficients "mean shape" for the same eye. The new Zernike coefficients differences (Zernike coefficients measurement minus mean coefficients) which are calculated for each measurement of one eye are transformed into a value referred to as residual rms with the aid of the formulae that are used to compute rms (see above). The mathematical steps as explained above render all calculated residual rms comparable.

Although the "mean shape" of every eye differs, this is not of any importance in the hypothesis testing, as justified by the following argument:

Every eye has different mean Zernike coefficients, referred to as "mean shape", but the mathematical way to determine the "mean shape" is the same for every eye.

Therefore, the “mean shape” is the standard we need to compare all the residual rms values from different eyes.

It is important to note, however, that every change in corneal shape, which is expressed with the value residual rms, is related to the “mean shape”, a virtual shape.

3.3.3 Calibration of instruments used in this study

The instruments which are described in this chapter from sections 3.2.3 to 3.2.10 were calibrated prior to the trek. Some important points should be considered. All tests were carried out in an air conditioned room. The temperature ranged between 19 and 21 degrees Celsius and the humidity ranged from 47% to 52%.

Values can not be measured objectively with two of the instruments; the slit lamp number 510L and the Welch Allyn ophthalmoscope. Here, signs should be detected subjectively and transformed into values with the help of the CCRLU grading scale. Following standardization of these subjective data it is possible to analyze them. The quality of these measurements depends on how skilled the observer is at obtaining and interpreting the images viewed using the slit lamp and ophthalmoscope.

To become as familiar as possible with these instruments, especially with the handling of the hand held slit lamp, the researcher carried out eye examinations first using a Zeiss slit lamp and then with a 90D Volk lens in combination with a Zeiss slit lamp. Shortly after this, the eyes were examined using the Slit lamp 510L and the Welch Allyn ophthalmoscope.

The Thommen 7000 altimeter and the Schneider aneroid barometer were calibrated together, because the similar structure of their components makes functionality absolutely comparable.

This altimeter is an aneroid barometer with an altitude scale (meter) combined with an air pressure scale (mbar) in front of the instrument (see chapter 3.2.4).

3.3.1 Altimeter and aneroid barometer

Both instruments were positioned in an air-tight box. While air was sucked out of the box, measurements were taken with both instruments simultaneously at different levels of air pressure. This procedure was repeated over an air pressure range from 940 mbar to 380 mbar (Table 3.3.1-1).

(1) Air pressure altimeter mbar	(1) Air pressure barometer mbar	(2) Air pressure altimeter mbar	(2) Air pressure barometer mbar
940	940	940	940
870	869	850	850
720	719	710	709
660	660	665	665
570	571	540	539
420	421	430	429
380	381	385	385

Table 3.3.1-1 Air pressure measured with an altimeter and a barometer. These data were obtained from two test sessions, (1) and (2). Pressure was measured at seven points from 940 mbar to 380 mbar.

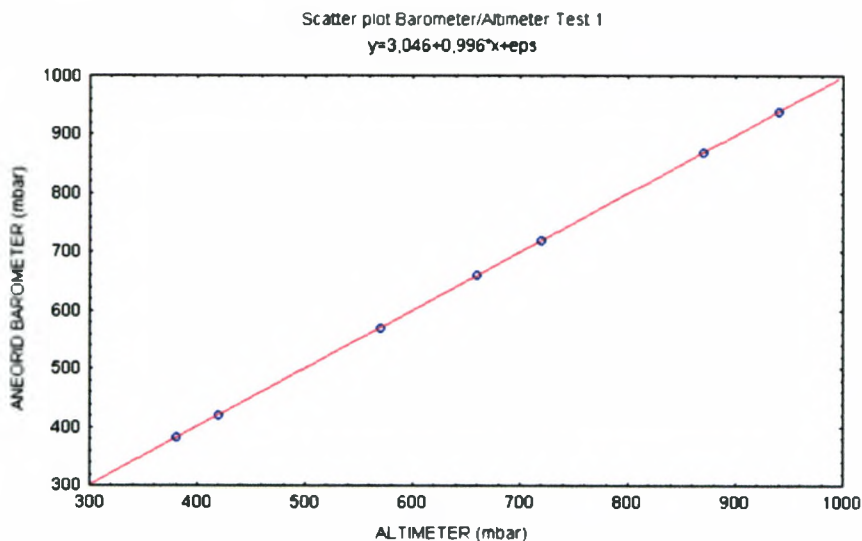


Figure 3.3.1-1 Scatter plot of data from the altimeter and aneroid barometer over an air pressure range from 940mbar to 380mbar (Test 1).

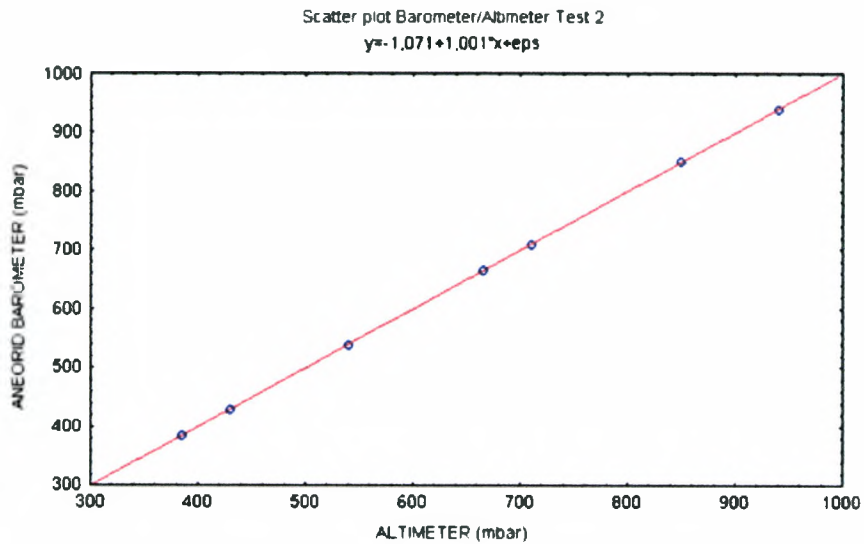


Figure 3.3.1-2 Scatter plot of data from the altimeter and aneroid barometer over an air pressure range from 940mbar to 380mbar (Test 2).

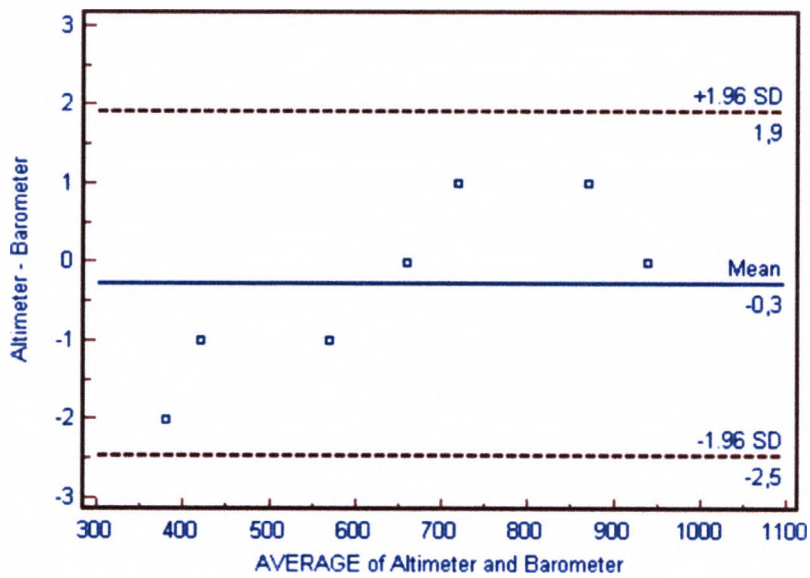


Figure 3.3.1-3 The Altman-Bland plot of the differences between the altimeter and the aneroid barometer in mbar for Test 1. The 'mean' line (bias) and the 95% confidence intervals for the differences are shown.

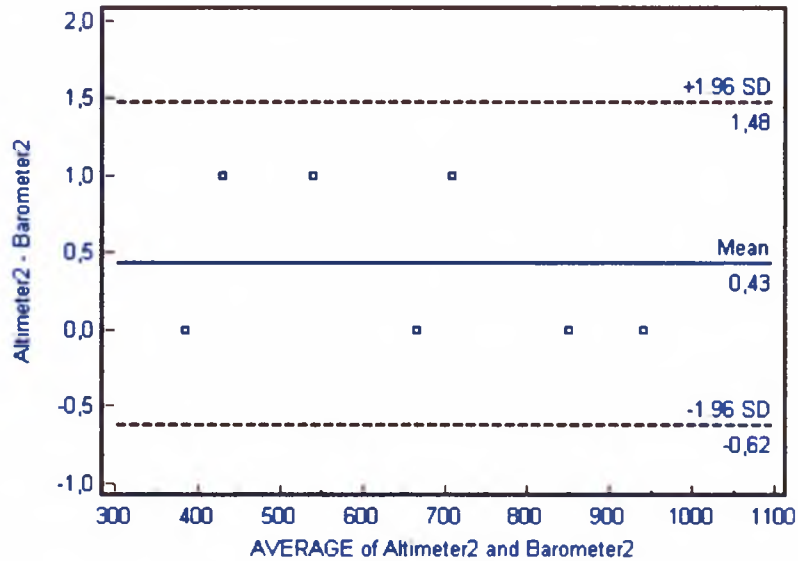


Figure 3.3.1-4 The Altman-Bland plot of the differences in mbar between the altimeter and the aneroid barometer for Test 2. The 'mean' line (bias) and the 95% confidence intervals for the differences are shown.

The data sets from both test phases confirm the good agreement between the tested instruments. This can be seen from the scatter plots of the two data sets (Figure 3.3.1-1, figure 3.3.1-2).

A closer consideration of the first test procedure reveals that two pressure values are identical, two values are smaller (1 mbar), and three values are greater (1 mbar) than the altimeter ones. Generally speaking, the barometer tends to measure lower values in a range from 940 mbar to 660 mbar and higher ones beneath 660 mbar. This tendency is reversed when the results of the second test procedure are analysed. Here, four values of both instruments are identical, and three barometer values are smaller than altimeter ones. Figure 3.3.1-3 shows that the first measurement procedure the altimeter values tend to be smaller than the barometer value. However the second procedure shows the opposite result. In both Bland-Altman plots (1986) the bias in the measurements is less than 1 mbar, therefore these results support the manufacturers' quality description of ± 1 mbar for the barometer and ± 8 m for the altimeter (corresponding to a measurement agreement of ± 1 mbar).

3.3.2 Thermometer

The tests were undertaken using as a “gold standard” two precision thermometers, that are usually part of an Assmann aspiration psychrometer, which were compared with two identical Möller Therm thermometers, model number 106705. The manufacturers of the psychrometer thermometers claim an accuracy of 0.2 °C from -10 °C to +60 °C. For the Möller Therm thermometer the manufacturers claim an accuracy of 1.0 °C from -30 °C to +50 °C for model number 106705. A range of temperatures from -20 °C to +35 °C were prepared for comparing all four instruments simultaneously. First a “cold pack” was mixed using 100 g of water ice and 31 g NaCl. The Möller Therm thermometers were inserted into the ice pack. When both thermometers showed -20 °C measurements were taken in steps of 5 °C until -10 °C, then the “psychrometer thermometers” were placed into the same bowl filled with ice and salt. Afterwards, the temperature of Möller Therm thermometers were taken in steps of one degree and “psychrometer thermometers” in steps of 0.5 degrees until +35 °C. From -2 degrees, the bowl containing the ice/salt mixture and the thermometers was slowly warmed to +35 degrees, and measurements taken as described above. Data from all instruments were then analysed to assess inter- and intra-instrument agreement.

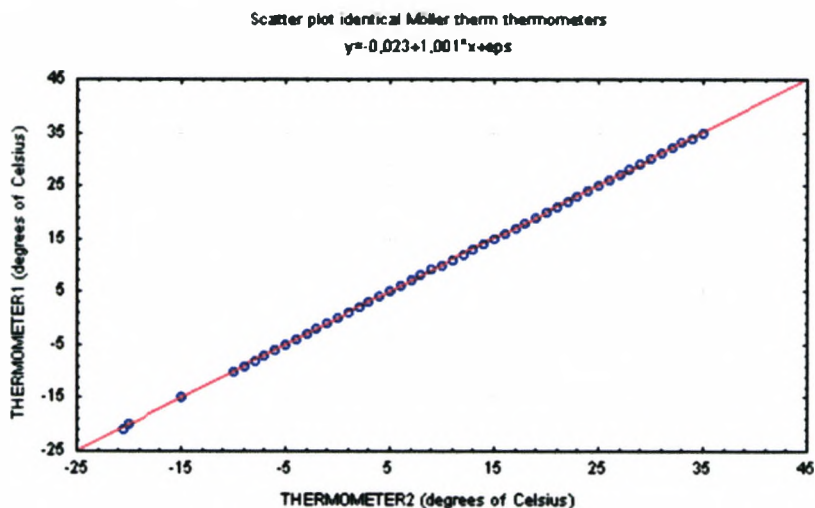


Figure 3.3.2-1 Scatter plot for temperatures recorded with the two Möller Therm thermometers.

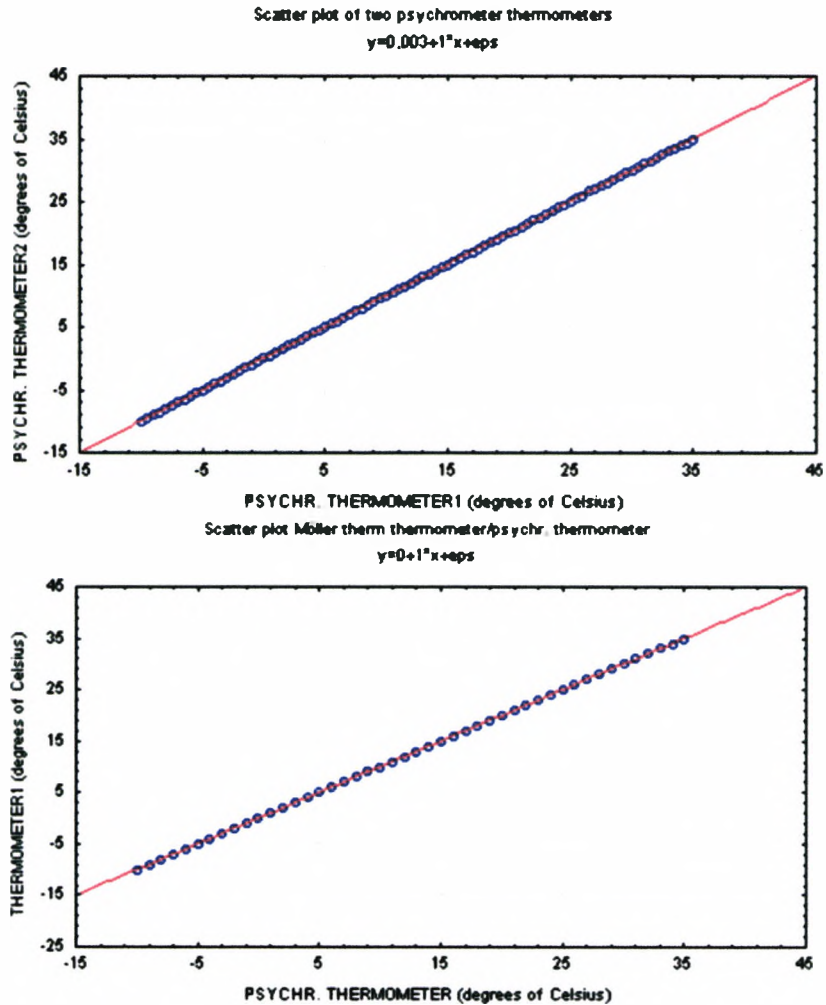


Figure 3.3.2-2 Scatter plot for temperatures recorded with the Möller therm thermometer and the psychrometer thermometer.

In consideration of the manufacturers' thermometer accuracy both types of instruments showed good agreement over the whole range of measured temperatures. In fact, both psychrometer thermometers measured identical temperatures throughout and fulfilled all expectations. This is an important result because these instruments will also be used to measure humidity. The difference between values recorded by one thermometer, which inserts into a wet wick, and the surrounding temperature determined by the second thermometer is related to a measure of the quantity of water evaporation.

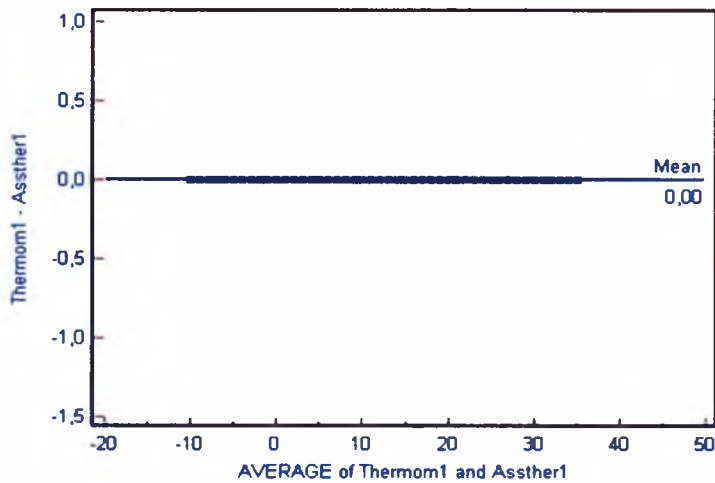
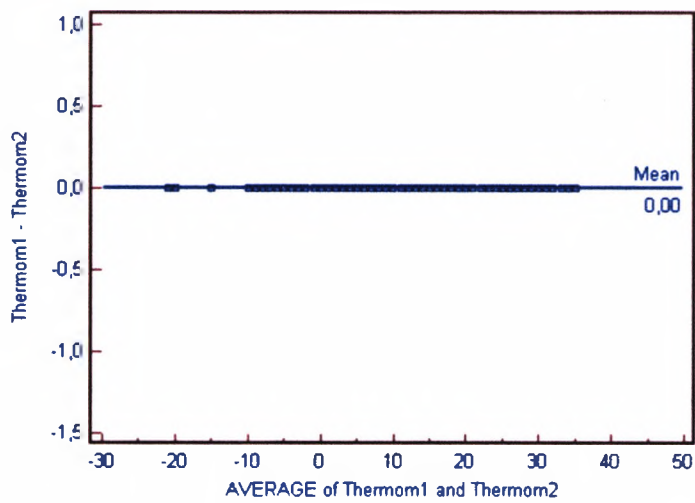
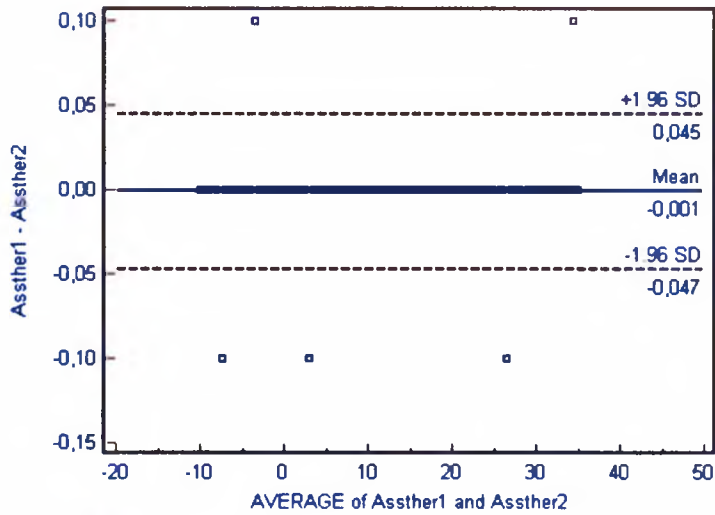


Figure 3.3.2-3 The Altman-Bland plots of the differences in temperature measurements plotted against their means for: Top figure, the two Assmann thermometers (rounding up/off 0.5 °C); Middle figure, the two Möller thermometers (rounding up/off 1.0 °C); Bottom figure, Assmann 1 and Möller 1 thermometers (rounding up/off 1.0 °C). The 'mean' line (bias) and the 95% confidence intervals, where relevant, for the differences are shown.

The Altman-Bland plots in figure 3.3.2-3 show excellent agreement between both Assmann aspiration psychrometers, both Möller Therm thermometers, and between the Assmann psychrometer 1 and Möller Therm thermometer 1. The values of the psychrometer thermometers are rounded up/off in steps of 0.5 degrees and the Möller thermometers in steps of 1 degree.

3.3.3 Hygrometer

The Assmann aspiration psychrometer pumps air along both precision thermometers to get fast accurate results (chapter 3.2.6). A table is used to measure the humidity with the help of two values, the surrounding temperature and the difference between the surrounding and evaporation temperatures. The manufacturers state a measurement tolerance of $\pm 1.0 \%$. It is used in this study to test the repeatability and accuracy of a second precision hygrometer (Fischer), which was also wrapped into a wet cloth for 20 minutes, by which point a humidity of 98 % is expected. After the wet cloth was removed the values of both hygrometers were compared until a surrounding humidity of 48% was reached. Then the instruments and bags containing magnesium chloride (which functions as a desiccant) were placed in an air-tight box. The lowest humidity that could be achieved with this equipment was 15%. Carrying out the tests using the box was very difficult because the wet wick had to be changed before each measurement was taken. However, the more occasions on which the box is opened, the greater is the risk that the humidity will rise inside the box. Additionally, the desiccant bags must not be placed under the wet wick of the psychrometer as this would produce unreliable results. For these reasons only four measurements were taken using the air-tight box (Table 3.3.3-1).

Humidity %					
Psychrom.	Hygrom.	Psychrom.	Hygrom.	Psychrom.	Hygrom.
98%	98%	66%	65%	24%	23%
90%	90%	60%	60%	15%	15%
85%	85%	54%	55%		
80%	80%	50%	50%		
75%	75%	45%	45%		
70%	70%	40%	40%		

Table 3.3.3-1 Humidity recorded by the Assmann Psychrometer and the Fischer Hygrometer over a range of humidity settings.

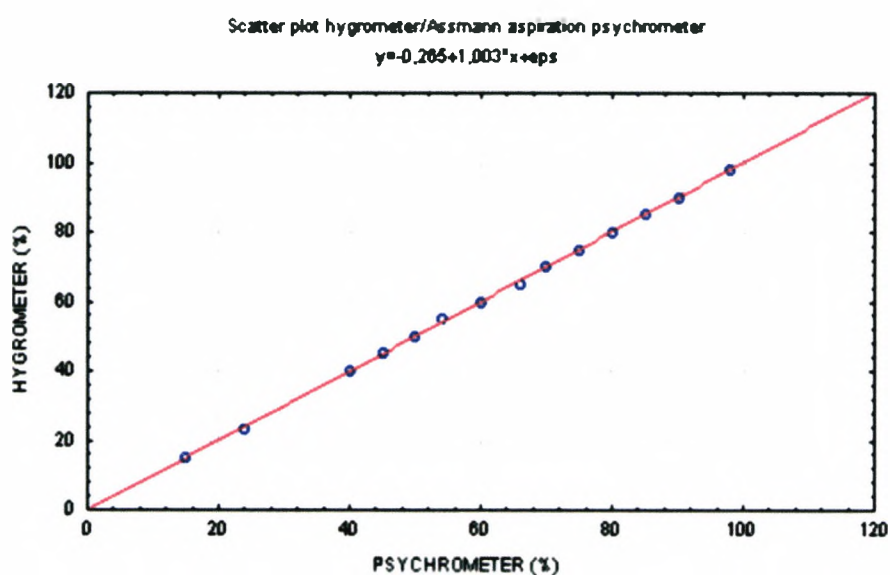


Figure 3.3.3-1 Scatter plot for humidity recorded with the Assmann Psychrometer and the Fischer Hygrometer.

In spite of the difficulties associated with carrying out these tests, Table 3.3.3-1 and the scatter plot in Fig3.3.3-1 indicate the good agreement between the hygrometers. Only three measurements of both instruments varied, and this was by a tolerable one per cent.

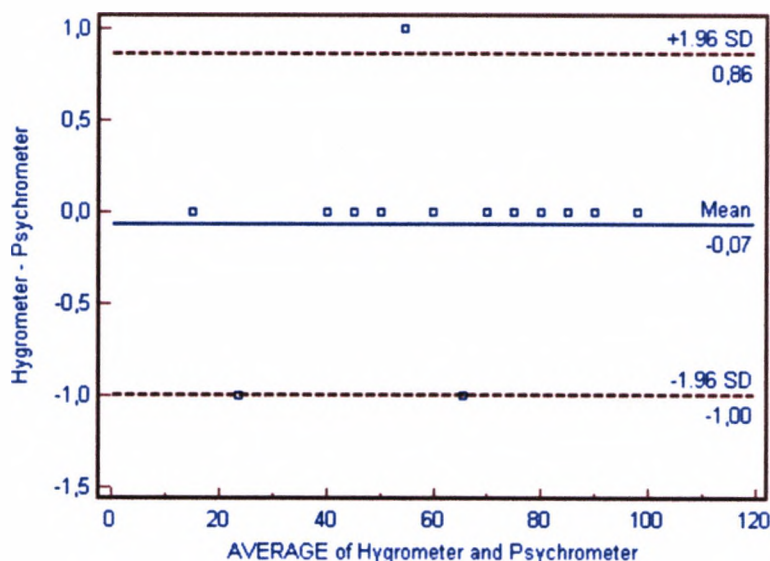


Figure 3.3.3-2 The Altman-Bland plot of the differences in humidity (%) measured by the Assmann Psychrometer and the Fischer Hygrometer. The 'mean' line (bias) and the 95% confidence intervals for the differences are shown.

This good agreement between the instruments is confirmed by the Altman-Bland plot (Figure 3.3.3-2), which shows minimal bias (-0.07%) and confidence intervals which are within 1%.

3.3.4 Tonometry

The Tono-Pen® XL and the Reichert AT 550 non contact tonometer were the instruments of choice. The ability to take a very fast measurement on the sclera, unproblematic handling, and the very small size were the main factors for selecting the Tono-Pen for the trek in Nepal (chapter 3.2.8). The non contact tonometer was used to obtain reference data for testing the reliability of the Tono-Pen. Before the test phase the tonometers were calibrated according to the manufacturers' recommendations. The Reichert AT 550 was new and was calibrated by a technician from the manufacturers. The method of calibration for the Tono-Pen is as follows:

- First the measurement button should be pressed twice with the instrument held perpendicularly pointing downwards.
- Immediately, after the display gives the instruction “up”, the tip of the tonometer is held in an upwards direction until a good calibration is confirmed. At this point the instrument is ready for measuring.

When the Tono-Pen is used the pressure measured on the sclera is converted to an estimate of the IOP by adding a correction factor which is taken from table 3.2.8-1. The mean of four estimated eye pressures using the Tono-Pen was compared with the mean of three non contact tonometer values. Both eyes of three subjects were measured 20 times (giving five IOP measurements in total for each eye) with the Tono-Pen and 15 times with the non contact tonometer (giving five IOP measurements in total for each eye).

Table 3.3.4-1 lists the mean values for both instruments. The risk that a single measurement from the sclera will be inaccurate because of the variability of pressure measurements using the Tono-Pen on the sclera led to the conclusion that the mean of four measurement values is more reliable than of one value. The negative aspect of using mean values is based on the fact that information on the variation of IOP with systole and diastole is lost.

IOP in mmHg				
	R. Tono P.	R. Non kon	L. Tono P.	L. Non Kon
Subject 1	13	11	14	12
	14	11	13	13
	11	12	14	11
	14	12	15	12
	15	13	16	12
Subject 1 SD	1.52	.84	1.14	.71
Subject 2	20	17	20	18
	18	17	21	18
	21	17	18	17
	20	18	19	17
	19	17	20	18
Subject 2 SD	1.14	.45	1.14	.55
Subject 3	20	14	16	14
	19	14	16	15
	17	14	19	14
	17	15	20	14
	18	15	19	15
Subject 3 SD	1.30	.55	1.87	.55

Table 3.3.4-1 The mean IOP of right and left eyes of three subjects. Each IOP in the table was the mean of either four Tono-Pen measurements or three non contact tonometer measurements. Five mean IOP values are listed for each subject. SD = standard deviation.

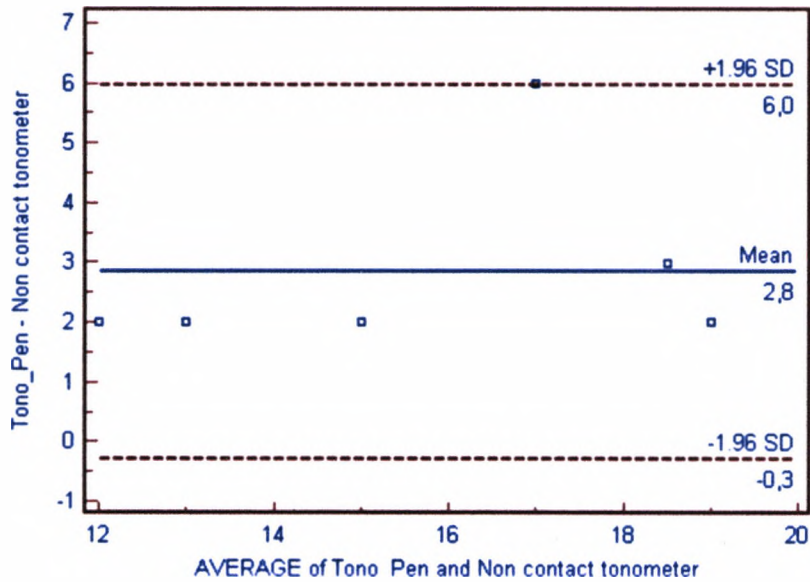


Figure 3.3.4-1 Agreement between the Tono-Pen and non-contact tonometer assessed using an Altman-Bland difference plot. Data is plotted for six eyes, using the first data pair of each eye shown in table 3.3.4-1. The unit of both abscissa and ordinate is mmHg.

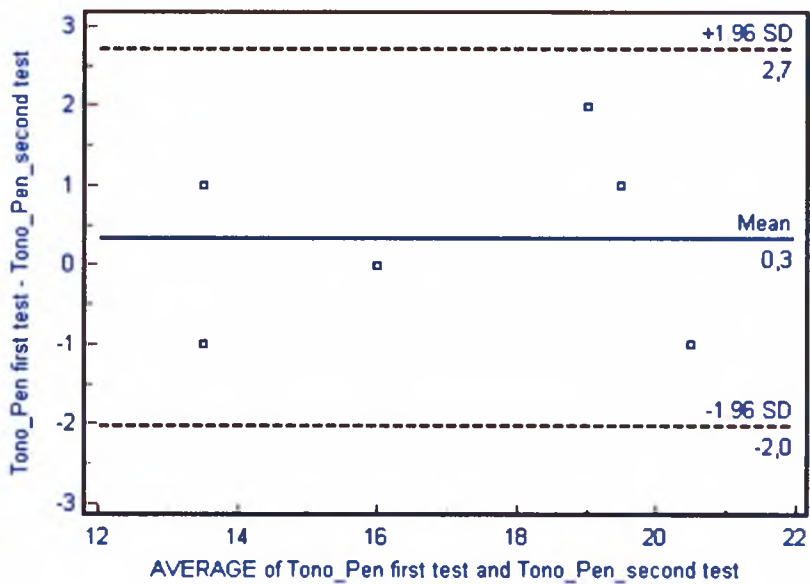


Figure 3.3.4-2 Repeatability of the Tono-Pen assessed using an Altman-Bland difference plot. Data is plotted for six eyes, using the first and second Tono-Pen measurement for each eye shown in table 3.3.4-1. The unit of both abscissa and ordinate is mmHg.

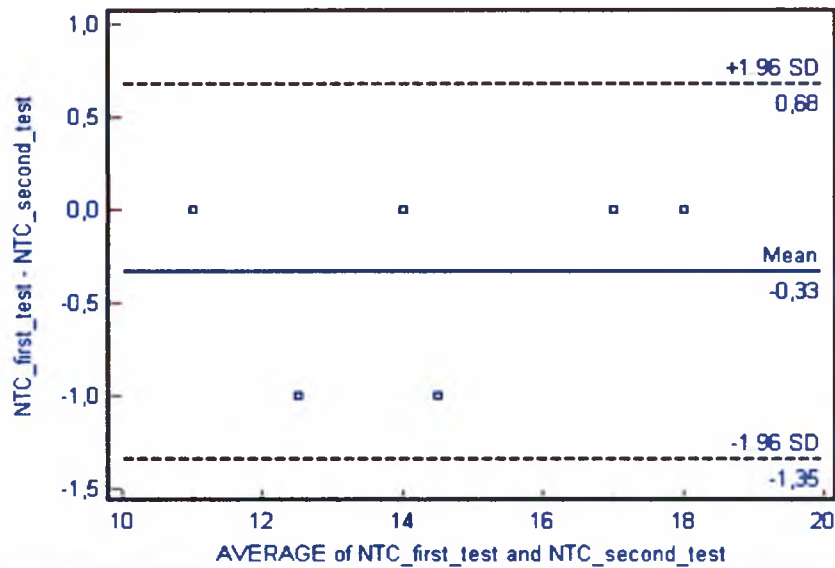


Figure 3.3.4-3 Repeatability of the non contact tonometer (NCT) assessed using an Altman-Bland difference plot. Data is plotted for six eyes, using the first and second NCT measurement for each eye shown in table 3.3.4-1. The unit of both abscissa and ordinate is mmHg.

For the six eyes tested, the agreement between the Tono-Pen and NCT can be assessed from the Altman-Bland difference plot (Bland and Altman, 1988). The mean value for the difference between the instruments, the bias, is 2.8 mmHg, with the Tono-Pen consistently giving higher measures of IOP than the NCT. There have been many method-comparison studies which have examined the accuracy of non-contact tonometers in relation to the gold standard Goldmann instrument. The vast majority of these studies conclude that NCTs provide clinically meaningful measures of IOP which equate to those obtained by the Goldmann instrument (Henson and Harper 1998).

In this small sample of eyes, the higher IOPs recorded with the Tono-Pen suggests that the conversion table provided by the manufacturers of the Tono-Pen XL to convert from measurements taken from the sclera at the limbus rather than from the cornea may be inaccurate (Table 3.2.8-1). However, the sample used to generate the difference plot in Figure 3.3.4-1 was small.

Furthermore, on the trek in Nepal the key factor regarding IOP was any relative change in IOP with altitude. For these reasons, the manufacturer's recommended correction factors were used for IOP recorded using the Tono-Pen on the trek.

For the six eyes tested, the test-retest repeatability of each tonometer, as assessed by the Altman-Bland plots is shown in Figures 3.3.4-2 and 3.3.4-3. Both instruments gave very similar mean differences (bias), for this small sample, between the first and second measurements (+0.3 mmHg for the Tono-Pen and -0.33 mmHg for the NCT). The 95% confidence interval for repeatability was greater for the Tono-Pen (-2.0 to +2.7 mmHg) than for the NCT (-1.35 to +0.68 mmHg), suggesting greater consistency of measurement with the NCT. However, this is hardly surprising when considered against the background of the inevitable loss of measurement accuracy associated with taking an IOP measurement from the sclera rather than the cornea.

A further measure of instrument repeatability is given by the repeatability standard deviation, computed from each set of five Tono-Pen and five NCT readings measured from the six tested eyes and shown in Table 3.3.4-1. These repeatability standard deviations are 1.14, 1.14, 1.14, 1.30, 1.52, and 1.87 mmHg for the Tono-Pen and 0.45, 0.55, 0.55, 0.55, 0.71 and 0.84 for the NCT, confirming the increased variability with the Tono-Pen.

3.3.5 Keratographer

During the trek in Nepal each cornea was to be measured with the keratographer three times every day; once each morning, once each noon, and once each evening. To assess the reliability of these measurements, two similar Oculus keratographers were used for the tests described in this section. The Oculus keratographer is a Placido keratographer, which means that a three-dimensional corneal shape description is computed from Placido circles projected onto the cornea (Schanzlin, and Robin, 1992).

The manufacturer (Oculus) instructs the user to carry out measurements on a well-defined glass ball which is part of the keratographer equipment. Before the agreement and repeatability of the instruments were tested, the calibration procedure was carried out, which involved measuring the glass ball with each instrument. The calibration process was successful, demonstrating that both instruments were accurately calibrated.

The repeatability and agreement of both instruments were tested on the right and left eyes of three normal subjects, comprising two female and one male aged between 35 and 45 years. In order to distinguish the data from each keratographer, the number 110x was used to indicate data from the first instrument and number 120x to indicate data from the second instrument. The symbol "x" is then replaced by the number of the measurement.

For example, the third measurement of keratographer one is indicated by the number 1103. The right eye Zernicke coefficients were measured five times consecutively with the first keratographer and this process was repeated with the second instrument. After computing the keratographer programme polynomial sequences, the Zernike polynomials and ellipsoid combination which describe the corneal shape was fitted and checked using the Professor Lingelbach programme (Chapter 3.2.10.1). Residual rms values were calculated from each data set for statistical analysis (Chapter 3.2.10.5, chapter 3.2.10.6). A similar approach has been used previously by Nigel, Diaz-Santana and Lara-Saucedo (2003), who demonstrated repeatability of ocular wavefront measurement using residual rms values.

Figure 3.3.5-1 and Figure 3.3.5-2 show how the Zernike coefficients of five measurements taken with two keratographers vary with each subject.

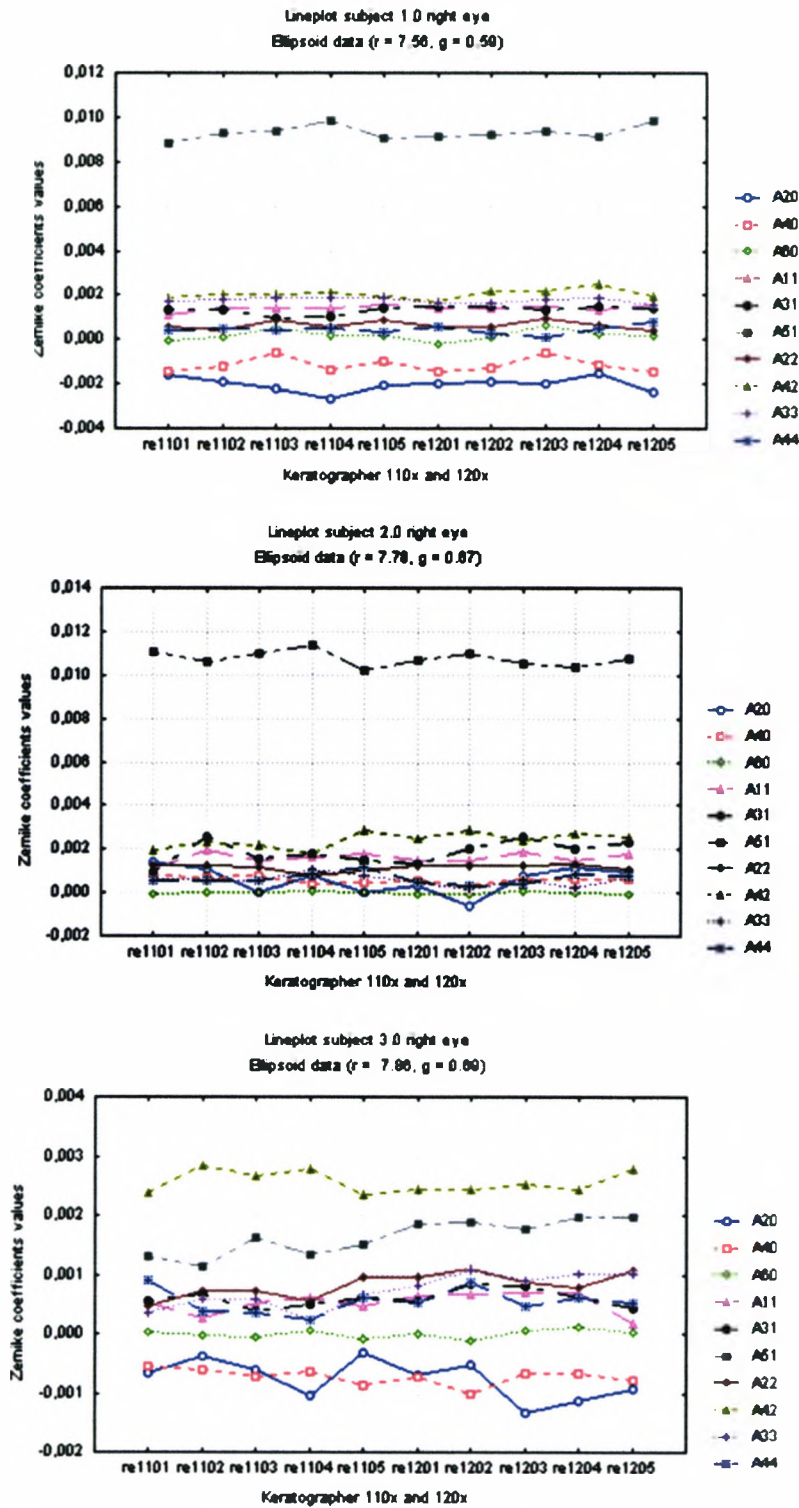


Figure 3.3.5-1 Variation in Zernike coefficients during the test phase of two keratographers on three subject's right eyes are shown. Measurements 1101-1105 were from the first keratographer and measurements 1201-1205 were from the second keratographer.

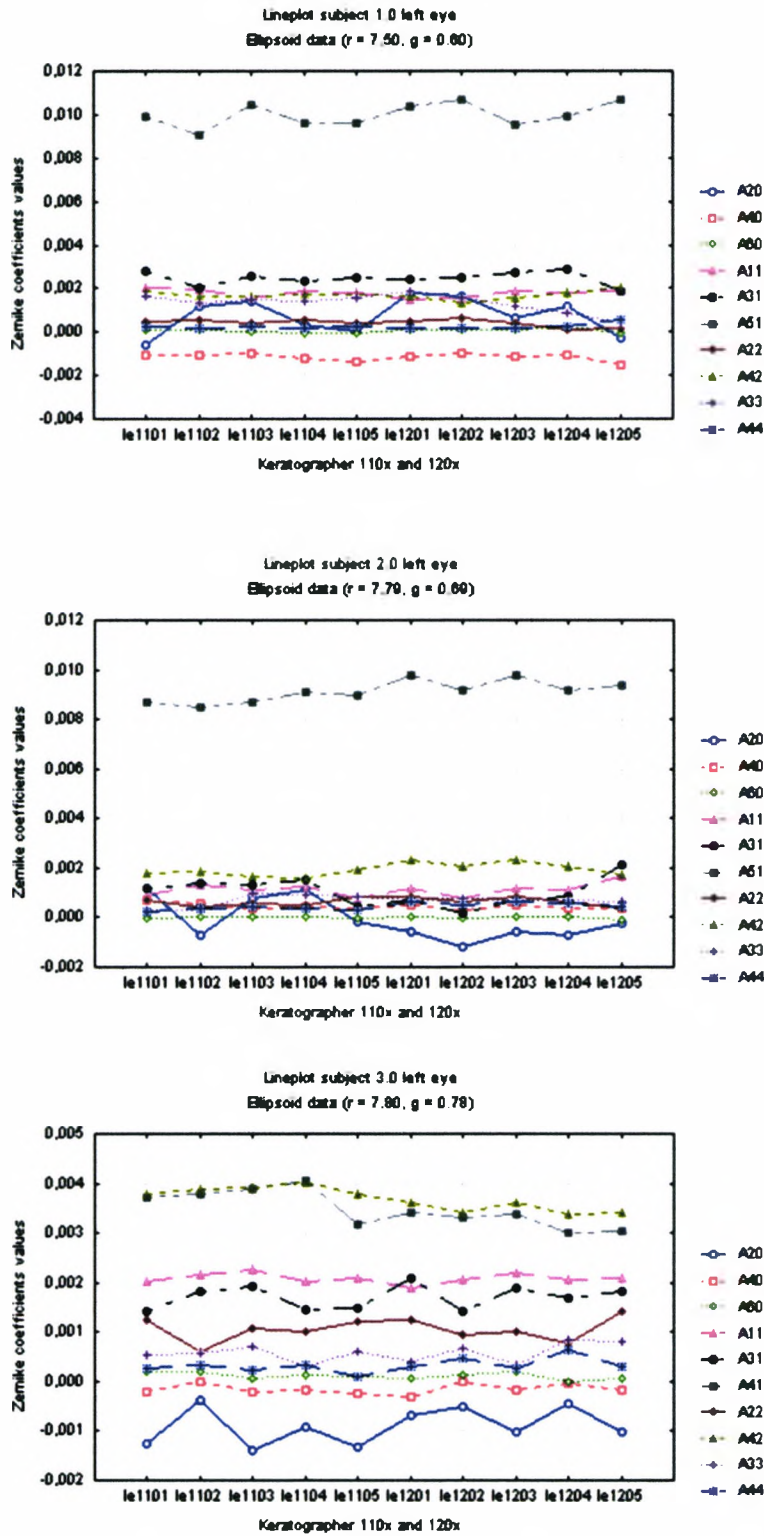


Figure 3.3.5-2 Variation in Zernike coefficients during the test phase of two keratographers on three subject's left eyes are shown. Measurements 1101-1105 were from the first keratographer and measurements 1201-1205 were from the second keratographer.

Interestingly, it is clear from these figures that Zernicke coefficient a_{51} consistently gives the highest values for all six eyes, and that Zernike coefficients a_{20} and a_{40} tend to have the lowest values. Any possible reasons suggested for a_{51} having the highest value Zernike coefficient must be speculative. However, a_{51} could play a central role in describing corneal shape irregularities because Zernike function₅₁ includes a term containing the variable p to the power of 5. No other angle-dependent Zernike function describing corneal shape has a term greater than p to the power of 4. The cornea is a human tissue therefore an absolute spherical shape can not be expected. Individual measurements were deleted, and repeated, when subjects closed their eyes during the measurement procedure or when projected circles were interrupted and therefore the oculus programme interpolated the gaps of the central circles.

Measurement number	Keratoghr. 110x	Keratogr. 120x	Keratoghr. 110x	Keratogr. 120x
	right eye res rms	right eye res rms	left eye res rms	left eye res rms
Subject1				
01	0.00065	0.00028	0.00079	0.00038
02	0.00042	0.00073	0.00045	0.00071
03	0.00038	0.00031	0.00054	0.00038
04	0.00040	0.00042	0.00074	0.00038
05	0.00048	0.00030	0.00030	0.00049
SD	0.00011	0.00018	0.00020	0.00014
Subject2				
01	0.00027	0.00012	0.00026	0.00025
02	0.00033	0.00031	0.00037	0.00028
03	0.00015	0.00036	0.00034	0.00015
04	0.00031	0.00027	0.00024	0.00036
05	0.00029	0.00028	0.00030	0.00024
SD	0.00007	0.00009	0.00006	0.00008
Subject3				
01	0.00036	0.00025	0.00079	0.00066
02	0.00011	0.00014	0.00041	0.00061
03	0.00034	0.00035	0.00044	0.00020
04	0.00042	0.00036	0.00025	0.00037
05	0.00019	0.00035	0.00042	0.00075
SD	0.00012	0.00009	0.00019	0.00021

Table 3.3.5-1 Residual rms values from the right and left eyes of three subjects tested five times with both keratographer 110x and 120x. Standard deviations (SD), are computed from each sample. Unit: $\times 10^6$ Microns.

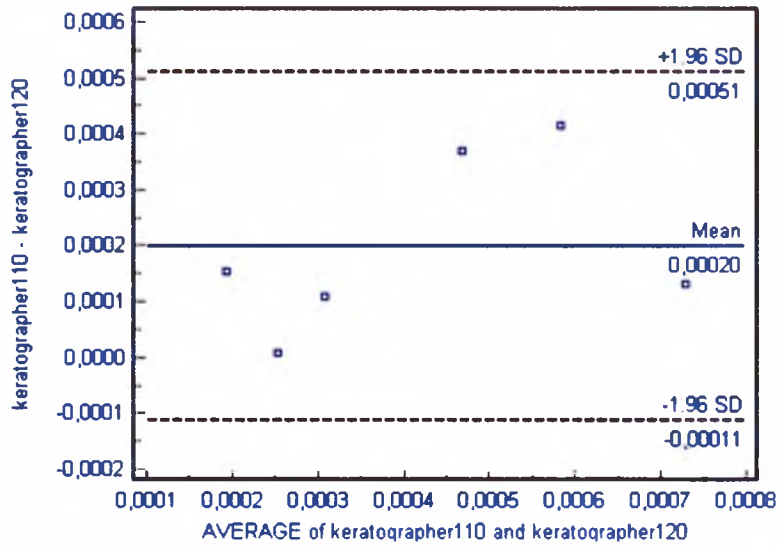


Figure 3.3.5-3 Agreement between keratographer 110x and keratographer 120x assessed using an Altman-Bland difference plot. Data is plotted for six eyes, using the first data pair of each eye shown in table 3.3.5-1. Unit: $\times 10^6$ Microns.

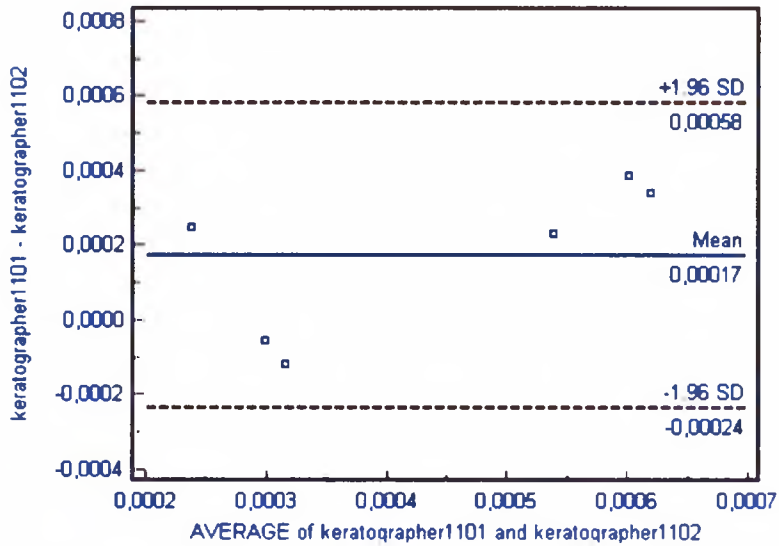


Figure 3.3.5-4 Repeatability of keratographer 110x assessed using an Altman-Bland difference plot. Data is plotted for six eyes, using the first and second keratographer 110x measurements for each eye shown in table 3.3.5-1. Unit: $\times 10^6$ Microns.

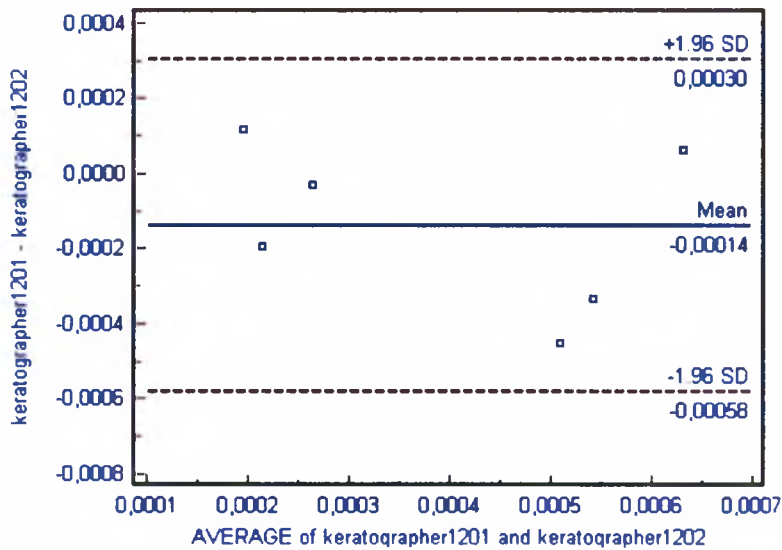


Figure 3.3.5-5 Repeatability of keratographer 120x assessed using an Altman-Bland difference plot. Data is plotted for six eyes, using the first and second keratographer 120x measurements for each eye shown in table 3.3.5-1. Unit: $\times 10^6$ Microns.

As noted in chapter 3.2.10.1, the best fitted ellipsoid is defined by two values r and g , which are stated during the fitting of a “master” corneal shape. Every corneal shape description of one eye includes the identical ellipsoid.

This ensures that the shape differences between measurements are completely determined by the Zernike polynomials. However, different eyes tested will normally have slightly different ellipsoids. In this case, the constant right and left eye ellipsoid data are demonstrated in figure 3.3.5-1 and figure 3.3.5-2 (see heading r, g). To avoid any influences of different ellipsoids when values from more than one eye are taken for further statistical consideration, the statistical tests are carried out using residual rms values. For the six eyes tested, the agreement between keratographer 110x and 120x can be tested using Altman-Bland difference plot (Bland and Altman, 1986). The mean difference between the instruments for rms measurements on these six eyes, the bias, is 0.0002.

Figures 3.3.5-4 and 3.3.5-5 show the repeatability of each keratographer as assessed by Altman-Bland plots. Both instruments give similar values for the absolute mean differences (bias), for this small sample.

For keratographer 110x the mean difference between first and second measurements is 170 Microns and for keratographer 120x the equivalent mean difference is 140 Microns. With this level of variability it would have been preferable to take more than one keratographer reading from each eye during each measurement session on the trek. Unfortunately, the practical difficulties of taking measurements on the trek did not allow repeated measurements to be taken with the keratographer at each session on each day (morning, noon and evening) on every subject. It was only possible to take one keratographer measurement on each eye in each measurement session. Therefore, some lack of precision in the recorded residual rms values has to be accepted. If keratographer measurements had been repeated at each session, then twice as much electrical power would have been necessary. It would have been very risky to be dependent on this elevated energy consumption, which had to be produced from the sun's energy, on the trek, because the trek passed through large shadow areas in Nepal. Furthermore, the time available to take the measurements at each daily stage was very limited. However, many morning, noon and evening measurements were taken from each subject at a range of altitudes over the course of the trek, which would help to minimise the effects of the variation in measurement of residual rms when mean residual rms values were statistically evaluated.

3.4 Summary

To investigate any corneal shape changes with altitude and the reasons for them, suitable tests have to be selected. Factors affecting corneal metabolism and, therefore, the corneal shape were discussed with reference to the relevant literature. These factors were air pressure, temperature, humidity, UV radiation, cosmic radiation, and intra ocular pressure, all of which can change during ascent to high altitudes and all of which have an influence on corneal metabolism.

The meteorological literature describes mathematical formulae with interactions involving all of the meteorological data which were measured in Nepal.

It is possible that if we measured, for example, the altitude, then all the other data could be found by calculation from other meteorological formulae.

But, for example, wind could influence local meteorological data so that the formulae are no longer reliable. The complexity of the weather variations in Nepal also serves to refute the idea of using mathematical formulae.

It is not necessary to measure UV-radiation because sun creams and sun glasses provide complete protection. However, there is no possible protection against cosmic radiation. However, to minimise the effects of possible cosmic radiation the test phase was carried out during a cosmic radiation minimum.

In an effort to make all the results of every test as reliable as possible, precision instruments should be taken to Nepal. Additionally, under no circumstances should any of the selected test procedures have any affect on corneal shape change. Selection and testing allowed the following instruments to be chosen for measurements on the trek:

- Fischer precision-aneroid barometer (range 400 hPa to 900 hPa \pm 1 hPa)
- Thommen altimeter 7000 (\pm 8 m, \pm 1 hPa)
- Möller Therm thermometer no. 106705 (range +50 $^{\circ}$ C to -30 $^{\circ}$ C, \pm 1 $^{\circ}$ C)
- Precision hygrometer Fischer model nr 122.01 (\pm 1 %)
- Slit lamp type 510L
- Tono-Pen tonometer
- Welch Allyn ophthalmoscope number 11730

The calibration of each of the barometer, altimeter, thermometer, hygrometer, and tonometer was tested against results from a “gold standard” second instrument to test how closely the data from both instruments agree. The test procedure showed a high degree of confirmation of each tested instrument to manufacturer tolerance, with the exception of the Tono-Pen.

Given the inevitable variability associated with taking IOP measurements from the sclera, the accuracy of the Tono-Pen was considered acceptable.

Signs detected by the Slit lamp type 510L and the Welch Allyn ophthalmoscope number 11730 were assessed subjectively and graded (CCLRU grading scale).

An Oculus keratographer delivered baseline data on the corneal shape which were transformed into an ellipsoid and Zernike coefficients combination using a programme computed by Professor Lingelbach. The shape fitting standard deviation of 0.0001 promises a high quality of corneal shape description. The ellipsoid makes it easier to manipulate and to transform graphs than is possible using only Zernike polynomials. Before each test procedure the keratographer was calibrated with a defined glass ball, then every corneal shape fitting was checked visually with the help of the Oculus contact lens programme.

Two series of five measurements were taken on both eyes of three subjects with two Oculus keratographers. Repeatability of the residual rms values was not as good as anticipated. However, it was comparable between the two keratographers and the variability was regarded as acceptable. Unfortunately, energy consumption and the need to limit the duration of each test session on the trek dictated that repeat measurements were not possible in Nepal.

Chapter 4. Standard measurements at low altitude

4.1 Introduction

A statistical analysis of keratographer measurements taken at low altitude is necessary to identify how the corneal shape changes in low altitude conditions. The results presented in this chapter have an important role to play in the interpretation of the results of the assessment of corneal change at high altitude discussed in chapter 6. Eleven subjects (eight non contact lens wearers and three contact lens wearers) were tested over a period of four days. Each subject attended every day for four days and had measurements taken on each day during the morning, at noon and in the evening. The results were taken over four days to allow mean Zernicke coefficients and mean residual rms values to be calculated. In this low altitude study none of the eleven subjects who participated were involved in the subsequent high altitude study. The results of the non contact lens wearer group and the contact lens wearer group were tested with variance analysis separately to detect any significant change in the cornea either in the morning, at noon, or in the evening, and to detect any significant change over the four days of the study. In addition, the variability of the z-value, which is defined as the difference between the highest and deepest point of corneal shape described with Zernike polynomials is discussed in this chapter.

4.2 Subjects and methods

4.2.1 Subjects

Eleven subjects were selected aged between 35 and 54 years. Three contact lens wearers (two women and one man), who had been soft lens wearers for a minimum of two years, were included.

Each subject wore their contact lenses for a minimum of 8 hrs a day, and all wore Bausch & Lomb Optima 38 (Polymacon Monomer A) lenses. The non contact lens wearing group consisted of three men and of five women.

To minimise any influence from the action of the immune system on the study's outcome, selected subjects had no problems with injuries, infections, infiltrations, inflammations, acid, or alkali burns on the cornea for a minimum of six months. Each subject was given a number e.g. x.11 or x.12, where x stands for the subject himself/herself, and the following number describes the study. The low altitude study is number 1 and the high altitude study is defined by number 2. The final number indicates whether the subject is a non contact lens wearer (1) or a contact lens wearer (2). For example, a contact lens wearer in the low altitude study could have one of following three numbers 1.12, 2.12, 3.12.

4.2.2 Anamnesis

Each subject was asked about their personal profile, their ocular history, their family ocular history, their general health history and health status, their family general health history and health status, and any medications and allergies.

Eye examination:

- Vision unaided OD, OS, OU
- Refraction sph, cyl, phoria tests
- Visual Acuity OD, OS, OU
- Ishihara Colour Vision Test
- Confrontation fields OD, OS,
- Amsler Grid test
- Eye pressure measured with Tono-Pen XL

- Pupil tests (Marcus Gunn Pupil)
- Pursuit test and saccades test
- Anterior chamber inspection

The anterior chamber angle was graded according to the system as described by van Herick et al. Retinal inspection was undertaken with a 90 dpt Volk lens in combination with a Zeiss slit lamp and hand held ophthalmoscope.

In particular, any subjects suffering from or at risk from a disease which could have an influence on eye pressure, for example glaucoma (either in the subject's eyes or in close family members' eyes), uveitis, or corneal surgery were excluded. Diabetes and high blood pressure are systemic diseases which could also influence the daily corneal shape change. Therefore, eyes with either condition or with a history of eye trauma were also excluded.

4.2.3 Contact lenses used for subjects in the low altitude study

Bausch & Lomb Optima 38 (Polymacon Monomer A) was used (Figure 4.2.3-1). The data on the lenses is as follows:

Subject 1.12:

Optima 38, sph +0.75 dpt, SAG 8.7, Diam \varnothing 14.0 optical zone 8.0 mm,
centre thickness 0.110mm/0.115mm

Optima 38, sph +1.0 dpt, SAG 8.7, Diam \varnothing 14.0, optical zone 8.0 mm,
centre thickness 0.110mm/0.115mm

Subject 2.12:

Optima 38, sph -1.50 dpt, SAG 8.7, Diam \varnothing 14.0 optical zone 9.0 mm,
centre thickness 0.060mm

Optima 38, sph -2.75 dpt, SAG 8.7, Diam \varnothing 14.0, optical zone 10.0 mm,
centre thickness 0.060mm

Subject 3.12:

Optima 38, sph $+3.50$ dpt, SAG 8.7, Diam \varnothing 14.0, optical zone 8.0 mm,
centre thickness 0.160mm/0.165mm

Optima 38, sph $+3.25$ dpt, SAG 8.7 Diam \varnothing 14.0, optical zone 8.0 mm,
centre thickness 0.160mm/0.165mm

Bausch & Lomb OPTIMA 38 Lenses

INDICATIONS

MYOPIA
 HYPEROPIA
 DAILY WEAR
 SUPERIOR HANDLING
 LATHE-CUT
 VIAL PRODUCT
 VISIBILITY TINT
 NATURAL TINTS

DESCRIPTION

An easy-to-fit low water content spherical soft lens manufactured using "Reverse Process III" technology, and designed for use in the correction of myopia and hyperopia on a daily wear basis. Low center thickness provides good oxygen transmission, while an increased mid-peripheral thickness allows good handling across the power range. The lathe-cut rear surface ensures good on-eye lens centration.

PARAMETERS

MATERIAL	Polymacon (Monomer A)
WATER CONTENT	38.6%
FDA MATERIAL GROUP	1
OXYGEN PERMEABILITY (Dk)	8.5x10 ⁻¹¹ W
OXYGEN TRANSMISSION (Dk/L)	14.00 x 10 ⁻⁹ (-3.00D @ Central)
	12.13 x 10 ⁻⁹ (-3.00D Avg. 6mm)
	5.63 x 10 ⁻⁹ (+3.00D @ Central)
	6.24 x 10 ⁻⁹ (+3.00D Avg. 6mm)
MANUFACTURING METHOD	Reverse Process III
BASE CURVES	8.4mm, 8.7mm, 9.0mm
DIAMETER	14.00mm
SAGITTAL DEPTH (minus powers)	3.82mm (8.4BC), 3.60mm (8.7BC), 3.38mm (9.0BC)
SAGITTAL DEPTH (plus powers)	4.02mm (8.4BC), 3.70mm (8.7BC), 3.53mm (9.0BC)
POWERS	-12.00D to +5.00D*
OPTICAL ZONE	8.00mm (+0.25D to +5.00D)
	9.00mm (-0.25D to -2.00D)
	10.00mm (-2.25D to -4.00D)
	9.00mm (-4.25D to -12.00D)
CENTER THICKNESS	0.060mm (-0.25D to -12.00D)
	0.100mm/0.105mm (+0.25D/+0.50D)
	0.110mm/0.115mm (+0.75 to +1.00D)
	0.120mm/0.125mm (+1.25 to +1.50D)
	0.130mm/0.135mm (+1.75 to +2.00D)
	0.140mm/0.145mm (+2.25 to +2.50D)
	0.150mm/0.155mm (+2.75 to +3.00D)
	0.160mm/0.165mm (+3.25 to +3.50D)
	0.170mm/0.175mm (+3.75 to +4.00D)
	0.180mm/0.185mm (+4.25 to +4.50D)
	0.190mm/0.195mm (+4.75 to +5.00D)
LENS MARKINGS	Large "B&L" (Eversion Indicator) and "S" opposing (8.4mmBC)
	Large "B&L" (Eversion Indicator) and "M" opposing (8.7mmBC)
	Large "B&L" (Eversion Indicator) and "F" opposing (9.0mmBC)
VISIBILITY TINT	Blue (100ppm reactive blue dye No.246) (N/A for NaturalTint)
LIGHT TRANSMITTANCE	CIE value average 96% (VisibleTint)
	CIE value average 82% (NaturalTint Blue)
	CIE value average 84% (NaturalTint Aqua)
	CIE value average 84% (NaturalTint Aqua)
	CIE value average 76% (NaturalTint Green)
REFRACTIVE INDEX	1.43
DISINFECTION METHODS	Heat
	Chemical
	Hydrogen Peroxide

* (-0.50D steps above -9.00D), 8.4mm & 8.7mm base curves not available above -9.00D)
 # (cm³O₂ x cm/(sec x cm² x mmHg) at 35° C.

Figure 4.2.3-1 Company information on lens type
 Optima 38.

For inclusion in the study the contact lens wearers had to wear the same type of lenses used for the altitude study, to facilitate comparison of results. For example, silicon hydrogel lenses with a higher DK/L could induce a slightly different change in corneal shape because of the higher oxygen supply to the cornea during contact lens wear.

Without knowledge of the influence of different types of lenses on the change of corneal shape, further discussion on the effects of the lenses would be impossible.

4.2.4 Methods

All tests were carried out in an air conditioned room. The air pressure ranged from 940 hPa to 958 hPa at an altitude of 520 m. The temperature was between 19 and 21 degrees Celsius and the humidity ranged between 48% and 55%. The surrounding conditions were checked with the precision instruments described in chapter 3.2. Before the eyes of every subject were measured with a keratographer (chapter 3.2.10), contact lenses were removed if worn, and the IOP was measured with a Reichert AT 550 non contact tonometer (chapter 3.3.4). The corneal shape was then measured on two occasions, three times a day (morning, at noon, and in the evening) for four days. Contact lens wearers wore their lenses throughout each day and removed them shortly before they went to bed.

4.2.5 Results of the low altitude study

Residual rms values were recorded from six groups; non contact lens wearers (right and left eye from eight subjects), or contact lens wearers (right and left eye from three subjects), and morning, noon or evening. Measurements were carried out over a period of four days. Table 4.2.5-1 shows descriptive statistics (mean, minimum, maximum, 0.25 Quartile, 0.75 Quartile, range, variance, and standard deviation) for each of the six groups described above. Interestingly, the greatest maximum values are calculated from measurements carried out in the morning. This could be explained by the phenomenon known as overnight corneal swelling, which is described in Mertz's study (1980), where he measured the overnight swelling of the eyes of nine subjects.

Results showed overnight corneal swelling to be approximately 4.5 %. The logarithmic recovery to baseline occurred within the first hour after eye opening.

The smallest range of residual rms values was detected in the noon group and the greatest range in the morning group for both contact lens wearers and non wearers. Regarding range depending on time of day, contact lens wearers and non contact lens wearers behave almost identically (Table 4.2.5-1).

Descriptive statistics residual rms standard measurements								
Res rms	Mean	Min	Maxim	0.25 th Quarti	0.75 th Quarti	Range	Varian	Stdv.
Morn-ncl	.0007	.0002	.0030	.0004	.0008	.0028	.0000	.0004
Noon-ncl	.0007	.0002	.0019	.0004	.0009	.0017	.0000	.0004
Even-ncl	.0007	.0001	.0023	.0004	.0009	.0022	.0000	.0004
Morn-cl	.0009	.0002	.0029	.0006	.0012	.0027	.0000	.0005
Noon-cl	.0008	.0002	.0020	.0006	.0010	.0018	.0000	.0004
Even-cl	.0008	.0002	.0022	.0005	.0010	.0019	.0000	.0004

Table 4.2.5-1 Every measurement is represented by one residual rms value. All residual rms values are divided into six groups. These are contact lens wearers and non contact lens wearers morning, noon, and evening. Every group is represented by all the measurements which were carried out during the test phase over four days. Unit: $\times 10^6$ Microns.

When we consider the distribution of the six groups more in detail, Table 4.2.5-1 and Figure 4.2.5-1 demonstrates an interesting fact. Both the mean and median values of the contact lens wearing group are greater at all times of the day than those of the non contact lens wearer group.

However, this result should be considered with caution because of the low subject numbers in the contact lens group (three subjects).

Additionally, the higher 0.75th quartile at all times of the day in the contact lens wearer group (0.75th quartile 0.0010, 0.0012) compared with the non contact lens group (0.75th quartile 0.0008, 0.0009) is also consistent with the tendency for residual rms values in the contact lens wearers group to be generally greater than residual rms values of the non contact lens wearer group.

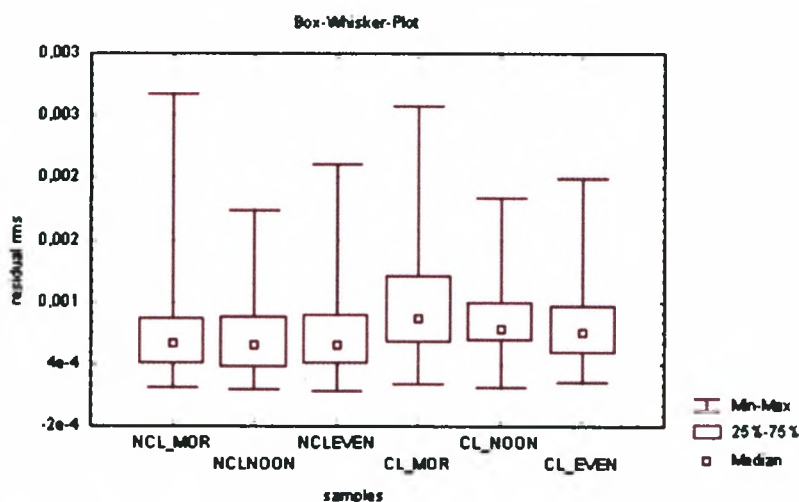


Figure 4.2.5-1 Box and whisker plots for the residual rms values at low altitude for both the contact lens wearing and non contact lens wearing groups.

4.2.5.1 Distributions of residual rms values and significance testing for daily corneal shape change

Prior to hypothesis testing, the best-fitting distribution was computed for both the non contact lens wearers, and the contact lens wearers for each of their morning, noon, and evening tests.

To establish the best fitted distribution for the data from the non contact lens wearer sample, "probability, probability" plots were used to check the fit of the following distributions, Beta-, Exponential-, Extreme-, Gamma-, Normal-, Raleigh-, and Weibull.

The red line in each graph describes the ideal theoretical distribution fit (Table 4.2.5.1-1). When the plotted points are positioned close to the red line, or on the line, the tested distribution represents the category under examination quite well. Only the best-fitting distribution is shown for each category (which was the Gamma distribution in all six categories), plus illustrations of how well the Normal distribution fits the data from each category.

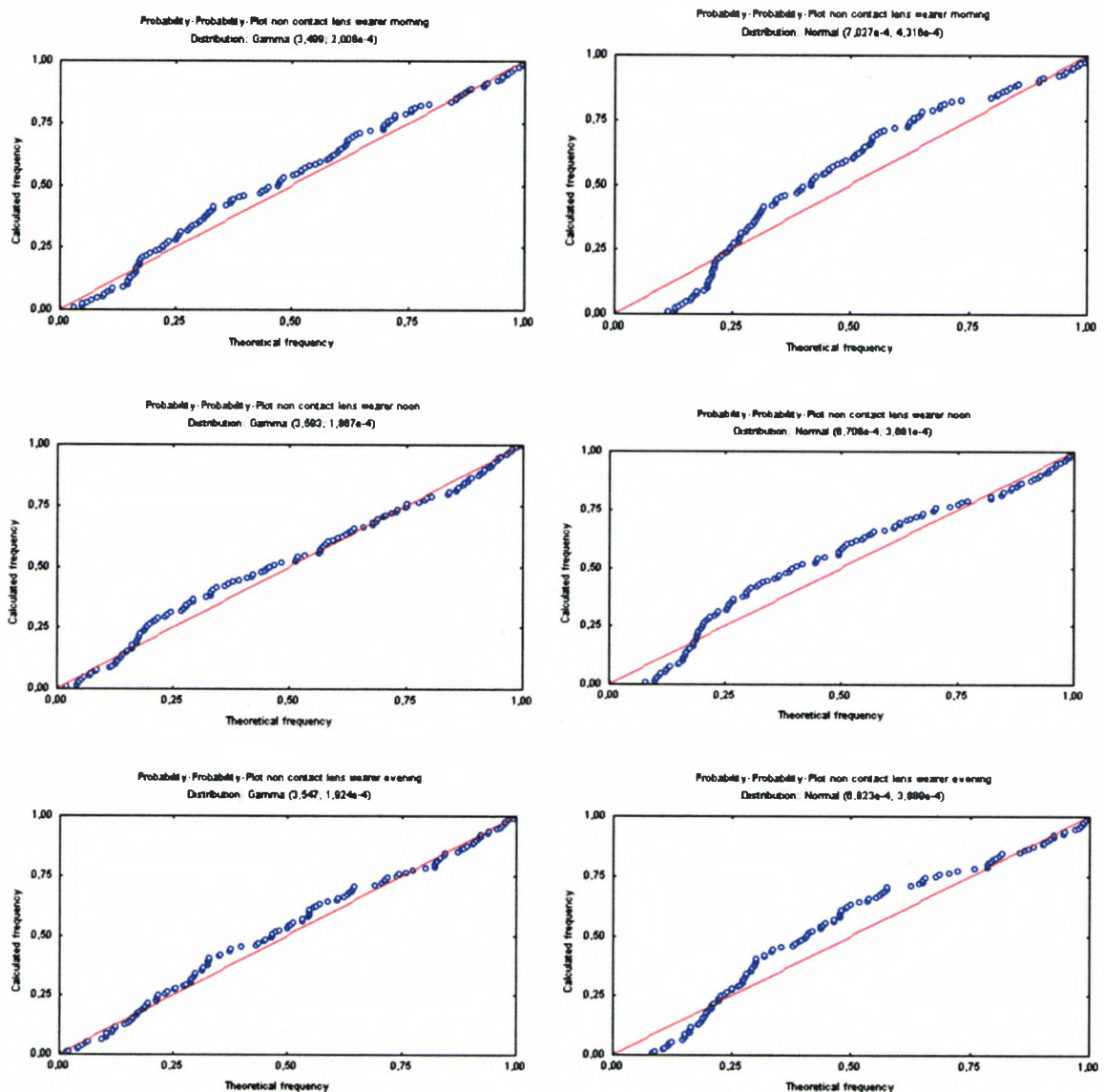


Figure 4.2.5.1-1 The left column shows the best fitted distribution for residual rms values for non contact lens wearers. The morning-, noon-, and evening data are best described by a gamma distribution. The right hand plots demonstrate how closely these data approach the Normal distribution.

The quality of the best fitted distribution (Gamma distribution) is expressed by the p-value calculated with the Kolmogorov-Smirnov test:

Non contact lens wearers morning → Gamma p = 0.36

Non contact lens wearers noon → Gamma p = 0.24

Non contact lens wearers evening → Gamma p = 0.53

Samples tested in figure 4.2.5.1-1 would be perfectly represented by the best fitting distribution when the p-value is 1. Although the Gamma distribution is the best fitting distribution, it does not represent the distribution of residual rms values of the tested samples particularly well.

As a result, the data from the morning, noon, and evening non contact lens wearers were tested for any significant daily variation in corneal shape change using variance analysis. The p-values were calculated using the F-test, a robust test with regard to moderate departures from normality (Winer, Brown, Michels, 1991). For this analysis, a mean difference is taken to be significant when the p-value < 0.05. A similar analysis was performed for the contact lens wearing sample.

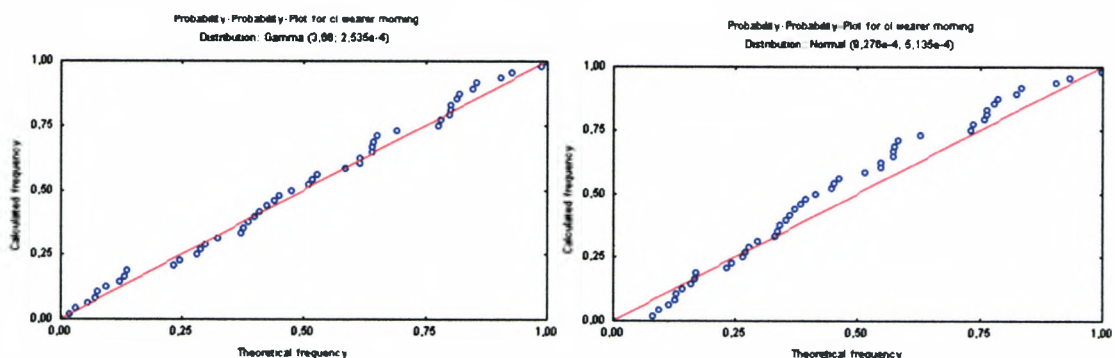
The variance analysis for the non contact lens wearers gives the following result:

STAT.	Non contact lens wearers					
General	Test daily stages morning, noon, and evening					
ANOVA	Degree of freedom (FG)					
EFFECT	FG	Mean	FG	Group	F	p-Value
	Mean	Variance	Group	Variance		
1	2	.0000	381	.0000	.213	.808

Table 4.2.5.1-1 Results of variance analysis using the F-test, testing for any diurnal variation in mean residual rms values for the non contact lens wearers group.

This demonstrates that there is no significant ($p = 0.808$) corneal shape change represented by residual rms values throughout the day in this subject sample. Additionally, the category non contact lens wearers was subdivided into morning, noon, and evening measurements to investigate for any significant corneal shape change over a four day test period. No significant corneal shape change was detected with the F-test. Results are as follows; morning tests (ANOVA, $F = 0.603$, $FG = 3$, $p = 0.62$), noon tests (ANOVA, $F = 1.189$, $FG = 3$, $p = 0.32$), and evening tests (ANOVA, $F = 2.06$, $FG = 3$, $p = 0.11$).

For the contact lens wearer samples, the “probability, probability” plots again reveal the Gamma function to be the best fitted distribution. The differences from a Normal distribution and the Gamma distribution fits are seen in figure 4.2.5.1-2.



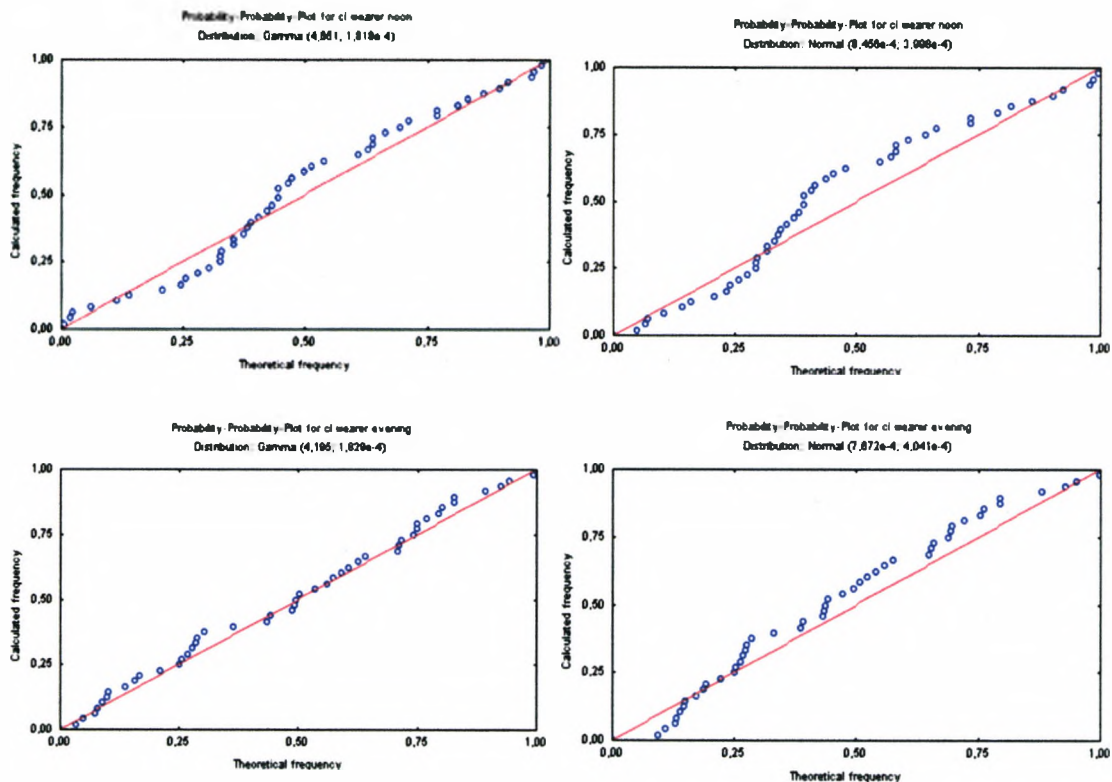


Figure 4.2.5.1-2 The left column shows the best fitted distribution for residual rms values for contact lens wearers. All data are best described by a gamma distribution. Right column shows how closely these data approach the Normal distribution.

The variance analysis carried out for the contact lens wearers category (Table 4.2.5.1-2) again finds no significant corneal shape change, as represented by the mean residual rms values, during the course of the day.

STAT.	Contact lens wearers					
General	Test daily stages morning, noon, and evening					
ANOVA	Degree of freedom (FG)					
EFFECT	FG	Mean	FG	Group	F	p-Value
	Mean	Variance	Group	Variance		
1	2	.0000	141	.0000	1.5783	.210

Table 4.2.5.1-2 Results of variance analysis using the F-test, testing for any diurnal variation in mean residual rms values for the contact lens wearers group.

Furthermore, the category of contact lens wearers was subdivided into morning, noon, and evening measurements to investigate for any corneal shape change over a four day test period. No significant corneal shape change was detected with the F-test. Results are as follows; morning tests (ANOVA, $F = 2.11$, $FG = 3$, $p = 0.11$), noon tests (ANOVA, $F = 2.29$, $FG = 3$, $p = 0.09$), and evening tests (ANOVA, $F = 1.13$, $FG = 3$, $p = 0.35$).

4.2.5.2 Zernike coefficients for both subject groups

Computing the mean of the Zernike coefficients shows that the values of coefficient a_{51} are greater than those of the other coefficients (Tables 4.2.5.1-3 and 4.2.5.1-4).

As noted above, the residual rms values of the contact lens wearers' measurements tend to be greater than those from the non contact lens wearers. It would be interesting to establish if one Zernike coefficient, or a small group, or all coefficients, of the contact lens wearers' corneal shape descriptions was/were responsible for the tendency towards greater residual rms values. It can be seen from Tables 4.2.5.1-3 and 4.2.5.1-4 that the contact lens wearers' mean values for most coefficients contribute to the tendency for the residual rms values to be higher in this group.

Mean of Zernike coefficients right eye										
subj	a20	a40	a60	a11	a31	a51	a22	a42	a33	a44
1.11	.0001	-.0014	.0002	.0013	.0015	.0106	.0010	.0021	.0017	.0005
2.11	-.0014	-.0008	-.0001	.0003	.0003	.0025	.0004	.0021	.0006	.0006
3.11	.0007	.0006	.0003	.0024	.0021	.0057	.0009	.0007	.0012	.0006
4.11	-.0013	-.0012	-.0001	.0007	.0009	.0029	.0004	.0027	.0003	.0010
5.11	-.0007	.0002	-.0000	.0017	.0013	.0113	.0012	.0026	.0005	.0008
6.11	-.0007	-.0007	.0002	.0012	.0012	.0081	.0008	.0012	.0012	.0004
7.11	-.0022	-.0005	.0002	.0008	.0009	.0062	.0012	.0025	.0005	.0006
8.11	-.0033	-.0013	.0001	.0007	.0007	.0069	.0007	.0027	.0010	.0005
Mean	-.0011	-.0006	.0001	.0011	.0011	.0068	.0008	.0021	.0009	.0006

Cl	a20	a40	a60	a11	a31	a51	a22	a42	a33	a44
1.12	-.0028	-.0022	-.0015	.0001	.0017	.0019	.0102	.0011	.0020	.0016
2.12	-.0018	-.0004	.0001	.0009	.0015	.0148	.0023	.0044	.0013	.0011
3.12	.0010	-.0010	-.0004	.0019	.0014	.0064	.0011	.0023	.0026	.0014
Mean	-.0012	-.0012	-.0006	.0010	.0015	.0077	.0045	.0026	.0020	.0013

Table 4.2.5.1-3 Zernike coefficients, and their means, of the right eyes of all subjects, both non contact lens wearers and contact lens wearers. Unit: $\times 10^6$ Microns.

Mean of Zernike coefficients left eye										
subject	a20	a40	a60	a11	a31	a51	a22	a42	a33	a44
1.11	.0004	-.0006	.0001	.0014	.0020	.0117	.0005	.0023	.0014	.0004
2.11	-.0012	-.0019	.0000	.0017	.0018	.0034	.0005	.0031	.0007	.0004
3.11	-.0021	-.0017	.0002	.0016	.0017	.0057	.0006	.0014	.0005	.0005
4.11	-.0021	-.0018	-.0000	.0018	.0020	.0032	.0009	.0034	.0005	.0003
5.11	.0011	.0011	-.0000	.0014	.0014	.0090	.0007	.0022	.0005	.0003
6.11	-.0003	.0002	.0001	.0008	.0012	.0103	.0007	.0010	.0009	.0006
7.11	-.0005	-.0009	.0001	.0010	.0011	.0095	.0013	.0017	.0010	.0004
8.11	-.0007	-.0007	.0000	.0005	.0006	.0103	.0006	.0026	.0007	.0003
Mean	-.0007	-.0008	.0001	.0013	.0015	.0079	.0007	.0022	.0008	.0004
Cl	a20	a40	a60	a11	a31	a51	a22	a42	a33	a44
1.12	.0001	-.0005	.0001	.0030	.0025	.0109	.0005	.0019	.0011	.0003
2.12	-.0022	-.0011	.0001	.0007	.0013	.0130	.0017	.0033	.0006	.0005
3.12	-.0001	-.0006	-.0001	.0031	.0021	.0120	.0007	.0030	.0015	.0004
Mean	-.0007	-.0007	.0000	.0022	.00196	.0120	.0020	.0027	.0011	.0004

Table 4.2.5.1-4 Zernike coefficients, and their means, of the left eyes of all subjects, both non contact lens wearers and contact lens wearers. Unit: $\times 10^6$ Microns.

subj	1.11	2.11	3.11	4.11	5.11	6.11	7.11	8.11	1.12	2.12	3.12
radius	7.53	7.85	7.3	7.85	7.78	7.74	7.34	7.75	7.58	7.41	7.52
g	0.60	0.66	0.73	0.62	0.61	0.62	0.72	0.61	0.6	0.69	0.63

Table 4.2.5.1-5 Radius and g value describing the ellipsoid for the right eye of each subject. Unit: Radius mm, $g \times 10^6$ Microns.

subj	1.11	2.11	3.11	4.11	5.11	6.11	7.11	8.11	1.12	2.12	3.12
radius	7.55	7.72	7.61	7.80	7.83	7.75	7.21	7.69	7.57	7.40	7.60
g	0.68	0.52	0.51	0.57	0.78	0.73	0.64	0.64	0.71	0.62	0.75

Table 4.2.5.1-6 Radius and g value describing the ellipsoid for the left eye of each subject. Unit: Radius mm, $g \times 10^6$ Microns.

4.2.5.3 z-value

The central corneal shape is comparable to an ellipsoid, therefore the highest point lies at the central cornea and the deepest point is positioned at the periphery. In this study a combination of a best fitted ellipsoid and Zernike polynomials are used to describe the corneal shape (Chapter 3.2.10.3-4). If we were to pull at the periphery of a best fitted ellipsoid until it became a flat disc, then the Zernike polynomials would describe a wavy three-dimensional shape with that flat disc as its base.

The difference between the highest and deepest points of the three-dimensional shape described above is defined as the z-value, a positive value. The z-value is not a constant for a given cornea, because it can vary as the corneal shape varies.

The bigger the z-value, the more a soft lens deforms (especially very thin soft contact lenses) and the more a hard lens tends to “wobble” on the cornea. Both of these influences, deformation and wobbling, lead to a reduced smooth corneal lens movement. Central corneal shapes with a diameter of 7mm were tested.

The range of each subjects' eye's z-values is an important measure of how the movement of the contact lens on the cornea could change as a result of corneal shape change. Table 4.2.5.3-1 lists the z-value range of each subject separately. The mean calculated from all the range values from both right and left eyes of the non contact lens wearer group shown in table 4.2.5.3-1 is 0.0085 mm and that of contact lens wearer group is 0.0126 mm. The normal central corneal thickness is between 0.49 mm and 0.56 mm (Kanski, 1995). The range of z-values for the contact lens wearers (approximately 2.5% of corneal thickness) is greater than the range for non contact lens wearers (approximately 1.5% of corneal thickness).

Descriptive statistics z-value (mm) right eye standard						
Subjects ncl	Mean	Minimum	Maximum	Range	Variance	Stdev.
1.11	.0220	.0195	.0263	.0068	.0000	.0018
2.11	.0097	.0073	.0153	.0080	.0000	.0019
3.11	.0196	.0099	.0231	.0132	.0000	.0031
4.11	.0132	.0097	.0164	.0067	.0000	.0016
5.11	.0245	.0223	.0275	.0052	.0000	.0013
6.11	.0211	.0175	.0245	.0070	.0000	.0020
7.11	.0168	.0133	.0204	.0071	.0000	.0019
8.11	.0180	.0139	.0248	.0109	.0000	.0027
Subjects cl	Mean	Minimum	Maximum	Range	Variance	Stdev.
1.12	.0223	.0186	.0270	.0083	.0000	.0021
2.12	.0317	.0245	.0386	.0141	.0000	.0036
3.12	.0203	.0141	.0268	.0128	.0000	.0031

Descriptive statistics z-value (mm) left eye standard						
Subjects ncl	Mean	Minim	Maxim	Range	Variance	Stdev.
1.11	.0263	.0195	.0299	.0104	.0000	.0021
2.11	.0110	.0092	.0152	.0060	.0000	.0016
3.11	.0125	.0072	.0192	.0120	.0000	.0029
4.11	.0139	.0106	.0200	.0094	.0000	.0032
5.11	.0195	.0168	.0237	.0069	.0000	.0017
6.11	.0263	.0210	.0340	.0130	.0000	.0028
7.11	.0184	.0160	.0222	.0062	.0000	.0015
8.11	.0226	.0181	.0255	.0074	.0000	.0018

Subjects cl	Mean	Minim	Maxim	Range	Variance	Stdev.
1.12	.0244	.0174	.0343	.0169	.0000	.0033
2.12	.0287	.0242	.0355	.0112	.0000	.0026
3.12	.0279	.0227	.0348	.0121	.0000	.0037

Table 4.2.5.3-1 Descriptive statistics of z-values for each subject. Right eye data is in the upper table; left eye in the lower.

4.2.5.4 Association between residual rms and intra ocular pressure

To check for any possible association between residual rms and intraocular pressure, three scatterplots were generated. Figure 4.2.5.4-1 shows, for the 22 eyes tested, the mean IOP recorded during the morning over the four days plotted against the mean morning residual rms value. Figures 4.2.5.4-2 and 4.2.5.4-3 show similar scatterplots for the noon and evening measurements. Three separate plots were constructed because IOP is known to vary diurnally.

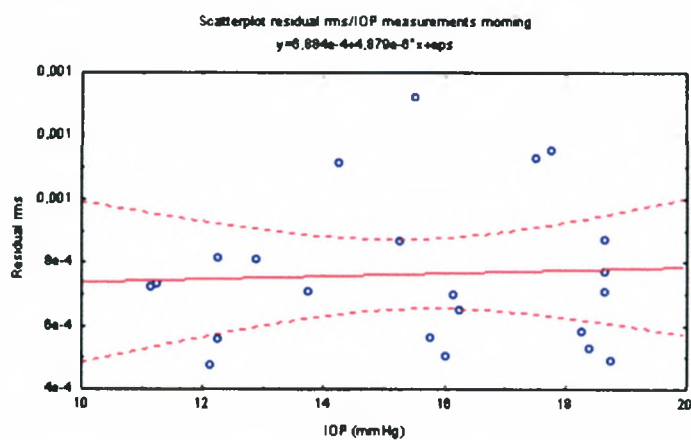


Figure 4.2.5.4-1 Scatterplot of mean residual rms value (abscissa) and mean IOP value (ordinate) for the 22 eyes studied. Measurements taken in the morning are plotted here.

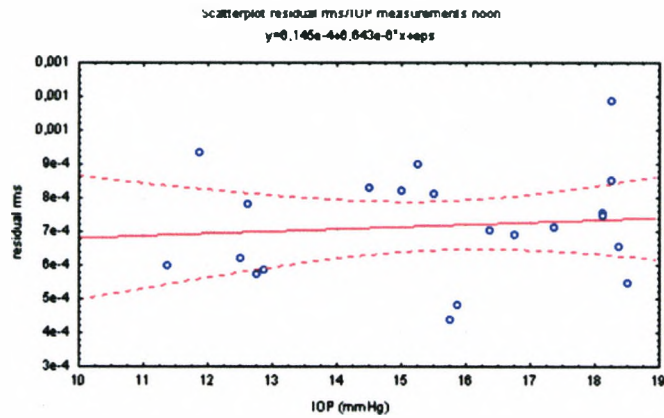


Figure 4.2.5.4-2 Scatterplot of mean residual rms value (abscissa) and mean IOP value (ordinate) for the 22 eyes studied. Measurements taken at noon are plotted here.

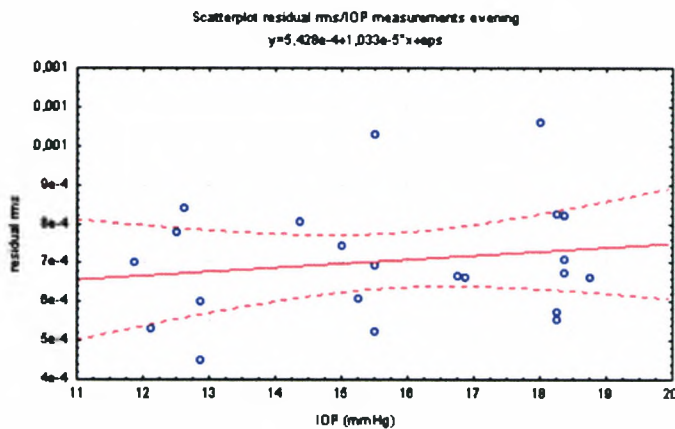


Figure 4.2.5.4-3 Scatterplot of mean residual rms value (abscissa) and mean IOP value (ordinate) for the 22 eyes studied. Measurements taken in the morning are plotted here.

The correlations are all low, with the correlation coefficients being; $r_{\text{morning}} = 0.06$, $r_{\text{noon}} = 0.10$, and $r_{\text{evening}} = 0.16$. The r values are equivalent to R^2 values of morning, noon, and evening of only 0.004, 0.01, and 0.03 respectively, indicating that 0.4%, 1%, and 3% respectively of the variation in residual rms is explained by the variation in intracocular pressure. All this strongly suggests that there is no linear association between residual rms and IOP.

4.2.6 Summary

One of the most important exclusion criteria for subject selection was that in no circumstances would any subject be included if they were taking any drugs and/or had any diseases that might have an influence on the standard measurements. The study tests were carried out in an air conditioned room in order to achieve as stable surrounding conditions as possible.

Although the Gamma distribution was the best-fitting distribution for each sample of subjects tested, it does not represent the distribution of residual rms values of any of the tested samples particularly well. As a result, the data from the morning, noon, and evening non contact lens wearers were tested for any significant daily variation in corneal shape change using variance analysis. The p-values were calculated using the F-test, a robust test with regard to moderate departures from normality. There was no statistically significant diurnal variation in corneal shape change for either contact lens wearers or non contact lens wearers. There is also a tendency for the mean residual rms values to be greatest in the contact lens wearers. The mean values of the Zernike coefficients show that the mean value of coefficient a_{51} is greater than the mean values of the other coefficients, while the coefficients a_{20} and a_{40} tend to be lower than the mean value of the other coefficients. The small sample sizes dictate that these findings should be interpreted with caution.

If the angle-dependent Zernike functions are compared directly, the function represented by coefficient a_{51} is the only one which includes the variable p to the power of 5 (Chapter 3.2.10.4.2). Therefore, this function plays a central role in the angle-dependent Zernike functions shape description.

The z-value is an important measure of how a contact lens moves on the cornea. In this study, the range of z-values for the contact lens wearers (about 2.5% of corneal thickness) is greater than the range for non contact lens wearers (about 1.5% of corneal thickness). There is no linear association between residual rms mean values and IOP.

Chapter 5. Methods and design of the study at high altitude

5.1 Introduction

One month before the trekking tour, the author assessed the subjects at the baseline altitude of 2000ft. This included the recording of baseline data relating to the health of the subjects' eyes and regarding the fit of the contact lenses. It was also the point at which the crucial reference residual rms data were recorded for each subject.

The high altitude study discussed in this and the following chapter was carried out in Nepal. The infrastructure of Western Europe is not comparable with that of the high altitude regions of Nepal. Therefore, once the trekking tour had begun the study had to be completely self-sufficient - in terms of everything from the electrical supply to the replacement parts that were carried to avoid any interruption of data collection. The weather was an incalculable risk factor. All this made it crucial that a suitable region in Nepal was chosen and that suitable equipment was chosen to permit the study to be self-sufficient – any failure to be self-sufficient would increase the risk of interruption to the study.

5.2 Electrical support

Two lead accumulators were used with the following technical data: The type no. was LC-R 1212P1, the voltage was 14.5 – 14.9 V, and the initial current had to be less than 4.8 A. A Portable Inverter transformed 12V/24V DC into 230 V AC with an efficiency of more than ninety per cent.



Figure 5.2-1 Trek logistics. One porter carried the instruments including the electrical equipment in a small container. The solar cells were placed on the back of the container. The accumulators were loaded while the porter carried the box.

Two solar modules with a total power of fifty watts loaded the accumulators while a porter carried a small container with the fixed solar modules on his back (Figure 5.2-1).

The formulae for the electrical power calculations were:

$P = U * I$; P = electrical power, U = voltage, I = current intensity, unit = W
Joules of energy = $U * I * t$; t = seconds, U = voltage, I = current intensity,
 t = time, unit = Wh (Kuchling, 1986).

The laptop power was calculated using the information from the laptop type plate (19V/2.6A). Therefore $p = 19 \text{ V} * 2.6 \text{ A} = 49.4 \text{ W}$. During the measurements the laptop was directly connected to one accumulator via a car adapter.

The 100 W keratographer power was connected via the inverter with one of the accumulators. The inverter's efficiency was more than ninety per cent, so we needed 110 W for the keratographer. It was estimated that one "test procedure" would take about twenty minutes, and there were three test procedures each day. Therefore, the total electrical power required per day for the laptop and keratographer was:

$$(50 \text{ W} + 110 \text{ W}) * (20 \text{ min} * 3) = 160 \text{ Wh.}$$

Batteries were carried for the other instruments, such as the Tono-Pen, the hand-held slit lamp and Welch Allyn ophthalmoscope.

The solar module's efficiency was 0.85 under ideal conditions, which means at noon, when the solar modules were positioned perpendicular to the sun. This was not always possible, and it was estimated that the total available sunshine power for a whole day would be approximately 2.5 hours of maximum sunshine power a day.

$W_{\text{solar}} = 100 \text{ W} * 0.85 * 2.5 \text{ h} = 212.5 \text{ Wh}$. 160 Wh were required each day and the solar modules delivered 212.5 Wh, so the electrical system was calculated to carry a reserve of approximately 52.5 Wh when the surrounding conditions were normal.

Risk factors for the electrical current supply were storms, prolonged fog, prolonged rain, a very cloudy sky, and a very low temperature. So the calculation had a risk factor which cannot be neglected. Accumulators with more power were impractical because they would be much heavier than the accumulators described here.

As a result of the weight of the equipment, it was not possible to have a reserve greater than 52.5Wh.

5.3 Preparation and test procedures

5.3.1 Preparation

The altitude study group consisted of twelve participants including nine subjects (three soft lens wearers, and six non-lens wearers) and three other participants.

The ages of the subjects (3 female and 6 male) ranged from 45 – 60 years. Two months before the trekking tour, at a meeting to discuss the principles which affect behaviour at high altitude, the author informed the subjects of their role during the tests and explained the measurements in detail. All risk factors associated with the tests were explained. The subjects all gave written informed consent to participate in the study.

5.3.2 Contact lenses used for subjects in the altitude study

One month before the trekking tour, the author assessed the subjects at the baseline altitude of 2000ft. The assessment included; taking a history and symptoms, carrying out an eye examination, and a soft contact lens fitting on the three contact lens wearers. The keratographer measurements, taken on each of the nine subjects' eyes were required as reference data (Table 5.3.2-1) and contribute to the analysis of the affects of altitude in Chapter 6.

Descriptive statistics of the residual rms values for the reference measurements								
Resrms	Mean	Min.	Max.	0.25 th Quarti	0.75 th Quarti	Range	Varian	Stdv.
Refmor	.0009	.0005	.0015	.0006	.0010	.0011	.0000	.0003
Refnoon	.0016	.0005	.0041	.0006	.0020	.0035	.0000	.0012
Refeven	.0010	.0003	.0050	.0005	.0011	.0047	.0000	.0009

Table 5.3.2-1 Descriptive statistics of residual rms reference values obtained during eye examinations carried out before the tour started. Unit: $\times 10^6$ Microns.

Two days following an eye examination on the contact lens wearers, the contact lenses arrived and the subjects immediately began wearing their lenses.

The quality of the fit and health of the eyes, judged by an assessment of the movement of the lenses, the contact lens surface and the cornea, was carried out every fifth day until two days before the trekking tour started.

Two types of contact lenses were used: Bausch & Lomb Optima Toric (Hefilcon B) lenses and Bausch & Lomb Optima 38 (Polymacon Monomer A).

The data on the lenses is as follows:

(Figure 4.2.3-1, Figure 5.2.-1, Figure 5.2-2).

Subject 1.22:

Optima Toric sph +250 cyl -4.25 AX 165, BC 8.90, Diam \varnothing 14.0,
optical zone 8.0 mm, centre thickness 0.231 mm/0.246 mm

Optima Toric sph +1.50 cyl -2.75 AX 180, BC 8.90, Diam \varnothing 14.0,
optical zone 8.0 mm, centre thickness 0.210 mm/0.225 mm

Subject 2.22:

Optima 38, sph +1.0 dpt, SAG 9.0, Diam \varnothing 14.0 optical zone 8.0 mm,
centre thickness 0.110mm/0.115mm

Optima 38, sph +1.25 dpt, SAG 9.0, Diam \varnothing 14.0, optical zone 8.0 mm,
centre thickness 0.120mm/0.125mm

Subject 3.22:

Optima 38, sph -2.75 dpt, SAG 8.7, Diam \varnothing 14.0, optical zone 10.0 mm,
centre thickness 0.060 mm

Optima 38, sph -2.50 dpt, SAG 8.7 Diam \varnothing 14.0, optical zone 10.0 mm,
centre thickness 0.060 mm

Polymacon - Group 1, Low Water, Non-Ionic *Optima 38*

The lens material polymacon is a hydrophilic random polymer of 2-hydroxyethyl methacrylate. The lens is 38.6% water by weight when immersed in a sterile solution of 0.4% sodium chloride and a borate buffer. The lens is tinted blue with up to 100 ppm of reactive blue dye 246. The resulting transparent material not only has good mechanical strength, but also behaves elastically, returning to its original shape after deformation. The refractive index of the material is 1.43.

Hefilcon B - Group 1, Low Water, Non-Ionic

The Bausch & Lomb Optima® Toric (hefilcon B) contact lens is made from a copolymer of 2-hydroxyethyl methacrylate and N-vinyl pyrrolidone, and is 45% water by weight when immersed in a sterile solution of sodium chloride and borate buffer.

Figure 5.3.2-1 Manufacturer's information (Bausch & Lomb) indicating some of the differences between the two contact lens types.

Bausch & Lomb OPTIMA TORIC Lenses

INDICATIONS

ASTIGMATISM
DAILY WEAR
VIAL PRODUCT

DESCRIPTION

An easy-to-fit low water content prism-ballasted toric soft lens manufactured using patented Toric Generating lathe-cutting technology, and designed for use in the correction of astigmatism on a daily wear basis. Comfort chamber design provides excellent comfort, while high modulus of material provides accurate and predictable orientation on the eye.

PARAMETERS

MATERIAL	Hellicon B
WATER CONTENT	45%
FDA MATERIAL GROUP	1
OXYGEN PERMEABILITY (Dk)	$13.0 \times 10^{-11}^*$
OXYGEN TRANSMISSION (Dk/L)	10.00 x 10 ⁻⁹ (-3.00D @ Central) 8.00 x 10 ⁻⁹ (-3.00D Avg. 6mm) 5.06 x 10 ⁻⁹ (+3.00D @ Central) 6.30 x 10 ⁻⁹ (+3.00D Avg. 6mm)
ORIENTATION METHOD	Prism-Ballasted
ORIENTATION INDICATORS	3 Laser Guide Marks Inferiorly (30° apart)
TORIC LOCATION	Front Surface
MANUFACTURING METHOD	Toric Generation (Lathe-Cut)
BASE CURVES	8.3mm, 8.6mm, 8.9mm
DIAMETER	14.00mm
POWERS (Sphere)	-9.00D to +6.00D
(Cylinder)	-0.75 to -4.25D (0.50D steps)
(Axes)	360° in 5° steps
OPTICAL ZONE	8.0mm
CENTER THICKNESS	0.100mm (-6.00D to -4.25D) 0.105mm to 0.121mm (-4.00D to -3.25D) 0.126mm/0.142mm (-3.00D to -2.25D) 0.147mm/0.168mm (-2.00D to -1.00D) 0.173mm/0.189mm (-0.75D to Plano) 0.194mm/0.204mm (+0.25D to +0.75D) 0.210mm/0.225mm (+1.00D to +1.75D) 0.231mm/0.246mm (+2.00D to +2.75) 0.252mm/0.273mm (+3.00D to +4.00D) 0.278mm/0.316mm (+4.25D to +4.80D)
LENS MARKINGS	3 Linear Laser Marks
VISITINT	Clear
REFRACTIVE INDEX	1.42
LIGHT TRANSMISSION	CIF Value approx. 97%
DISINFECTION METHODS	Heat Chemical Hydrogen Peroxide

* $(\text{cm}^2\text{O}_2 \times \text{cm}/(\text{sec} \times \text{cm}^2 \times \text{mmHg}))$ at 35°C.

Figure 5.3.2-2 Manufacturer (Bausch & Lomb) information on lens type Optima Toric.

5.3.3 The test procedure performed morning, noon, and evening

The test procedure carried out during the altitude study consisted of the following tests in this order:

- Air pressure
- Altitude
- Temperature

- Humidity
- Contact lens fit (where applicable)
- Corneal examination
- Eye pressure
- Central retinal examination
- Keratographer measurement.

A brief summary of the instruments (described in detail in chapter 3.2) for testing the meteorological surrounding conditions follows;

- The air pressure was measured with a Fischer barometer model nr 104-002 modified for high altitudes.
- The altitude was measured with a Thommen 7000 altimeter. Since air pressure influences the altimeter, every change in air pressure was taken into account when adjusting the altimeter. In addition, we had two maps showing the altitude of some points we passed during our trekking tour. These points were also used as corroboration points to adjust the altimeter (Chapter 3.2.4).
- A mercury thermometer Möller Therm model number 106705 showed the temperature while the humidity was measured with a precision hygrometer Fischer model nr 122.01

The following measurements were performed on the subjects in detail:

The fit of the contact lenses was assessed for the contact lens wearers. This comprised a test of the contact lens movement, an examination of the contact lens surface with the slit lamp,



Figure 5.3.3-1 The soft lens fitting was tested before the measurements were performed with the keratographer.

and the subjects' observations on the wearing comfort of the contact lenses.

The corneal examination was performed with a hand-held slit lamp.

1. The corneal surface was inspected with a broad slit to detect injuries, irregularities, inflammation, the colour of the tear film to assess the oily layer with the help of the reflected illumination, neo-vascularization, infiltrations, striae, and other abnormalities.

2. Secondly, the small slit was used to identify Descemet folds.

The intraocular pressure was measured with the Tono-Pen XL. The instrument was newly calibrated each day before the first subject was measured. In every measurement block the measurements were taken at the same point on the sclera, below and adjacent to the limbus at the cornea, of each eye. After four measurements were performed on one eye, the instrument calculated the mean of the measurements automatically. The IOP was obtained from a conversion table provided by the manufacturer (Table 3.2.8-1) and the computed mean.

The central retinal examination was carried out with the ophthalmoscope, and chief emphasis was on the typical retinal changes that may be seen at high altitudes such as, retinal haemorrhages (including flame-shape haemorrhages), cotton wool spots, blood vessel engorgement, tortuosity and papilloedema.

The findings for the cornea and contact lens fitting were recorded using the CCLRU-grading scale.

Before each subject was assessed with the keratographer they were instructed on their role during the measurement. A small camera in the centre of the Placido circles helped to control the eye position relative to the Placido circles.

The measurement was performed automatically, shortly after the eye had been centred. The base data were transformed into a combination of ellipsoid and Zernike coefficients after completion of the trekking tour.

5.4 Description of the tour

5.4.1 The choice of the region for the tests

Normally mountaineers remain at high altitude for some weeks. They are a long way from the base camp and the weather often changes for the worse. Mountain climbers, therefore, often have to stay in their base camp until the weather improves. Sometimes they must wait several days before they are able to climb up to a mountain peak, which means that many trekking tours last about three weeks. The surrounding conditions such as air pressure, temperature, humidity, and altitude change quickly. The human body, including the eyes, have to adapt to these changing conditions.

For this reason trekking tours are an ideal opportunity to test changes in the corneal shape during the acclimatisation phases. Nepal is one of the best regions in the world to test this hypothesis because Nepal has very high mountains as well as reliable information on weather and trekking tours. The latitude of Nepal is the same as that of the Central Sahara – between 26 degrees 22 seconds north and 30 degrees 27 seconds north. The longitude is 80 degrees 40 seconds east to 88 degrees 12 seconds east.

The best time of year to carry out scientific activities in the Himalayas is in November due to the stable weather conditions during this time. The months from June to the beginning of October are not suitable for such research because of the monsoon. In Nepal the monsoon comes not from the Southwest like in India, but from the Southeast. The monsoon brings much more rain to the eastern part of Nepal than to the western part.

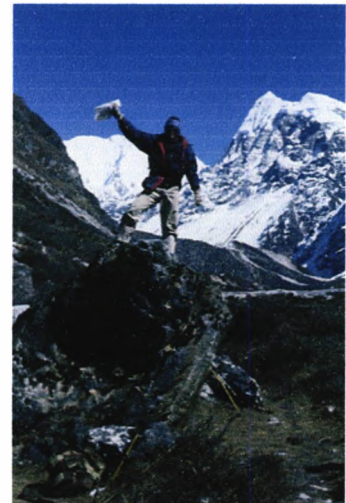


Figure 5.4.1-1 Location of the first base camp at Kyangjin. 12600 ft.

In December the northeast monsoon brings rain to the eastern part of Nepal. A very complex wind system found on high mountain chains and the position near the equator are responsible for the variability of different climatic conditions in some valleys. When a trekking tour goes from one valley to another it is possible that the surrounding climatic conditions may change completely. The temperature depends on the height, the region, and the season. Normally in spring it is warm, in summer it is hot, in autumn it is warm, and winter is very cold. In November the weather is very stable but it becomes colder week by week (Aubert, 1996). Sometimes it snows, which makes it very difficult to reach some locations.

Northern Nepal is marked by high mountains and deep valleys. Trekking tours use particular paths, which normally allow the tours to complete their treks even when the weather is bad. These familiar pathways minimize the risk of having to interrupt a tour. We chose Lang tang, whose latitude is about 28 degrees north (near Tibet). During our tour the altitude changed quite often and the path was familiar (Figure 5.4.1-2).

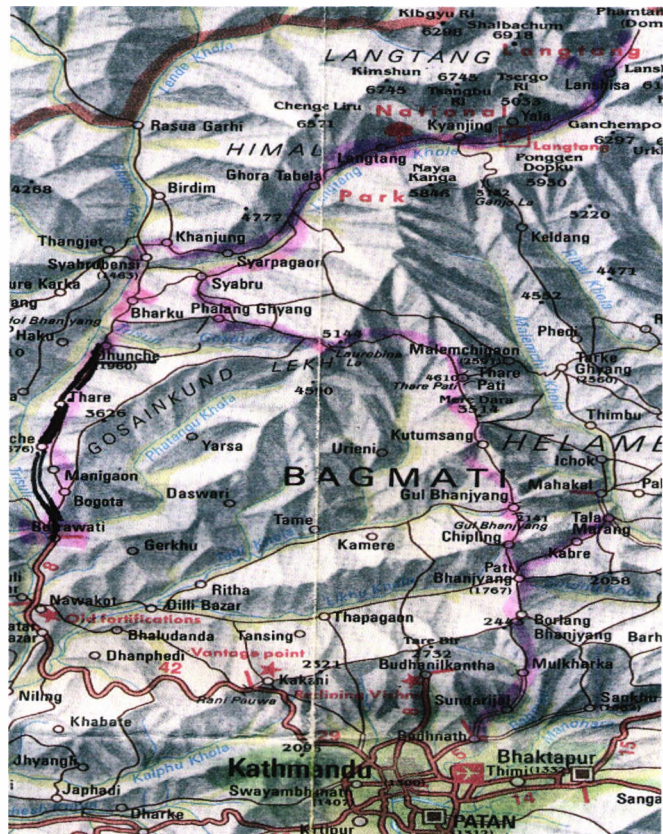


Figure 5.4.1-2 Map showing the path taken on the trekking tour in Northern Nepal.

5.4.2 Equipment



Figure 5.4.2-1 The equipment used for the measurements and personal belongings one day before the tour started. The equipment weighed 48 kg.

All the instruments described above were transported in a metal box with foam material inside. Small tents for two persons and one large community tent were transported with us. The furniture in our community tent consisted of two folding tables and one small folding chair for each trekker. The community tent was our dining room and the location for the study tests. During the night the outside temperature sometimes fell below minus 20



Figure 5.4.2-2 The subjects were instructed how to behave before the measurements were taken. We had tables and chairs with us to perform the keratographer measurements.

degrees Celsius. To protect the instruments against these low temperatures they placed in the author's sleeping bag and the metal box with the medical instruments inside was placed between two trekkers in the middle of a tent. Inside the tent and outside the sleeping bags a temperature of approximately plus 9 degrees Celsius was maintained overnight.

The manufacturer of the laptop guaranteed the laptop's screen functionality when the surrounding temperature is above five degrees Celsius. The laptop and the other instruments functioned without complications throughout the trekking tour, although it was sometimes necessary to replace a fuse for the inverter and the insulation for the solar cell cables broke twice. The insulation was repaired with adhesive tape. The porter was advised to handle everything very carefully (especially the metal box).

One problem remained insoluble: the sun refused to shine on some days. An electrical power generator would have been too heavy. One week before the start of the tour the Meteorological Institute in Munich informed the author that due to a stable weather front in Kathmandu we would probably have no problems with the weather. The tour party included twenty-two porters, three cooks, and three sherpas.

5.4.3 The trekking tour

Lang tang is a very large valley. It begins at Syrabru Berisi (4590 ft) and ends between two mountains, Lang tang Ri (23,630 ft) and Porong Ri (25,260 ft) at an altitude of 21,650 ft. The Lang tang valley follows a river called Lang tang Khola until Drichung Pu (14,430 ft). Lang tang Khola has its source in Drichung Pu. At this point a large glacier (Lang tang Tsang) begins.

Nubamathang was the last stop made by our group in the Lang tang valley shortly before the glacier begins. The first measurement block was carried out in Kathmandu (4400 ft) on the evening before we left the capital.

After a seven-hour bus ride from Kathmandu to Dhunche (where an evening and morning test procedure was conducted at 6500 ft) the trekking tour began the following day. The group ascended slowly to Syrabru (7400 ft). This path was chosen in order to ensure a good acclimatisation phase. Syrabru (evening and morning tests at 7400 ft) was the second station where the tour stayed for the night.

The group went down to the deepest point (noon tests at 5600 ft) of Lang tang valley, where we arrived around noon. Then we ascended to Lama Lodge (evening and morning test procedures at 8100 ft) to camp for the night. On the way we passed by Ghora Tabela (noon tests at 9970 ft) to reach Lang Tang (evening and morning test procedures at 11,400 ft) to spend the night. After having lunch near Kyangjin Khar (noon test procedure at 12,400 ft) we arrived at our base camp in Kyangjin Khar (Figure 5.4.1-1 evening test procedure at 12,600 ft).

To achieve better acclimatisation, the group ascended to Nubamathang (morning tests at 13,800 ft) and returned to Kyangjin Khar (evening measurements at 12,600 ft). When we returned an inhabitant informed us that two mountaineers had ascended Gangtsa La (16,800 ft), but they had had problems because it had snowed one week before. This path was much more difficult because of snow. Furthermore, they had not had enough water with them. The mountaineers had been found dead on the same day we arrived in Kyangjin Khar. The reason for the death of these two mountaineers is speculative. One body was found near the path and the other was found 500m away from the path. The path is well defined so it is possible that both mountaineers were suffering from acute mountain sickness and one of them wanted to go back to get help but was not able to find the right path. Our plan was to open a second camp near Yala Peak (18,110 ft) in a small valley (\approx 16,400 ft), but when we heard of the deaths our mountain guide and the author ascended to the small valley to test the surrounding conditions. There was deep powder snow and it was very cold. After we returned all the participants ascended to the top of a mountain called Kyimoshung (\approx 16,000ft). Evening measurements were taken after we returned to Kyangjin Khar.

One subject in our group experienced physiological problems and had to break off the trekking tour at Kyangjin Khar. He was taken out by helicopter.

One day later, we decided to ascend the top of a mountain called Tsergo Ri (morning and evening tests in Kyangjin Khar), returning the same day.

In the following days we spent one night at Nat. P. Lodge (morning test procedure at 9800 ft), one night between Nat. P. Lodge and Bambu Lodge (noon and evening measurements at 8000 ft and 6700 ft, respectively) and one night at Bambu Lodge (noon and evening tests at 7500 ft) before returning to Syrabru (noon test procedure at 7400 ft).

The next day's goal was Shing Gompa (noon test procedure at 11,000 ft), which is on the opposite side of Lang tang valley.

This side is usually a very foggy region where the fog comes in the morning and disperses in the evening every day. One day later we ascended Gosaikund (evening tests at 14,300 ft) and stayed there for the night.

Next day we tried first to climb an unnamed mountain (\approx 17,000 ft) but there was too much snow about 200 ft below the peak, so we climbed to the top of a nearby peak (16,700 ft) near the mountain and came down across the Laurebina Pass (noon test procedure at 15,100ft but not complete). The following days we went to Pal Mere Dora (12,000 ft), Kutumsang (noon measurements at 8100 ft), Chisopani (7200 ft), returning to Kathmandu (evening tests at 4400 ft).

The fog around Shing Gompa and the low temperatures at Gosaikund caused the electrical support from the accumulators to fail. The accumulators had to be recharged once a day. One measurement block was performed in Kutumsang (8100 ft). One day later, the accumulators had to be recharged for the whole day. Then we arrived back in Kathmandu valley (Figure 5.4.1-2), and we stayed in Kathmandu for one day before flying home. Everyone in the party was in a good health when we arrived back in Kathmandu.

The important stages in the trekking tour were as follows:

03.11. Kathmandu 4400 ft

04.11. Dhunche 6500 ft

05.11. Syrabru 7400 ft

06.11. Deepest point Lang tang 5600 ft

06.11. Lama Lodge 8100 ft

- 07.11. Ghora Tabela 9970 ft
- 07.11. Lang Tang 11,400 ft
- 08.11. Kyangjin Khar 12,600 ft
- 09.11. Nubamathang 13,800 ft
- 10.11. Kyangjin Khar 12,600 ft
- 11.11. Tsergo Ri 16,500 ft
- 11.11. Kyangjin Khar 12,600 ft
- 12.11. Nat. P. Lodge 9800 ft
- 13.11. Bambu Lodge 7500 ft
- 14.11. Syrabru 7400 ft
- 15.11. Shing Gompa 11,000 ft
- 16.11. Gosaikund 14,300 ft
- 17.11. Peak 16,700 ft
- 17.11. Laurebina 15,100 ft
- 17.11. Pal Mere Dora 12,000 ft
- 18.11. Return to deepest point
5900 ft
- 18.11. Kutumsang 8100 ft
- 19.11. Chisopani 7200 ft
- 20.11. Kathmandu 4400 ft
- 21.11. Kathmandu 4400 ft

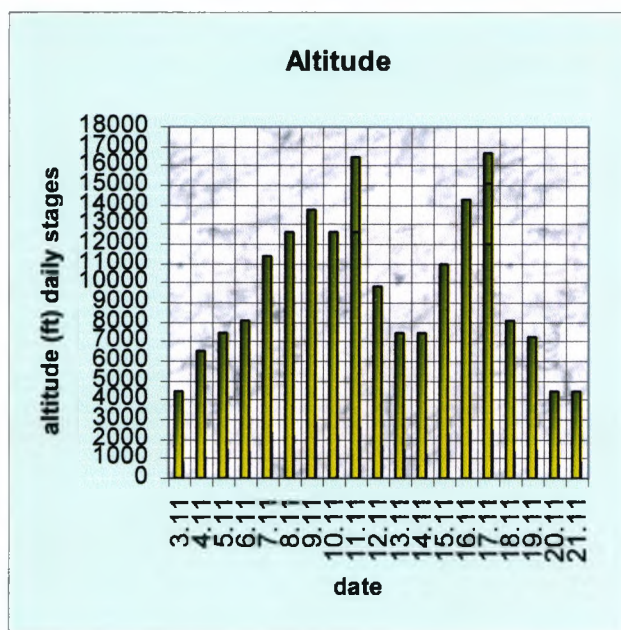


Figure 5.4.3-1 The maximum altitude of every daily stage of the trek.

5.5 Summary

One month before the trekking tour, the author assessed the subjects at the baseline altitude of 2000ft, and recorded the reference residual rms data for each subject.

Carrying out a self-sufficient study in Nepal required the electrical support to be chosen to ensure as far as possible that all instrumentation would function without interruption during the whole test phase.

Additionally, preparations were made to ensure that other factors did not cause interruption of the tests. Besides replacement parts, food, tents, sleeping bags and so on, keeping all the subjects healthy throughout the trekking tour should be mentioned as a main aim of the tour organization! Thus the choice of a suitable region for the tests played a central role in the design of the trekking tour. Chapter 2.2.7.1 states that the human body acclimatizes in steps, therefore the altitude should rise steadily on the trek up to our maximum of 17,000ft.

In consideration of the elevated physical effort required by acclimatisation alone, it is important that the trekking tour should not be too difficult for the subjects. That was one of the reasons why the altitude study was carried out in Lang tang, a very large valley, with a return to Kathmandu. The valley begins at Syrabru Berisi (4590 ft) and ends between two mountains, Lang tang Ri (23,630 ft) and Porong Ri (25,260 ft) at an altitude of 21,650 ft. Nine subjects were tested, three female and six men, aged between 45 and 60 years. Three of them were soft contact lens wearers.

Measurements of surrounding conditions, eye examinations, and keratographer measurements were taken morning, noon and evening throughout the tour in Nepal. The measurements were documented, with some interruption during the third week of the trekking tour. We passed a very foggy region which led to a reduced availability of electrical power and which prevented the author taking measurements three times a day.

Chapter 6. High altitude study

6.1 Introduction

The interactions between environmental conditions and their influence on the eye at high altitude were established with the help of literature on the topic. This chapter describes the procedure followed to perform the hypothesis tests on the data collected at high altitude, and comments on some of the outcomes of this analysis.

To facilitate the statistical analysis it was necessary to render all the corneal shape measurements comparable, hence the value residual rms was introduced in section 3.2.10.6. This represents the corneal shape alterations of each eye separately. The background to the statistical hypothesis tests are described graphically and completed with the aid of ANOVA analysis. After the ANOVA tests, any significant changes in corneal shape have been examined in more detail with the Duncans' MRT procedure. Associations between residual rms values and other parameters are investigated.

6.2 Data from the high altitude study

One special aspect of outdoor studies compared with studies carried out in low pressure chambers is the fact that surrounding conditions, for example humidity, temperature, and air pressure, can change simultaneously and spontaneously. Thus statistical evaluations, especially discussions of correlations between corneal shape change and surrounding conditions, can become particularly complex. Nevertheless, there are two pressing reasons for carrying out the tests outdoors, firstly the acclimatisation of the human body to altitude takes some days, with the length of the acclimatisation period depending on the altitude a mountaineer intends to ascend.

Secondly the weather conditions found in nature can not be completely simulated in a low pressure chamber. For the high altitude study the corneal shape measurement data are considered from several different aspects.

6.3 Descriptive statistics

All the residual rms values computed from corneal shape measurements carried out at high altitude (higher than 1000m) are divided into six categories; non contact lens wearers and contact lens wearers, and these two groups are further subdivided into morning (Morn-ncl, Morn-cl), noon (Noon-ncl, Noon-cl), and evening (Even-ncl, Even-cl). The reference measurements taken from the subjects before ascending to altitude are divided into morning- (Refmor), noon- (Refnoon) and evening categories (Refeven). One month before the tour started the reference measurements were taken from every subject (section 5.3.2). These reference categories contain residual rms values which demonstrate corneal shape change of the subjects recorded under common surrounding conditions at low altitude.

Table 6.3-1 shows the differences between the above categories in terms of mean, minimum, maximum, 0.25 quartile, 0.75 quartile, range, variance, and standard deviation. It is interesting to note the following:

The means of the residual rms values for the contact lens wearers tend to be greater than the means of the other categories.

The ranges of the rms values for the contact lens wearers are greater than those of the non contact lens wearers, and the contact lens wearers evening range is the greatest of all the values recorded. This increased range is less obvious from the 0.75 quartile, which reflects the influence of an outlier in the contact lens wearers evening measurement category. The Box and Whisker Plots (Fig. 6.3-1) give a further overview of the differences between categories. Here, the similarity between the median values of the non contact lens and contact lens wearing groups and the influence of outliers are apparent.

Descriptive statistics of the residual rms values for the reference and altitude measurements								
Resrms	Mean	Min.	Max.	0.25 th Quarti	0.75 th Quarti	Range	Varian	Stdv.
Refmor	.0009	.0005	.0015	.0006	.0010	.0011	.0000	.0003
Refnoon	.0016	.0005	.0041	.0006	.0020	.0035	.0000	.0012
Refeven	.0010	.0003	.0050	.0005	.0011	.0047	.0000	.0009
Morn-ncl	.0017	.0003	.0057	.0009	.0024	.0054	.0000	.0011
Noon-ncl	.0015	.0004	.0065	.0008	.0018	.0062	.0000	.0011
Even-ncl	.0015	.0003	.0050	.0008	.0019	.0047	.0000	.0011
Morn-cl	.0017	.0005	.0085	.0009	.0023	.0081	.0000	.0013
Noon-cl	.0021	.0005	.0090	.0011	.0030	.0086	.0000	.0013
Even-cl	.0018	.0003	.0104	.0008	.0020	.0101	.0000	.0017

Table 6.3-1 Descriptive statistics of the residual rms values for all tested subjects. Unit: $\times 10^6$ Microns.

Although the standard deviations of the reference data do vary between morning, noon and evening, the reference sample sizes are too small for reliable statistical tests. It was not possible to collect more reference data as a result of the very limited time available before the trek began. Table 6.3-1 shows data to four places after the decimal point, which is sufficient to identify trends.

Variances are shown in Table 6.3-1 and they only contribute from the sixth place after the decimal point (difference between smallest- and greatest variance, which were taken into consideration different sample sizes, is 16.6%).

It is clear that the residual rms values are not very evenly distributed in their categories. This phenomenon is most apparent in the contact lens wearers for the evening measurement category.

The descriptive statistics for high altitude samples compared with those for low altitude samples generally show higher sample mean residual rms values at high altitude, and greater maximum residual rms values at high altitude.

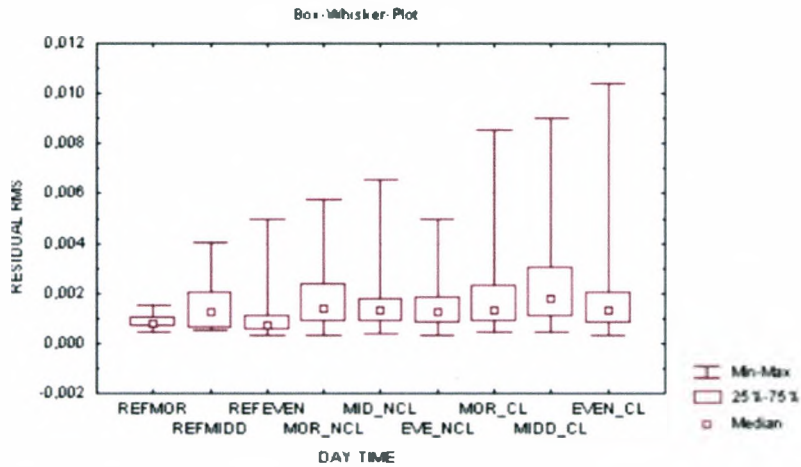


Figure 6.3-1 Descriptive summary of residual rms values using Box and Whisker Plots.

Chapter 3.2.10.4.3 demonstrates the Zernike functions graphically. To identify which Zernike coefficient(s) mean value(s) dominate(s) it helps to understand how the corneal shape is comprised. Which coefficient has the greatest influence on residual rms values?

To begin to answer this question the Zernike coefficients are described by means of mean values computed for every coefficient and subject separately.

The results are summarized in table 6.3-2 and table 6.3-3.

The data defining the ellipsoid for each eye are presented in table 6.3-4.

Mean of Zernike coefficients for the subjects' right eyes										
Subject	a20	a40	a60	a11	a31	a51	a22	a42	a33	a44
1.21	-.0117	-.0021	-.0000	.0016	.0029	.0075	.0007	.0027	.0019	.0010
2.21	-.0013	-.0017	-.0000	.0007	.0009	.0018	.0006	.0014	.0014	.0008
3.21	.0021	.0006	.0002	.0021	.0023	.0022	.0008	.0015	.0009	.0008
4.21	.0012	-.0009	.0003	.0010	.0008	.0052	.0007	.0018	.0013	.0004
5.21	-.0002	-.0011	.0001	.0020	.0019	.0130	.0010	.0018	.0012	.0010
6.21	.0011	.0004	.0002	.0014	.0021	.0089	.0009	.0016	.0013	.0009
Sum/6	-.0015	-.0008	.0001	.0015	.0018	.0064	.0008	.0018	.0013	.0008
Cl	a20	a40	a60	a11	a31	a51	a22	a42	a33	a44
1.22	.0316	.0000	-.0005	.0857	.0114	.0606	.0025	.0055	.0026	.0013
2.22	-.0024	-.0026	.0002	.0019	.0019	.0049	.0008	.0014	.0011	.0010
3.22	-.0004	-.0010	.0001	.0009	.0018	.0077	.0009	.0040	.0025	.0015
Sum/3	.0096	-.0012	-.0007	.0295	.0050	.0244	.0014	.0036	.0021	.0013

Table 6.3-2 Mean values of each Zernike coefficient for the right eye of each subject. Unit: $\times 10^6$ Microns.

Mean of Zernike coefficients for the subjects' left eyes										
Subject	a20	a40	a60	a11	a31	a51	a22	a42	a33	a44
1.21	-.0015	-.0029	-.0001	.0023	.0023	.0050	.0009	.0028	.0011	.0010
2.21	-.0023	-.0021	-.0001	.0013	.0012	.0029	.0006	.0020	.0014	.0012
3.21	-.0011	-.0009	.0002	.0021	.0027	.0049	.0006	.0020	.0011	.0009
4.21	-.0031	-.0015	.0002	.0015	.0011	.0039	.0003	.0023	.0010	.0006
5.21	.0000	-.0005	.0002	.0042	.0031	.0052	.0012	.0020	.0016	.0012
6.21	-.0000	-.0011	.0000	.0016	.0025	.0113	.0013	.0027	.0015	.0012
Sum/6	-.0013	-.0015	.0007	.0021	.0021	.0055	.0008	.0023	.0013	.0010
Cl	a20	a40	a60	a11	a31	a51	a22	a42	a33	a44
1.22	.0173	-.0017	-.0003	.0550	.0069	.0408	.0014	.0029	.0023	.0012
2.22	-.0019	-.0021	.0000	.0016	.0019	.0083	.0013	.0020	.0012	.0014
3.22	.0002	-.0004	.0003	.0011	.0017	.0043	.0005	.0033	.0019	.0016
Sum/3	.0052	-.0014	0	.0192	.0035	.0178	.0011	.0027	.0018	.0014

Table 6.3-3 Mean values of each Zernicke coefficient for the left eye of each subject. Unit: $\times 10^6$ Microns.

Subject	1.21	2.21	3.21	4.21	5.21	6.21	1.22	2.22	3.22
Radius mm (RE)	8.08	7.45	7.84	7.55	7.74	7.57	7.07	7.98	7.26
g (RE)	0.61	0.62	0.75	0.70	0.57	0.81	0.58	0.54	0.63

Subject	1.21	2.21	3.21	4.21	5.21	6.21	1.22	2.22	3.22
Radius mm (LE)	7.83	7.42	7.85	7.66	7.72	7.46	7.19	7.95	7.33
g (LE)	0.53	0.62	0.59	0.66	0.67	0.63	0.58	0.63	0.74

Table 6.3-4 Values of the radius and g values of the ellipsoid for each subject. RE = Right eyes, LE = Left eyes. Unit: $g \times 10^6$ Microns.

The mean value of coefficient a_{51} when compared to the other coefficients is highest for almost every subject. Zernike function $Z_{5,1}(\rho, \alpha)$ influences the corneal shape mainly peripherally. Furthermore, most of the coefficient mean values are greater for subjects belonging to the contact lens wearing group than for those in the non contact lens wearing group.

Each coefficient represents the quantitative influence of a Zernike function on the description of the corneal shape. The structure of this Zernike function ($Z_{n,m}(p,\alpha)$) also has an influence on the description of the corneal shape. Therefore, for a complete discussion of the quantitative influences of coefficients on corneal shape, the structure of their Zernike functions ($Z_{n,m}(p, \alpha)$) should also be taken into consideration, with the help of formulae described in section 3.2.10.5. Index n shows the greatest power in each Zernike function. That power is calculated from values which range between 0 and 1. The greater the power of those values the smaller the result and therefore the smaller is the influence of Zernike functions themselves on the corneal shape. That influence is computed in a number of steps. First, Zernike coefficients of spherical aberration are divided by the term $(n+1)^{0.5}$ and Zernike coefficients of angle dependent aberrations are divided by the term $(2*(n+1))^{0.5}$. Second, in order to get positive numbers, the results from step one are squared. The average influence of Zernicke coefficients on corneal shape is calculated from the values “ $a_{n,m}$ sum/6” and “ $a_{n,m}$ sum/3” taken from table 6.3-2, and table 6.3-3.

The coefficient with the lowest average influence on corneal shape is a_{60} (between 0 and $1.4E-09$). The coefficient with highest average influence on corneal shape is a_{51} (between $2.5 E-06$ and $4.9 E-05$).

6.4 Distributions of residual rms values and significance testing for the non contact lens wearers and contact lens wearers groups

Prior to hypothesis testing, the best-fitting distribution was computed for the samples (categories) non contact lens wearer morning tests (MORN-NCL), noon tests (NOON-NCL), and evening tests (EVEN-NCL), and the contact lens wearer morning tests (MOR-CL), noon tests (NOON-CL), and evening tests (EVEN-CL). The best-fitting distribution was selected from the following with the aid of the Likelihood Method; Beta, Exponential, Extreme, Gamma, Lognormal, Normal, Raleigh, and Weibull distributions.

Figures 6.4.1 – 6.4.12 demonstrate the differences between the best-fitting distributions for the study data compared to the theoretical distribution. The red line in each graph describes the ideal theoretical distribution fit. When the plotted points are positioned close to the red line, or on the line, the tested distribution represents the category under examination quite well. Only the best-fitting distribution is shown for each category (which was the Gamma distribution in all six categories), plus illustrations of how well the Normal distribution fits the data from each category.

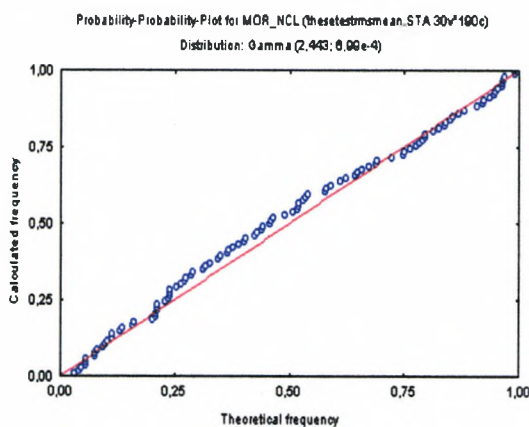


Figure 6.4-1 Graph illustrating how well the distribution of residual rms values is described by the Gamma distribution for the non-contact lens wearing group (morning tests).

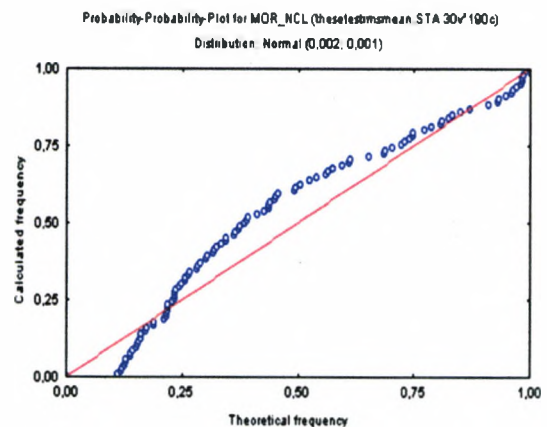


Figure 6.4-2 Graph illustrating how well the distribution of residual rms values is described by the Normal distribution for the non-contact lens wearing group (morning tests).

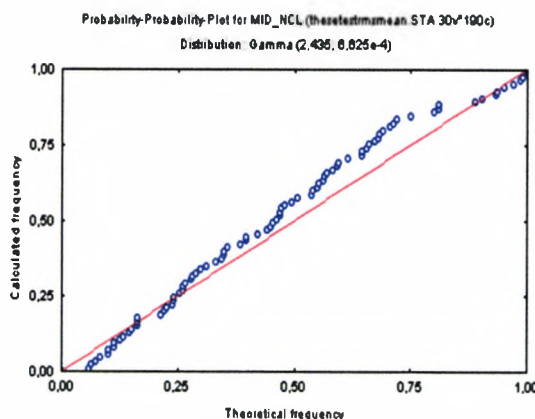


Figure 6.4-3 Graph illustrating how well the distribution of residual rms values is described by the Gamma distribution for the non-contact lens wearing group (noon tests).

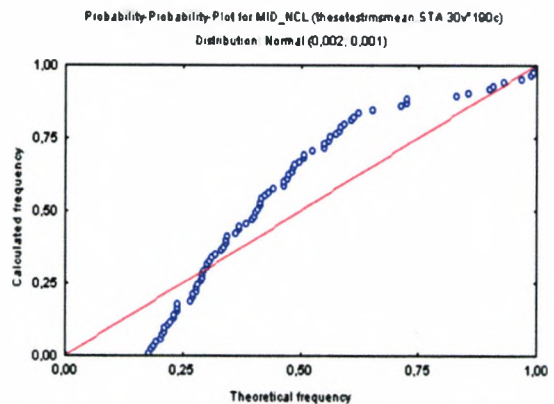


Figure 6.4-4 Graph illustrating how well the distribution of residual rms values is described by the Normal distribution for the non-contact lens wearing group (noon tests).

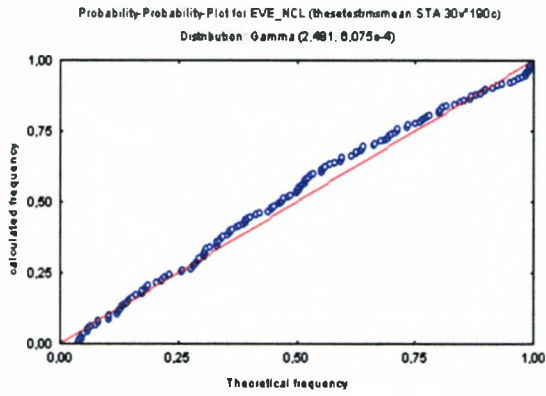


Figure 6.4-5 Graph illustrating how well the distribution of residual rms values is described by the Gamma distribution for the non-contact lens wearing group (evening tests).

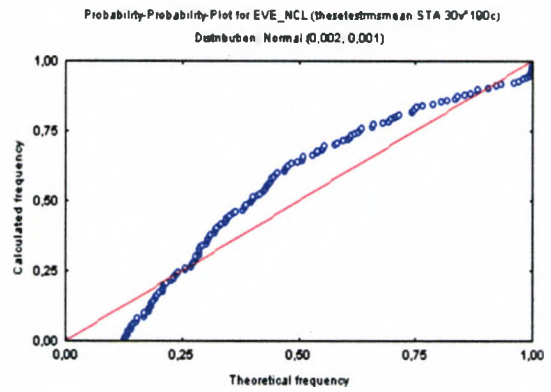


Figure 6.4-6 Graph illustrating how well the distribution of residual rms values is described by the Normal distribution for the non-contact lens wearing group (evening tests).

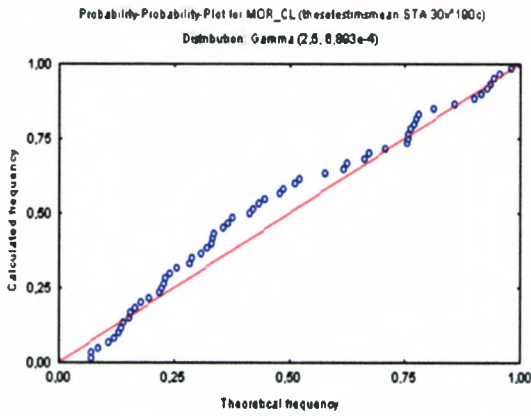


Figure 6.4-7 Graph illustrating how well the distribution of residual rms values is described by the Gamma distribution for the contact lens wearing group (morning tests).

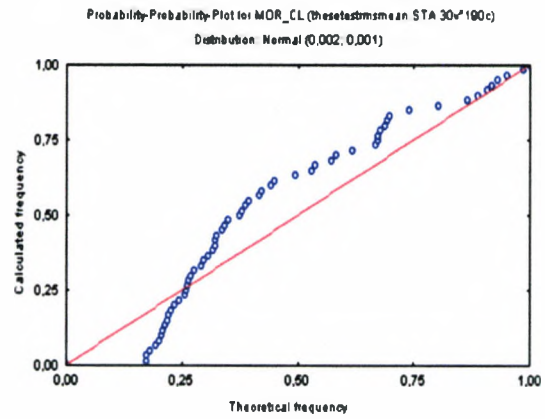


Figure 6.4-8 Graph illustrating how well the distribution of residual rms values is described by the Normal distribution for the contact lens wearing group (morning tests).

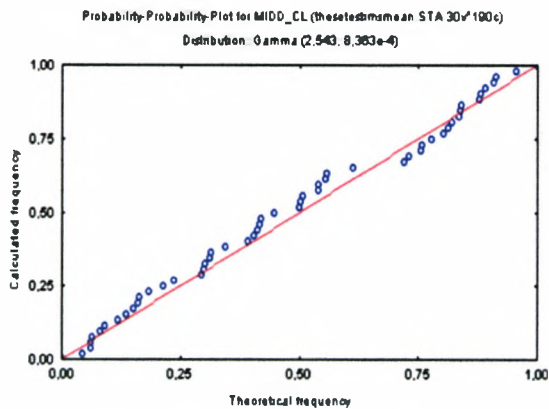


Figure 6.4-9 Graph illustrating how well the distribution of residual rms values is described by the Gamma distribution for the contact lens wearing group (noon tests).

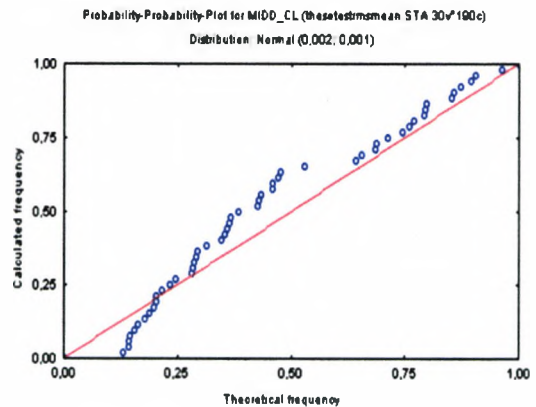


Figure 6.4-10 Graph illustrating how well the distribution of residual rms values is described by the Normal distribution for the contact lens wearing group (noon tests).

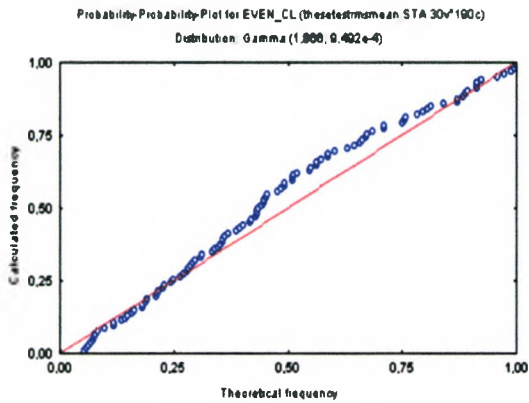


Figure 64-11 Graph illustrating how well the distribution of residual rms values is described by the Gamma distribution for the contact lens wearing group (evening tests).

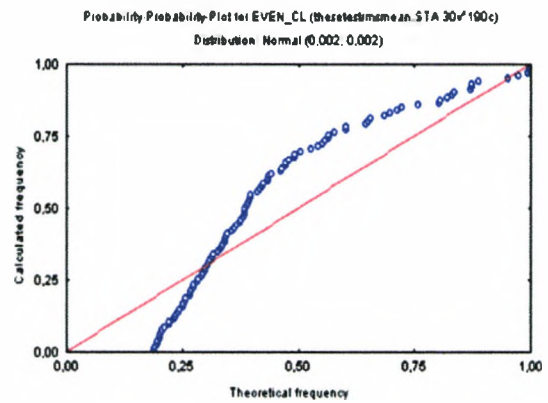


Figure 6.4-12 Graph illustrating how well the distribution of residual rms values is described by the Normal distribution for the contact lens wearing group (evening tests).

The Gamma distribution invariably gave the best fit for the tested data samples for MORN-NCL, NOON-NCL, EVEN-NCL, MORN-CL, NOON-CL and EVEN-CL. The parameters of the Gamma distribution, shape and scale parameter, are shown in figures 6.4.1 - 6.4.12

The reference data, collected at low altitude from subjects on the trek, were also best described by the Gamma distribution for morning, noon and evening measurements.

Figures 6.4-13 – 6.4-24 illustrate in more detail how well each tested sample is represented by the Gamma, and Normal distributions. The p-value of significance for the fit is estimated with the aid of the Chi square test and should be seen as a measure of the quality of distribution fitting. A p-value of significance of less than 0.05 suggests that the quality of the sample distribution shown in figures 6.4-13 – 6.4-24 is not an acceptable fit with the theoretical distribution. It should be noted that the scales of the abscissas of the left hand gamma distribution and the right hand normal distribution are slightly different.

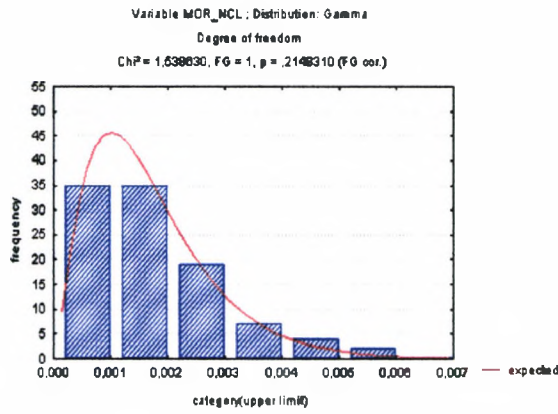


Figure 6.4-13 Graph illustrating the fit of the Gamma distribution to the residual rms values for the non contact lens wearing group (morning tests).

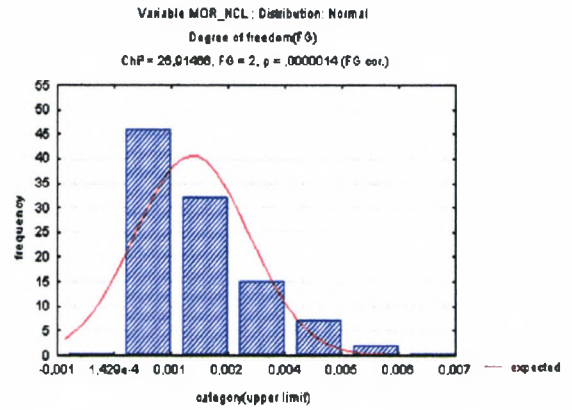


Figure 6.4-14 Graph illustrating the fit of the Normal distribution to the residual rms values for the non contact lens wearing group (morning tests).

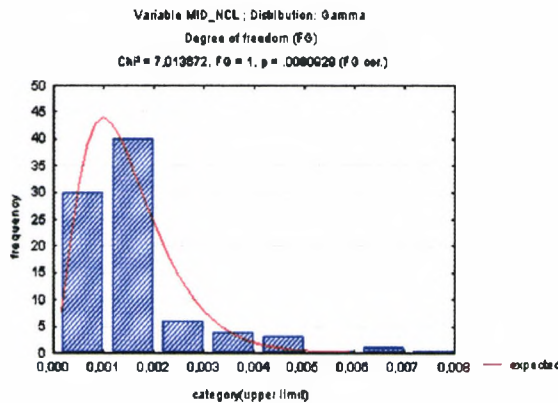


Figure 6.4-15 Graph illustrating the fit of the Gamma distribution to the residual rms values for the non contact lens wearing group (noon tests).

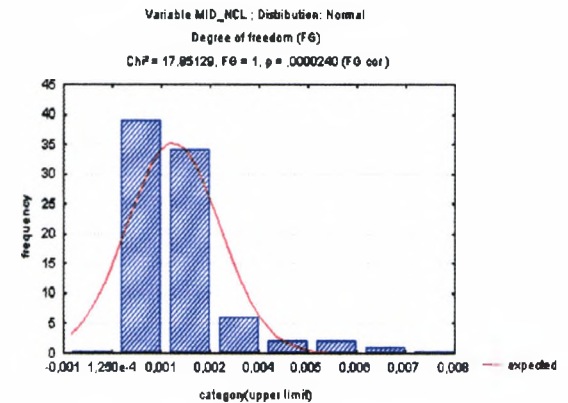


Figure 6.4-16 Graph illustrating the fit of the Normal distribution to the residual rms values for the non contact lens wearing group (noon tests).

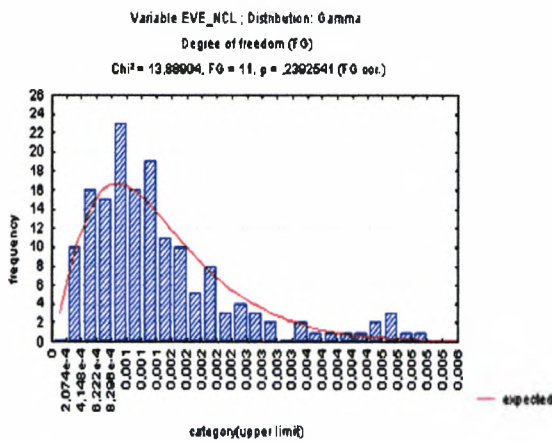


Figure 6.4-17 Graph illustrating the fit of the Gamma distribution to the residual rms values for the non contact lens wearing group (evening tests).

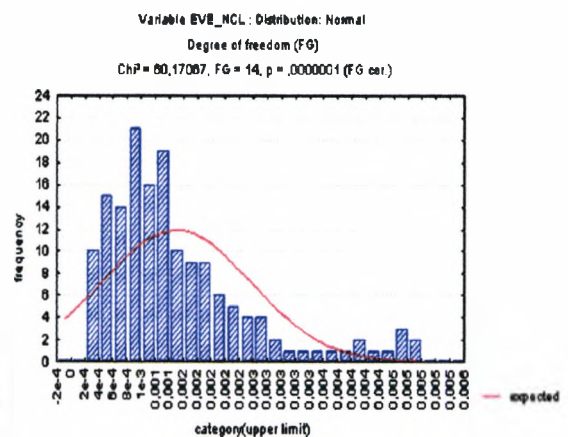


Figure 6.4-18 Graph illustrating the fit of the Normal distribution to the residual rms values for the non contact lens wearing group (evening tests).

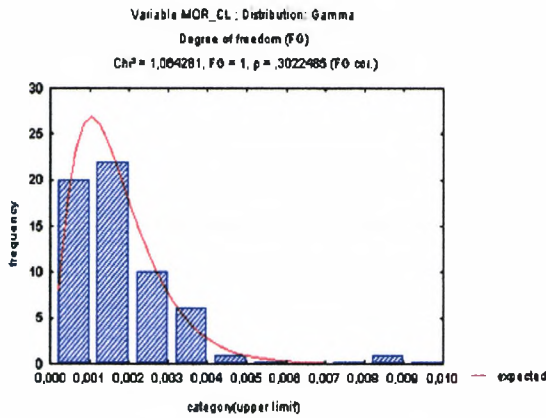


Figure 6.4-19 Graph illustrating the fit of the Gamma distribution to the residual rms values for the contact lens wearing group (morning tests).

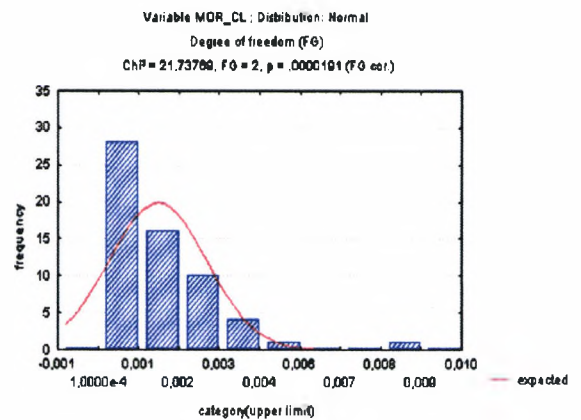


Figure 6.4-20 Graph illustrating the fit of the Normal distribution to the residual rms values for the contact lens wearing group (morning tests).

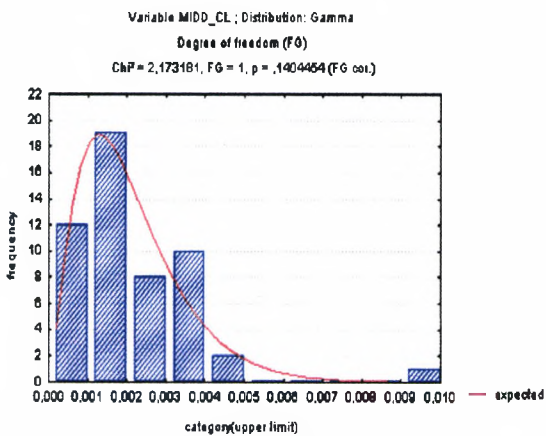


Figure 6.4-21 Graph illustrating the fit of the Gamma distribution to the residual rms values for the contact lens wearing group (noon tests).

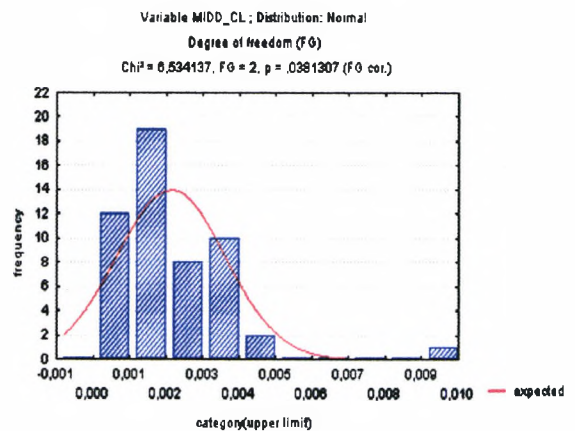


Figure 6.4-22 Graph illustrating the fit of the Normal distribution to the residual rms values for the contact lens wearing group (noon tests).

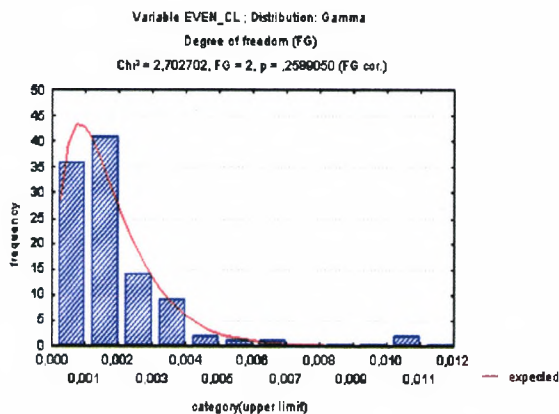


Figure 6.4-23 Graph illustrating the fit of the Gamma distribution to the residual rms values for the contact lens wearing group (evening tests).

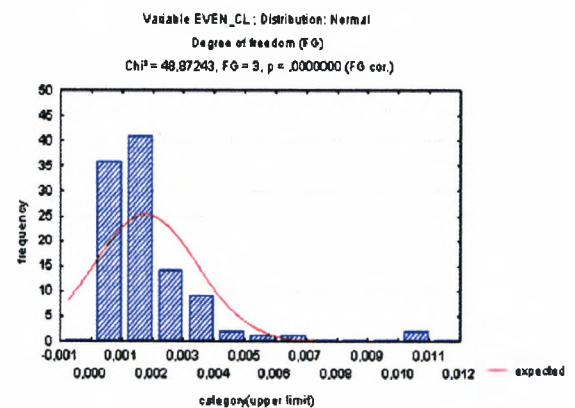


Figure 6.4-24 Graph illustrating the fit of the Normal distribution to the residual rms values for the contact lens wearing group (evening tests).

For each category it is clear that the normal distribution fit is not acceptable (p-value of significance less than 0.05, Figure 6.4-13 to figure 6.4-24). However, the sample sizes used in the altitude study are small and do not give enough information to be certain of the nature of the population distribution.

6.5.1 Significance analysis and hypothesis testing

All residual rms values of a population that are perfectly normally distributed would be ideal for almost every kind of hypothesis test. However, the graphical distribution tests show that the normal distribution does not describe the sample data in a way that is superior to the Gamma distribution.

Nevertheless, variance analysis tests have been conducted with the F-test to establish if there is any significance in the differences between the variances of the group and the variances of each sample's mean. The p-values were calculated using the F-test, a robust test with regard to moderate departures from normality (Winer, Brown, Michels, 1991). In addition, Duncans' MRT test was carried out to establish which group means were significantly different from the others tested. Duncans' MRT test is a conservative test which is designed to control the overall Type 1 error rate (Altman, 1991).

There are some important points worth considering in testing the hypothesis put forward at the end of Chapter 2 that "The cornea is able to adapt to changing conditions and does not exhibit a statistically significant change in corneal shape up to 16,400 ft." In chapter two it was established that changing environmental conditions at altitude, such as humidity, oxygen rate, air pressure, temperature, cosmic radiation, and UV radiation, could induce corneal shape changes. Also, there may be complex interactions between the environmental conditions. However, when the interaction of two surrounding conditions is considered in isolation from all the other influences, it is possible to describe such interactions mathematically.

The literature shows that when altitude changes, all the surrounding conditions change too. Therefore, the altitude has an influence on the change in the surrounding conditions. Furthermore, the effects of weather are very complex. This makes it necessary to consider the meteorological data for the trekking tour separately.

The data were subdivided into categories according to the altitude at which measurements were taken in order to determine the effects of altitude on corneal shape. Five altitude samples (or categories) were specified for the variance analysis. The first sample contains all measurements which were conducted up to 3280 ft (1000 m). In this sample the residual rms values are estimated by each subject's reference measurements. The second sample contains all the measurements which were performed up to 6560 ft (2000 m) and so on up until the fifth sample. The fifth sample contains all the measurements which were taken at higher than 13,120 ft (4000 m). Each group contained measurements collected over an altitude range of 1000m. This altitude interval was selected because it included approximately two of the standard 1500ft acclimatisation steps (1000m = 3280 ft), and to ensure that sufficient data were collected within each group to allow hypothesis testing. The variance analysis was conducted on every category of subject (non contact lens wearers morning tests, non contact lens wearers noon tests, non contact lens wearers evening tests, contact lens wearers morning tests, contact lens wearers noon tests, and contact lens wearers evening tests) separately.

One part of the hypothesis "...and does not exhibit a statistically significant change in corneal shape..." needs to be defined. The variance analysis of the changes in corneal shape was set to flag up a statistically significant difference when $p < 0.05$ as computed with the F-test. When the cornea is not able to adapt to changing conditions, it exhibits a statistically significant corneal shape change (H_a).

Conversely, when the cornea is able to adapt to change conditions, there is no statistically significant change in the corneal shape (H_0).

Let us briefly examine mathematical aspects of the hypothesis test:

$H_a: \alpha_i \neq 0$ respectively $H_a: \mu_i \neq \mu$ for $i = 1, 2, 3, 4, 5$

$H_0: \alpha_i = 0$ respectively $H_0: \mu_i = \mu$ for $i = 1, 2, 3, 4, 5$

The advantage of testing every category separately is that any significant corneal shape changes that are dependent on the time of day can be identified. All tests were performed using a statistics computer programme and an F-test table (Trampisch et al, 1997).

The table shows all F values which are computed at the 0.95th centile depending on the degree of freedom mean and degree of freedom group. All values from the said table are described with the variable $F_{a,b,c}$.

Meaning of the variable indices:

a = degree of freedom Mean

b = degree of freedom Group

c = 0.95th centile

6.5.2 Hypothesis tests

Each of the six categories, contact lens wearers and non contact lens wearers, subdivided into morning, noon, and evening test procedures, is tested at the five altitude samples.

6.5.2.1 Non-lens wearers' morning tests (MOR-NCL)

STAT. ANOVA	Non contact lens wearers Test daily stage morning Degree of freedom (FG)					
EFFECT	FG	Mean	FG	Group	F	p-Value
	Mean	Variance	Group	Variance		
1	4	.0000	97	.0000	1.8628	.1232

Table 6.5.2.1-1 Variance analysis for the category non lens wearers, morning tests at the five altitude samples. The test is for any variation in mean residual rms values with altitude.

Stat. ANOVA	Analysis
	tab.6.5.2.1-1
Altitude sample nr. (measured altitude)	Mean residual rms value
1 (up to 3280 ft)	0.0009
2 (3280 - 6560 ft)	0.0020
3 (6560 - 9840 ft)	0.0016
4 (9840 - 13120 ft)	0.0017
5 (>13120 ft)	0.0020

Table 6.5.2.1-2 Mean residual rms value for each altitude sample. Non contact lens wearers, morning tests.

The variable $F_{4,97,0.95} = 2.465$ compared with the calculated variable $F = 1.863$ (Table 6.5.2.1-1) shows the following result:

$F_{4,97,0.95} > F$ therefore $H_0 = 0$, hence it follows that there is no statistically significant change with altitude in corneal shape recorded in the mornings and the hypothesis has to be accepted. Table 6.5.2.1-2 shows the means of the residual rms values for the five altitude samples for the non contact lens wearers. The table and the graph show that the corneal shape change tends to increase the higher the mountaineer ascends. But the residual rms mean for sample 2 is greatest (seen with six places after the decimal point).

The same result is illustrated by the medians of the Box and Whisker Plot). Interestingly, the greatest residual rms value is positioned in the second sample and not as might be expected in the fifth sample (Figure 6.5.2.1-1).

The ordinate of every Box and Whisker Plot shown in each of the following hypothesis tests represents the residual rms values of the described sample. In this category the corneal shape is changing, but the change is not enough to be considered significant (with respect to the 0.95th centile).

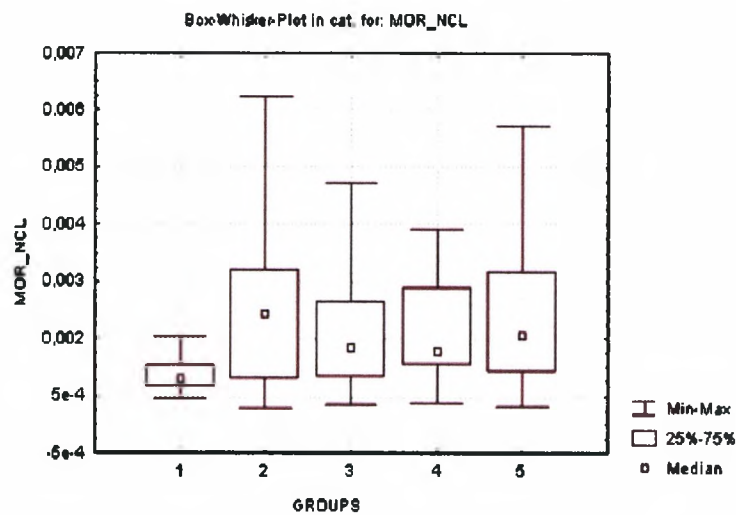


Figure 6.5.2.1-1 The residual rms values in each of the altitude samples are compared for the non lens wearers' category for their morning tests.

6.5.2.2 Non-lens wearers' noon tests (NOON-NCL)

In this case the variable $F_{4,79,0.95} = 2.487$ and is greater than the computed variable $F = 0.371$ (Table 6.5.2.2-1). In other words $H_0 = 0$, and the hypothesis has again to be accepted i.e. there is no significant difference in mean residual rms values in the five altitude samples.

STAT. ANOVA	Non contact lens wearers					
	Test daily stage noon					
	Degree of freedom (FG)					
EFFECT	FG	Mean	FG	Group	F	p-Value
	Mean	Variance	Group	Variance		
1	4	.0000	79	.0000	.3715	.8283

Table 6.5.2.2-1 Variance analysis for the category non lens wearers, noon tests at the five altitude samples. The test is for any variation in mean residual rms values with altitude.

Stat. ANOVA	Analysis
	tab.6.5.2.2-1
Altitude sample nr. (measured altitude)	Mean residual rms value
1 (up to 3280 ft)	0.0016
2 (3280 - 6560 ft)	0.0014
3 (6560 - 9840 ft)	0.0014
4 (9840 - 13120 ft)	0.0017
5 (>13120 ft)	0.0018

Table 6.5.2.2-2 Mean residual rms values for each altitude sample.
Non contact lens wearers, noon tests.

The means for each sample behave differently compared with the category of non contact lens wearers' morning tests. For the noon tests, the corneal shape changes were greater in the first sample compared with the second and third samples. However, the corneal shape change rose from the third to the fifth sample (Table 6.5.2.2-2).

In addition, the Box and Whisker Plot shows that the range of residual rms values is smaller for the second and fifth altitude samples than for the other samples. The maximum residual rms value is in the fourth sample, although one might expect it to be in the fifth sample because the greatest mean residual rms value for the measurements in this sample was found at the highest altitudes. The mean and the median of the fifth altitude sample are consistent with this expected behaviour (Figure 6.5.2.2-1).

One feature apparent from the residual rms box and whisker plots is the presence of obvious outliers in the data. Altman (1991) suggests a strategy for checking the influence of outliers on the statistical analysis. This involves carrying out the analysis both with and without the suspicious values.

Trampisch, Windeler, Ehle, and Lange (1997) identify two types of outlier; inner fence, and outer fence outliers. The inter-quartile range (IQ), which is the difference between the 0.25th – and 0.75th quartiles, is a key factor in defining the inner and outer fence outliers. Inner fence outliers lie between the IQ multiplied by 1.5 plus the 0.25th Quartile (lower inner fence) or plus the 0.75th Quartile (upper inner fence), and IQ multiplied by 3 plus the 0.25th Quartile (lower outer fence) or plus the 0.75th Quartile (upper outer fence). Outer fence outliers are greater than the upper outer fence or less than the lower outer fence. For the category of non contact lens wearers for the noon measurements there are two outer fence outliers. When these two values are deleted there is no change in the conclusion from the variance analysis, ANOVA ($F = 0.31$, $df_g = 4$, $p = 0.86$).

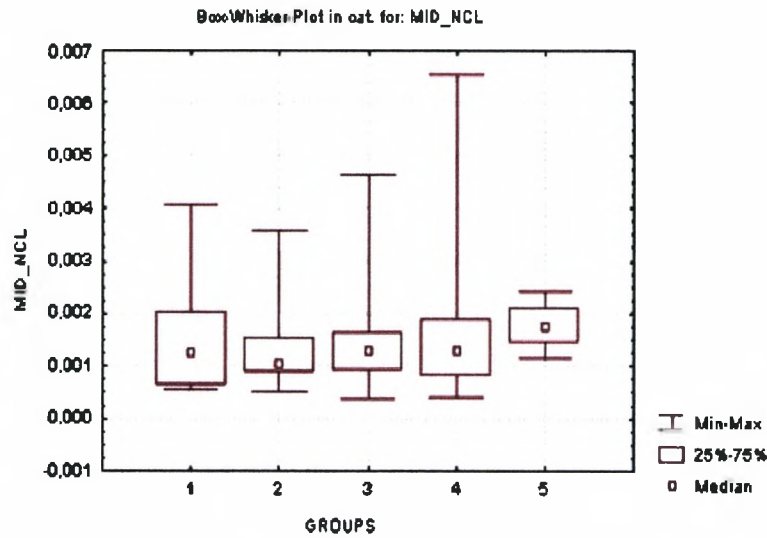


Figure 6.5.2.2-1 The residual rms values in each of the altitude samples are compared for the non lens wearers category for their noon tests.

6.5.2.3 Non-lens wearers' evening tests (EVEN-NCL)

The 0.95th centile is expressed by $F_{4,153;0.95} = 2.431$ in this category (EVE_NCL). The computed value $F = 3.752$ is greater than the value $F_{4;153;0.95}$. Therefore $H_0 \neq 0$, which means the null hypothesis is rejected (Table 6.5.2.3-1), and there is a significant difference in mean residual rms values with altitude.

STAT. ANOVA	Non contact lens wearers Test daily stage evening Degree of freedom (FG)					
EFFECT	FG	Mean	FG	Group	F	p-Value
	Mean	Variance	Group	Variance		
1	4*	.0000*	153*	.0000*	.3752*	.0061*

Table 6.5.2.3-1 Variance analysis for the category non lens wearers, evening tests at the five altitude samples. The test is for any variation in mean residual rms values with altitude.

Stat. ANOVA	Analysis
	tab.6.5.2.3-1
Altitude sample nr. (measured altitude)	Mean residual rms value
1 (up to 3280 ft)	0.0010
2 (3280 - 6560 ft)	0.0018
3 (6560 - 9840 ft)	0.0016
4 (9840 - 13120 ft)	0.0017
5 (>13120 ft)	0.0018

Table 6.5.2.3-2 Mean residual rms values for each altitude sample. Non- contact lens wearers, evening tests.

In this category the mean for the fifth sample is greatest (seen with six places after the decimal point, Table 6.5.2.3-2) and the mean of sample 1 is lowest. Although the mean declines from sample 2 to sample 3 and rises again from sample 3 to sample 5, all these values are similar (Figure 6.5.2.3-1). Sample 1, containing the reference measurements, also has a few extreme residual rms values but the range of the lowest 75% of residual rms values is smaller than in the other samples.

Duncan's MRT test was performed to indentify which pairs of residual rms values are significantly different. Duncan's test indicates that significant pairs of groups are only found when sample 1 is paired with other samples (Table 6.5.2.3-3). The mean residual rms value for samples 2, 4 and 5 are significantly greater than for sample 1 ($p = 0.034$, $p = 0.037$, and $p = 0.028$ respectively).

Duncan's MRT test α 5% group comparison is described by p-values					
Significance $p < 0.05$. Category - non-contact lens wearers' evening test					
Sample (mean)	1 (0.0010)	2 (0.0018)	3 (0.0016)	4 (0.0017)	5 (0.0018)
1 (0.0010)		.034*	.098	.037*	.028*
2 (0.0018)	.034*		.547	.910	.892
3 (0.0016)	.098	.547		.594	.484
4 (0.0017)	.037*	.910	.594		.817
5 (0.0018)	.028*	.892	.484	.817	

Table 6.5.2.3-3 Duncan's test results showing the sample means that are significantly different at the $p < 0.05$ level. These are marked with an asterisk.

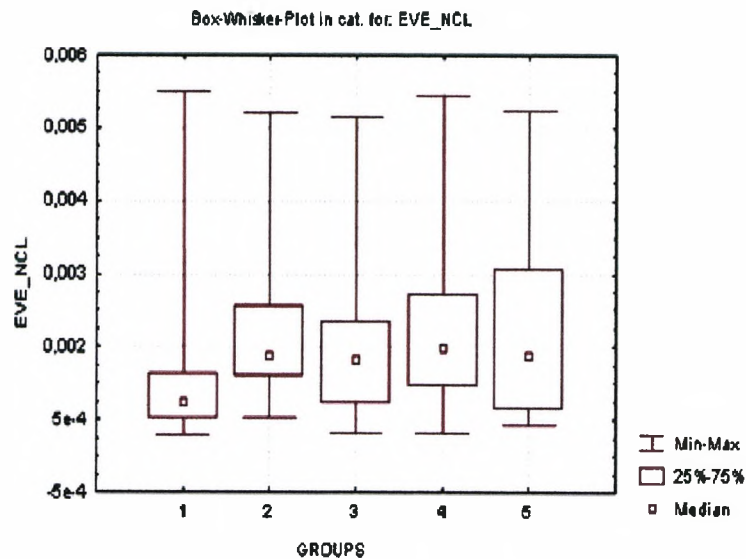


Figure 6.5.2.3-1 The residual rms values in each of the altitude samples are compared for the non-lens wearers category for their evening tests.

6.5.2.4 Contact lens wearers morning tests (MORN-CL)

$F_{4,55;0.95} = 2.540$ compared with $F = 1.470$, hence

$F_{4,55;0.95} > F$. The hypothesis has to be accepted because $H_0 = 0$ (Table 6.5.2.4-1).

STAT. ANOVA	Contact lens wearers Test daily stage morning Degree of freedom (FG)					
EFFECT	FG	Mean	FG	Group	F	p-Value
	Mean	Variance	Group	Variance		
1	4	.0000	55	.0000	1.4703	.2237

Table 6.5.2.4-1 Variance analysis for the category lens wearers, morning tests at the five altitude samples. The test is for any variation in mean residual rms values with altitude.

Stat. ANOVA	Analysis
	tab. 6.5.2.4-1
Altitude sample nr. (measure altitude)	Mean residual rms value
1 (up to 3280 ft)	0.0009
2 (3280 - 6560 ft)	0.0014
3 (6560 - 9840 ft)	0.0020
4 (9840 - 13120 ft)	0.0013
5 (>13120 ft)	0.0020

Table 6.5.2.4-2 Mean residual rms values for each altitude sample. Contact lens wearers, morning tests.

The mean of sample 3 is highest, followed by sample 5 (Table 6.5.2.4-2). It is clear from the Box and Whisker plot (Figure 6.5.2.4-1) that there is an obvious outlier in sample 3. If this outlier is ignored, the corneal changes in sample 5 are greater than those in sample 3. This outlier was identified as the only outer fence outlier (Chapter 6.5.2.2) in this data set. After deleting the outer fence outlier the variance analysis produced the same conclusion as above, ANOVA ($F = 1.86$, $df_g = 4$, $p = 0.12$).

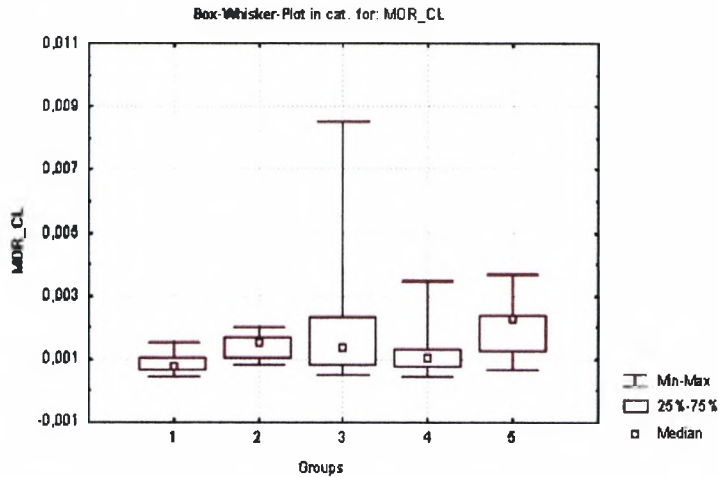


Figure 6.5.2.4-1 The residual rms values in each of the samples are compared for the category lens wearers, morning tests.

6.5.2.5 Contact lens wearers' noon tests (NOON-CL)

For this test the values of $F_{4,47,0.95} = 2.570$ and $F = 0.139$ show the following relation, $F_{4,47,0.95} > F$ and $H_0 = 0$, so the hypothesis is accepted (Table 6.5.2.5-1).

STAT.	Contact lens wearers					
ANOVA	Test daily stage noon					
	Degree of freedom (FG)					
EFFECT	FG	Mean	FG	Group	F	p-Value
	Mean	Variance	Group	Variance		
1	4	.0000	47	.0000	.3392	.9668

Table 6.5.2.5-1 Variance analysis for the category lens wearers, noon tests at the five altitude samples. The test is for any variation in mean residual rms values with altitude.

Stat. ANOVA	Analysis
	tab.6.5.2.5-1
Altitude sample nr. (measure altitude)	Mean residual rms value
1 (up to 3280 ft)	0.0022
2 (3280 - 6560 ft)	0.0020
3 (6560 - 9840 ft)	0.0021
4 (9840 - 13120 ft)	0.0021
5 (>13120 ft)	0.0032

Table 6.5.2.5-2 Mean residual rms values for each altitude sample. Contact lens wearers, noon tests.

In this category, sample 5 has the highest mean. But there are fewer measurements in sample 5 compared to the other samples because not many test procedures were performed at an altitude higher than 13,120 ft (Table 6.5.2.5-2). One reason for this is that the electrical support broke down on the Laurebina Pass (15,100 ft), as a result of passing through a very foggy area on the previous day. The fog impaired the loading procedure of the electrical accumulators. On Laurebina Pass there was not enough power to carry out the measurements at noon at an altitude of 15,100 ft. This is one of the reasons that the sample size of altitude sample 5 is very low. The maximum residual rms value in all samples was the obvious outlier in sample 1 (Figure 6.5.2.5-1). This was the only outer fence outlier (chapter 6.5.2.2) in this data set. After deleting the outer fence outlier the variance analysis produced the same conclusion as above, ANOVA ($F = 0.37$, $df_g = 4$, $p = 0.83$).

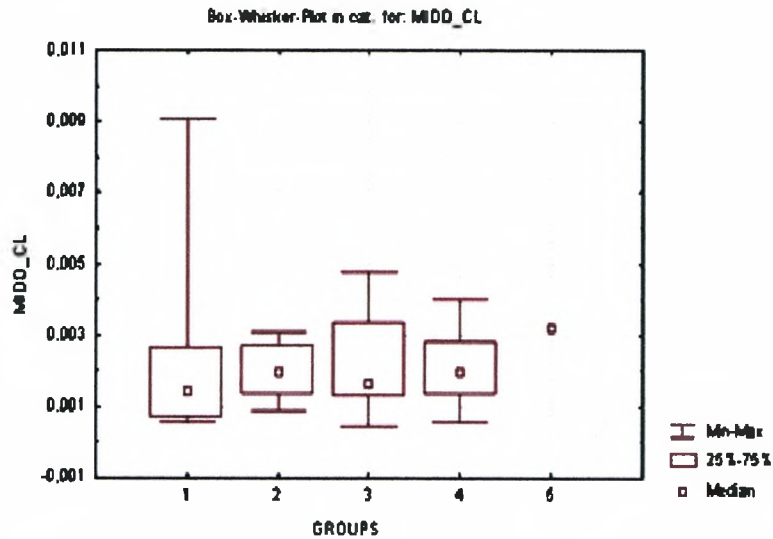


Figure 6.5.2.5-1 The residual rms values in each of the altitude samples are compared for the contact-lens wearers category for their noon tests.

6.5.2.6 Contact lens wearers evening tests (EVEN-CL)

In this case the values of $F_{4,101;0.95} = 2.462$ and $F = 6.076$ produced the following result:

$F_{4,101;0.95} < F$, hence it follows $H_a \neq 0$ and the null hypothesis is rejected, as it was for the category of non-lens wearers for their evening measurements (Table 6.5.2.6-1).

STAT. ANOVA	Contact lens wearers					
	FG	Mean	FG	Group	F	p-Value
	Mean	Variance	Group	Variance		
1	4*	.0000*	101*	.0000*	6.0762*	.0002*

Table 6.5.2.6-1 Variance analysis for the category contact-lens wearers, evening tests at the five altitude samples. The test is for any variation in mean residual rms values with altitude.

Stat. ANOVA	Analysis
	tab.6.5.2.6-1
Altitude samples nr. (measure altitude)	Mean residual rms value
1 (up to 3280 ft)	0.0010
2 (3280 - 6560 ft)	0.0031
3 (6560 - 9840 ft)	0.0020
4 (9840 - 13120 ft)	0.0021
5 (>13120 ft)	0.0026

Table 6.5.2.6-2 The mean residual rms values of each altitude sample. Contact lens wearers, evening tests.

Sample 2 has the greatest mean and the greatest maximum value. Duncan's MRT test was performed to identify which pairs of residual rms values are significantly different. Duncan's test indicates that significant pairs of groups are only found when sample 1 is paired with other samples (Table 6.5.2.3-3). The mean residual rms value for samples 2 and 5 are significantly greater than for sample 1 ($p = 0.004$, $p = 0.020$ respectively).

Duncan's MRT test α 5% sample comparison is described by p-values Significance $p < 0.05$. Category - contact lens wearers' evening test					
Sample (mean)	1 (0.0010)	2 (0.0031)	3 (0.0020)	4 (0.0021)	5 (0.0026)
1 (0.0010)		.004*	.188	.117	.020*
2 (0.0031)	.004*		.086	.147	.496
3 (0.0020)	.188	.086		.728	.257
4 (0.0021)	.117	.147	.728		.389
5 (0.0026)	.020*	.496	.257	.389	

Table 6.5.2.6-3 Duncan's test results showing the sample means that are significantly different at the $p < 0.05$ level. These are marked with an asterisk.

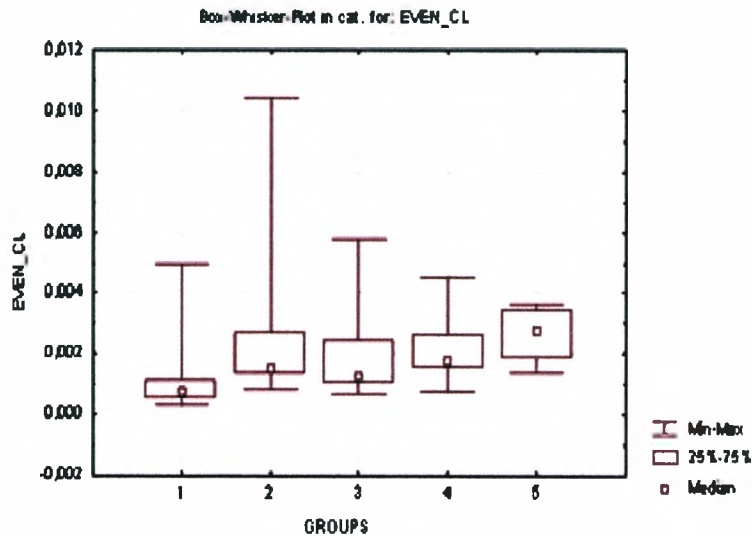


Figure 6.5.2.6-1 The residual rms values in each of the altitude samples are compared for the contact-lens wearers category for their evening tests.

There were four outer fence outliers identified in the category of contact lens wearers evening measurements (Chapter 6.5.2.2). After deleting the outer fence outliers the variance analysis produced the same conclusion as above, ANOVA ($F = 8.15$, $df_g = 4$, $p = 0.00001$).

6.5.2.7 A short summary of the tests:

MORN-NCL: The hypothesis is accepted.

NOON-NCL: The hypothesis is accepted.

EVEN-NCL: The hypothesis is rejected.

MORN-CL: The hypothesis has to be accepted.

NOON-CL: The hypothesis is accepted.

EVEN-CL: The hypothesis is rejected.

There are statistically significant increases in residual rms values with altitude identified by ANOVA testing for both non contact lens wearers and contact lens wearers for their evening tests.

Further analysis with Duncan's MRT test allows the identification of statistically significant changes between pairs of samples for these evening tests, and revealed a tendency for sample 1 (the reference sample) to have significantly lower residual rms values than other samples (2, 4 & 5 for non contact lens wearers, and 2 & 5 for contact lens wearers). Therefore, for this small sample, the outcome of the analysis is that for morning and noon tests the hypothesis is accepted and, although there is a tendency for residual rms to increase with altitude, this increase is not statistically significant. However, the tendency for residual rms to increase with altitude is statistically significant for the evening tests for both non contact lens wearers and contact lens wearers.

6.5.3 Maximum and minimum residual rms values described graphically

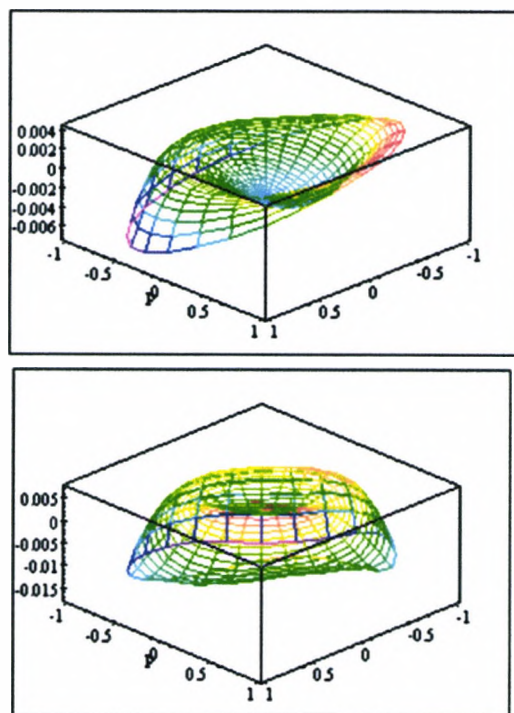


Figure 6.5.3-1 Both graphics show only the Zernike polynomials element, without the ellipsoid component, of corneal shape of subject 1.21, left eye. The base is described by a unit circle with radius one. The upper graphic is drawn using data giving minimum residual rms values and the lower graphic with data giving maximum residual rms values.

It is helpful to give an example to illustrate the difference in corneal shape between the situations when the maximum and minimum residual rms values for corneal shape were obtained. The corneal shape is described by a combination of Zernike polynomials and an ellipsoid (see chapter 3.2.10-3 and 3.2.10-4). The example chosen is the corneal shape change of the left eye of subject 1.21 as described by the Zernike polynomials while the ellipsoid data remain constant.

The upper graphic in Figure 6.5.3-1 illustrates the corneal shape for the minimum residual rms value recorded on day 8 at an altitude of 3800 m and the lower graphic is the corneal shape for the maximum residual rms value recorded on day 6 at an altitude of 2500 m. Both measurements were carried out in the first week of the trek, during the first phase of subject acclimatisation. The three-dimensional graphs of corneal shape measurements show a smaller height dimension when residual rms is at a minimum compared with when residual rms is a maximum (Figure 6.5.3-1).

6.6 Corneal shape change during the test period compared to corneal shape change during normal conditions

To investigate corneal shape change at altitude the maximum residual rms value for all subjects from the reference measurements was used as a cut-off point. Three separate cut-off points were used for morning, noon, and evening measurements. Any residual rms values found at altitude which were greater than the reference maximum residual rms value for that time of day were recorded. The number of residual rms measurements that were above this cut-off point was expressed as a percentage of the total number of residual rms values recorded during the testing period at altitude.

For the purpose of further analysis, all the residual rms values for all subjects (contact lens wearers and non contact lens wearers) are divided into three samples, morning, noon and evening.

The best fitting distribution from the following distributions was selected with the aid of the Likelihood Method; Beta, Exponential, Extreme, Gamma, Lognormal, Normal, Raleigh, and Weibull distributions (Figure 6.6-1 to 6.6-3).

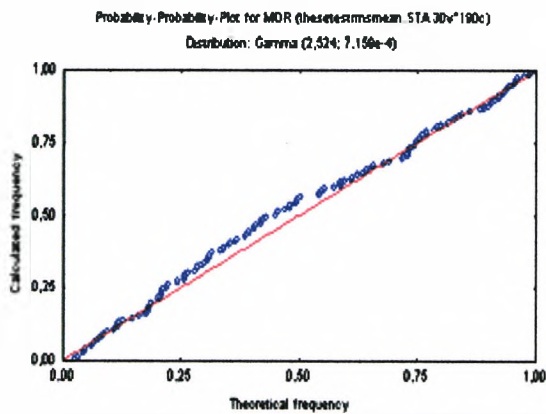


Figure 6.6-1 Graph illustrating how well the distribution of all residual rms values is described by the Gamma function (morning tests).

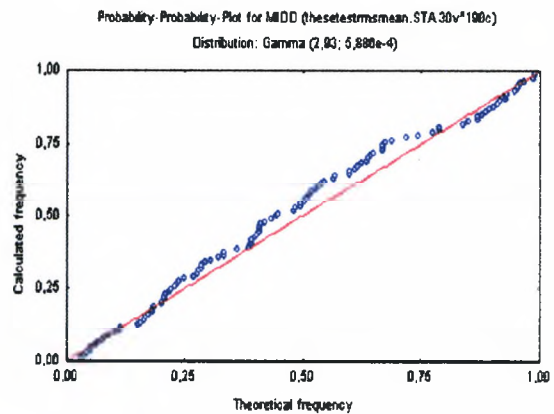


Figure 6.6-2 Graph illustrating how well the distribution of all residual rms values is described by the Gamma function (noon tests).

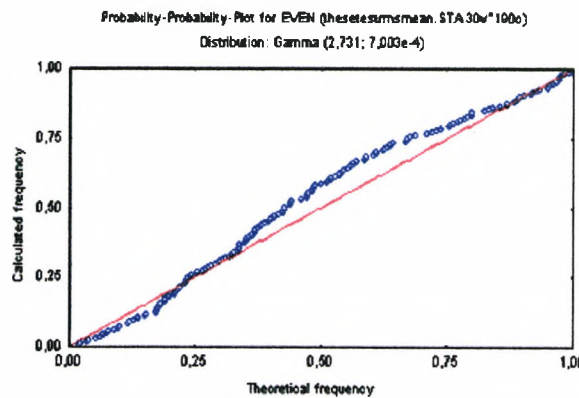


Figure 6.6-3 Graph illustrating how well the distribution of all residual rms values is described by the Gamma function (evening tests).

The Gamma distribution is the best-fitting distribution for all three samples. The frequency distributions of the residual rms values at altitude are shown in figures 6.6-4 to 6.6-6, together with the maximum residual rms values for the reference measurements.

Residual rms maximum morning = 0.0036

Residual rms maximum noon = 0.0041

Residual rms maximum evening = 0.00499

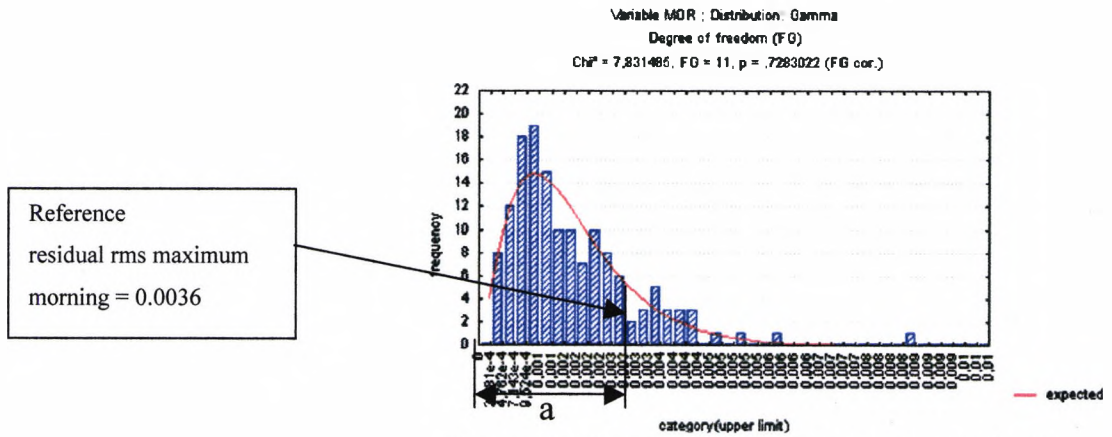


Figure 6.6-4 Gamma frequency distribution computed for all residual rms results for morning tests.

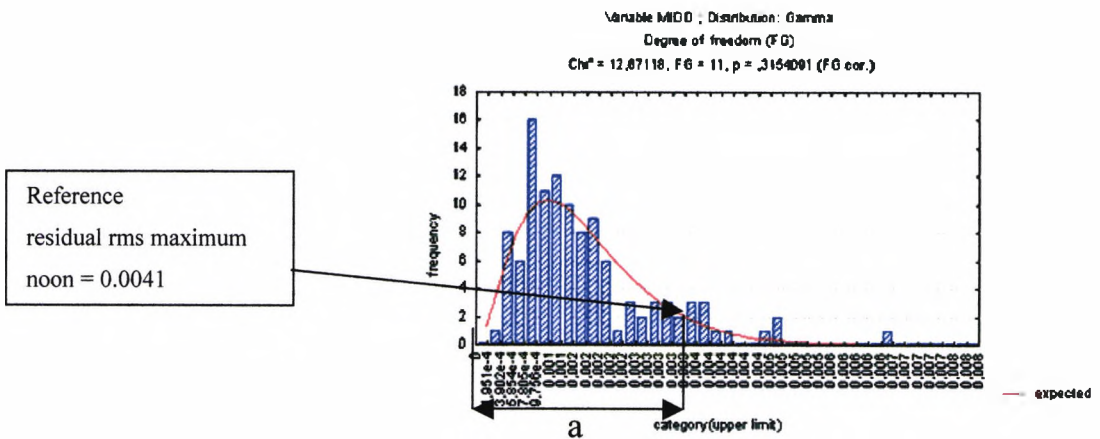


Figure 6.6-5 Gamma frequency distribution computed for all residual rms results for noon tests.

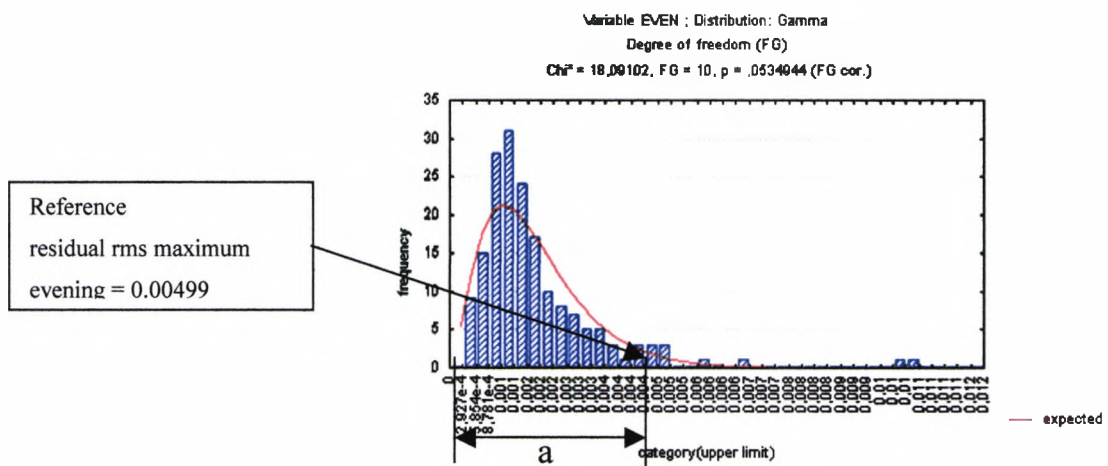


Figure 6.6-6 Gamma frequency distribution computed for all residual rms results for evening tests.

The test period residual rms values that are lower than the reference residual rms maximum are described by the variable “a” in percentage terms. The cumulative values observed are:

“a” morning = 90.79 %,

“a” noon = 96.29 %

“a” evening = 97.73 %

Hence the proportion of residual rms values which are greater than the reference residual rms maximum ranges from 2.27 % to 9.21 % of all values, depending on the time of day. The highest figure occurs in the morning, which could be explained by the phenomenon known as overnight corneal swelling, which is described in Mertz’s study (1980), where he measured the overnight swelling of the eyes of nine subjects. Results showed overnight corneal swelling to be approximately 4.5 %. The logarithmic recovery to baseline occurred within the first hour after eye opening.

6.7 Associations between the various meteorological parameters

Häckel (1999) observed that if stable weather conditions are expected, then air pressure, humidity, and temperature are reduced during ascent to high altitudes.

For hypothesis testing, we defined our five residual rms samples according to the altitude at which measurements were carried out. It can be said that altitude is a summary of changing surrounding conditions and their influence on corneal shape change. In this section, the data were analysed for any association between the altitude, the humidity, air pressure and temperature.

First any linear association between the altitude and the humidity, air pressure and temperature respectively was tested. The raw data are shown in table 6.7-1. The scatterplots of the data are shown in figures 6.7-1 to 6.7-4. The regression line is shown together with its 95% confidence interval.

Altitude (ft)	Humidity (%)	Air pressure (mbar)	Temperature (°C)
4400	65	830	24
6500	70	737	22
6500	69	704	8
7400	74	697	16
7400	72	762	9
5600	80	676	14
8100	80	676	12
8100	55	618	8
9970	50	573	25
11400	55	571	12
11400	50	540	2
12400	30	520	26
12600	71	524	5
13800	51	518	5
12600	42	460	10
12600	38	519	17
16500	48	440	6
12600	38	542	12
9800	69	627	-2
8100	49	623	23
4700	88	702	6
7500	62	711	21
7500	65	711	11
7400	49	704	19
11000	30	587	19
14300	34	582	6
14300	39	481	4
15100	35	500	18
12000	50	725	18
4400	69	875	17

Table 6.7-1 Humidity, air pressure, and temperature recorded during the trek at the specified altitudes.

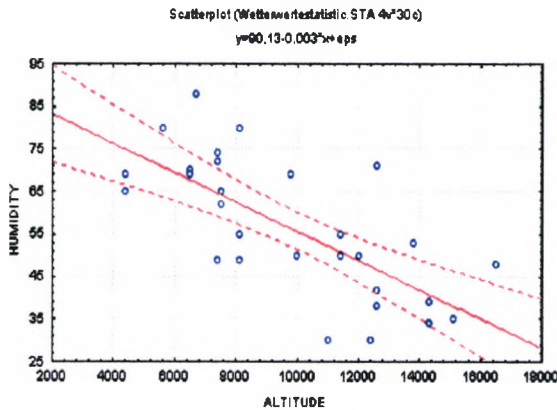


Figure 6.7-1 Scatterplot of humidity vs altitude. The regression line is shown in red, flanked by the 95% confidence limits for the regression line.

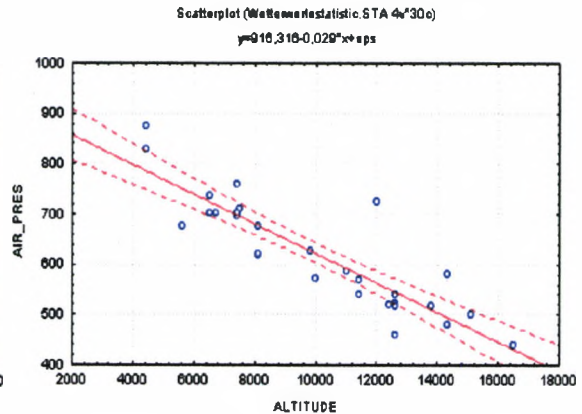


Figure 6.7-2 Scatterplot of air pressure vs altitude. The regression line is shown in red, flanked by the 95% confidence limits for the regression line.

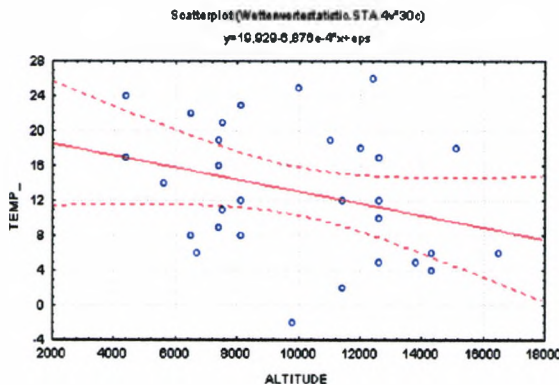


Figure 6.7-3 Scatterplot of temperature vs altitude. The regression line is shown in red, flanked by the 95% confidence limits for the regression line.

Summarizing all the scatterplots, the higher the region, the lower the temperature, the lower the air pressure, and the drier the air. All these findings conform to the literature. Two of the meteorological variables, the air pressure, and the humidity show a very strong linear association with the altitude (humidity/altitude $r = -0.710$, $p = 0.00$ and air pressure/altitude $r = -0.886$, $p = 0.00$).

The correlation between the temperature and the altitude is weak and not statistically significant, but the tendency for reduced temperature at altitude can be seen clearly from the scatterplot (temperature/altitude $r = -0.306$, $p = 0.099$).

6.8 z-values

The z-value is the difference between the extreme values - the maximum and minimum - of a shape prescribed by Zernike polynomials. Table 6.8-1 and table 6.8-2 present the descriptive statistics of every subject tested at altitude divided into right and left eyes.

Descriptive statistics z-value (mm) right eye altitude						
Subjects ncl	Mean	Minim	Maxim	Range	Variance	Stdev.
1.21	.0378	.0183	.0581	.0398	.0001	.0117
2.21	.0117	.0061	.0187	.0126	.0000	.0041
3.21	.0077	.0027	.0100	.0073	.0000	.0016
4.21	.0174	.0113	.0286	.0172	.0000	.0040
5.21	.0306	.0241	.0444	.0204	.0000	.0047
6.21	.0192	.0103	.0325	.0223	.0000	.0057
Subjects cl	Mean	Minim	Maxim	Range	Variance	Stdev.
1.22	.2026	.1572	.3453	.1881	.0008	.0284
2.22	.0167	.0103	.0303	.0200	.0000	.0048
3.22	.0243	.0163	.0329	.0167	.0000	.0052

Table 6.8-1 Descriptive statistics of the z-values for both non contact lens wearers and contact lens wearers. Data for the subjects' right eyes are presented here. SD = standard deviation.

Descriptive statistics z-value (mm) left eye altitude						
Subjects ncl	Mean	Minim	Maxim	Range	Variance	Stdev.
1.21	.0196	.0144	.0246	.0102	.0000	.0021
2.21	.0173	.0113	.0346	.0233	.0000	.0051
3.21	.0147	.0090	.0223	.0134	.0000	.0042
4.21	.0170	.0097	.0347	.0250	.0000	.0049
5.21	.0240	.0128	.0557	.0429	.0001	.0081
6.21	.0326	.0194	.0516	.0322	.0001	.0098
Subjects cl	Mean	Minim	Maxim	Range	Variance	Stdev.
1.22	.1913	.1252	.2290	.1038	.0011	.0334
2.22	.0225	.0118	.0322	.0204	.0000	.0046
3.22	.0170	.0089	.0338	.0249	.0000	.0056

Table 6.8-2 Descriptive statistics of the z-values for both non contact lens wearers and contact lens wearers. Data for the subjects' left eyes are presented here. SD = standard deviation.

For most subjects the right and left eyes' mean z-values were markedly different, with only one non lens wearer (4.21) and one lens wearer (1.22) having similar right and left z-values. A high mean z-value suggests possible difficulties achieving a smooth contact lens movement on the cornea during contact lens fitting. There is a tendency for the mean z-values for contact lens wearers, for both the right and left eyes, to be higher than those of the non contact lens wearers. A large range of z-values, as described in table 6.8-1 and table 6.8-2, was found in two non lens wearers (0.0398 mm in subject 1.21's right eye, and 0.0429 mm in subject 5.21's left eye) and notably in one contact lens wearer (0.1881 mm and 0.1038 mm in subject 1.22's right and left eyes respectively). This represents a very variable difference between the highest and deepest points in a 7mm circle of the corneal shape.

Any suggested cause for these high ranges must be speculative, but a possible reason could be found in some alteration to corneal metabolism or to the pump mechanisms of the corneal epithelium or the corneal endothelium (Chapter 1.41 – 1.43).

Subject 1.22 wore toric contact lenses on both eyes. These lenses were much thicker than the other contact lenses worn by the other two lens wearers and toric lenses have, therefore, less oxygen transmission than the non toric lenses. The combination of altitude hypoxia and the reduced oxygen transmission of the contact lenses could have induced the much greater z-values compared with the other subjects.

The risk of contact lens wear inducing irritations rises dramatically when movement of the contact lens is influenced by a very variable z-value. The greatest range of z-values was 0.1881 mm in a contact lens wearer (1.22). Achieving a satisfactory contact lens fit for this patient would represent a clinical challenge.

Any conclusions drawn from these small samples should be made with caution, but contact lens wear during acclimatisation appears to affect the change in corneal shape more than non lens wear. As further evidence for this statement, the standard deviation (SD) of the z-values for the contact lens wearers was greater than the SD of the non contact lens wearers. The SD of the contact lens wearers ranges between 0.0048 mm and 0.0284 mm for right eyes and between 0.0046 mm and 0.0334 mm for the left eyes. In comparison, the SD of the non contact lens wearers ranges from 0.0016 mm to 0.0117 mm for the right eyes and from 0.0021 mm to 0.0098 mm for the left eyes.

6.9 Altitude and z-value

The descriptive statistics in section 6.8 give details of the minimum and maximum z-values for each subject who took part in the altitude study.

It is interesting to establish the altitudes at which the maximum and minimum z-values were recorded in Nepal. Table 6.9.1 gives a short overview.

Subject	z-value right eye at altitude (ft)		z-value left eye at altitude (ft)	
	Maximum	Minimum	Maximum	Minimum
1.21	6700	8100	7500	4400
2.21	10000	13700	6500	13700
3.21	16400	12500	10000	7500
4.21	14300	12500	14300	6500
5.21	12500	12500	11400	6700
6.21	14300	6700	7400	12500
1.22	4400	1700	6700	6500
2.22	8100	4400	12500	12500
3.22	6500	12500	7500	9800

Table 6.9-1 Altitudes at which maximum and minimum z-values were recorded.

It could be expected that the minimum z-values would be associated with lower altitudes and vice versa, as a result of reduced oxygen supply at high altitude which will eventually influence corneal metabolism (Chapter 1.41 and chapter 2.2.6.2). This is the case for 9 of the 18 eyes. Three eyes had identical or virtually identical altitudes for maximum and minimum z-values. For three right eyes and three left eyes the altitude at which the minimum z-value was recorded was higher than that at which the maximum z-value was recorded. Interestingly, both the right and left eyes of contact lens wearer subject nr. 3.22 and of non contact lens wearer subject nr. 2.21 show minimum z-values computed from measurements carried out at higher altitudes than the altitude at which the maximum z-value was recorded.

The difference in altitudes between the right and left eyes at which the maximum z-values were recorded was less than or equal to 1000ft in only 3 subjects and was more than 3000ft in 5 subjects. For the minimum z-values, only one subject had a difference between eyes in altitudes at which the minimum z-values were recorded of less than 1000ft with 7 subjects having a difference of more than 3000ft (Figure 6.9-1).

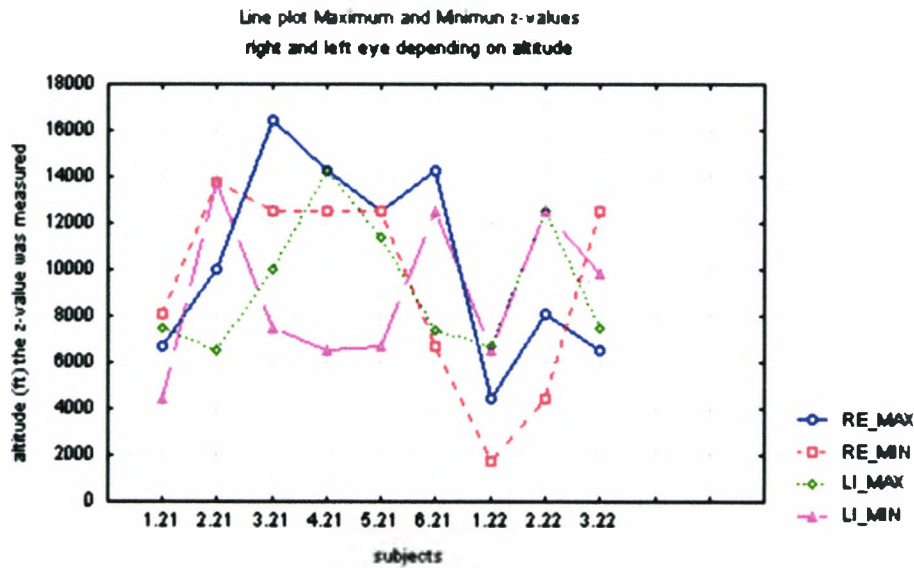


Figure 6.9-1 Altitudes at which the minimum and maximum z-values were recorded for each subject.

All this suggests that there is little tendency for z-values to vary with altitude. The z-value is an interesting parameter, but only conveys two-dimensional information regarding the three-dimensional corneal shape, unlike rms and residual rms values.

6.10 Results of eye examinations during the test period

At the beginning of every measurement procedure an eye examination was conducted on every tested eye, as described in chapter 5.3.3. The following grading scale was used to allow statistical analysis:

Anterior segment of the eye:

1. Injuries and irregularities of the cornea, iris and conjunctiva were described in detail. When the results of the tests were negative, a minus sign was recorded.

2. Infiltrations were counted and their depth within the layers of the cornea noted by recording the number of the deepest layer involved (from one to five).
3. Striae and Descemet folds were counted and their location described as being central or peripheral, and superior, inferior, nasal, or temporal.
4. Bulbar injections and limbal injections were determined with the aid of the CCRLU grading scale, classifying injection from the first to the fourth degree.
5. Contact lens movement was split up into three degrees of movement. The movement can be tested while the subject blinks, when the inferior limbus and the inferior rim of the contact lens were observed. Movement of a contact lens ≥ 1 mm was assigned as degree one. Movement of a contact lens < 1 mm but ≥ 0.5 mm was assigned as degree two, and contact lens movement of less than 0.5 mm was assigned as degree three. The contact lens wearers were invited to report any complaints and problems they had wearing the lenses.

The retina:

1. Any haemorrhages were identified. If the result was positive, the record was marked with a plus sign and when no haemorrhages were found a minus sign was recorded. The expansion of any haemorrhages was measured with a scale in the ophthalmoscope.
2. Cotton wool spots were counted and the area in which the cotton wool spots occurred was identified.
3. Tortuosity and papilloedema were marked with a plus sign when they occur and with a minus sign when they do not. Blood vessel diameter can be determined with the aid of the A/V ratio e.g. 2/3, 3/4, 4/5...

Anterior eye		Retina	
Injuries and irregularities of the cornea, iris and conjunctiva	-	Haemorrhages, highlighting flame shape haemorrhages	-
Infiltrations and depth of any infiltrations	-	Cotton wool spots	-
Striae and descemet folds	-	Tortuosity and papilloedema	-
Bulbar infections and limbus infections	-	Change in blood vessel size	+*
With two subjects, contact lens movement changed from degree one to degree two at an altitude of 11,400 ft. For one subject the contact lens movement changed to degree two at 12,600 ft.			+*

Table 6.10-1 Summary of the results from all subjects of eye examinations during the trek.

A minus sign = no abnormalities found. A plus sign = the sign was found in some subjects.

The A/V ratio of two subjects (subject nr. 6.21 and subject nr. 1.22) changed from 2/3 to 3/4 when we arrived at an altitude of 12,600 ft (Table 6.10-1). After we returned to Syrabru at 7400ft the A/V ratio had returned to 2/3.

Subsequently an A/V ratio 2/3 was constantly measured on both subjects for the rest of the test period.

The degree of contact lens movement changed for all three subjects during the trek (Table 6.10-1). A summary of these changes is shown in Table 6.10-2.

Subject one	Subject two	Subject three
Kyangjin Khar 12,600 ft deg. 2	Kyangjin Khar 12,600 ft deg. 2	Kyangjin Khar 12,600 ft deg. 2
Syrabru 7400 ft deg. 1	Bambu lodge 7500 ft deg 1	Bambu lodge 7500 ft deg. 1
Gosaikund 14,300 ft deg. 2	Gosaikund 14,300 ft deg. 2	Gosaikund 14,300 ft deg. 2
Kutumsang 8100 ft deg. 1	Kutumsang 8100 ft deg. 1	Kutumsang 8100 ft deg. 1

Table 6.10-2 The stages of the trek at which a change in contact lens movement was detected. Every subject's contact lens movement was measured to be degree 1 at the beginning of the tour.

The contact lens movement test was performed during each measurement block, so it is possible that the movements may have changed a little before or after the stages given in Table 6.10-2. None of the three contact lens wearers felt comfortable wearing their lenses at altitudes higher than 12,000 ft. Nevertheless, all of them wore the lenses up to 16,500 ft and during the whole test period every day.

6.11 Association between residual RMS values and other parameters

In this section any associations between corneal shape changes, as defined by residual rms values, and measurements of humidity, air pressure, temperature and altitude are investigated.

6.11.1 Association between residual rms and humidity

The first stage in this procedure was to draw a scatterplot of the data for each eye of each subject. Each of these scatterplots reveals little tendency for residual rms and humidity to be associated. A typical scatterplot is shown for the right eye of subject 1.21, and the scatterplot with the greatest r-value is presented for the left eye of subject 4.21 tested at high altitude (figure 6.11.1-1). The right eye scatterplot of subject 1.21 and left eye scatterplot of subject 4.21 show contrary tendencies for the association between residual rms and humidity. For one eye (subject 1.21), the slope of the best-fitting straight line is positive but for the other eye (subject 4.21) the slope is negative. However, the weakness of any linear association between residual rms and humidity is confirmed by the values of the typical correlation coefficient for subject 1.21's right eye ($r = 0.21$, $p = 0.31$) and the maximum correlation coefficient obtained for subject 4.21's left eye ($r = -0.54$, $p = 0.02$). To put this further into perspective, the R^2 values (given by the square of r) can be calculated.

These are 0.04 for the right eye of subject 1.21 and 0.29 for the left eye of subject 4.21 respectively, indicating that typically only 4% and maximally only 29% of the variability in residual rms is explained by the variation in humidity.

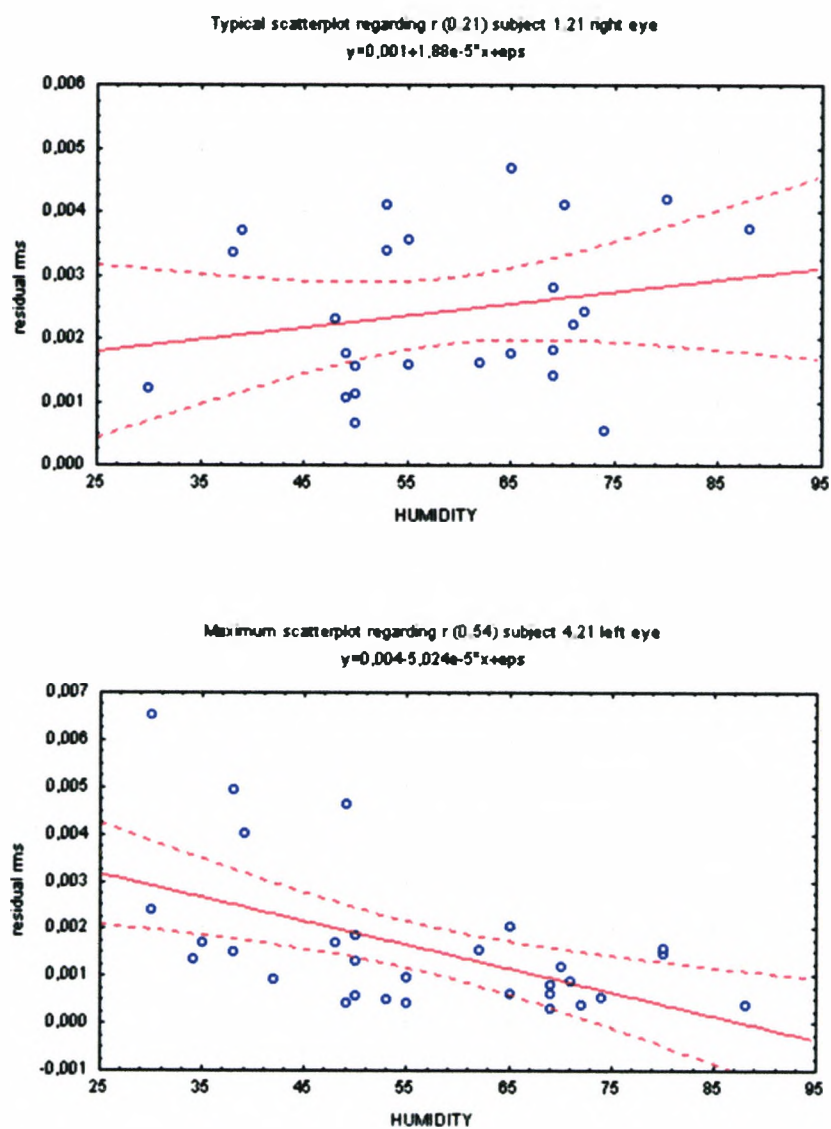


Figure 6.11.1-1 Scatterplot of residual rms values plotted against humidity for the right eye of subject 1.21 (typical scatterplot) and left eye of subject 4.21 (scatterplot with maximum r value).

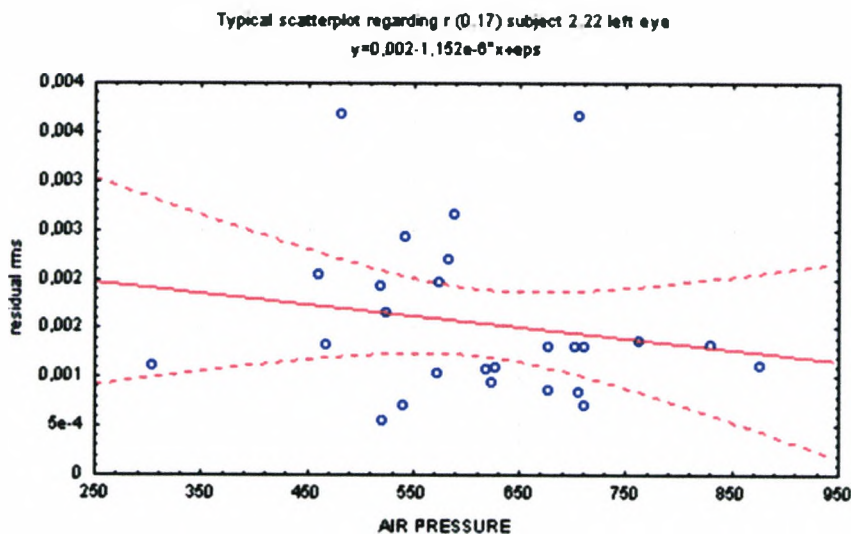
Interestingly, for all the eyes tested, half of the best-fitting straight lines to the data have a positive slope and half have a negative slope. The correlation coefficients lie between $r_{\min} = 0.02$ and $r_{\max} = 0.54$, with $r_{\text{mean}} = 0.24$.

The maximum r value of 0.54, as demonstrated above, is equivalent to an R^2 value of only 0.29, indicating that 29% of the variation in residual rms is explained by the variation in humidity, while the R^2 of the mean correlation is only 6%.

All this strongly suggests that there is no linear association between residual rms and humidity.

6.11.2 Association between residual rms and air pressure

Again, examination of each of the scatterplots reveals little tendency for residual rms and air pressure to be associated. A typical scatterplot is shown for the left eye of subject 2.22, and the scatterplot with the maximum r -value is presented for the left eye of subject 2.21 (figure 6.11.2-1).



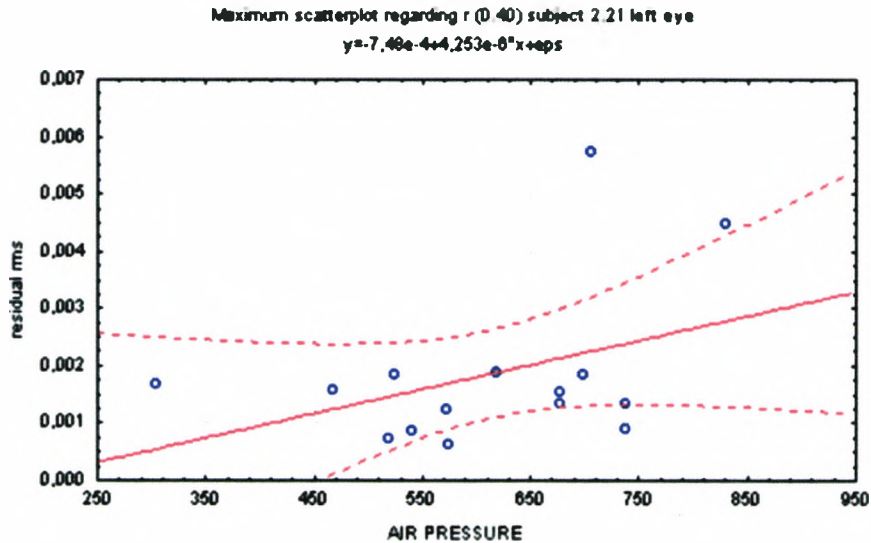


Figure 6.11.2-1 Scatterplot of residual rms values plotted against air pressure for the left eye of subject 2.22 and left eye of subject 2.21.

Once again the slope of the best-fitting straight line is negative for one eye (subject 2.22) but for the other eye the slope is positive (subject 2.21). Eight of the best-fitting straight lines have a positive slope, with 10 having a negative slope. The correlations are all low, with the correlation coefficients lying between $r_{\min} = 0.02$ and $r_{\max} = 0.40$, with $r_{\text{mean}} = 0.18$. The maximum r value of 0.40 is equivalent to an R^2 value of only 0.16, indicating that 16% of the variation in residual rms is explained by the variation in air pressure, while the R^2 of the mean correlation is only 3%. All this strongly suggests that there is also no linear association between residual rms and air pressure.

6.11.3 Association between residual rms and temperature

A typical scatterplot is shown for the left eye of subject 6.21. Additionally the scatterplot with the maximum r -value is presented for the right eye of subject 2.21 (figure 6.11.3-1). One would expect that, the higher the temperature, the greater the residual rms values (because of elevated evaporation of tears).

However, the slope of the best-fitting line of the left eye of subject 6.21 in figure 6.11.4-1 is negative, rather than the expected positive slope. The scatterplot of the right eye of subject 2.21 does reveal a positive slope.

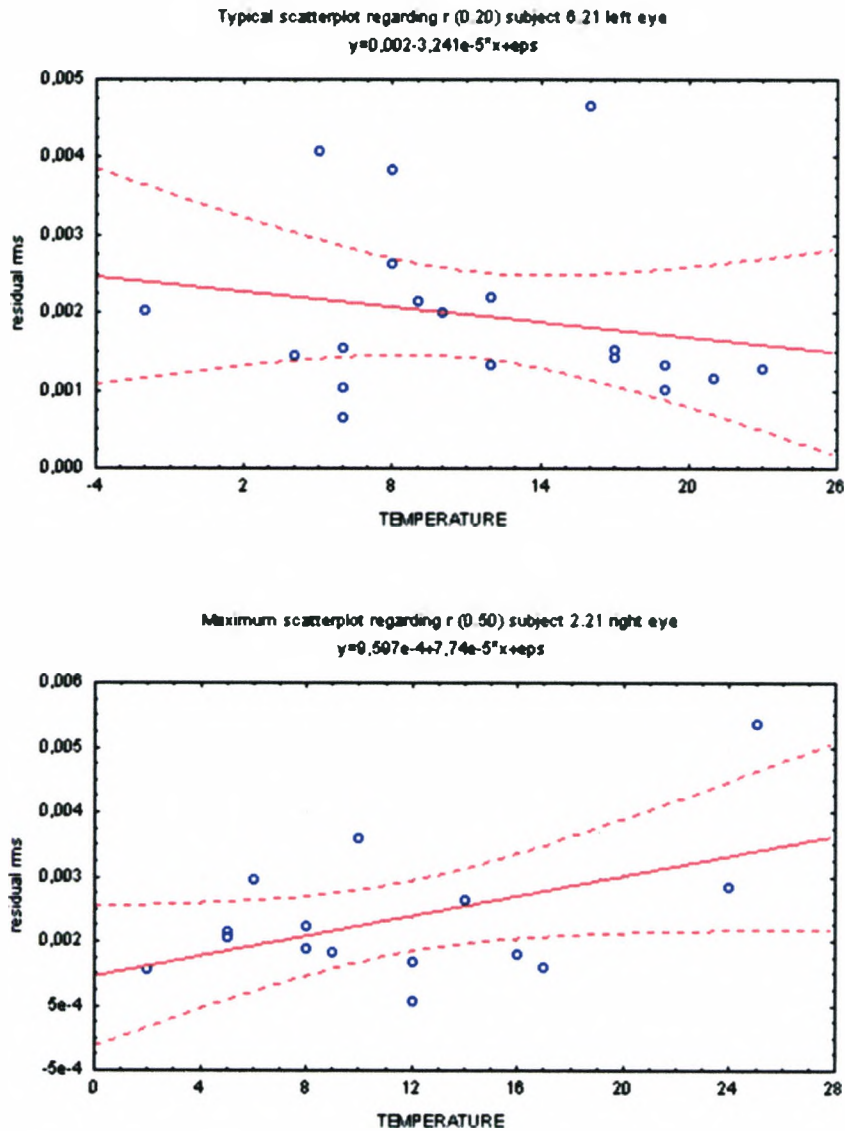


Figure 6.11.3-1 Scatterplot of residual rms values plotted against temperature for the left eye of subject 6.21 and right eye of subject 2.21.

Again, the weakness of any linear association is demonstrated by the values of the correlation coefficient of the left eye of subject 6.21 ($r = 0.20$, $p = 0.32$) and the correlation coefficient of the right eye of subject 2.21 ($r = 0.50$, $p = 0.06$).

Nevertheless, twelve of the eighteen best-fitting straight lines have a positive slope, suggesting that there may be some weak tendency for higher temperatures to be associated with higher residual rms values. But analysis of the correlation coefficients, which lie between $r_{\min} = 0.04$ and $r_{\max} = 0.50$, with $r_{\text{mean}} = 0.20$, show that any association is extremely weak indeed. The maximum r value of 0.50 is equivalent to an R^2 value of only 0.25, indicating that 25% of the variation in residual rms is explained by the variation in temperature, while the R^2 of the mean correlation is only 4%. All this strongly suggests that there is no linear association between residual rms and temperature.

Most corneal shape measurements were performed at between 8 degrees Celsius and 22 degrees Celsius. Although these tests were conducted at high altitudes, the temperature was higher than might have been expected. The reason for these relatively high temperatures is that Nepal is located at 26 degrees 22 seconds north. This is the same latitude as the Central Sahara (Chapter 5.4).

6.11.4 Associations between residual rms and altitude

Once again each of these scatterplots reveals little tendency for residual rms and air pressure to be associated. A typical scatterplot is shown for the left eye of subject 1.22, and the scatterplot with the maximum r -value, from the left eye of subject 2.21, is presented (figure 6.11.4-1). In both examples the best-fitting straight line has a negative slope.

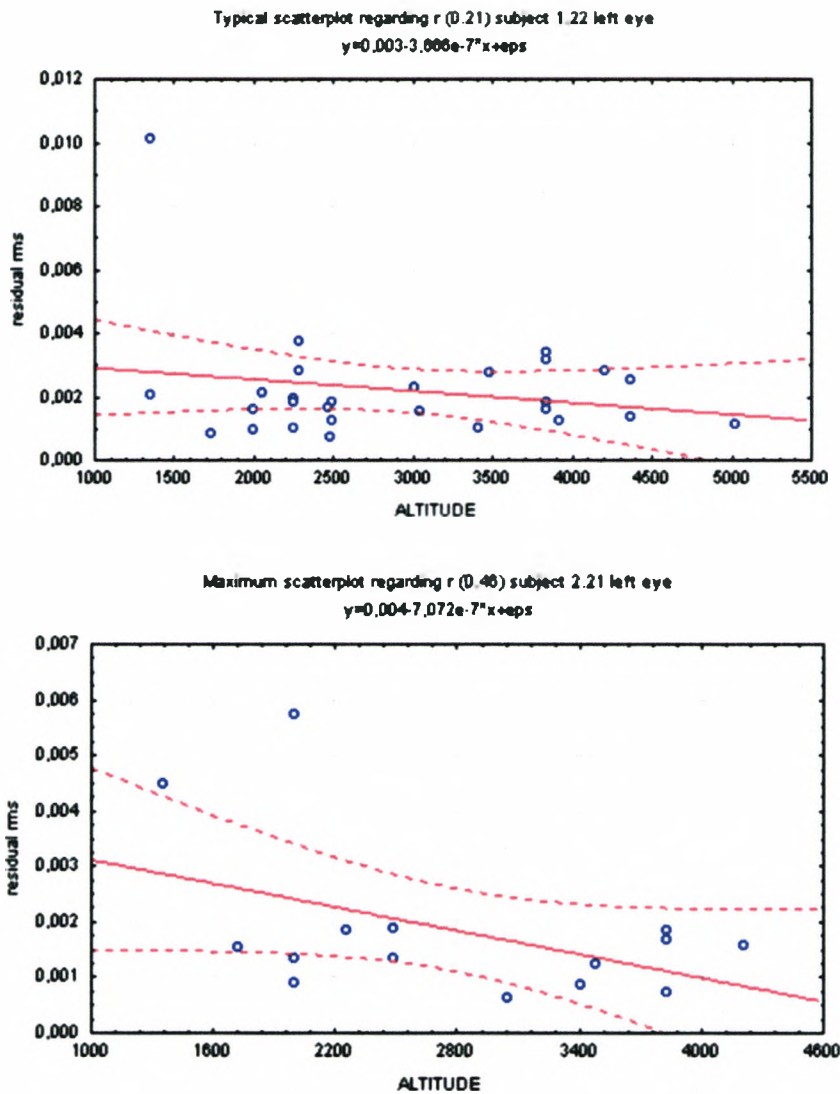


Figure 6.11.4- Scatterplot of residual rms values plotted against altitude for the left eye of subject 1.22 and the left eye of subject 2.21.

Eleven of the best-fitting straight lines have positive slopes (i.e. the higher the altitude, the greater the residual rms value) and 7 have negative slopes.

Correlation coefficients are between $r_{\min} = 0.02$ and $r_{\max} = 0.46$, with $r_{\text{mean}} = 0.19$. The maximum r value of 0.46 is equivalent to an R^2 value of only 0.22, indicating that 22% of the variation in residual rms is explained by the variation in altitude, while the R^2 of the mean correlation is only 4%. These results indicate that there is no linear association between residual rms and altitude.

The following means for the correlation coefficients were calculated from each data block:

Humidity/residual rms	$r_{\text{mean}} = 0.24$
Air pressure/residual rms	$r_{\text{mean}} = 0.18$
Temperature/residual rms	$r_{\text{mean}} = 0.20$
Altitude/residual rms	$r_{\text{mean}} = 0.19$

Table 6.11.4-1 The mean correlation coefficient r_{mean} for the association between residual rms values for eighteen tested eyes and their meteorological parameters.

The conclusion from all these analyses is that there is very little or no association between residual rms and the parameters tested i.e. humidity, air pressure, temperature, and altitude. The adaptation of the human body to the steadily changing parameters described above and the complex interactions between the meteorological parameters are probably responsible for the absence of any linear associations.

6.12 Summary and discussion

The residual rms value plays a central role in the hypothesis tests performed in this chapter. The method of calculation of residual rms values has been described in chapter 3.2.10.6. A total of eighteen eyes were tested in Nepal. All the residual rms values computed from every corneal shape measurement were divided into nine categories; morning tests, noon tests, and evening tests for each of the following categories, reference measurements, measurements on non contact lens wearers and measurements on contact lens wearers.

The descriptive statistics for high altitude samples compared with those for low altitude samples (both the “reference” data in Chapter 6 and the low altitude study in Chapter 4) generally show higher sample mean residual rms values at high altitude, and greater maximum residual rms values at high altitude.

Each altitude sample contains obvious outliers, as can be clearly seen in the box and whisker plots (Fig 6.3-1).

Generally, the residual rms values of the contact lens wearer samples tend to be greater than the residual rms values of the non contact lens wearer samples.

Unfortunately, the practical difficulties of taking measurements on the trek did not allow repeated measurements to be taken with the keratographer at each session on each day (morning, noon and evening) on every subject. It was only possible to take one keratographer measurement on each eye in each measurement session. Therefore, some lack of precision in the recorded residual rms values has to be accepted. However, many morning, noon and evening measurements were taken from each subject at a range of altitudes over the course of the trek, which would help to minimise the effects of the variation in measurement of residual rms when mean residual rms values were statistically evaluated.

Analysis of the descriptive statistics for the Zernicke coefficients for all subjects revealed that the coefficient with the lowest average influence on corneal shape was a_{60} (between 0 and $1.4E-09$). The coefficient with the highest average influence on corneal shape was a_{51} (between $2.5 E-06$ and $4.9 E-05$).

For the hypothesis tests the residual rms values for the contact lens wearer and non contact lens wearer categories described above were divided into samples depending on the altitudes at which the measurements were carried out. Each sample contained measurements collected over an altitude range of 1000m. This altitude interval was selected because it included approximately two of the standard 1500ft acclimatisation steps ($1000m = 3,280$ ft), and to ensure that sufficient data were collected within each sample to allow hypothesis testing. The first sample contains all measurements which were conducted up to 3,280 ft. In this sample the residual rms values are calculated from each subject's reference measurements. The second sample contains all the measurements which were performed up to 6,560 ft, and so on up to the fifth sample. The fifth sample contains all the measurements which were taken at altitudes higher than 13,120 ft.

For these five samples, six hypothesis tests were performed using ANOVA – these were for both the non contact lens wearer and contact lens wearer categories, further subdivided into morning, noon, and evening tests. Additionally, if a statistically significant ANOVA result was obtained, Duncan's MRT test was used to establish which group means were significantly different from the others tested.

There are statistically significant increases in residual rms values with altitude identified by ANOVA testing for both non contact lens wearers and contact lens wearers for their evening tests. The low altitude reference sample 1 had statistically significantly lower mean residual rms values than samples 2 and 5 for both contact lens wearers and non wearers, and the mean of sample 1 was also statistically significantly lower than sample 4 for the non wearers.

This contrasts with the data from the low altitude study described in Chapter 4, in which all measurements were taken at a constant altitude. Here there was no significant change in mean residual rms values with time of day (morning, noon or evening) or for measurements taken over a four day period for either contact lens wearers or for non contact lens wearers.

Fischer (2005) showed that the human body of mountaineers ascending to high regions is mainly influenced by reduced oxygen levels as a result of low air pressure at high altitude. Acclimatisation is achieved in stages, with the first stage beginning at 9,000 ft, and with the following stages occurring at every subsequent 1,500 ft. The required acclimatisation period for an individual is variable. It is accepted that no further acclimatisation is possible above about 17,000 ft (Albrecht, and Albrecht, 1967).

The minimum oxygen tension to prevent corneal swelling has been stated to be 74 mmHg (Holden, Sweeney, and Sanderson, 1984). This figure comes from a study which generated low levels of oxygen tension artificially, but 74 mmHg corresponds to an oxygen tension which is usually measured at an altitude of approximately 17,500 ft, which is an altitude to which the human body should still be able to acclimatize.

There is evidence from the current study that statistically significant corneal shape change, which may be the result of corneal swelling, may occur at levels below 17,500 ft, especially in contact lens wearers.

Any conclusions drawn from these small samples should be made with caution, but a contact lens can be considered as a membrane in front of the cornea which can induce reduced oxygen supply to the corneal epithelium, resulting in corneal shape change as indicated by raised residual rms values. Furthermore, the tendency for residual rms values of the high altitude samples to be greater than those of the low altitude samples suggests that the acclimatisation of the human body during the ascent to high regions could have an influence on corneal shape change represented by residual rms values.

Before each corneal shape measurement in Nepal, the temperature, humidity, altitude, and air pressure were recorded. The humidity was greater than might be expected at high altitude in November. Also, the temperature was higher than might be expected for these altitudes in November. However, the region of choice for the trek was close to the equator and therefore the temperatures measured in Nepal were not exceptional (Chapter 5.4.1). For each subject, correlation analysis revealed very little or no linear association between residual rms and the parameters tested i.e. humidity, temperature, air pressure, or altitude. This fact is demonstrated by the low correlation coefficients (r_{mean}) shown in table 6.11.5-1. From visual inspection of the scattergraphs, no obvious association (linear or otherwise) was apparent for any subject between residual rms and any of the parameters measured. This suggests that the acclimatisation of the human body and the interactions happening in the human body during acclimatisation (Chapter 2.27) are complex processes that make corneal change difficult to predict.

Transient changes in retinal vasculature occurred in two subjects on the trek. Similar changes in retinal vasculature have been reported previously (Schumacher and Petajan, 1975), in a study in which the fundi of mountaineers at high altitude were monitored. Contact lens movement increased in all three contact lens wearers at the higher altitudes encountered on the trek.

The z-value is the distance between the highest and deepest points of the corneal shape described by the Zernike coefficients. It gives two-dimensional information on a three-dimensional construction.

It is interesting to investigate the change in z-value for each eye separately, because a great change in z-values could have an influence on contact lens movement on the cornea during lens wear. For the calculation of z-values, a diameter of 7mm of the central area of the corneal shape was considered. There is a tendency for the mean z-values of contact lens wearers, for both the right and left eyes, to be higher than those of the non contact lens wearers. This suggests that wearing contact lenses at altitude may have an influence on z-values. Furthermore, at low altitude the greatest range of a non contact lens wearer's z-value is 0.0132 mm compared with 0.0429 mm at high altitude, and the greatest range of a contact lens wearer's z-value is 0.0169 mm at low altitude compared with 0.1881 mm at high altitude (see Chapter 4.2.5.3 for low altitude data). This suggests that the variability of z-values increases with altitude, and that this increase in variability is greater in contact lens wearers. A particularly large range of z-values at altitude, as described in table 6.8-1 and table 6.8-2, was found in two non lens wearers (1.21 right eye, and 5.21 left eye) and notably in one contact lens wearer (1.22 right and left eyes). Variations in z values on the scale noted on the trek have clinical implications for the comfortable wear of contact lenses at altitude, and could be the result of changes to the corneal epithelial or endothelial pump mechanisms.

However, an analysis of the altitudes at which the maximum and minimum z-values were achieved for each subject suggests that there is little tendency for z-values themselves to vary consistently with altitude in an individual subject. The main conclusion from Chapter 6, which should be interpreted with caution due to the small samples, is that the hypothesis is rejected for the evening measurements at altitude when a statistically significant corneal shape change was detected.

These corneal shape changes are likely to be the result of a combination of a reduced oxygen partial pressure at high altitudes, possibly exacerbated by fatigue, and, for contact lens wearers, the effects of the contact lens on the cornea.

Chapter 7. Discussion and Summary

7.1 Introduction

Changes in corneal shape at altitude have not been the subject of research, but are of great relevance to mountaineers. There is considerable anecdotal evidence based on reports from high altitude mountaineers of reduced visual acuity at high altitudes. The current surge in numbers of those ascending Everest, at a height of 8850 m, has added to the volume of these reports. The reduced visual acuity is presumably the result of corneal oedema resulting from the reduced oxygen concentration in the atmosphere, and corneal oedema could contribute to corneal shape change. When the cornea is subjected to experimentally-induced reduced oxygen levels at low altitude there is no consensus as to the level of oxygen which leads to corneal oedema.

Eleven subjects were tested to determine the daily corneal shape change and the corneal shape change over four days in low altitude conditions, and nine subjects were tested at high altitudes in Nepal. The analyses of both studies, followed by a comparison of the results, do reveal a tendency for the corneal shape to change with altitude. However, there is a need for further studies to confirm these findings. Therefore, this thesis should be seen as a starting point and a stimulus for further research in this area. The results from both studies are summarised and discussed on the following pages. In addition, the outcome of testing the hypothesis “The cornea is able to adapt to changing conditions and exhibits no statistically significant change in the corneal shape up to 16,400 ft” is discussed by considering different aspects of the changing conditions. In particular, the meteorological influencing factors were critically examined to assess their influence on the changes in the shape of the cornea during the stay at high altitude in Nepal.

Furthermore, the following questions were addressed:

- How does the corneal shape change, at low and high altitudes, both with and without contact lenses being worn?
- Is the extent of the corneal shape change relevant to comfortable contact lens wear?
- What are the main influencing factors at work in corneal shape change?

7.2 Corneal shape change at low altitude

7.2.1 Keratographer accuracy considered in detail

The corneal shape covers a horizontal length which ranges in the healthy human eye from 11.0 – 12.5 mm (mean 11.6 mm) and a vertical height which ranges from 10.0 – 11.5 mm (mean 10.7 mm) (Baron, 1981). In this study, a central corneal area of 7 mm in diameter is described using the Professor Lingelbach programme and only this area of the cornea is measured in the research presented in this thesis.

The keratographer used for this research employs circles of a Placido disc (object) which are reflected by the cornea and then photographed. This two-dimensional image is taken to describe the three-dimensional corneal shape. However, this two-dimensional image of circles on the cornea does not provide enough information for an exact calculation of the three-dimensional corneal shape, therefore a method has to be utilized to compensate for these gaps in the information required. One method to provide this additional information required is as follows. A reference image taken from a well-defined glass ball is compared with a Placido circle image of a cornea which is photographed by the keratographer. The differences between the circles on both pictures supplies the information which is necessary to compute a three-dimensional corneal shape with the help of a mathematical algorithm. However, this method only delivers exact data when the corneal shape is spherical or almost spherical.

The greater the deviation from a sphere, the less reliable are the results using this method (Schanzlin and Robin, 1992).

Additionally, Placido circles reflected from the cornea are often not photographed in full, particularly at the periphery of the cornea. The main causes for interrupted circles are shadows thrown from the subject's nose and eye lids. These shadow areas lead to gaps in the corneal shape information.

The Oculus keratographer programme utilises a mathematical algorithm which compensates for the problem of lack of sphericity of the cornea described above and also interpolates the corneal shape description at areas where there are gaps in the circles. However, these compensatory procedures do introduce approximations into the calculations of the three-dimensional corneal shape and changes in the shape such as those investigated in this study.

The outputs from the mathematical algorithm are polynomial sequences. These sequences form the bases for all the two and three-dimensional corneal shape considerations of the Oculus keratographer programme analysed in this thesis. The choice of the central corneal area of 7 mm in diameter described above ensures that there are very few gaps in the circles that require interpolation by the Oculus keratographer programme and which, therefore, could influence the measurements of corneal shape change. If a larger diameter had been chosen, then the number of interpolated areas would have increased dramatically.

In chapter 3.3.5 the agreement between two Placido keratographers is discussed, with residual rms values shown on Altman-Bland difference plots. The difference in the mean rms values between the instruments is 0.00020 (bias) and the 95% confidence intervals for the differences was from 0.00051 to -0.00011. The repeatability of each keratographer was also assessed by an Altman-Bland plot. Both keratographers present similar absolute mean difference values of 0.00017 and 0.00014 (bias). It was hoped that better repeatability would have been achievable. Taking several residual rms readings and averaging them at each measurement session would have been the ideal way to improve the quality of these data.

However, time pressures and the need to conserve precious electricity on the trek dictated that only one keratographer reading could be taken at each measurement session. This undoubtedly affected the precision of recorded residual rms values, but this single measurement procedure had to be adopted, and it represents just one of the compromises that are essential when coping with conditions as arduous as those encountered at high altitude in Nepal. There have been studies which have assessed the repeatability and accuracy of other video keratographers, in most cases by comparing central radii and sagittal radii. These parameters are not easily comparable with the results for residual rms values. Carvalho (2005) discussed the wave-front error which is induced by Zernike polynomials when they are used for corneal shape description. The quantitative influence of wave-front error on corneal shape description based on Zernike polynomials depends on the quantity of Zernike terms and the complexity of the corneal surface. In the current Nepal study, where the corneal shapes of subjects and Zernike terms were taken at low and high altitude, the wave-front error is about 16 μm . This is 16% of the maximum standard deviation (100 μm) which was defined for corneal shape fitting by the Professor Lingelbach programme (chapter 3.2.10.2).

7.2.2 Measurement of IOP

In a small sample of six eyes, consistently higher IOPs were recorded with the Tono-Pen XL tonometer than with the “gold standard” air puff tonometer. This suggests that the conversion table provided by the manufacturers of the Tono-Pen XL to convert from measurements taken from the sclera at the limbus, rather than from the cornea, may be inaccurate (Table 3.2.8-1). However, the sample used to generate the difference plot in Figure 3.3.4-1 was small. Furthermore, on the trek in Nepal the key factor regarding IOP was any relative change in IOP with altitude. For these reasons, the manufacturer’s recommended correction factors were used for IOP recorded using the Tono-Pen on the trek.

7.2.3 Low altitude study

To analyse the daily corneal shape change at low altitude eleven subjects were divided into two categories. The first category included three contact lens wearers (two women and one man), who had been soft lens wearers for a minimum of two years. The second category included eight non contact lens wearers (five women and three men).

Both categories were further subdivided into morning tests, noon tests, and evening tests, giving a total of six groups. Measurements were taken over a four day period. The conclusions that emerged are presented in the following sections but all should be treated with caution, given the small samples studied.

7.2.3.1 Tests of significant daily corneal shape change

Each residual rms value represented a keratographer measurement and is a measure for corneal shape change (chapter 3.2.10.6). The greatest maximum residual rms values were calculated from measurements carried out in the morning samples (Table 4.2.5-1). This could be explained by the phenomenon known as overnight corneal swelling, which is described in Mertz's study (1980), where he measured the overnight swelling of the eyes of nine subjects. Results showed overnight corneal swelling to be approximately 4.5 %. The logarithmic recovery to baseline occurred within the first hour after eye opening. Murray and colleagues (1985) described deswelling of the cornea after hypoxia. Central corneal thickness changes were monitored in nine subjects who wore low water content hydrogel lenses of varying thickness for 3h in both open and closed eye conditions. They stated that deswelling appears to occur in two phases, first at a rapid initial rate which is followed by a slower rate. The time taken for the deswelling process to return corneal thickness to baseline depends on the increase in thickness of the cornea and can last for up to 90 minutes. Contact lens wear or closed eyes have a similar effect, since in both cases the corneal oxygen supply is reduced.

Additionally, soft contact lens wear itself leads to an increase in corneal thickness (Chapter 2.2.6.2).

From the descriptive statistics, there is a slight tendency for the residual rms values to be higher in contact lens wearers in this small sample. As evidence, both the mean and median rms values for the non contact lens wearers were lower than those of the contact lens wearers at all times of the day.

Furthermore, the 0.75th quartile was greater at all times of the day in the contact lens wearers. All this could result from the influence of reduced oxygen supply during contact lens wear (Chapter 2.2.6).

In 1995, Rom and colleagues assessed the eyes of ten subjects to investigate the relationship between corneal oedema and topography. The right eye of every subject was exposed to an anoxic environment for 2 hours using a nitrogen chamber goggle. The left eyes served as controls. Immediately after the goggle was removed, topographic measurements and optical pachometry were taken from four locations, one in each of the central, nasal, temporal, and inferior cornea. The cornea was described in Dioptres of power following recording of the keratometric data. On the one hand, the average percentage thickening for each area was: 16.4% centrally, 6.3% temporally, 6.3% superiorly, and 9.2% inferiorly. On the other hand, the topographic data demonstrated no significant change from the baseline in each of the four areas. Furthermore, there was no significant correlation between corneal thickening in any area measured and changes in corneal topography.

There is evidence from the current study that corneal topography is affected by contact lens wear, unlike the results of the statistical analysis from the Rom study. It could be argued that data on corneal shape change derived using Zernike polynomials is more reliable than data, such as that from the Rom study, from only four fixed points defined on the cornea and used to describe corneal shape change.

There was no evidence to suggest that corneal shape change, as assessed by residual rms values, varies during the day for either the non contact lens wearer category ($p = 0.808$) or for the contact lens wearer category ($p = 0.210$).

This result is valuable in itself but, in addition, was used later in the thesis as baseline data to compare with the results of diurnal variation in residual rms values obtained at altitude. Data were collected over four days in these 11 subjects at low altitude to allow corneal shape change over time to be investigated when altitude remains constant. No significant corneal shape change occurred over four days for the morning, noon, or evening tests.

7.2.3.2 Change in z-value (the distance between the highest and deepest points of a cornea)

For contact lens fitting it is valuable to know the difference between the extreme values (i.e. the three-dimensional shape's highest and deepest points) of a corneal shape. As explained on page 142, the central corneal shape is comparable to an ellipsoid, therefore the highest point lies at the central cornea and the deepest point is positioned at the periphery. In this study a combination of a best fitted ellipsoid and Zernike polynomials are used to describe the corneal shape (Chapter 3.2.10.3-4). If we were to pull at the periphery of a best fitted ellipsoid until it became a flat disc, then the Zernike polynomials would describe a wavy three-dimensional shape with that flat disc as its base.

The difference between the highest and deepest points of the three-dimensional shape described above is defined as the z-value, a positive value. The z-value is not a constant for a given cornea, because it can vary as the corneal shape varies. The z-values obtained from the contact lens wearers tend to be greater than those of the non contact lens wearers in the low altitude study.

The range between minimum and maximum values shows similar behaviour. (Chapter 4.2.5.3). The average range of z-values of the non contact lens wearer samples shown in table 4.2.5.3-1 is 0.0085 mm and the average range of z-values of the contact lens wearer samples is 0.0126 mm. The z-values can be regarded as an indicator of probable contact lens movement on the surface of the cornea (see chapter 7.3.3).

7.3 Corneal shape change at high altitude

7.3.1 Hypothesis test

Once again, the two categories of contact lens wearers' and non contact lens wearers' residual rms values were divided into morning, noon, and evening groups. Some of the conclusions from the high altitude study are identical to those at low altitude. In particular, the residual rms values of the contact lens wearers tend to be greater than those of non contact lens wearers (Chapter 6.3, and chapter 6.4). The descriptive statistics of the high altitude study, when compared with those from the low altitude study, demonstrate greater residual rms values and a greater range of residual rms values at high altitude (Chapter 4.2.5, and chapter 6.3).

The effects of altitude on residual rms values were evaluated by statistical hypothesis testing for each category of morning, noon, and evening tests. There were statistically significant increases in residual rms values with altitude, identified by ANOVA testing, for both non contact lens wearers ($p = 0.0061$) and contact lens wearers ($p = 0.0002$) for their evening tests. Further analysis with Duncan's MRT test allows the identification of statistically significant changes between pairs of samples for these evening tests, and revealed a tendency for sample 1 (the reference sample) to have statistically significantly lower residual rms values than other samples (2, 4 & 5 for non contact lens wearers, and 2 & 5 for contact lens wearers). It appears that the human body's adaptation to the presence of less oxygen in the air at high altitude and the physical effort expended by the tour participants during a whole day in Nepal does have a measurable influence on the corneal shape change (Chapter 2.2.7.1).

Altitude sample number 1 includes all measurements which were carried out up to an altitude of 3,280 feet (1000m). Kathmandu lies at 4,400 feet of altitude and was the starting point of the trek. So the altitude sample number 1 included only the reference measurements taken at the baseline altitude of 2000 ft.

Butler (1999) discusses how the air pressure declines when altitude increases. A reduced air pressure leads to fewer gas molecules, especially oxygen molecules, in the air. On the trek, there was a strong linear association between the drop in air pressure recorded with increasing altitude ($r = -0.89$; $p = 0.00$, chapter 6.7). As described above, the cornea swells when the oxygen supply is reduced. So it could be expected that the higher the altitude the higher the risk of corneal swelling.

One feature apparent from the residual rms box and whisker plots in Chapter 6 is the presence of some obvious outliers in the data. The influence of these outliers was addressed using the strategy suggested by Altman (1991). This involves carrying out the statistical analysis both with and without the suspicious values. When the most obvious outliers are identified using the method described by Trampisch, Windeler, Ehle, and Lange (1997), and excluded from the subsequent statistical analysis, there is no change in the conclusions of any of the variance analysis (ANOVA) tests described above, thus reinforcing these conclusions.

7.3.2 Meteorological data and its influence on the test subjects

Kreutzig (1997) and Jefferson et al (2002) have determined that the higher a mountain-climber ascends, the lower the air pressure, the temperature and the humidity. The mountain-climber's body must adjust to these altered conditions. The pH value of the blood changes and this has a negative effect on the quantity of oxygen transported by the erythrocytes. This causes the number of erythrocytes in the blood to rise and the blood becomes thicker (Kreutzig, 1997). As stated above, the air pressure declines with increasing altitude in an almost linear fashion during the testing phase.

The humidity also reduced in a linear manner with increasing altitude ($r = -0.71$, $p = 0.00$). Temperature also drops with increasing altitude ($r = -0.31$, $p = 0.099$), though this linear association was much less marked. The average temperature was $13.1\text{ }^{\circ}\text{C}$ and the average humidity was 55.97% .

As a result of the geographic location of the trek, the temperatures measured during the day when the sun was shining were relatively high, but often fell rapidly to below $-20\text{ }^{\circ}\text{C}$ after sundown. Temperatures at night were not particularly important, as the test subjects were in warm tents at this time. Humidity was also unexpectedly high (Chapter 6.7). The reason for this was that the trek took place along a river in the Lang Tang valley, a high-altitude area where fog is common. Interestingly, the highest humidity measured was 88% at 6,700 feet and not, as expected, in lower-lying regions. The contact lens wearers possibly had a slight advantage over the non contact lens wearers with regard to maintaining the moisture of their eyes, for their contact lenses were kept in saline solution while the measurements were carried out. This helped to moisten the eyes of the contact lens wearers following insertion of their lenses. Because there was relatively high humidity on the trek, however, the moisture added to the eyes probably did not have any major impact on the values measured for the changes in the corneal shape. The linear association between the residual rms values and humidity was low ($r_{\text{mean}} = 0.24$), and a similar lack of linear association was found between residual rms values and air pressure ($r_{\text{mean}} = 0.18$), temperature ($r_{\text{mean}} = 0.20$), and altitude ($r_{\text{mean}} = 0.19$) (Chapter 6.11). These results should be treated with caution because the meteorological conditions changed rapidly during the whole test phase in Nepal. It should be noted that each one of the environmental parameters discussed here can affect the others, so there are undoubtedly interactions between them.

7.3.3 The range of the maximum and minimum z-values

It might be expected that the higher the altitude attained the greater the measured z-value, as a result of corneal reaction to the reduced oxygen supply in the air at high altitudes (Chapter 2.2.1, and chapter 2.2.6.2).

However, an analysis of the z-values of the 18 eyes tested on the trek revealed that in six of these eyes (involving four subjects) the altitude at which the minimum z-value was recorded was actually higher than that at which the maximum z-value was recorded. This could be because tissues in the human body are embedded in complex interactions of the metabolic activities at work during changing surrounding conditions (Kreutzig, 1997). As a result, changes in corneal shape with altitude cannot be predicted consistently.

The range of the z-values obtained during the test period gives quantitative data which may indicate how a contact lens could move on the corneal surface during the trek. It is interesting to compare the range of z-values for both lens wearers and non lens wearers at low and high altitudes (Chapter 6.8, and chapter 4.2.5.3). The ranges of z-values for the non contact lens wearers were; right eyes, 0.0073 mm to 0.0398 mm, and left eyes between 0.0102 mm and 0.0429 mm at high altitudes. At low altitude the non contact lens wearers' right eye range is between 0.0052 mm and 0.0132 mm, and their left eye range is from 0.0062 mm to 0.0130 mm.

For the right eyes of the contact lens wearers the range of z-values obtained at high altitudes were from 0.0167 mm to 0.1881 mm and for the left eyes were from 0.0204 mm to 0.1038 mm. The equivalent ranges at low altitude for the contact lens wearers' right eyes were between 0.0083 mm and 0.0141 mm and for the left eyes from 0.0112 mm to 0.0169 mm.

There is a tendency for the mean z-values for contact lens wearers, for both the right and left eyes, to be higher than those of the non contact lens wearers at both low and high altitude. There is also a tendency for a greater range of z-values to be found in contact lens wearers. This was most notable in one contact lens wearer (0.1881 mm and 0.1038 mm in subject 1.22's right and left eyes respectively). This represents a very variable difference between the highest and deepest points in a 7 mm circle of the corneal shape and complicates the challenge of achieving a satisfactory contact lens fit. The reason for these increased ranges of z-values could be some alteration to corneal metabolism or to the pump mechanisms of the corneal epithelium or the corneal endothelium.

The risk of contact lens wear inducing irritations rises dramatically when movement of the contact lens is influenced by a very variable z-value. This elevated range of z-values at high altitude should undoubtedly be taken into consideration during lens fitting for mountaineers who wish to ascend to high altitudes.

7.3.4 Eye inspection

A change in the retinal artery-vein ratio from $2/3$ to $3/4$ was detected in two trekkers after they reached their camp in Kyangjin Khar at an altitude of 12,600 feet for the first time. After arriving once again in Syrabru (7,400 feet), however, the retinal artery-vein ratio had returned to the $2/3$ level in these two subjects and remained at this level for the remainder of the trek. Karaküçük and Ertuğrul Mirza (2000) noted that altitude has potential undesirable effects on the retina. Ascents over 3000m produce engorgement and tortuosity of retinal vessels due to hypoxia and hemoconcentration.

Indicators of physiologic stresses on the cornea, such as tear debris, conjunctival injection, and corneal epithelial staining, are seen more frequently at altitude in contact lens wearers as a result of the dry air and low oxygen levels (Flynn et al, 1988). The lenses of all three contact lens wearers in the current study began to fit more tightly at altitudes of 12,000 feet or higher, and all had reduced lens movement (from their baseline of grade 1 to grade 2) at some point during the trek (Chapter 6.10). Reduced lens movement may be attributable to the corneal changes at altitude described above. The contact lens can be seen as a membrane on the surface of the cornea which reduces the oxygen supply to the corneal epithelium. Additionally, a reduced oxygen partial pressure at high altitude does have an influence on corneal metabolism resulting in an oedematous reaction of the cornea (Chapter 2.2.6.2).

It is clear from this study, on an admittedly small sample of contact lens wearers, that contact lens wearers who want to climb to high altitudes should take glasses with them in their backpack in reserve.

7.4 Addressing the three questions posed in Chapter 7 section 1

The questions are addressed as follows:

- How does the corneal shape change, at low and high altitudes, both with and without contact lenses being worn?

The range of residual rms values at high altitude of those in the non contact lens wearers and contact lens wearers categories are clearly greater than those of both categories measured at low altitude. At both low altitude and high altitude, the mean residual rms values of those in the contact lens wearer category tend to be greater than the residual rms values of those in the non contact lens wearer category (Chapter 4.2.5, and chapter 6.3). So corneal shape tends to change with altitude and changes are greater in contact lens wearers.

- Is the extent of the corneal shape change relevant to comfortable contact lens wear?

The subjective impression gained from the three trekkers wearing contact lenses suggests this question can be answered in the affirmative for this small sample. None of the trekkers found it comfortable wearing contact lenses at altitudes of greater than 12,000 feet (Chapter 6.10). An elevated z-value range at high altitude in a subject could be an indicator of more uncomfortable lens wear at high altitudes compared to low altitudes (Chapter 7.3.3).

- What are the main influencing factors at work in corneal shape change?

The main influencing factors with respect to the changes in corneal shape were the acclimatisation to altitude (mainly as a result of reduced oxygen in the air) and fatigue in the evening as a result of the high levels of physical exertion during the trek (Chapter 2.2.7.1 and chapter 2.2.7.2).

7.5 Suggestions for further research

This work has given rise to some further questions which should be addressed:

- Albrecht and Albrecht (1967) stated in their study that the human body is only capable of acclimatising up to 17,300 feet. If mountain-climbers ascend beyond this altitude, their body only deteriorates. Holden, Sweeney and Sanderson (1984) determined that there must be a minimum of 74 mm Hg oxygen pressure in order to avoid a swelling of the cornea. 74 mm Hg oxygen pressure corresponds to an altitude of 17,500 feet above sea level (Butler 1999). It would be interesting to know how the corneal shape changes at altitudes over 17,000 feet.
- It should also be remembered that in this study the test subjects were only tested over an 8 hour period. It would be valuable to test the subjects over a longer period of the day, although this has major implications for the supply of electricity and the logistical difficulties of taking measurements in darkness and in tents.
- In chapter 2.2.1 humidity and the factors that cause it to vary were discussed. Different climatic conditions prevail on a glacier. It would be fascinating to discover how the shape of the cornea would change on a glacier with or without contact lenses wear.
- Altitude acclimatization may affect visual acuity, contrast sensitivity and other measures of visual performance. However, it is known that visual acuity does not change up to an altitude of 15 000 ft (Butler, 1999). Although of interest, the practical limitation imposed on this study made impossible to carry out additional tests to investigate visual performance.

7.6 Main conclusions

All the conclusions from this thesis should be interpreted with caution, due to the small samples. However the main conclusion is that the cornea does exhibit significant changes in corneal shape with increasing altitude up to 16,700 ft. These significant changes were found in both contact lens wearers and non wearers for their evening tests.

The corneal shape changes detailed in this thesis are likely to be the result of a combination of a reduced oxygen partial pressure at high altitudes, possibly exacerbated by fatigue, and, for contact lens wearers, the effects of the contact lens on the cornea.

References

- ACOSTA M. C., BELMONTE C., and GALLAR J. (2001).
Sensory experiences in humans and single-unit activity in cats evoked by
polymodal stimulation of the cornea.
Journal of Physiology 534 (2): 511-525.
- ALBRECHT E., and ALBRECHT H. (1967).
Metabolismus unter O₂-Mangel im Höhenklima.
Pflügers Archiv 293: 1-18.
- ALTMAN DG. (1991)
Practical statistics for medical research.
Chapman & Hall, London
- ANDRESKO G., and SCHOESSLER J. P. (1980).
The Effect of Humidity on the Dehydration of Soft Contact Lenses
on the Eye.
International Contact Lens Clinic 7: 210-212.
- AUBERT H.J. (1996).
Nepal.
(Cologne: DuMont).
- AUFSCHNAITER P., MIEHE G., and SCHNEIDER CH. (1990).
Langthang Himal-Ost.
(Austria: Freytag-Berndt und Artaria Wien).
- AUFSCHNAITER P., MIEHE G., and SCHNEIDER CH. (1990).
Langthang Himal-West.
(Austria: Freytag-Berndt und Artaria Wien).

BAILEY I. L., and CARNEY L. G. (1973).
Corneal Changes From Hydrophilic Contact Lenses.
American Journal of Optometry 50 (1): 299-304

BARON H. (1981).
Kontaktlinsen.
(Heidelberg: Verlag Optische Fachveröffentlichung GmbH P13-18).

BERGHOLD F., SCHAFFERT W., and PALLASMANN K. (1991).
Voraussetzungen und Richtlinien für die Akklimatisation an große
und extreme Höhen zur Vorbeugung der Höhenkrankheit.
Wiener Medizinische Wochenschrift (11): 242-248.

BERKE A. (2002).
Hypoxie und Hornhaut.
Deutsche Optiker Zeitung (4): 90-96.

BERMAN E. R. (1991).
Biochemistry of the Eye.
(New York: Plenum Press P97, p98, p103-105, p115-117).

BLAND J.M., and ALTMAN D.G. (1986).
Statistical methods for assessing agreement between two methods of clinical
measurement.
Lancet: 307-310.

BLAUSTEIN B. H. (1996).
Ocular Manifestations of Neurologic Disease.
(St. Louis, Missouri: Mosby-Year Book, Inc. P21-26).

BOHL W., and ELMENDORF, W. (2005).

Technische Strömungslehre.

(Würzburg: 13th EDITION Vogel Verlag P75-77, p368-371).

BONANNO J. A., STICKEL T., NGUYEN T., BIEHL T., CARTER D.,
BENJAMIN W. J., and SARITA SONI P. (2002).

Estimation of Human Corneal Oxygen Consumption by Noninvasive
Measurement of Tear Oxygen Tension While Wearing Hydrogel Lenses.

Investigative Ophthalmology & Visual Science 43 (2): 371-376.

BOURASSA S., BENJAMIN W. J., and BOLTZ R. L. (1991).

Effect of humidity on the deswelling function of the human cornea.

Current eye research 10 (6): 493-500.

BURK A., and BURK R. (1996).

Checkliste Augenheilkunde.

(Stuttgart: Georg Thieme Verlag P125-129).

BUTLER F. K. Jr. (1999).

The Eye at Altitude.

International Ophthalmology Clinics 39 (2): 59-78.

CARVALHO L. A. (2005).

Accuracy of Zernike Polynomials in Characterizing Optical Aberrations and the
Corneal Surface of the Eye.

Investigative Ophthalmology & Visual Science 46 (6): 1915-1926.

CASEBEER J. C. (1973).

Effects of Air Travel on Contact Lens Wearer.

American Journal of Optometry 76 (1): 165-166.

CATANIA L. J. (1995).

Primary care of the anterior segment.

(Connecticut: Appleton & Lange P205-206).

COHEN S. R., POLSE K. A., and MANDELL R. B. (1990).

Humidity effects on corneal Hydration.

Investigative ophthalmology & visual science 31 (7): 1282-1289.

DAVIS N., DIAZ-SANTANA L., and LARA-SAUCEDO D. (2003).

Repeatability of Ocular Wavefront Measurement.

Optometry and Vision Science 80 (2): 142-150.

DIXON J. M., and BLACKWOOD L. (1991).

Thermal variations of the human eye.

Transactions of the American Ophthalmological Society 89: 183-193.

DONSHIK P. C., SUCHECKI J. K., and EHLERS W. H. (1995).

Peripheral corneal infiltrates associated with contact lens wear.

Transactions of the American Ophthalmological Society 93: 49-64.

EFRON N., MUTALIB H. A., PEREZ-GOMEZ I., and

KOH H. H. (2002).

Confocal microscopic observations of the human cornea following overnight contact lens wear.

Clinical and Experimental Optometry 85 (3): 149-155.

ENG W. G. (1979).

Survey on Eye Comfort in Aircraft: 1. Flight Attendants.

Aviation, Space, and Environmental Medicine 50 (4): 401-404.

ENG W. G., HARADA L. K., and JAGERMAN L. S. (1982).
The Wearing of Hydrophilic Contact Lenses Aboard a Commercial Jet
Aircraft: I. Humidity Effects on Fit.
Investigative Ophthalmology & Visual Science 53 (3): 235-238.

ENG W. G., RASCO J. L., and MARANO J. A. (1978).
Low Atmospheric Pressure Effects on Wearing Soft Contact Lenses.
Aviation, Space, and Environmental Medicine 49 (1): 73-75.

ETLING D. (1996).
Theoretische Meteorologie.
(Braunschweig/Wiesbaden: Vieweg Verlag P29-44).

FISCHER R. (2005).
Damit Bergreuden nicht zum Albtraum werden.
MMW Fortschritte der Medizin 147 (38): 28-30.

FLYNN W. J., MILLER R. E., TREDICI T. J., and BLOCK M. G. (1988).
Soft Contact Lens Wear at Altitude: Effects of Hypoxia.
Aviation, Space, and Environmental Medicine 59: 44-48.

FLYNN W. J., MILLER R. E., TREDICI T. J., BLOCK M. G.,
KIRBY E. E., and PORVINES W. F. (1987).
Contact Lens Wear at Altitude: Subcontact Lens Bubble Formation.
Aviation, Space, and Environmental Medicine 58: 1115-8.

FORTH W., HENSCHLER D., RUMMEL W., FÖRSTERMANN U., and
STARKE K. (2001).
Pharmakologie und Toxikologie.
(München: Urban & Fischer Verlag P746, p747,p531-533).

FREEMAN R. D., and FATT I. (1973).

Environmental influences on ocular temperature.

Investigative Ophthalmology 12 (8): 596-602.

FREYLER H. (1985).

Augenheilkunde für Studium Praktikum und Praxis.

(Wien, New York: Springer Verlag P81-90).

HÄCKEL H. (1999).

Meteorologie.

(Stuttgart: Eugen Ulmer GmbH & Co. P32-37, p39-46, p53-70, p386-387).

HAPNES R. (1980).

Soft Contact Lenses Worn At A Simulated Altitude of 18000ft.

ACTA Ophthalmologica 58: 90-95.

HEINRICH W., ROESLER S., and SCHRAUBE H. (1999).

Physics Of Cosmic Radiation Fields.

Radiation Protection Dosimetry 86 (4): 253-258.

HENSON D.B., and HARPER R.A. (1998).

Do non-contact tonometers read high?

Ophthal Physiol Opt 18: 308-310.

HOCKWIN O. (1985).

Biochemie des Auges.

(Stuttgart: Enke Verlag P21-25, p30, p36, p41).

HOLDEN B. A., and MERTZ G. W. (1984).

Critical Oxygen Levels to Avoid Corneal Edema for Daily and Extended Wear Contact Lenses.

Investigative Ophthalmology & Visual Science 25: 1161-1167.

HOLDEN B. A., SWEENEY D. F., and SANDERSON G. (1984).

The Minimum Precorneal Oxygen Tension to Avoid Corneal Oedema.

Investigative Ophthalmology & Visual Science 25: 476-480.

HUPFER P., and KUTTLER W. (2005).

Witterung und Klima.

(Wiesbaden: 11th EDITION Teubner Verlag P87-92).

JEFFERSON J. A., ESCUDERO E., HURTADO M. E., PANDO J., TAPIA R., SWENSON E. R., PRCHAL J., SCHREINER G. F., SCHOENE R.B., HURTADO A., and JOHNSON R. J. (2002).

Excessive erythrocytosis, chronic mountain sickness, and serum cobalt levels.

The Lancet 359: 407-408.

JOHNSON M. H., BOLTZ R. L., and GODIO L. B. (1985).

Deswelling of the Cornea After Hypoxia.

American Journal of Optometry & Physiological Optics 62 (11): 768-773.

KAMPIK A., and GREHN F. (1996).

Das äußere Auge.

(Stuttgart: Ferdinand Enke Verlag P1-3).

KANSKI J. J. (1995).

Clinical Ophthalmology.

(London: Butler&Tanner Ltd P100-101).

KARAKÜÇÜK S., and ERTUĞRUL MIRZA G. (2000).

Ophthalmological effects of High Altitude.

Ophthalmic Research 32: 30-40.

KAUFMAN H. E., BARRON B. A., and MCDONALD M. B. (1998).

The Cornea.

(Boston:2nd Edition Butterworth-Heinemann P14, p15, p19, p20, p22, p28-41).

KAUFMAN P. L., and ALM A. (2003).

Adlers Physiology of the Eye.

(St. Louis, Missouri: Mosby P47-51, p59, p62, p69-70, p91).

KHEN J. A., DAVIS, M., GRAHAM C. E., TRANK J., and

WHITACRE M. M. (1991).

Comparison of Oculab Tono-Pen Readings Obtained From Various
Corneal and Scleral Locations.

Arch Ophthalmology 109: 1444-1446.

KLYCE S. D. (1981).

Stomal Lactate Accumulation Can Account For Corneal

Oedema Osmotically Following Epithelial Hypoxia In The Rabbit.

Journal of Physiology 321: 49-64.

KOLOZVÁRI L., NÓGRÁDI A., HOPP B., and BOR Z. (2002).

UV Absorbance of the Human Cornea in the 240- to 400 nm Range.

Investigative Ophtalmology & Visual Science 43 (7): 2165-2168.

KREUTZIG T. (1997).

Biochemie.

(Suttgart: Gustav Fischer Verlag P349, p358).

KUCHLING H. (1986).

Taschenbuch der Physik.

(Frankfurt/Main: Harri Deutsch Verlag P41-50, p152, p216-217, p394-396, p608-609).

KÜHNEL W. (1999).

Taschenatlas der Zytologie Histologie und mikroskopischen Anatomie.

(Stuttgart: Thieme Verlag P455, p457, p459).

LAMBERTS D. W., FOSTER S., and PERRY H. D. (1979).

Schirmer Test After Topical Anesthesia and the Tear Meniscus Height in Normal Eyes.

Arch Ophthalmology 97: 1082-1085.

LEMP M. A., MATHERS W. D., and SACHDEV M. S. (1990).

The effects of contact lens wear on the morphology of corneal surface cells in the human.

Transactions of the American Ophthalmological Society 88: 313-325.

LEWIS T., and FINGERET M. (1993).

Primary Care of the Glaucomas.

(Norwalk, Connecticut: Appleton & Lange P107-118).

LINGELBACH B. (1999).

Zernike-Polynome.

Zur praktischen Augenheilkunde 20: 157-164.

LÜLLMANN H., MOHR K., and ZIEGLER A. (1996).

Taschenatlas der Pharmakologie.

(Stuttgart: Thieme Verlag P86-95, p98-107).

MADIGAN M. T., MARTINKO J. M., and PARKER J. (2000).
Brock Mikrobiologie.
(Heidelberg: Spektrum Akademischer Verlag P143-144, p330-332, p455-459).

MALCONIAN M. K., ROCK P. B., REEVES J. T., CYMERMAN A., and
HOUSTON C. S. (1993).
Operation Everest 2: Gas Tensions in Expired Air and Arterial Blood at
Extreme Altitude.
Aviation, Space, and Environmental Medicine 64 (1): 37-42.

MANDELL R. B., and FARREL R. (1980).
Corneal swelling at low atmospheric oxygen pressures.
Investigative Ophthalmology & Visual Science 19 (6): 697-702.

MATHERS W. D., BIMATAO G., and PETROLL M. (1993).
Ocular water evaporation and the dry eye. A new measuring device.
Cornea 12 (4): 334-340.

MAURICE K. H., GARNER L. F., LEGG S., and FARIS J. (1995).
Effects of Exposure to Simulated Altitudes on Visual Fields,
Contrast Sensitivity, and Dazzle Recovery.
Aviation, Space, and Environmental Medicine 66 (3): 243-246.

MEEK K. M., DENNIS S., and KHAN S. (2003).
Changes in the Refractive Index of the Stroma and Its Extracellular Matrix
When the Cornea Swells.
Biophysical Journal 85: 2205-2212.

MERTZ G. W. (1980).
Overnight swelling of the living human cornea.
American Journal of Optometry 51 (3): 211-213.

MIEYAL P. A., DUNN M. W., and SCHWARTZMAN M. L. (2001).
Detection of Endogenous 12-Hydroxyeicosatrienoic Acid
in Human Tear Film.

Investigative Ophthalmology & Visual Science 42 (2): 328-332.

MURRAY H. J., ROGER L., and LOUIS B. G. (1985).

Deswelling of the Cornea After Hypoxia.

American Journal of Optometry & Physiological Optics 62 (11): 768-773.

NAUMANN G. O. H. (1997).

Pathologie des Auges.

(Heidelberg: Springer Verlag P9-10, p24-28).

NELSON A. C., and TOBIAS C. A. (1983).

Rapid development of corneal lesions in rats produced by heavy ions.

Advance Space Research 3 (8): 195-209.

NGUYEN T., SONI P. S., BRIZENDINE E., and

BONANNO J. A. (2003).

Variability in hypoxia-induced corneal swelling is associated with variability in
corneal metabolism and endothelial function.

Eye Contact Lens 29 (2): 117-125.

NIGEL D., DIAZ-SANTANA L., and LARA-SAUCEDO D. (2003).

Repeatability of Ocular Wavefront Measurement.

Optometry and vision science 80 (2): 142-150.

PITTS D. G., BERGMANSON J. P., and CHU L. W. (1987).

Ultrastructural analysis of corneal exposure to UV radiation.

Acta Ophthalmologica (Copenh.) 65 (3): 263-273.

PLATA R., CORNEJO A., ARRATIA C., ANABAYA A., PERNA A.,
DIMITROV B. D., REMUZZI G., and RUGGENENTI P. (2002).

Angiotensin-converting-enzyme inhibition therapy in altitude
polycythaemia: a prospective randomised trial.

The Lancet 359: 663-666.

PODSKOCHY A. (2004).

Protective role of corneal epithelium against ultraviolet radiation damage.

Acta Ophthalmologica Scandinavica 82 (6): 714-721.

POLSE K. A., BRAND R. J., COHEN S. R., and
GUILLON M. (1990).

Hypoxic Effects on Corneal Morphology and Function.

Investigative Ophthalmology & Visual Science 31 (8): 1542-1554.

POLSE K. A., and MANDELL R. B. (1970).

Critical Oxygen Tension at the Corneal Surface.

Arch Ophthalmology 84: 505-508.

POLSE K. A., SARVER M. D., and HARRIS M. G. (1975).

Corneal Edema And Vertical Striae Accompanying The Wearing Of
Hydrogel Lenses.

American Journal of Optometry 52 (3): 185-191.

ROM M. E., KELLER W. B., MEYER C. J., MEISLER D. M., CHERN K. C.,
and LOWDER C. Y. (1995).

Relationship between Corneal Edema and Topography.

The CLAO journal 21 (3): 191-194.

SACHSENWENGER M. (1994).

Augenheilkunde.

(Stuttgart: Hippokrates Verlag GmbH P130-131).

SCHANZLIN D., and ROBIN J. B. (1992).

Corneal Topography Measuring and Modifying the Cornea.

(New York: Springer Verlag P2-24).

SCHIRMER H., BUSCHNER W., CAPPEL A., MATTHÄUS H., and
SCHLEGEL M. (1989).

Wetter und Klima.

(Mannheim: Meyers Lexikonverlag P28-33).

SCHUMACHER G. A., and PETAJAN J. H. (1975).

High Altitude Stress and Retinal Hemorrhage. Relation to Vascular Headache
Mechanisms.

Arch. Environ Health 30 (5): 217-221.

SINGH G., and BHINDER H. S. (2003).

Closed chamber thermometry and humidity measurements in normal and dry
eye patients: a pilot study.

European Journal of Ophthalmology 13 (4): 343-350.

SMITH H. (1999).

Quantifying Radiation Risks.

Radiation Protection Dosimetry 86 (4): 259-262.

SMOLIN G., and THOFT R. A. (1994).

The Cornea.

(Boston: 3rd EDITION Little Brown and Company P5, p7, p11, p13, p439-444).

STAPLETON F., TAN M. E., PAPAS E. B., EHRMANN K., GOLEBIEWSKI B., VEGA J., and HOLDEN B. A. (2004).

Corneal and conjunctival sensitivity to air stimuli.

British Journal of Ophthalmology 88: 1547-1551.

TAYLOR H. R., WEST S. K., ROSENTHAL F. S., MUNOZ B., HENRY S., ABBEY H., and EMMETT E. A. (1988).

EFFECT OF ULTRAVIOLET RADIATION ON
CATARACT FORMATION.

The New England Journal Of Medicine 319 (22): 1429-1433.

TOMMASINO L. (1999).

In-Flight Measurements Of Radiation Fields And Doses.

Radiation Protection Dosimetry 86 (4): 297-301.

TRAMPISCH H. J., WINDELER J., EHLE B., and LANGE S. (1997).

Medizinische Statistik.

(Heidelberg: Springer Verlag P211-264).

UNIACKE C. A., AUGSBURGER A., and HILL R. M. (1971).

Epithelial Swelling With Oxygen Insufficiency.

American Journal of Optometry 48 (7): 565-568.

WANG L., DAI W., and LU L. (2005).

Ultraviolet irradiation-induced K(+) channel activity involving p53 activation in corneal epithelial cells.

Oncogene 24 (18): 3020-3027.

WATKINS J. R. (1966).

Corneal topography and contact lens relationships.

Journal of the American Optometric Association 37 (3): 224-228.

WEST J. B. (2004).

The Physiologic Basis of High-Altitude Diseases.

Annals of Internal Medicine 141: 789-800.

WINER B. J., BROWN D. R., and MICHELS K. M. (1991).

STATISTICAL PRINCIPLES IN EXPERIMENTAL DESIGN.

(New York: McGraw-Hill P100-101).

WOLKOFF P., NOJGAARD J. K., TROIANO P., and

PICCOLI B. (2005).

Eye complaints in the office environment: precorneal tear film integrity influenced by eye blinking efficiency.

Occupational and Environmental Medicine 62 (1): 4-12.

APPENDIX

Assumptions and definition of terms

12V/24V DC / 230 V AC the inverter consists of a primary spool 12V/24V and secondary spool 230 V.

Acclimatisation is the ability of the body to adapt to changes in surrounding conditions.

Acute mountain sickness (AMS) is the most common manifestation of altitude sickness and involves headache, loss of appetite, nausea, fatigue, and insomnia.

ANOVA/MANOVA variance analysis or multiple variance analysis for the testing of the hypothesis

Apoptosis designates programmed cell death to renew tissue.

2,3 Bisphosphoglycerate is produced during anaerobe glycolysis.

CCLRU Grading Scales describes irregularities in the eye in quantitative terms. This makes it possible to examine such irregularities using statistical methods.

Cosmic radiation compared with UV radiation do ionize. Ninety-eight of cosmic radiation is made up of nuclei and γ -radiation, and only two per cent electrons or positrons.

DNA desoxyribonucleic acid.

Enalapril is an angiotensin-converting enzyme-inhibitor

Erythropoietin is produced in the kidneys and controls the erythropoiesis.

$f_{absolute}$ designates absolute humidity, which shows the momentary water vapour mass in the air. The unit is kg/m^3

f_{max} designates maximum humidity, which shows the maximum water vapour mass in the air. The unit is kg/m^3

$f_{relative}$ designates relative humidity and is measured with a hygrometer.
The unit is %

Hemoglobin saturation shows the quantity of oxygen the hemoglobin binds.
(Unit %)

Hemogrtid shows the quantity of erythrocytes in the blood.

HETE 12-hydroxyeicosatetraenoic acid is a product of arachidonic acid metabolism.

HETrE 12-hydroxyeicosatrienoic acid is a product of arachidonic acid metabolism.

Hyperpnea designates more and stronger breathing than normal.

IOP intra ocular pressure, which in this work is measured with a Tono-Pen XL.

The Levene test tests how the variances of the groups are homogenous for variance analysis.

Lorentz force acts on an electron moving through a magnetic field to derive a field direction at a 90° angle.

Measurement block is the term used for all measurements performed which are related in time, for example: morning measurement block, noon measurement block, and evening measurement block.

Paracrine means that there is a direct effect but it is not transported through blood circulation.

Polycythaemia is used to describe a state where the quantity of erythrocytes in the blood is higher than normal.

Proteinuria describes when proteins are excreted through the urine.

PRPH per cent recovery per hour. Corneal swelling induced by closed eyes and a thick contact lens in front of the cornea. The per cent recovery per hour is measured as an indication of corneal pH.

Residual rms represents the difference in the Zernike coefficients between one measurement and the mean coefficients of the same eye as one value.

Rms is a variable that is the square root of the sum of the squared Zernike coefficients.

Ruhepuls denotes the pulse after a period of relaxation. The best time for measuring the pulse is immediately after waking up in the morning.

SGTP Serum-Glutamate-Pyruvate-Transaminase is a zyttoplasmic enzyme which is present in the liver.

Solar flares take place on the surface of the sun, predominantly during periods of high or significant changes in solar activity, occasionally releasing large amounts of energy in sudden local outbursts of γ -rays, hard and soft x-rays and radio waves. These are solar flare events.

Stress lens is a very thick soft lens that is used to induce corneal swelling.

UV radiation is a radiation that does not ionise. It is divided into UV-A (320 - 400 nm), UV-B (290 - 320 nm) and UV-C (100 – 290 nm).

Water vapour mass represents the quantity of water vapour in the air. The unit used is kg.

Water vapour pressure of saturation is the maximum amount of water vapour in the air. The saturation point of water vapour pressure depends on the temperature.

Zernike polynomials are circle polynomials. Zernike polynomials describe optical surfaces with a base area of a circle. Each coefficient describes a lens error for the optical surface with the base of the wave fronts.